Addendum

Question: The examiner understands that the candidate constructed a refrigeration system test rig, but wonder why the refrigeration characteristics such as the refrigeration capacity and the COP of the system are not presented in the thesis.

Answer: One of the major objectives of this thesis is to study the feasibility of solving the problem of air leaking into the adsorption refrigeration system which works at vacuum pressure. In order to see the progress of the adsorption and the cooling effect (eg, dew, frost) objectively, the evaporator is made with glass, and it is not insulated. This arrangement, on the other hand, makes it difficult to precisely measure the refrigeration capacity. Therefore, the experimental refrigeration capacity and the Coefficient of Performance (COP) of the system are not presented.

Question: Some key points of heat transfer analyses on the collector/desorption bed need to be clarified, for instance:

- o The desorption process is a problem of forced convection with variable fluid properties; why did the candidate model the problem as a conduction problem (Eq. 4.1)? Justification is needed in this regard.

- o Comparing Eqs. (4.1) and (4.16), why is the term

$$\partial^2 T / \partial z^2$$

omitted? Physically, both the concentration and the temperature vary along the z-axis.

Answer: Yes, the desorption process is also a problem of forced convection with variable fluid properties. But the main concern here is the fixed bed being heated by the boundary, the pipe. For a fluid flowing at steady rate through the voids in a column, to simplify the calculation, it could be approximately taken as a conduction problem, and one of the expressions of the effective (apparent) bed conductivity is given by Flix and Neill (McAdams, *Heat Transmission*, 1954).

Yes. Eq. (4.1) is the general one. In our application, the main concern here is the fixed bed, especially the adsorbent particles, being heated by the boundary. Since the heat (solar radiation) falling on the pipe is the same along the axis, to simplify the calculation, it is assumed that there is no temperature gradient in the adsorbent particle column along the z-axis. So that term

$$\partial^2 T / \partial z^2$$

is omitted in Eq. (4.16).

Question: The data presented in Figs 4.4 and 4.5 need to be explained because it is strange why all the temperatures at different radial positions fall in a single linear line.

Answer: I feel a little bit strange too. I think there are several reasons for the results.
- ➤ The diameter of the pipe is small.
- ➤ The effective thermal conductivity of the packed bed is high (with the gas flowing through the bed, the temperature distribution is even radially).
- ➤ The accuracy of thermal couples is limited ($\pm 0.3°C$).

Question: The definition of the temperature difference given by Eq. (5.37) lacks physical sense. The use of log mean temperature will avoid the problem encountered by the candidate for calculating outlet temperatures.

Answer: Yes, the log mean temperature difference is definitely a good one. The reason to use the temperature difference defined by Eq.(5.37) is that it is simple and easy for the following calculation.

A SOLAR ADSORPTION REFRIGERATION SYSTEM OPERATING AT NEAR ATMOSPHERIC PRESSURE

Ying You, Dip., MEngSci.

A thesis submitted in fulfilment of the requirements for the degree of

Doctor of Philosophy

GIPPSLAND SCHOOL OF ENGINEERING
MONASH UNIVERSITY

JUNE 2001

Contents

Abstract

To solve the leaking problem faced by solar adsorption refrigeration systems currently working at vacuum pressure, this thesis carried out a comprehensive study on the hypothesis of adjusting the system's working pressure to around atmospheric by using a selected adsorbent and introducing a pressure adjusting gas in the system.

The first chapter presents the hypothesis of the research. Then the objectives and scopes of this study are identified. The related previous studies are also comprehensively reviewed.

Chapter two firstly describes the selection of the adsorbent, the refrigerant, and the pressure-adjusting gas. Then, the pressure - temperature - concentration relationships for Molecular Sieve 5A — Methanol, and Activated Carbon 207E — Methanol are tested, respectively. The key thermodynamic properties (e.g., the heat of adsorption) are also determined here in mathematical expressions.

The experimental study of the system is the task of chapter 3. Activated carbon/methanol is finally selected as the adsorbent/refrigerant pair, and helium as the pressure-adjusting agent. Then the setting up of the indoor simulation refrigeration rig developed for working arour ʰe atmospheric pressure, and the experimental procedures are described. The results of the experiments are presented in the following chapters with the theoretical results.

Chapter 4 describes the heat transfer analysis on the collector pipe in the heating and the heating/desorption processes. A semi-empirical equation of the temperature variation with time in the collector pipe is obtained.

Chapter 5 contains the energy analysis on the cycle. The energy balance equation is firstly extended to the situation with heat depletion. The relationship of Coefficient of Performance (COP) of the cycle and the operation temperatures is derived and shown on figures. The COP of the system without the pressure-adjusting gas is also shown in the figures for the convenience of comparison.

Adsorption analysis is conducted in chapter 6 since the inert gas in the system increases the adsorption resistance for the refrigerant. Based on the analysis on the adsorption mechanisms, some derivates (eg. the rate of adsorption and cooling) were derived and expressed in equations and figures. The experimental data are also shown in the figures.

In a complete and advanced analysis, the *quality* of energy should also be analyzed. In chapter 8, firstly the exergy for mixtures and the *irreversibility* are developed. Then a detailed exergy analysis on the processes and the whole cycle is carried out.

The foregoing work is based on the constant heating flux. A simulation of the performance of the system powered by solar radiation which changes with time is conducted in chapter 8. This simulation can be refereed in the prototype design. An index of the useful formulae is also presented in this chapter.

In the last chapter of thesis (chapter 9), some suggestions are presented for the prototype design.

This study shows the hypothesis proposed here can be realized and the models presented here describe the performance of the system well. This study may be of benefit to the effects to remove the leaking problem faced by the systems currently working at vacuum pressure.

Statement

This thesis, except with the committee's approval contains no material which has been accepted for the award of any other degree or diploma in any university or other institution and to the best of the candidate's knowledge, the thesis contains no material previously published or written by another person, except where due reference is made in the text of the thesis.
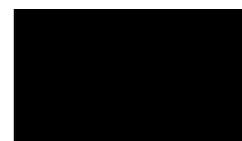
Ying You

Acknowledgments

Work described in this thesis was carried out at the School of Engineering at Gippsland, Monash University.

Most of All, the author wishes to thank his supervisor, Professor Jim Jarvis, Head of the school, for his kind concern and support to the author.

Special thanks are owed to Dr Eric Hu (the author's principal supervisor, now at Deakin University) for his invaluable advice, guidance, and encouragement over the entire period of research. Dr Hu led the solar utilisation research group at Gippsland School of Engineering where the research was initiated.

Thinks are also due to all members who have helped with the project, especially Dr Mir-Akbar Hessami (the Department of Mechanical Engineering, Clayton), A/Professor Ibrahim Yousef, and A/Professor David Wood (the University of Newcastle) for their comments, and Mr Ian Bowden, Mr Ken Phelps and Mr Glenn Azlin for their wonderful work without that the experimental projects could not have been pursued.

The author is indebted the Commonwealth Department of Education, Training, and Youth Affairs (DETYA) for providing the fund for the solar refrigeration project, and Monash University for providing the Monash Graduate Scholarship (MGS) which made this study possible.

Finally, the author wishes to thank all members of his family, especially his hardworking parents, his wife and his son for their understanding and support.

Nomenclature

a	Solid particle surface area	I_{dir}	Direct irradiance
	or activity	I_r	Reflect irradiance
	or where context indicates	I_0	Extraterrestrial irradiance
A	Area	j_H	j-factor for heat transfer
	or where context indicates	j_M	j-factor for mass transfer
b	Stream exergy parameter	k	Thermal conductivity
B	where context indicates	K	Henry's constant
c	Specific heat		or extinction coefficient
	or concentration for liquid	k_B	Boltzmann's constant
	or partial pressure for gas	k_f	External mass transfer
	or where context indicates		coefficient
C	where context indicates	k_p	Particle-phase mass transfer
c_p	Constant pressure specific		coefficient
	heat	k_{of}	Overall transfer coefficient to
c_v	Constant volume specific		the surface area of the
	heat		particle
c_s	Specific heat for entropy	k_{op}	Overall transfer coefficient to
COP	Coefficient of Performance		the volume of the particle
d	Diameter	KE	Kinetic energy
D	Diameter	l	Length
	or Parameter in D-A	L	Length
	equations		or distance between two
	or diffusivity		surfaces
D_e	Effective intrapellet	m	Mass
	diffusivity		or integer (1, 2, or 3)
D_K	Knudsen diffusivity	M	Molecule weight
D_M	Molecular diffusivity	n	Parameter of the D-A
D_p	Pore diffusivity		equation
D_{pM}	Pore molecular diffusivity		or number of pellets per
D_s	Surface diffusivity		volume
D_z	Axial dispersion coefficient		or day of year
e	where context indicates		or glazed number
E	Energy	N	Mole numbers
E_t	Equation of time		or glazed number
e_x	Specific exergy	Nu	Nusselt number
E_x	Exergy	$p.P$	Pressure
$E_x{}'$	Exergy function	Pe	Peclet number
f	Fugacity	Pr	Prandtl number
	or dilution factor for	PE	Potential energy
	irradiance	q	the amount adsorbed in
	or where context indicates		equilibrium
F	Free energy	q_0	Maximum amount of
	or radiation shape factor		adsorbate in the adsorbent
Fo	Fourier number	Q	Heat flow
G	Gibbs function	Q_a	Non-convective heat transfer
h	Specific enthalpy		per area
	or heat transfer coefficient	Q_v	Heat generation per unit
H	Enthalpy		volume
	or length of the hot surface	Q'	Heat generation in a system
i	Relative exergy loss	r	Radius
I	Irreversibility		or correlation coefficient
I_{dif}	Diffuse irradiance	R	Radius

	or gas constant
Ra	Rayleigh number
R_c	Contact thermal resistance
Re	Reynolds number
s	Specific entropy
S	entropy
Sc	Scmidt number
t	Time
t_{as}	Apparent solar time
t_{ls}	Local standard time
T	Temperature
u	Specific internal energy
U	Internal energy
	or heat transfer coefficient
u_s	Superficial velocity
v	Specific volume
V	Volume
	or velocity
W	Work
	or volume of the adsorbate adsorbed in a unit mass of adsorbent
W_0	Maximum volume of adsorbate in a unit mass of adsorbent
x	The mass of the adsorbate adsorbed in a unit mass of adsorbent
	or the mole fraction
x_0	Maximum mass of adsorbate in a unit mass of adsorbent
z	Elevation
	or axial coordinate/distance

Greek letters

α	Thermal diffusivity
	or absorptivity
β	Affinity coefficient
	or volume coefficient
γ	Activity coefficient
Δ	Change
δ	Solar declination
ε	Adsorption potential
	or emissivity
	or voidage
	or Lennard-Jones force constant
	or exergetic efficiency
η	Efficiency
θ	Excess temperature
	or incident angle
θ_p	Tilt angle of the collector plane
θ_s	Zenith angle
θ'	Angle of refraction
λ	Latitude

μ	Viscosity
	or chemical potential
ν	Kinematic viscosity
ρ	Density
	or reflectivity
σ	Collusion diameter
	or entropy generation
	or Stefan-Boltzmann constant
ϕ	Circumferential coordinate
	or plane-solar azimuth
ϕ_p	Plane azimuth
ϕ_s	Solar azimuth
τ	Transmissivity
	or tortuosity factor
τ_a	Transmissivity considering only absorption
τ_r	Transmissivity neglecting absorption
ω	Solar hour
Ω	Collusion integral

Subscripts

a	Apparent quantity
	or atmosphere
act	Actual
ad	adsorbent
b	Adsorption/desorption bed
	or back casing of the collector
c	Property at critical point
	or at condenser state
	or cooling effect
	or convective heat transfer
$c'g$	Collector/generator
CM	Control mass
CV	Control volume
d	diffuse
de	Desorption quantity
e	Effective quantity
	or exit state
	or property at evaporator state
ev	Evaporator
ex	Exit (outlet) state
f	Saturated liquid
	or flow process
fg	Difference in property for saturated vapour to saturated liquid
g	Saturated vapour
	or glass
	or ground
gro	Gross quantity
h	Heating process

He	Helium
i	Inlet state
in	Inlet state
L	Liquid
	or loss
leak	Leakage
loc	Local state
mix	Quantity for mixture(s)
Meth	Methanol
nf	Non-flow process
net	Net quantity
o	Centre line of the collector tube
p	Adsorption pellet/particle or collector pipe
pr	Pressure-adjusting gas
pro	projected
$\underline{Q}$	Quantity related to heat
r	Refrigerant or radiative heat transfer
rec	Receiver
ref	Reference state
rev	Reversible
s	Saturated state or solid or surface of the bed or solar

t	Collector tube or top of the pipe
tot	Total amount
u	Useful
v	Quantity per unit volume
V	Vapour
W	Quantity related to work
θ	Incident angle
0	Restricted dead state

Superscripts

ch	Chemical property
tm	Thermomechanical property
tot	Total amount
0	Unrestricted dead state
.	Dot over symbol denotes time rate
-	Bar over symbol denotes average quantity or partial mole property
~	Wave-line over symbol denotes mole quantity
*	Quantity in equilibrium with the related quantity

1

Literature Review and Tasks of the Thesis

1.1 BACKGROUND

Energy and the environment are two of the most important issues in the current world. Nowadays most electricity is generated by consuming fossil fuels such as coal, oil and natural gas. Not only do fossil fuels have a limited life but their combustion emissions have serious negative impacts on our environment such as adding to the greenhouse effect and causing acid rain. As a potential clean and sustainable energy source, solar energy is getting more and more attention.

In many places around the world, especially in the third world countries and some rural and isolated areas in the tropical zone, refrigeration techniques are much needed to preserve foodstuffs and medical supplies and for air conditioning. However, the lack of infrastructure, especially the lack of a reliable energy supply, and the lack of trained service personnel prevent the use of conventional refrigeration methods. On the other hand, solar radiation is ubiquitous, and solar radiation is very strong in the tropical zone where there is much need for refrigeration air conditioning. Solar energy is often the only readily available energy source there, and solar-powered refrigeration technology has the potential to store perishable food and vaccines and for air conditioning for these parts of the world. Even in the urban areas, the use of solar energy can help to reduce the emission of the combustion products exhausted from the conventional power plants.

1.2 SOLAR REFRIGERATION

Refrigeration is defined as the process of extracting heat from a lower temperature heat source, substance, or cooling medium, and transferring it to a higher temperature heat sink. A refrigeration system is a combination of components and equipment connected in a sequential order to produce the refrigeration effect. The refrigeration systems commonly used for general purposes can be classified as vapor compression systems and sorption systems. The former are driven by mechanical (electrical) energy and the latter are driven by thermal energy.

Normally there are two ways of refrigeration powered by solar energy. One is to convert solar radiation to electricity by means of photovoltaic cells (ASHRAE, 1996; Kreith and West, 1997) to run an ordinary vapor compression refrigerator. Though the small size (50 litre) PV refrigerators are available, it is necessary to reduce the cost otherwise it is difficult to afford by the user in developing

countries if there is no financial assistance from the government or other sources. Another problem related to PV refrigerator is that it employs a conventional compression refrigerator using HCFCs as the refrigerants. The HCFCs still have some ozone depletion potential (ODP) and high global warming potential (GWP), which has resulted in the global phase-out schedule (Wang, 1993). As the alternative refrigerants are explored, new refrigeration forms are also actively exploited.

The second method uses solar thermal radiation to drive the sorption (absorption or adsorption) refrigeration systems. Sorption refrigeration devices are heat-operated cycles. They use much less, even no, electrical energy as compared with the vapour compression cycles. Furthermore, they can use environmentally benign working fluids such as ammonia, methanol or water as refrigerant thus reducing the use of HCFCs. Among them the absorption refrigeration systems such as water-lithium bromide absorption, ammonia-water absorption and ammonia-water-hydrogen cycles (ASHRAE, 1994) have been thoroughly studied and widely used; however, it is the adsorption and solid sorption cycles that have a distinct advantage in using waste heat in relatively low temperatures like that collected by flat-plate solar collectors. Unlike the steam driven absorption chiller and the direct-fired systems, there is no need to consume fossil fuels. Furthermore, the supply of sunshine and the need for refrigeration both reach maximum levels in the same seasons. Therefore, the solar adsorption and solid sorption refrigeration seem to be the promising refrigeration technique.

1.3 RESEARCH HYPOTHESIS

Although there have been many studies on solar refrigeration systems and some advanced systems have been developed, unfortunately, no solar refrigeration systems or chillers have widespread practical application. One of the shortcomings is that all the solar refrigeration systems currently studied work either at high positive pressure ranges, such as ammonia refrigeration systems, or at high vacuum ranges like water and methanol refrigeration systems. For example, the water system usually works in the 1.24-92.5 mmHg pressure range; and the methanol system normally works at 10-400 mmHg pressure range. In refrigeration systems working at the high positive pressure ranges, the refrigerant can escape to the environment, which not only results in the decrease of the refrigeration performance but may also endanger the health of local people, especially for highly toxic substances such as ammonia. For refrigeration systems working at the high vacuum ranges, the maintenance of the high vacuum degree in the whole system is critical for such systems' performance. This makes it difficult to deliver the refrigeration units to, and maintain them in, the above mentioned remote areas where such units are in much demand. That is one of the main reasons why to date such green refrigeration units/air conditioners have not yet been popularised commercially. So far there has been no study addressing this problem. To solve the leakage problem faced by the solar adsorption system current working in the vacuum pressure, a research hypothesis

has been put forward by the author that the working pressure of the system could be adjusted to atmospheric by using some proper adsorbent and introducing some pressure-adjusting gas in the system. This thesis conducts a comprehensive study on this hypothesis.

1.4 OBJECTIVES AND SCOPES

The general objectives and scopes of this research are to:

- justify the research hypothesis by experiment;
- understand the working mechanisms of such systems and evaluate the performance to reveal and evaluate the factors affecting the performance of the system;
- explore the possibility of implementing the idea to the vacuum adsorption refrigeration systems powered by solar radiation.

The research includes the following specific objectives. They are to:

- provide the guidelines and experience for the selection of the suitable adsorbent / refrigerant pair and the pressure-adjusting gas;
- develop the refrigeration experimental rig which can work at about atmospheric pressure;
- understand the heat transfer characteristics of the collector/generator in the heating and heating/desorption process;
- evaluate the coefficient of performance (COP) of the refrigeration system;
- reveal the adsorption characteristics for the collector/adsorption bed for the adsorption/ refrigeration process;
- evaluate the exergy (availability) analysis for the components/process and the cycle of the refrigeration system;
- evaluate the performance of the refrigeration cycle powered by solar radiation by simulation; and
- provide suggestions/guidelines for the design of such a prototype.

The project consists of the following scopes.

- The selection of the adsorbent, refrigerant and the pressure-adjusting gas, and the investigation of the relationship of pressure-temperature-concentration (P-T-x) for the adsorbent/refrigerant pairs by test.
- The development of the refrigeration experimental rig working at about atmospheric pressure, and conducting experimental tests.
- The heat transfer analysis for the collector/generator for the heating and heating/desorption process.
- The first law of thermodynamics (energy) analysis of the refrigeration system.

- The adsorption mass transfer analysis for the collector / adsorption bed for the adsorption / refrigeration process.

- The exergy (availability) analysis for the components/process and the cycle of the refrigeration system.

- The simulation of the performance of the refrigeration cycle powered by solar radiation.

- Suggestions and guidelines for the design of such a prototype.

1.5 RELATED LITERATURE REVIEW

1.5.1 Principle of Solar Adsorption Refrigeration

Almost all solid materials have the capacity to adsorb/absorb water vapor and gases by physical and/or chemical forces. The solid materials used on adsorb/absorb purpose are called the adsorbents. The moisture or gases adsorbed/absorbed can be driven out from the adsorbent by heating, and the cooled 'dry' adsorbents can adsorb/absorb moisture or gases again. The popular adsorbents are some solid salts, silica-gal, zeolite, and activated carbon.

It is convenient to describe the adsorption refrigeration cycles in a P-T-x (Pressure-Temperature-Concentration) diagram as shown in Figure 1.1. The ideal cycle consists of two isoster (constant-volume) processes (1-2 and 3-4) and two isobar (constant-pressure) processes (2-3 and 4-1).

The cycle starts from state 1 (in the morning) as the sun rises. The temperature of the collector/generator increases thus the pressure increases until state 2 is reached. After the temperature of the collector/generator reaches the desorption threshold temperature (state 2), the heating/generation process starts. In this process, the temperature of the collector rises, while the pressure remains at the condenser pressure. During the isobaric process, the adsorbate is driven off until the minimum concentration of the refrigerant (corresponding to the maximum temperature). During this process, the generated vapour is condensed in the condenser and is collected in the receiver/evaporator.

When the collector/adsorption bed is cooled by the ambient in the evening, the pressure in the collector/adsorption bed decreases until the evaporating pressure (state 4). Then the adsorbent starts to adsorb the vapour vaporised at the evaporator thus the refrigerating effect is produced. This process ends when the concentration of adsorbate in the adsorbent reaches the maximum (state 1). The cycle is then repeated.
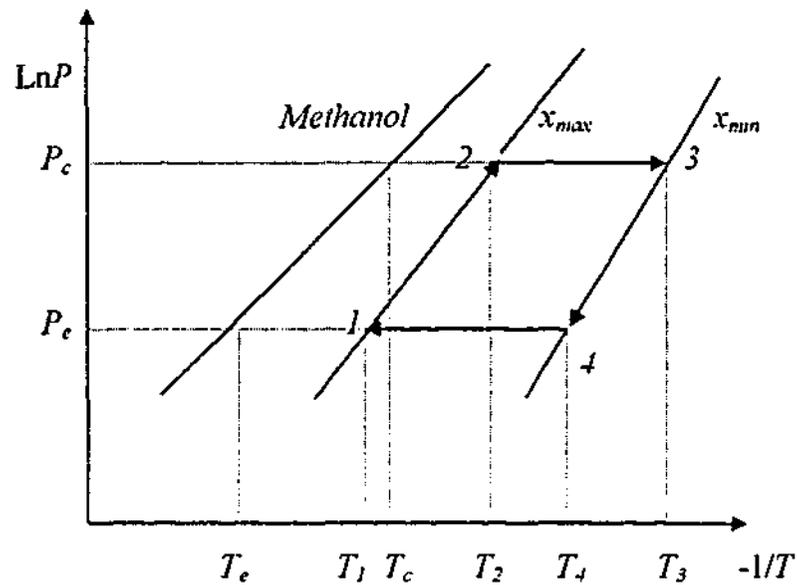
Figure 1.1 The P-T-x diagram of the ideal basic adsorption cycle

1.5.2 The Popular Adsorbent-Refrigerant Pairs

Solid Salts and the Refrigerants

Michael Faraday in 1824 first discovered the sorption refrigeration principle (Hahre, 1988) and he used AgCl-NH$_3$ as the working pair and got the cooling effect. But AgCl has several shortcomings and was abandoned.

Nielsen and Worsφe-Schimdt (1977) built an indoor test rig and investigated the heat and mass transfer in the adsorption and desorption processes for Calcium-Ammonia. After detailed investigations on NH$_3$—CaCl$_2$ and NH$_3$—SrCl$_2$, Nielsen (1981) concluded that solid CaCl$_2$ and SrCl$_2$ could be used for solar refrigeration. Worsφe-Schimdt (1979) designed a demonstration plant for a net amount of cooling of approximately 8000 kJ per day. The testing showed that the process COP was 0.34 and the total solar COP was 0.096. Iloeje (1985) tested a Calcium-Ammonia solar refrigerator over the annual climate variations at Nsukka, Nigeria. He also investigated the effect of charging pressure on COP with three different pressures and carried out the parameter analysis on the performance of the NH$_3$—CaCl$_2$ solar refrigeration. Based on his experimental work, he and his coworkers (1995) developed a simple mathematical model and computer program to the system and carried out the parametric study on the system with the view to optimising the design.

A better but more expensive working pair is SrCl$_2$-NH$_3$. Dornier, a Germany Company, manufactured a solar refrigerator which uses the compound material IMPEX (80%SrCl$_2$+20%Graphite) as the adsorbent and NH$_3$ as the adsorbate (Bansal et al., 1997). The heat

was supplied by an evacuated solar heat pipe. The IMPEX has a high coefficient for heat and mass transfer and a good adsorption property. The refrigeration capacity is 1.5 kWh per day. Bansal et al. (1997) carried out the theoretical and experimental analyses to this refrigerator using the meteorological data for Delhi. The maximum theoretical COP was 0.143, but the testing COP was only 0.081. They thought that the weaker solar radiation due to the pollution and dust was the reason for the low testing COP and suggested a redesign of the system according to the local meteorological condition. Erhard and Hahne (1997) also carried out the theoretical and experimental study on the $SrCl_2$-NH_3 system and made a simulate program.

Silica-Gal and the Refrigerants

In 1930s' G. E. Hulse invented silica-gal—sulfur oxidised adsorption refrigeration system. Plank and Kuprianoff (1960) investigated the possibility of using silica-gal—propanone in solar refrigeration systems. Eggers-Lura (1978) designed an adsorption refrigeration system. Sakoda and Suzukii (1984) investigated the silica-gal—water adsorption system for solar cooling. Sakoda and Suzuki (1986) built a small silica-gal—water cooling unit and proposed a simple model which can interpret the experimental results well. Their sensitivity study showed that the heat transfer area between the adsorbent packed bed and its container had a considerable effect on the COP and they suggested that the heat transfer area should be approximately 0.4 m^2/kg adsorbent to obtain the solar thermal COP of 0.4. Kluppel and Gurgel (1988) reported a solar cooled drinking fountain using silica gel – water pair with an average COP of 0.07. Cho and Kim (1992) developed a test set and a simulation code to study the effects of component heat transfer rate on the cooling capacity of a silica-gal—water adsorption cooling machine. Watable and Yanadori (1994) studied the cooling characteristic of silica gal—ethanol. Tanaka et al. (1983) carried out an experimental study on a compact silica-gal—water refrigeration system which was thought to have a better performance than the traditional ones. There also have been several cycles proposed to reduce heat inherent in batch-cycle operation and hence improve cycle efficiency. Saha et al. (1995) investigated analytically the performance of a three-stage silica-gal—water adsorption chiller to use the near-ambient temperature waste heat between 55 and 4.°° and experimentally, by Saha and Kashiwagi (1997). Boelman et al. (1997) studied the influence of thermal capacitance and heat exchanger UA-valued on the cooling capacity, power density, and COP of a silica gel-water chiller. Alam et al. (2000) investigated the effect of heat exchanger design on the system performance of silica gel adsorption refrigeration systems.

Zeolite (and Zeolite Molecular Sieves) and Refrigerants

The possibility of using the zeolite-water pair was studied as early as 1974 (Techernev, 1974). Techernev (1974, 1978, 1982, 1984) studied solar cooling with zeolite, and he built and tested a small cooling cabinet with the volume of 100 dm^3. Meunier and Mischler (1979) and Guilleminot et al. (1980) also reported the application of zeolite. Guilleminot and Meunier (1981) tested a small experimental unit. Monnier and Dupont (1982) carried out the numerical optimization and field testing for a zeolite-water close cycle solar refrigeration. Grenier et al. (1988) built a large experimental solar adsorption cold store with the area of the collectors $0.8m^2$ and the volume of the cooling space 12 m^3. In Guilleminot's and Grenier's cases, the net solar COP was about 0.1, the efficiency of the collectors was approximately 0.33 and the cycle COP was also 0.33. Hinotani and Kanatani (1983) made a small experimental apparatus to obtain fundamental data for the design of the Zeolite-Water solar refrigeration system. The performance of the system was simulated with an evacuated glass tube collector with heat pipe. The COP of the system was from 0.02 to 0.05. After aging test on several metals, it was suggested copper should be used for further industrial development. These results showed that the Zeolite-Water could be used either in the small or the large refrigeration systems.

Shelton et al. (1989) conducted a ramp wave analysis of a solid – vapour heat pump using zeolite—ammonia pair. The heat transfer fluid is circulated to reduce the heat required from the external source by heat recovery.

Hajji et al. (1991) carried out a dynamic analysis for a solar adsorption refrigerator using zeolite 13X-water and Chabazite-methanol as working pairs. Zhu et al. (1992) investigated experimentally the 13X zeolite – water chiller. Chang and Roux (1995) carried out a thermodynamic analysis for a solar zeolite refrigeration system.

The Zeopower Company produced a Zeolite-Water solar refrigerator a long time ago (Tchernev, 1979). It was reported that the system could produce 9.8 kg ice per day per m^2 of collector area for a total solar input of 20 MJ/m^2 under the typical climatic condition of Boston. Later, the Zeopower Company developed another solar Zeolite-Water solar refrigerator for the domestic and recreational markets (Tchernev, 1984) which could produce about 0.9 kWh for each square meter of collector with a solar input of 6 kWh and the efficiency is 15% according to the report.

In order to improve the efficiency of adsorption refrigeration, Tan and Wang (1998) researched the double effect cascade adsorption systems using silica-water/zeolite-water and zeolite-water/zeolite-water respectively.

Activated Carbon and Refrigerants

Pons and Guilleminot (1986) designed an activated carbon-methanol solar adsorption ice maker and built a prototype in Orsay. The solar collector was 6 m² in area and contained 130 kg of A.C., the condenser was air-cooled and the evaporator had a net production of 30-35 kg ice per sunny day. The net solar COP was 0.12. Pons and Grenier (1987) presented the experimental data from this prototype. The measured net solar COP was 0.12 when the incident solar energy Q_i was 22 MJ/m² and 0.1 when Q_i was 19 MJ/m². Based on the *P-T-x* data determined by Sridhar (1987), Exell (1987) designed and fabricated a charcoal-methanol ice maker. The solar collector was 0.97 m² and contained 18 kg charcoal. 2.5 kg ice at -1 to -3°C could be produced for a good day. Passos and Escobedo (1989) presented an analytical model for the solar adsorption cooling cycle using the activated carbon-methanol pair. Medini et al. (1991) set up a non-valve active carbon-methanol solar ice maker with the 0.8 m² collection surface with a view to build an industrial machine. This machine produced 4 kg of ice per day in summer. With a collection efficiency of 0.41, it is possible to obtain a gross solar COP of 0.15. However, because of insufficient insulation of the ice bank, the net COP obtained was half that value. Tan et al. (1992) studied an active carbon-methanol solar ice maker with the collector area 1.1 m² and the refrigerator volume 103 litres. The maximum net COP of the machine was 0.15 and the experimental value was about 0.11. Boubakri et al. (1992) reported their experimental study of three charcoal-methanol ice makers with the collecto-condese (assembly of solar collector and condenser in a unique component) operated in Agadir, Morocco. They obtained a nominal production of 4 kg of ice per square meter collector for 60% of the period of the experiment. The net solar COP was between 0.08 and 0.12. Huang et al. (1992) built a prototype of solar powered ice maker (no valve cycle and air natural cooling). The results showed that the this refrigerator could produce 4.5 kg ice per day in winter and 2-3 kg ice per day in summer. The net solar COP was 0.1-0.12 and 0.08 respectively. Critoph (1994) built and tested an active carbon-ammonia solar refrigerator for vaccine cooling. The collector was 1.4 m² and contains 17 kg of carbon. It is possible to produce up to 4 kg of ice per day in a diurnal cycle. Bentayeb et al. (1995) introduced a model which took account of the real operation for an activated carbon-methanol solar refrigerator. Their numerical simulation showed that the behaviour of the refrigerator is different from one climate to the other. Critoph (1996) presented the results of heat transfer tests on a carbon-ammonia experimental generator together with future plans for a one ton per day solar ice maker. Hu (1996) presented some further applications of the program developed and validated before in the investigation of the non-valve carbon-methanol solar refrigerator. Follin et al. (1996) studied the influence of microporous characteristics of activated carbon on the performance of an adsorption cycle for refrigeration. Chen et al. (1997) studied the activated carbon – ethanol refrigeration system and showed that ethanol could be a substitute for methanol. Wang et al. (1997) investigated the

feasibility of using active carbon fibre (ACF) as the adsorbent in adsorption refrigeration and found that ACF-methanol has good potential as an adsorption refrigeration pair. Li and Sumathy (1999) built a solar ice maker using activated carbon and methanol with an exposed area of 0.92 m² and about 4-5 kg ice could be produced with the COP of about 0.1-0.12. Wang et al. (1999) developed an activated carbon–methanol adsorption refrigerator using spiral plate heat exchangers as absorbers, and more than 2.6 kg ice per day per kg activated carbon with a COP of 0.13 can be obtained. Li et al. (2000) designed an adsorption bed for activated carbon – methanol refrigeration system.

Douss and Meunier (1989) proposed a cascading adsorption cycle in which an active carbon-methanol cycle is topped by a zeolite-water cycle. This arrangement makes it possible to obtain, for example, both steam and ice with reduced heat input from the external source.

Grenier and Pons (1983) pointed that the COP of activated carbon-methanol system was higher than those of zeolite sieves—water systems at about 120°C. Meunier et al. (1986) compared synthetic zeolite—water, synthetic zeolite—methanol, and charcoal-methanol combinations and found that the activated-charcoal-methanol gave a better COP generally, but that the zeolite—water system was better when the difference between the nighttime ambient temperature and the evaporating temperature was particularly high. After comparing AC35-methanol with zeolite 13X-water, Meunier suggested that the zeolite combination would be superior only when the temperature lift (adsorption—evaporating temperature) exceeded 45°C. But the comparison was based on the heat input. Taking account of the collector efficiency which decreases with increasing temperature, the charcoal-methanol combination might be superior at even higher temperature lifts.

Owing to the differences in the raw material used, the activated condition (activated temperature, etc.), process employed and the degree of activated (activated time, etc.), the properties of the activated carbon such as porosity, pore size, and surface area for adsorption vary from one application to another. The adsorption properties for individual particular activated charcoal and methanol combination are normally tested in laboratories.

Sridhar (1987), Eltom and Sayigh (1994), Passos et al. (1986), Grenier and Pons (1983), and Hu and Exell (1993) tested the adsorption capacities for different charcoals. Based on his COP calculation of ideal cycles, Hu (1993) pointed out that the charcoal 207E4 from UK was suitable for ice making for tropical areas (high peak collector temperature). Hu (1998) also studied the thermal decomposition of methanol in solar powered adsorption refrigeration systems.

2

Working Substance: The Selection and the Adsorption Equilibrium

Before considering the solar adsorption refrigeration system, the adsorbent/refrigerant working pair must be selected and its adsorption property evaluated. The adsorbent we are searching for should have selective adsorption property in addition to the other general adsorption properties required. In this chapter, the possible working pairs and the pressure-adjusting agent were selected from general considerations, and the adsorption properties for the working pairs were tested. The adsorption equilibrium was described by Dubinin and Astakhov (D-A) equation, and the test data (pressure P, temperature T, and concentration x) were expressed in the $\ln P$ — $-1/T$ chart. Some of the thermodynamics of adsorption (the heat of adsorption and the desorption and the adsorption threshold temperatures) for the following analyses were also conducted in this chapter. The heat of adsorption was determined by employing the Clausius-Clapeyron equation, while the desorption and the adsorption threshold temperatures were determined by three approaches. It is shown that the D-A Equation and Simplified Pressure Equation approach is simple and accurate.

2.1 THE PRELIMINARY SELECTION FOR ADSORBENT, REFRIGERANT AND PRESSURE-ADJUSTING AGENT FOR OUR PURPOSE

The selection of the working substance for our purposes, i.e., to make the system work at about atmospheric pressure, should be based on the two sets of properties required:

- The general adsorptive properties, i.e., in solar application temperature range, it needs to work well.
- The adsorbent should have selective adsorption property, i.e., it should not adsorb the pressure-adjusting agent.

The *adsorbent* used in industry usually has a micro-porous structure. An ideal adsorbent for refrigeration should meet the following requirements: The specific surface area should be large and there should be the micropores; The adsorption capacity should be large; The adsorption force should be small and the regeneration temperature should be low; The heat of adsorption should be small; There is no reaction with the adsorbate; The velocity of adsorption should be quick so it is easy to achieve the adsorption equilibrium; The specific heat should be small and conduction heat transfer high, so to quicken the adsorption/desorption processes; High hardness or resistance to

abrasion; The flow resistance for gases should be small; Being able to be regenerated and reused many times; Easy to available; Cheap; etc.

An ideal *refrigerant* for adsorption refrigeration should meet the following requirements. High enthalpy of evaporation at the required evaporator temperature; Low freezing temperature; Relatively high critical temperatures; Positive evaporating pressure; Relatively low condensing pressure; Good heat transfer characteristics; Low water solubility; Inertness and stability; Nonflammability; Nonexplosive when mixed with air; Nontoxicity; Nonirritability; Noncorrosive; Relative low cost; Be easy to detect in case of leaks.

It is almost impossible to find an adsorbent and a refrigerant to satisfy all the above-mentioned requirements. The most used adsorbent in refrigeration is silica gel, zeolite, and activated carbon and the most used refrigerants are ammonia, water, and methanol.

2.1.1 The Refrigerant — Methanol

We would like our new refrigerator to have the potential of making ice, so *methanol* is chosen as the refrigerant. The advantages of using methanol as the refrigerant are:

- It can evaporate at a temperature below $0°C$ (its Melting Point is $-93.9°C$);
- Its molecule is small (4 A) and it can be easily adsorbed in micropores with the diameter less than 20 A;
- Its normal boiling point ($65°C$) is higher than room temperature, which means the methanol refrigeration system always works at pressures lower than atmospheric. It is the leakage problem of this kind of systems that this research is aimed to solve.
- Its enthalpy of vaporisation is significant (about 1100 kJ/kg), so a good COP of its cycle may be expected.
- Non-irritability.
- Non-corrosive.

2.1.2 The Pressure-adjusting Agent — Some Inert Gases

It is known that the saturation temperature of vapour in a gas mixture depends only on the vapour's partial pressure and would not be affected by the presence of the other gases. Therefore, some gas may be filled in the system to raise the pressure of the system to atmospheric pressure. In order to achieve this goal some points should be met.

Firstly the gas should not react with the rest of the system (the machine material, the adsorbent, and the adsorbate). Thus some *inert gas* may be a good choice. Secondly, in order to act as the pressure-adjusting agency, the gas should not be condensed in the working temperature range nor adsorbed by the adsorbent. Inert gases such as Helium and Argon meet these requirements.

2.1.3 The Adsorbent — Molecular Sieves and Activated Carbon

The adsorbent for our proposes should have a selective adsorption property. That is to say, the adsorbent should adsorb the refrigerant only and should not adsorb the pressure-adjusting gas.

The molecular sieves have an excellent property for selective adsorption. Zeolite *Molecular Sieves (MSs)* are highly porous dehydrated crystalline zeolite. The pores are precisely uniform in diameter and of molecular dimensions. Therefore, they adsorb selectively only those molecules which are small enough to enter the pore system. That is why they are called molecular sieves. Besides, their adsorptive performance is strongly affected by the polarity, the polarizability, the bond character, and the molecular weight of the adsorbed substance. The 'Sieving" action, and the high affinity for a certain adsorbate give them their unique properties as molecular adsorbent. Therefore, zeolite molecular sieves are the first materials selected naturally as the adsorbent for our purpose.

Since the critical molecular diameter of methanol is 0.44 nm, the pore diameter of the adsorbent selected should be greater than that value, so the adsorbent can adsorb the vapour molecules of the refrigerant, the methanol. *5A MS* (pore diameter 0.5 nm) and *13X MS* (pore diameter 1.0 nm) meet this requirement.

It is also true that the diameters of the inert gases are smaller than the pore diameter of the chosen adsorbent (the critical molecular diameter of argon is 0.38 nm and helium is 0.2 nm), but their polarities and molecular weights determine that they can be displaced by methanol. Here Helium, a weaker affinity inert gas, is chosen as the pressure-adjusting agency. Argon will also be tried in the experiment to see the effect of the density (molecular weight) of the gas on the cycling.

Carbon has been known throughout history as an adsorbent, and it has been well documented that *Activated Carbon* (carbonaceous material like coal, lignite, wood, nut shell, petroleum and sometimes synthetic high polymers thermal decomposed and then activated with steam or carbon dioxide at elevated temperature 700-1000°C) and methanol pair has an excellent refrigeration performance. The advantages of using activated carbon as the adsorbent are:

- Activated Carbon has a significant capacity of adsorption.

- Activated Carbon + Methanol can work at as high as 150°C without decomposition. Hence Activated Carbon + Methanol seems to be a suitable pair for a solar refrigeration system working at the temperature range that the flat-plate collectors can reach.
- Activated Carbon can be made to suit particular applications by varying the activation time and temperature, etc.
- Activated Carbon can be manufactured easily by local industry.
- Activated Carbon is cheap.

All the above-mentioned advantages show that the Activated Carbon + Methanol seems to be a good pair for solar refrigeration with the flat-plate collectors.

Carbon Molecular Sieve (CMS) is an interesting form as of activated carbon since it not only retains the advantages of the activated carbon, e.g., high adsorption capacity and easy desorption, but also has a uniform and narrow micropore size distribution. Both of the characteristics seem to be important for our purpose. As for the zeolite molecular sieve, it is the difference of the affinities of the gas and the vapour to the adsorbent, rather than the 'sieving action' of the adsorbent, decides the priority of the adsorption. Fortunately, inert gases are hardly adsorbed by common adsorbents in the normal temperature range. Therefore, some inert gas can be used in the system as the carrier gas, and activated carbon, rather than carbon molecular sieve, as the adsorbent.

2.2 SOME THEORETICAL BACKGROUND

2.2.1 The Physical and Chemical Properties of Pure Methanol

The vapour pressure P (Pa) of methanol in a limited temperature range can be described by Antoine equation (Boublik et al, 1973; see also Cheng and Kung, 1994)

$$\log P = 10.20587 - 1582.271/(T - 33.424) \tag{2.1}$$
$$288.0 \text{ K} < T < 356.8 \text{ K, error} < 0.06\%$$

with an error less than 0.06%. For a wider range of temperature, Dauber and Danner (1984) suggested

$$\ln P = 109.93 - 7471.3/T - 13.988 \ln T + 0.015281\, T \tag{2.2}$$
$$175.6 \text{ K} < T < 512.6 \text{ K, error} < 1\%$$

For saturated density of methanol liquid ρ_s (kg/m^3), Dauber and Danner (1984) suggested

$$\ln \rho_s = 3.6541 + 1.62055\,[1 + (1 - T/512.63)^{0.17272}] \tag{2.3}$$
$$175.6 \text{ K} < T < 512.6 \text{ K, error} < 1\%$$

Based on the table given by Liley (1982), Exell et al. (1987) computed the properties of methanol as a function of temperature from the regression formulas:

Saturation vapour pressure in bar:

$$\ln P_s = 12.6973 - 4024.37/T - 87582.885/T^2 \tag{2.4}$$

$$250K < T < 337.5K \text{ with maximum error of } 2.9\%$$

$$337.5K < T < 420K \text{ with maximum error of } 0.1\%$$

Saturated density of methanol liquid ρ_s (kg/m^3) with maximum error of 0.25%:

$$\rho_s = 937.911 - 0.058267T - 0.001459T^2 \tag{2.5}$$

Since the equations regressed by Exell et al. (1987) are simple and also precise in the part of the temperature range in our application, they will be used mainly in this research.

2.2.2. Isotherm Adsorption Equation: D-A Equation

The widely used description of activated carbon adsorption is the D-A equation which was developed by Dubinin and Astakhov (1970) from the potential theory originally put forward by Polanyi, and Berenyi. This equation is also used for other adsorbents such as molecular sieves in adsorption refrigeration analysis. The basis of the potential theory of adsorption is that at the surface of the solid adsorbent the molecules of the gas are compressed by the forces of attraction acting from the surface to a certain distance into the surrounding space. Therefore, in micropores comparable to the size of adsorbate molecule, the adsorbate molecules are attracted by the wall surrounding the micropores and start to fill the micropore volumetrically. Dubinin (1960) studied the adsorption characteristic curve and derived the following equation (Dubinin - Radushkevich equation)

$$W = q/\rho = W_0 exp(-k\varepsilon^2/\beta^2) \tag{2.6}$$

where W is the volume filled by the adsorbate, q is the amount adsorbed and ρ is the density of the adsorbed phase, W_0 is the maximum volume of the adsorbate adsorbed by the adsorbent, m^3/kg adsorbent; k is a parameter which depends upon the number and size distribution of micros, i.e., that is a function of the structures of the adsorbent only and its value does not depend on the adsorbate. The difference in adsorption properties of different vapours from those of the standard vapor (normally benzene) is accounted by an affinity coefficient β which characterise the polarizability of the adsorbate and is a function of adsorbate only, ε is the adsorption potential which is defined as the difference in free energy between the adsorbed phase and the saturated liquid. For one mole of an ideal gas

$$\varepsilon = \Delta F = \int_P^{Ps} VdP = -RT\ln(P/P_s) \tag{2.7}$$

where ΔF is the free energy change, R is the gas constant, T is the absolute temperature of the adsorbent/adsorbate, P_s is the saturated vapour pressure of the adsorbate at temperature T, and P is the equilibrium gas-phase partial pressure of the adsorbate;

Substituting for ε into Eq. (2.6), the Dubinin-Radushkevich (D-R) equation is written as

$$W = W_0 exp(-D(T\ln(P_s/P))^2) \tag{2.8}$$

where $D=kR^2/\beta^2$ and W_0 and D are determined by experimental measurement.

Eq. (2.8) is valid for temperature sufficiently below the critical temperature T_c ($T<0.8T_c$). For methanol $T_c=239°C$.

Since it was found experimentally that for some substances there were deviations from the above expression, Dubinin and Astakhov (1970) introduced an improved and more general form of the D-R equation, which is called the D-A equation, to fit the experimental data better. The D-A equation contains a third variable n and the form is

$$W = W_0 exp\{-D[T\ln(P_s/P)]^n\} \tag{2.9a}$$

or

$$x = x_0 exp\{-D[T\ln(P_s/P)]^n\} \tag{2.9b}$$

where n is usually between 1 and 3, and equals 2 in the D-R equation, and x is the mass concentration.

Taking logarithms we obtain the linear form

$$\ln W = \ln W_0 - D[T\ln(P_s/P)]^n \tag{2.10}$$

The parameters W_0 and D can be determined experimentally by plotting $\ln W$ vs $[T\ln(P_s/P)]^n$ for a variety of values of n from measurements of W, T and P.

The introduction of the new parameter n helps to improve the fit but it does not necessarily have any direct physical meaning (Critoph, 1988). Pons and Grenier (1986) also pointed out that the D-A equation is not thermodynamically correct near saturation because the predicted heat of adsorption does not tend to the heat of vaporisation of the adsorbate. The D-A equation is known to deviate from experimental data for very small and very large values of W. They suggested a linear potential expression which does not have this defect but it is not necessary for the work in this study.

2.2.3. Isotherm Adsorption Equation: $\ln P$ — -$1/T$ Equation

The saturation pressure P_s of the refrigerant can be approximately expressed as a function of temperature as following (Smith, 1996)

$$\ln P_s = A - B/T \tag{2.11}$$

where A and B are constants.

For methanol, according to Eq.(2.4), A and B can be determined by following expressions:
(a) at a state with temperature T

$$A = 12.6973 + 87582.885/T^2 \tag{2.12a}$$

and

$$B = 4024.37 + 175165.77/T \tag{2.13a}$$

and (b) in a process the average A and B

$$A = 12.6973 + 87582.885/(T_l \, T_u) \tag{2.12b}$$

and

$$B = 4024.37 + 87582.885(1/T_l + 1/T_u) \tag{2.13b}$$

where T_l and T_u are the lower and the upper temperatures in the range the saturation methanol experiencing in the process.

Similarly, the pressure-temperature relationship of an adsorbate can also be simply expressed as

$$\ln P = b*(-1/T) + a \tag{2.14}$$

To determine a and b (the intercept and the slope for a constant mass concentration line on the $\ln P$ vs -$1/T$ diagram, respectively), rewrite D-A equation $\ln W = \ln W_0 - D(T\ln(P_s/P))^n$ as

$$\ln P = c*(-1/T) + \ln P_s \tag{2.15}$$

where $c = (\ln(W_0/W)/D)^{1/n} = (\ln(x_0/x)/D)^{1/n}$ and x is the mass of the adsorbate adsorbed.

Substitute Eq. (2.11) into Eq. (2.15), we have Eq. (2.14) ($\ln P = b*(-1/T) + a$), and

$$b = c + B = (\ln(W_0/W)/D)^{1/n} + B, \text{ and } a = A \tag{2.16}$$

With a series of a and b, a set of lines for a particular adsorbate/adsorbent pair can be drawn in the $\ln P$ — -$1/T$ † diagram. The parameters W_0, D, n, and thus b are determined by adsorption test. In order to make the diagram more readable, the pressure P rather than $\ln P$ is denoted in the y-axial and T in the x-axial along with $-1/T$ in practice. Fig. 1.1. shows such a diagram and an ideal adsorption refrigeration cycle in the diagram schematically.

2.2.4 Heat of Adsorption — Clausius-Claperyon Equation

Under the assumption that the specific volume of the gas is much greater than that of the liquid, the specific volume of the liquid is negligible, and if the pressure is low enough so the gas can be treated as the ideal gas, the equilibrium vapour-liquid phase transformation for a pure fluid can be expressed by *Clausius-Claperyon* equation (Smith, et al. 1996)

$$d\ln P_s / dT = h_{fg} / RT^2 \tag{2.17}$$

where h_{fg} is the latent enthalpy of the liquid to vapour phase transformation.

The Clausius-Claperyon equation is also applicable to gas adsorption equilibrium. The analogous equation for adsorption is (Smith, 1996)

$$(\partial \ln P / \partial T)_x = h_{ad} / RT^2 \tag{2.18}$$

where the subscript x signifies that the derivative is taken at constant concentration adsorbed and h_{ad} is the *isosteric (constant volume) heat of adsorption* and is a function of the concentration x, the mass of refrigerant adsorbed per unit mass of adsorbent.

Rewrite the Eq (2.17) and (2.18), we get

$$h_{fg} = \frac{d\ln P}{d(-1/T)} R \tag{2.19}$$

and

$$h_{ad} = \left(\frac{\partial \ln P}{\partial (-1/T)} \right)_x R \tag{2.20}$$

which mean that h_{fg} and h_{ad} can be obtained from the slopes of the equilibrium lines for the pure refrigerant and for a constant concentration x on the $\ln P$ vs $-1/T$ diagram.

---

† A thermally isolated system can be put into a state of negative temperature. If temperature were defined as the negative reciprocal of the conventional temperature, ie, New temperature $\theta = -1/$ Old temperature T, temperature would vary smoothly from minus infinity (what we now called absolute zero) through zero, and on to plus infinity (Atkins, 1994).

Comparing Eq. (2.20) with Eq. (2.14), it is easy to see

$$h_{ad} = b \times R \tag{2.21}$$

That is to say that the heat of adsorption h_{ad} is just the multiplication of the slope b of a constant concentration line on $\ln P$ vs $(-1/T)$ diagram and the gas constant R.

2.2.5 The Desorption and the Adsorption Threshold Temperatures

In Fig. 1.1, T_2 and T_4 are the threshold temperatures at which the desorption and adsorption starts respectively, P_c is the condenser pressure and P_e is the evaporator pressure, respectively.

It is difficult to measure the threshold temperatures experimentally. Nevertheless, it can be determined by three theoretical approaches.

By Clausius-Claperyon Equation

Integration of Eq. (2.17) from state e to c, and Eq. (2.18) from state 1 to 2

$$\ln \frac{P_c}{P_e} = \int_{T_e}^{T_c} \frac{h_{fg}}{RT^2} dT \tag{2.22}$$

and

$$\ln \frac{P_c}{P_e} = \int_{T_1}^{T_2} \frac{(h_{ad})_{x_{max}}}{RT^2} dT \tag{2.23}$$

Since the values of h_{ad} and h_{fg} only change a little in the integration temperature ranges, they may be supposed to be constants, or thought as the average values over the temperature range. Therefore

$$\ln P_c - \ln P_e = \left(\frac{1}{T_e} - \frac{1}{T_c} \right) h_{fg} / R \tag{2.24}$$

and

$$\ln P_c - \ln P_e = \left(\frac{1}{T_1} - \frac{1}{T_2} \right) (h_{ad})_{x_{max}} / R \tag{2.25}$$

Equating the two integrals gives

$$\frac{1}{T_2} = \frac{1}{T_1} - \frac{h_{fg}}{(h_{ad})_{x_{max}}} \left(\frac{1}{T_e} - \frac{1}{T_c} \right) \tag{2.26}$$

Similarly

$$\frac{1}{T_4} = \frac{1}{T_3} + \frac{h_{fg}}{\left(h_{ad}\right)_{x_{min}}} \left(\frac{1}{T_e} - \frac{1}{T_c}\right) \tag{2.27}$$

By D-A Equation and Pressure Equation

We have shown that the *D-A* equation can be rewritten as Eq. (2.15) and the saturation pressure P_s of the refrigerant can be evaluated by Eq (2.4). The general form for Eq (2.4) can be expressed as

$$\ln P_s = A_0 + A_1/T + A_2 T^2 \tag{2.28}$$

where A_0, A_1, and A_2 are constants.

Combining Eq. (2.15) and Eq. (2.28) yields

$$(A_0 - \ln P)T^2 - (c - A_1)T + A_2 = 0 \tag{2.29}$$

Thus

$$c = (A_0 + \frac{A_1}{T} + \frac{A_2}{T^2} - \ln P)T \tag{2.30}$$

and

$$T = \frac{(c - A_1) \pm \sqrt{(c - A_1)^2 - 4A_2(A_0 - \ln P)}}{2(A_0 - \ln P)} \tag{2.31}$$

and the larger value should be taken respectively for T.

The desorption threshold temperature T_2 is given by

$$T_2 = \frac{(c_{x_{max}} - A_1) \pm \sqrt{(c_{x_{max}} - A_1)^2 - 4A_2(A_0 - \ln P_c)}}{2(A_0 - \ln P_c)} \tag{2.32}$$

where $c_{x_{max}} = (A_0 + \frac{A_1}{T_1} + \frac{A_2}{T_1^2} - \ln P_e)T_1$.

The adsorption threshold temperature T_4:

$$T_4 = \frac{(c_{x_{min}} - A_1) \pm \sqrt{(c_{x_{min}} - A_1)^2 - 4A_2(A_0 - \ln P_e)}}{2(A_0 - \ln P_e)} \tag{2.33}$$

where $c_{x_{min}} = (A_0 + \frac{A_1}{T_3} + \frac{A_2}{T_3^2} - \ln P_c)T_3$.

The larger value should be taken respectively for T_2 and T_4.

For example, if T_1=293.15 K (20°C), T_3=383.15 K (110°C), T_e=268.15 K (-5°C), and T_c=308.15 K (35 °C), in case of methanol, $\ln P_e$=-3.5287, $\ln P_c$=-1.2848, A_0=12.6973, A_1=-4024.37T, A_2=-87582.885, it is calculated that T_2=337.39 K and T_4=332.32 K.

By D-A Equation and the Simplified Pressure Equation

Eq. (2.14) ($\ln P = b*(-1/T)+ a$) can be rewritten as

$$T = b/(a - \ln P) \tag{2.34}$$

That means

$$T_1 = b(x_{max})/(a_1 - \ln P_e) \tag{2.35}$$

and

$$T_2 = b(x_{max})/(a_1 - \ln P_c) \tag{2.36}$$

where P_e and P_c is the evaporator and the condenser pressure, respectively, and $a_1=A(T_1)$.

Therefore

$$T_2 = \frac{a_1 - \ln P_e}{a_1 - \ln P_c} T_1 \tag{2.37}$$

Similarly, we have

$$T_4 = \frac{a_3 - \ln P_c}{a_3 - \ln P_e} T_3 \tag{2.38}$$

where $a_3=A(T_3)$.

For example, if T_1=293.15 K (20°C), T_3=383.15 K (110°C), T_e=268.15 K (-5°C), and T_c=308.15 K (35°C), in case of methanol, $\ln P_e$=-3.5287, $\ln P_c$=-1.2848, a_1=13.7165, and a_3=13.2939, then T_2=337 K, and T_4=332.04 K, which is almost the same as that from the pressure equation (337.39K and 332.32K, respectively). Therefore, the simplified pressure equation is precise enough for our application.

Considering $a_1 \approx a_3$, from Eq. (2.37) and (2.38), it can be seen that

$$T_2 / T_1 \approx T_3 / T_4 \tag{2.39}$$

This is the relationship of the four temperatures widely used by other literatures. It is rather simple in form, but it should be pointed out that it is only an approximate expression (most of the literatures have not made it clear). Eq. (2.37) and (2.38) will be used in this thesis to determine T_2 and T_4.

2.3 TEST OF ADSORPTION PROPERTY (*P-T-x*)

2.3.1 The Test Rig for *P-T-x* Relationship Test

As mentioned above, the *P-T-x* (pressure, temperature, and concentration) diagram for the working pair (adsorbent/adsorbate) is a powerful and convenient tool for analysing a particular adsorption refrigeration cycle. The test rig used to investigate the *P-T-x* relationship for the adsorbent/adsorbate pairs at Monash University is shown in Fig. 2.1.
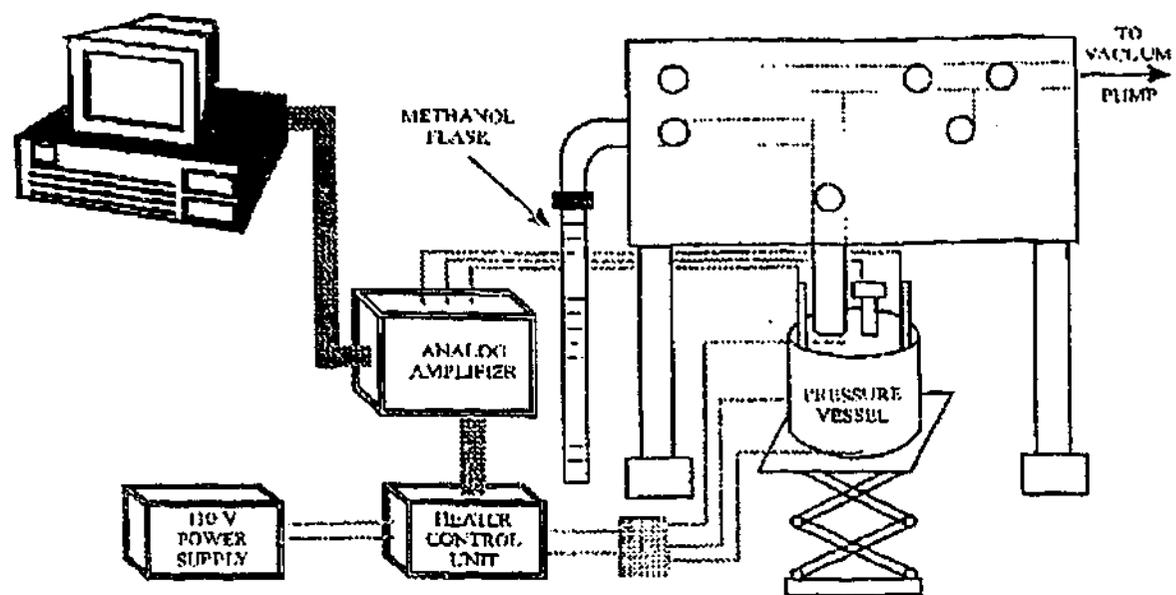

Figure 2.1 The test rig for the *P-T-x* relationship

2.3.2 Experimental Procedures

This test measures the changes in pressure *P* for given changes of *T* for fixed concentrations *x*. The procedures are

1) Put the desorbed adsorbent sample in the pressure-monitored vessel (the short cylindrical vessel).

2) Charge the adsorbate (methanol) into the graduated glass tube (the long methanol flask).

3) Heat and Vacuum the adsorbent sample to remove gases from the adsorbent.

4) Vacuum the adsorbate tube to remove gases from the adsorbate space.

5) Let the adsorbent adsorb a certain amount (volume) of adsorbate.

6) Heat the pressure-monitored vessel from the initial (ambient) temperature to 50°C (the maximum temperature of the pressure sensor) by step of 5°C. The time step is set by 15 minutes (this time

step is enough for the adsorption equilibrium to set up from one state to the next state). When the maximum temperature is reached, let the pressure vessel cool down to the ambient temperature.

7) Repeat step 6 three times to obtain average values for one concentration.

8) Repeat step 5 to 7 for other concentrations.

2.3.3 Experiment Data Process: 5A Molecular Sieve — Methanol

The first working pair was 5A molecular sieve and methanol. The test data are listed in table1.

Table 1 *P-T-x* Data of 5A Molecular Sieve — Methanol Adsorption

	W (l/kg)	0.048066	0.065344	0.07279	0.08126	0.086792	0.089443	0.091952
T (K)	Ps (kPa)	P (kPa)						
288.15	9.79046	0.025455	0.110299	0.209834	0.440721	0.687866	1.608008	4.038168
293.15	12.87508	0.037052	0.156582	0.294633	0.611043	0.946485	2.180762	5.391182
298.15	16.76695	0.053225	0.21956	0.408779	0.837466	1.287721	2.925751	7.123953
303.15	21.63405	0.07551	0.304288	0.560749	1.135297	1.733335	3.885254	9.32242
308.15	27.66992	0.105861	0.417058	0.760977	1.523148	2.309582	5.109547	12.08716
313.15	35.09601	0.146748	0.565624	1.022193	2.023446	3.047867	6.657925	15.53495
318.15	44.1639	0.201261	0.75946	1.359788	2.662987	3.985452	8.599782	19.80047
323.15	55.15765	0.273223	1.010041	1.79222	3.473542	5.166206	11.01574	25.03788

By varying the value of n, a linear relationship of $\ln W$ and $(T\ln(P_s/P))^n$ with the best correlation coefficient r was obtained. For the 5A molecular sieve and methanol, when $n=2.34$, $r=0.997$. The D-A Representation is shown bellow.


$$y = -0.0018x - 9.2809$$
$$R^2 = 0.9945$$

$(T\ln(Ps/P))$^2.34*E-5
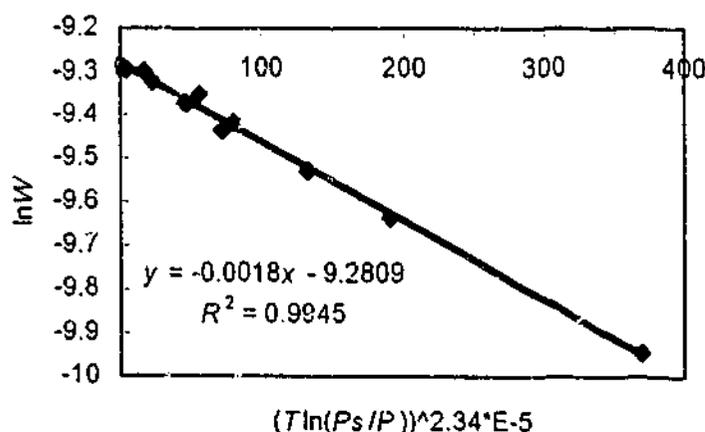
Figure 2.2 The D-A Representation for 5A molecular sieve and methanol

From the D-A Representation, it was found that and $W_0 = 9.3817 \times 10^{-5}$ m³/(kg adsorbent) and $D = 0.0018172 \times 10^{-5}$. Therefore

$$\ln P = [B + 2032.1116(-\ln W - 9.2809)^{1/2.34}](-1/T) + A \qquad (2.40a)$$

or

$$\ln P = [B + 2032.1116(-\ln x - 2.5748)^{1/2.34}](-1/T) + A \qquad (2.40b)$$

where $x = \rho W$ and $\rho = \rho_{s(sc)} = 817.378$ kg/m³ (Eq. 2.5).

The *P-T-x* (pressure, temperature, and concentration) relationship is shown in the $\ln P$—$-1/T$ chart as Figure 2.3.
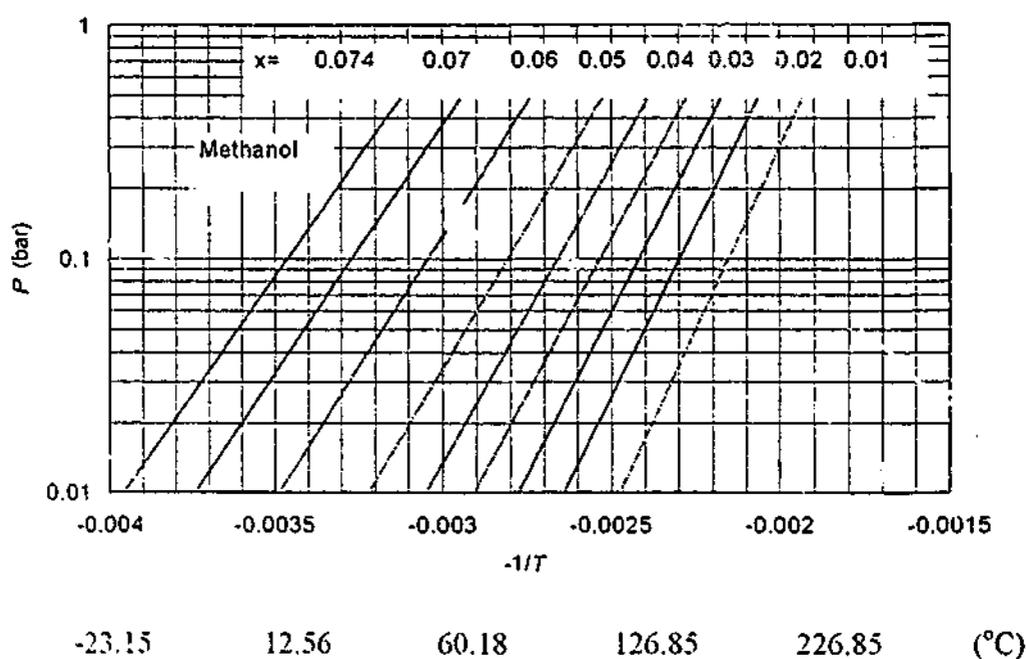
Figure 2.3 The P-T-x relationship chart for 5A MS and Methanol

From the $\ln P$—$-1/T$ diagram, it can be seen that in the temperature range the flat-plate solar adsorption refrigeration system working (eg, 20-110°C), the concentration change is not large. For example, taking the evaporator temperature $T_e = -5$°C, the condenser temperature $T_c = 35$°C, the morning temperature (the temperature of the collector in the beginning of the heating) $T_1 = 20$°C, and the peak temperature $T_3 = 110$°C, the maximum concentration is about 0.065, the minimum concentration is about 0.041, and the change of the concentration is only about 0.024. That means that 5A molecular sieve and methanol is not a good working pair for solar refrigeration. The activated carbon may be a better adsorbent for our purpose.

2.3.4 Experiment Data Process: Activated Carbon 207E4 — Methanol

Based on the results of the adsorptive tests of Hu and Excell (1993), charcoal 207E4 pellet was chosen as the adsorbent for the next test. The test data are listed in table 2.

Table 2 *P-T-x* Data of activated carbon 207E4 — Methanol Adsorption

T (K)	W (l/kg)	0.035786	0.071688	0.11757	0.137061	0.206101	0.275371	0.335187
	Ps (kPa)	P (kPa)						
288.15	9.79046	9.531104	9.593498	9.629752	9.661348	9.706761	9.744977	9.764135
293.15	12.87508	12.53975	12.62044	12.66732	12.70817	12.76688	12.81629	12.84105
298.15	16.76695	16.33749	16.44084	16.50088	16.55321	16.6284	16.69167	16.72338
303.15	21.63405	21.08894	21.22015	21.29636	21.36277	21.45821	21.5385	21.57875
308.15	27.66992	26.9839	27.14905	27.24498	27.32856	27.44866	27.5497	27.60034
313.15	35.09601	34.2396	34.44579	34.56556	34.6699	34.81983	34.94595	35.00916
318.15	44.1639	43.10295	43.35843	43.50681	43.63608	43.82181	43.97804	44.05634
323.15	55.15765	53.85285	54.1671	54.34959	54.50857	54.73698	54.9291	55.02538

Adjusting the value for *n* to maximise the linearity of the relationship of $\ln W$ vs. $[T\ln(P_s/P)]^n$. Since $n=1.34$, the correlation coefficient is 0.9967. The D-A Representation is shown in Fig. 2.4.
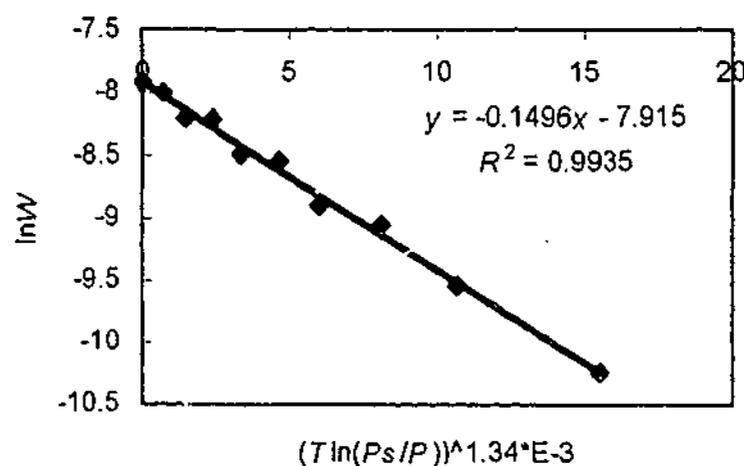

Figure 2.4 The D-A Representation for Activated Carbon 207E and Methanol

From the D-A Representation, it is found that $D=0.14962 \times 10^{-3}$ and $W_0 =0.365\times10^{-4}$ m³/(kg adsorbent). Therefore

$$\ln P = [B+715.2952(-\ln W-7.915)^{1/1.34}](-1/T)+A \qquad (2.41a)$$

or

$$\ln P = [B+715.2952(-\ln x-1.209)^{1/1.34}](-1/T)+A \qquad (2.41b)$$

where $\rho = \rho_{s(-sc)} = 817.378$ kg/m³ (Eq. 2.5).

The $\ln P$—$-1/T$ chart expression of the above relationship is shown in Fig. 2.5.
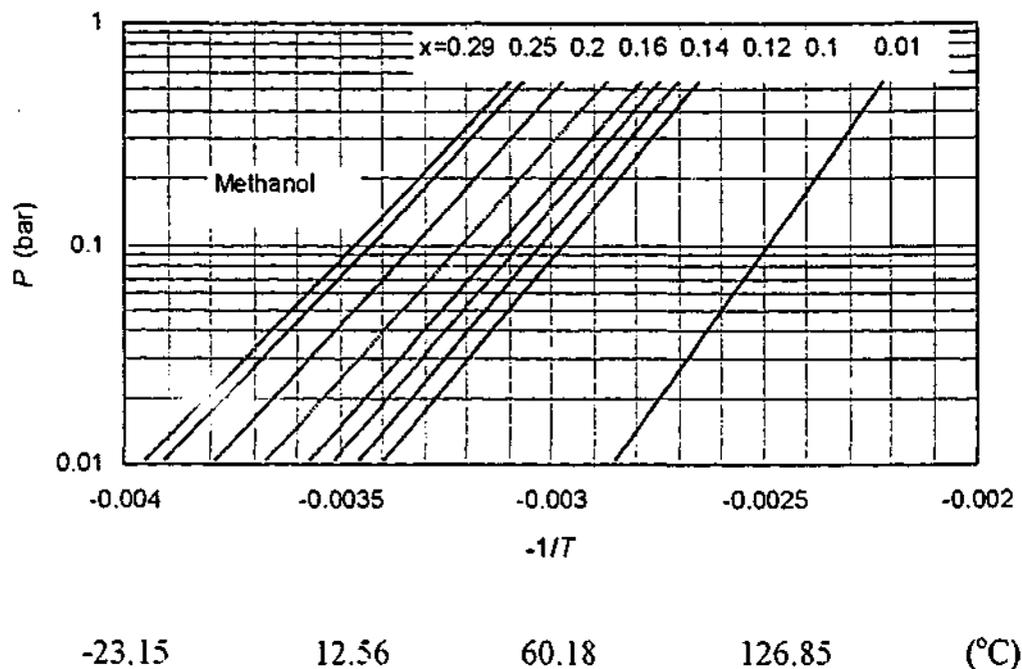
Figure 2.5 The *P-T-x* relationship chart for Activated Carbon 207E and Methanol

From the ln$P$— -$1/T$ diagram, it can be seen that in the temperature range the flat-plate solar adsorption refrigeration systems, the concentration change is large. For example, taking the evaporator temperature T_e=-5°C, the condenser temperature T_c=35°C, the morning temperature (the temperature of the collector in the beginning of the heating) T_1=20°C, and the peak temperature T_3=110°C. the maximum concentration is about 0.18, the minimum concentration is about 0.0636, and the change of the concentration is about 0.1164! That means that activated carbon 207E and methanol is an excellent working pair for solar refrigeration.

3

The Experimental Study of the Adsorption Refrigeration System Working at near Atmospheric Pressure

In the preceding chapter, the adsorbent/refrigeration pairs (Molecular Sieves/Methanol and Activated Carbon/Methanol) were selected and the adsorption property was tested. In this chapter, the refrigeration experiment is described. Firstly, no pressure-adjusting gas was used in the system. This experiment determined the working pair which is suitable for the refrigeration cycle. Then, the working pair is used in the refrigeration experiment with pressure-adjusting gas. The experimental rig working around atmospheric pressure was thus developed from first principles and experimental trials. The experimental results carried out in the experimental rig are presented in the following chapters with the theoretical results.

3.1 REFRIGERATION OBSERVATION (WITHOUT PRESSURE-ADJUSTING GAS)

The theoretical judgment from the investigation of the P-T-x diagrams in the last chapter indicated that 5A MS and methanol is a poor working pair, while Activated carbon 207E4 and methanol is an excellent working pair, for solar refrigeration. For refrigeration application, analysis from the P-T-x diagram is insufficient, and refrigeration cycle experiments should be carried out. Firstly, no pressure-adjusting gas was charged in the refrigeration system. If a working pair does not work in the refrigeration cycle even without the pressure-adjusting gas, it must be eliminated. The adsorbent/refrigerant pairs passing this test (i.e., without the pressure-adjusting gas) will be tested further in the refrigeration system charged with pressure-adjusting gas in the next steps. In this section, several MSs and methanol, and activated carbon and methanol are used in the refrigeration experiment, respectively.

3.1.1 The Refrigeration Observation Rig

The sketch of the refrigeration rig at this stage is shown in Fig. 3.1. The main components and equipment of the rig are as follows:

a. Container A. This spherical container is used to contain the adsorbent and it acts as the adsorption bed/generator. The temperature of the adsorbent is maintained by the Thermoline Thermal Convection Bath.
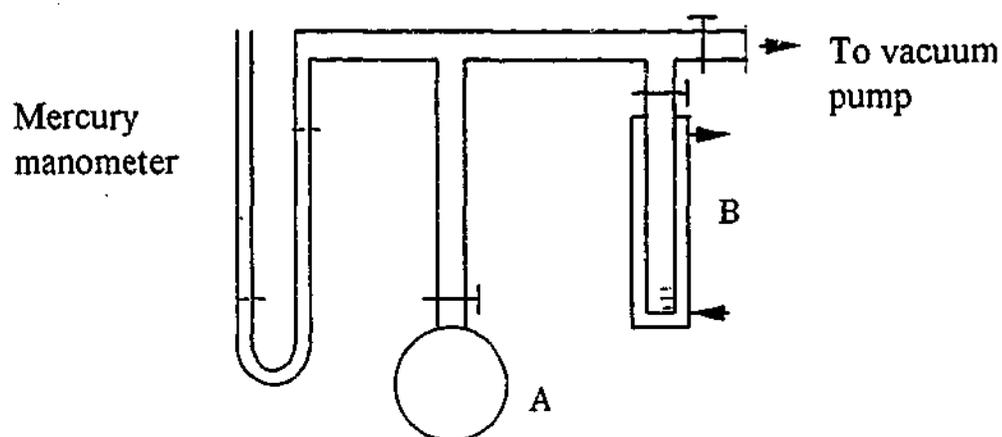
Fig. 3.1 The sketch of the refrigeration observation rig

b. Column B. This cylindrical container acts as the evaporator/condenser. It is composed of an inner tube and an outer tube. The refrigerant is in the inner tube which is calibrated in millilitres. The refrigerant can be maintained at a constant temperature by circuiting the constant temperature water through the "channel" between the two walls and through the Thermoline Precision Refrigerated/Circulator.

c. Thermoline Thermal Convection Bath (was not shown in Fig.3.1). This is used to control and maintain the temperature of the adsorbent evenly by submerging the container A in the oil. The bath can only be used for heating and the nominal temperature range is 0-100°C. The maximum temperature of the bath is 115°C, which is about the same value as the flat-plate solar collector can achieve. Oil ('Repco" Motor Oil SAE 20W-50), rather than water, is used for this application as the oil allows the temperature to rise more than 100°C without vaporisation and the good conductivity of oil makes the temperature distribute more evenly.

d. Thermoline Precision Refrigerated/Circulator (was not shown in Fig.3.1). This equipment is used to control the water at the desired temperatures and make the water circulate in the channel of container B thus to control the temperature of the refrigerant (methanol) at the desired temperatures.

The whole system was constructed from glass. There are two reasons for this. Firstly if the methanol container is transparent, the process of the adsorption could be 'seen'. Secondly glass is easier to process than metal and it is also easier to make the components/system airtight.

3.1.2 Molecular sieve 5A — methanol

The refrigeration experiment showed that *molecular sieve 5A* could adsorb methanol readily. However, it was found that there was hardly any condensation during the desorption process even

though the desorption temperature is set at as high as 110°C (the temperature the normal flat-plate solar collect can achieve). The reason may be that the bond between MS 5A and methanol is too strong so that it is nearly impossible to desorb methanol from MS 5A in the normal temperature range the flat-plate solar collect can achieve. So molecular sieve 5A was excluded.

3.1.3 Molecular sieve 13X — methanol

It has been reported that *molecular sieve 13X* and water can work well for air conditioning. The pore diameter of MS 13X is 1 nm, far larger than that of MS 5A (0.5 nm). Therefore, it should be easier to drive out the adsorbate from MS 13X than from MS 5A. MS 13X and methanol was also tried. Unfortunately, it was also found that there was hardly any condensation during the desorption process even though the desorption temperature is set at as high as 110°C too. So molecular sieve 13X was excluded.

3.1.4 Activated Carbon 207E4 —Methanol

The next candidate of the adsorption/refrigeration pair is activated carbon/methanol. Based on the reasons mentioned by Hu (1992), activated carbon 207E4 pellet is chosen as the adsorbent in our next refrigeration observation. The system using activated carbon and methanol works satisfactorily in the test rig (Fig. 3.1).

From the above work, it can be seen that even though an adsorbent can adsorb an adsorbate, there is no guarantee that the pair is suitable for solar refrigeration purposes. In order to save the trouble to measure the P-T-x relationship for a pair which may turn out to be unsuitable, the refrigeration observation experiment with no pressure-adjusting gas may be conducted first. If it works, then the P-T-x relationship of this pair will be tested, and the refrigeration effects with pressure-adjusting gas will be tried. By this way, the unworkable pair can be eliminated readily, and a suitable working pair can be selected. That is why we did not test molecular sieves 13X /methanol adsorption characteristics in the previous chapter.

In view of the investigation and observation results we have obtained, the following work would focus on the study of activated carbon-methanol as the adsorbent-refrigerant pair.

3.2 REFRIGERATION OBSERVATION (WITH PRESSURE-ADJUSTING GAS) — THE DEVELOPMENT OF THE WORKABLE REFRIGERATION TEST RIG

3.2.1 The Observation in the Old Test Rig

In the following experiment, activated carbon 207E4/methanol was selected to as the adsorption/refrigerant working pair. Firstly, the refrigeration observation experiment with pressure-adjusting gas was carried out in the same experiment rig as shown in Fig. 3.1. The first pressure-adjusting gas charged in the system was Argon. It was found that, with Argon, the desorption/condensing process worked, but the adsorption/evaporating process was too slow. Helium was tried as the pressure-adjusting gas then with the wish that the lighter gas may occupy the upper part of the rig and leave the space close to the adsorption bed for the refrigerant vapour, but there is almost no difference in the adsorption/evaporating rates between Argon and Helium. It was suspected that the inert gas blocked the adsorption of methanol vapour. This means that the experiment rig shown in Fig. 3.1 is not suitable for the refrigeration experiment with the pressure-adjusting gas; Therefore, the refrigeration experiment rig was modified several times and a new experiment rig is developed as described below.

3.2.2 The New Experiment Rig

Photograph 3.1 shows the workable vision of the refrigeration rig which is also schematically shown in Fig. 3.1.

Compared with Fig. 3.1, some modifications have been made. The modifications and the new instrument and components in the rig are

a) A stainless steel cylindrical column A takes the place of the spherical glass container A in the previous rig. The cylindrical shape is the common shape of a solar collector. To heat the adsorption bed/regenerator (column A) evenly, a heating mat is wrapped around it. Stainless steel, rather than glass, is used as the material of the shell to ensure that there is no danger of breaking. The stream (gas and/or vapour) enters from the bottom and leaves it from the top. This direction of flow is in accordance with the direction of the natural convection. A set of thermocouples is inserted into the pockets (was not shown in the figure) to measure the temperature distribution of the bed in different depths.

**Photograph 3.1** The refrigeration experimental rig
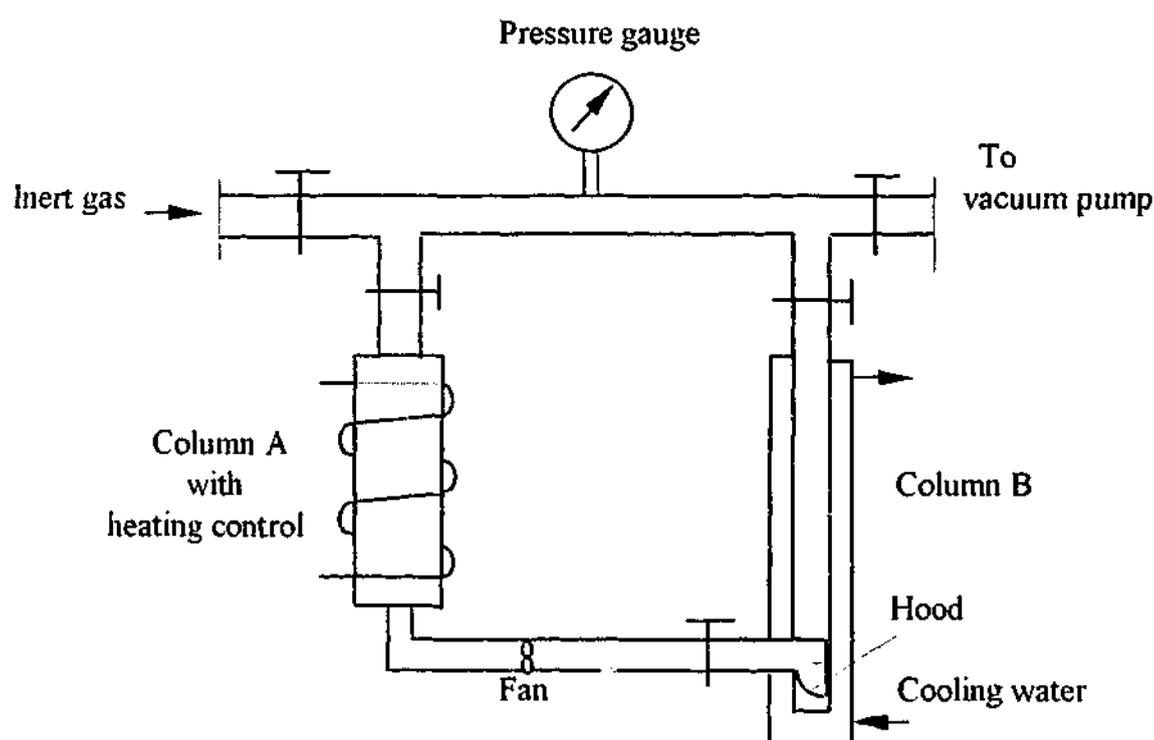
Figure 3.2 The schematic of the refrigeration experimental rig

b) The addition of a pipe connecting column A and column B at the bottoms of each component to provide/complete the path for the gases circulating within the system. To reduce the adsorption mass transfer resistance further, a small circulation fan is installed in the connection tube, and a round hood with an elliptical shaped opening is put in the evaporator (column B).

c) The Heating Mat and the Monitor. The heating mat is monitored and controlled by the EUROTHERM Model 94. This set is used to heat and maintain the temperature of the adsorption bed. It is only used for heating.

d) The Circulating Fan. The fan is used to make the gas and vapour circulate. The fan used here is MULTICOMP, 40mm, 12V and is supplied by Farnell Electronic Components Pty Ltd.

e) The Pressure Gauge. The pressure of the system is measured by an Active Strain Gauge, ASG-2000-NW16, D357-28-000, and is displayed by an Active Digital Display, ADD D395-56-000. The ASG and the ADD are connected by the adaptor cable D400-03-060.

f) Thermoline Precision Refrigerated/Circulator. The same as used in Fig 3.1.

Except the adsorption bed/regenerator (column A), the components and connecting tubes in the experiment rig were constructed in glass based on the same reasons as in section 3.1.

Before the test rig was assembled, all the fittings were cleaned very carefully several times with absolute ethanol (C_2H_5OH) to get rid of any dirt and grease. After drying, different greases/compounds were used in different connections to seal them. These greases/compounds are 'Apiezon L', 'Apiezon Q', and Dow Corning High Vacuum Grease. The 'Apiezon L' was thinly coated on the coupling surfaces of the fittings working in the low temperature districts. The 'Apiezon Q' was covered on the external surfaces of the fittings if necessary. Dow Corning High Vacuum Grease was thinly coated on the coupling surfaces of the fittings working in the high temperature areas. Though Dow Corning High Vacuum Grease can provide a steady seal and work better at high temperatures, it is harder to clean off when the glass is recycled. Therefore, it is only used for the fittings where it is necessary.

Before the experiment was conducted, the assembled system was examined several times to ensure airtightness. Each time, the system was vacuumed then closed and left for one week to see the pressure change of the system. After the leaking fittings were detected and the leaking problem was solved by proper cleaning and careful reassembling the fittings, the experiment was started.

3.3 THE EXPERIMENT PROCEDURES

3.3.1 The Refrigeration Observation Experiment Procedures and Results

Each time after the experiment rig being modified, the observation experiment is conducted. The purpose of this observation is to see whether the modified refrigeration rig works with an inert gas in the system. The procedures of this experiment in the new experiment rig are

a) Regenerate the adsorbent. Put the adsorbent in a furnace and heat it. Since the maximum temperature the furnace in our laboratory is 250°C, the regeneration lasted 2-3 days. As soon as the adsorbent was taken out from the furnace, isolate the regenerated adsorbent from air. Weigh

the regenerated adsorbent with scale then and charge them into the container A. The charged adsorption bed was then heated to about 115°C; meanwhile, it was vacuumed to regenerate the adsorbent furthermore.

b) Turn off the valve to the vacuum pump for two days to see whether the loaded system is still in a good vacuum condition. Owing to the reassembly of the loaded container, the airtightness of the tested system might be affected, therefore, so it is necessary to check it again.

c) If the system is not absolutely airtight, the most likely site for a leak is the container A's connection. Detach the connection, clean both of the male and female connections, and resemble the connection again. Then vacuum the system and repeat step b until the system is made airtight again.

d) After making the system airtight, isolate the adsorption bed by closing the valves and open the valve to the methanol container and vacuum the container. This vacuuming process lasted about 3 minutes or until the methanol level dropped a litter (usually 2.5 mm, here it was about 5 ml). The pressure of the system rises a bit due to the evaporation of methanol.

e) Close the valve to the vacuum pump, and open the valve to the adsorption bed to charge the system with methanol. The methanol was maintained above 0°C with hair drier to prevent the container from breaking owing to the cooling and to shorten the time for the charging process. The amount of methanol charged was calculated by means of the P-T-x relationship of the activated carbon-methanol (Corresponding to the evaporator temperature of 2°C and the morning temperature of 20°C. The amount of methanol charged for that condition is sufficient for the evaporator temperature equal to, and less than, 2°C, and the morning temperature equal to, and greater than, 20°C). After charging the system with the required amount of methanol, close the valve to isolate the methanol container from the system.

f) Close the valves to isolate the adsorption bed and other related components and let the adsorption bed cooled down to the ambient temperature. Then open the valve to the gas tank and to the vacuum pump. Vacuum the hose and the tube between the gas tank and the system for 30 minutes and then close the valve to the vacuum pump. Charge Helium to the system to about one atmospheric pressure.

g) Heat the bed to start the desorption/condensing process. The temperature of the bed (column A) was set at 100°C with the heating mat to simulate the solar collector at its peak temperature. The column B acted as condenser now (in the refrigeration process late, it would act as evaporator). The condenser temperature was set at 35°C (for typical ambient temperature) by circulating the cooling water cooled and circulated by the Thermoline Precision Refrigerated/Circulator around Column B. The fan was also turned on to help the condensation. This process was conducted until the level of the methanol condensed could not increase any

more (about three hours from our previous experiment). Then tuin off valves to isolate the bed and let the bed cool down to the ambient temperature.

h) Drain the water from the channel in container B (condenser/evaporator).

i) Open valves to the bed and turn on the fan to start the adsorption/refrigeration process.

j) Change the flow rate of the fan by adjusting the power input (the valves were fully open) and repeat the steps g to i. The flow rates of the fan corresponding to the different power inputs were measured in advance.

k) Compare the observation results to find a favourable flow rate.

l) Using Helium as the pressure-adjusting gas, in one set of the experiment, the system's pressure was between 1.013—1.29 bar in the whole cycle. In this case, the superficial velocity of the bed was 0.3 m/s, and ice and frost (cooling effect) could be observed at the surface of the column B (near the bottom, Photograph 3.2).

The ice and frost formed here
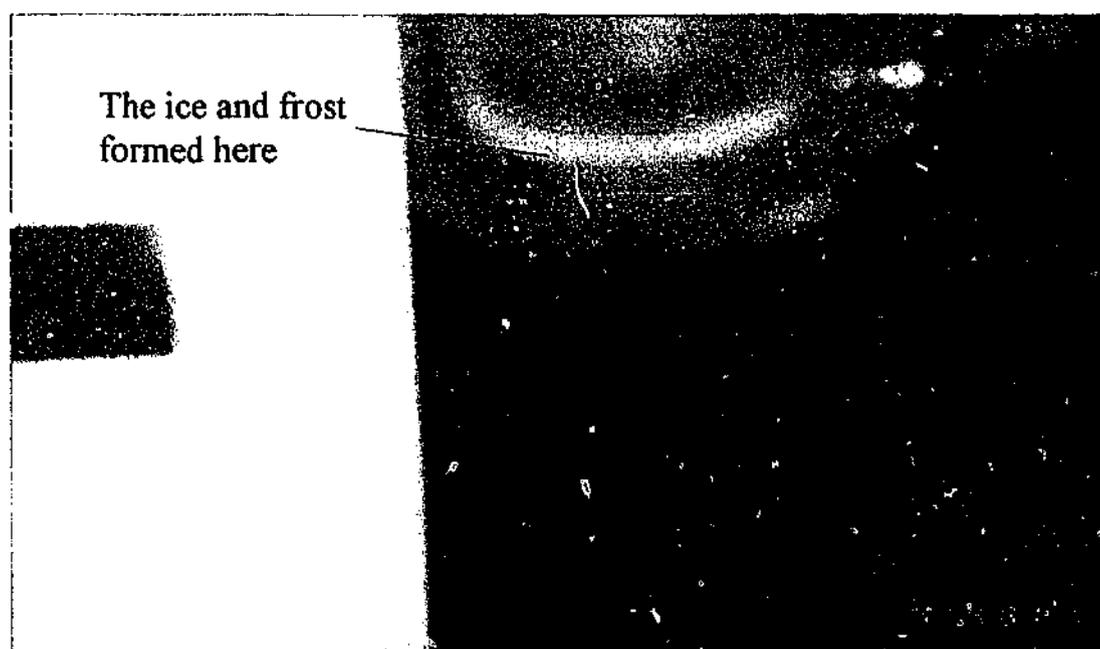
Photograph 3.2 The ice and frost formed at the surface of the column B

The experiment shown that adsorption refrigeration system using activated carbon-methanol as the working pair, and inert gas, the pressure-balancing agent does work. The introduction of the inert gas, no doubt, increases the mass transfer resistance for methanol diffusion. The investigation of the mass transfer mechanism in this case is the task of Chapter 6.

3.3.2 The Refrigeration Experiment Procedures (for Readings' Taking)

After the observation experiment, the refrigeration experiment was conducted using the following procedures.

a) Let all the refrigerant in the evaporator in the observation experiment to be evaporated and adsorbed by the bed.

b) Heat the bed with the heating mat at the heat flux about 821 W/m^2 (the typical solar irradiance).

c) When the temperature of the central line of the bed reaches the desorption threshold temperature (which was calculated by the method in chapter 2), turn on the fan to help the condensation of the refrigerant (the superficial velocity of the bed was 0.3 m/s). Heat the bed (column A) to the temperature of 75, 85, 95, and 105°C, in the different experiments, respectively, to simulate different peak temperatures in the flat-plate solar collector. Actually, this peak temperature range was founded to be favourable for the coefficient of performance of the system from theoretical analysis (chapter 5). The column B acted as condenser now. The condenser temperature was set at 30, 35, and 40°C, respectively (some typical values), by circulating the cooling water cooled and circulated by the Thermoline Precision Refrigerated/Circulator around Column B. This process was continued until the bed released the theoretical amount of the refrigerant (measured by the graduation on the condenser, column B).

d) Turn off valves to isolate the bed and let the bed being cooled down to the ambient temperature.

e) Open valves to the bed and turn on the fan to start the adsorption/refrigeration process.

f) Maintain the evaporator temperature by adjusting the temperature and the flow rate of the cooling water cooled and circulated by the Thermoline Precision Refrigerated/Circulator. Since the Thermoline Precision Refrigerated/Circulator was supposed to cool and circulate water, the evaporator temperature was maintained at 2°C here. (With antifreeze solutions, the evaporator temperature could be maintained below 0°C.)

Take the readings at certain time intervals in the heating processes. In the adsorption process, since the adsorption rate changes with time, to get a good record of the adsorption rate, the times corresponding to the methanol level interval, rather than the methanol levels, are recorded. The results are described in following chapters with the theoretical data.

4

Heat Transfer Analysis on the Collector/Desorption Bed in the Heating Processes

This chapter describes the heat transfer analysis on the collector/bed in the heating processes. The purpose of this analysis is to investigate the temperature distribution with position and time in the collector tube in the heating and the heating/desorption processes to provide information for other analyses (eg, performance analysis and mass transfer analysis). The physical and mathematical models are proposed and the effective (apparent) parameters for the desorption bed are determined. Then, the numerical solution is obtained, and it is compared with the experimental data. By this way, a semi-empirical equation is obtained. Part of the work of this chapter has already been published (Publication 14).

4.1 PHYSICAL AND MATHEMATICAL MODELS

Physical Model

Historically, there are two kinds of models in analysing the heat and mass transfer in carbon/methanol bed:

(1). Uniform temperature model.   The bed porous mass diffusion controlled the kinetics of the sorption (Ruthven and Lee, 1981). It was assumed that both the thermal conductivity of the individual adsorbent particle and the effective thermal conductivity of the particle bed were large enough to maintain a uniform temperature throughout the entire adsorbent sample. This assumption is valid when the adsorption bed is very compact and the adsorbent is in thin slabs;

(2). Uniform pressure model.   The bed heat conduction controls the kinetics of the sorption (Guileminot and Meunier, 1987). It was assumed that (a) pressure was uniform in the reactor, which is valid when thick beds of high porosity are used, and (b) the heterogeneous medium was regarded as an equivalent continuous medium. In this model, all mass transfer resistances were neglected. Based on the uniform pressure model, Passos (1989) developed a similar model by introducing a linear driving force equation to account for the resistance to mass transfer.

Both of the above-mentioned models have some applications but neither of them is very suitable to our case. Another model is needed.

The collector is composed with a set of parallel tubes charged with the cylindrical adsorbent (AC) pellets. The mixture of the adsorbate (methanol) vapour and the inert gas is forced through the bed by a fan to enhance the heat and mass transfer. Neglecting the side-effect of the collector casing, every tube is in identical condition. Thus, only one needs be analysed.

In the collector tubes, there are three heat transfer mechanisms: (a) conduction by the solid and the gases; (b) convection of the gases; and (c) the heat pipe effect associated with the mass transfer.

The so-called heat pipe effect is that during the heating desorption process a portion of the desorbed adsorbate (methanol) vapour, which is originally adsorbed in the adsorbent in the liquid form, migrates form the outer hotter zones (or layers) of the bed and re-adsorbed by the inner colder adsorbent zones (or layers).

The following assumptions were made.

(1). There is no temperature gradient along the axis of the tube, since the sun shine falling on the tube is the same along the axis.

(2). The adsorbent/adsorbate are in local thermodynamic equilibrium.

(3). The specific heat of the adsorbed species is the same as the bulk liquid adsorbate.

(4). There is no circumferential temperature gradient, since the heat conductivity of the metal pipe is much higher than that of the adsorbent bed.

Mathematical Model

The general three-dimensional heat-conduction equation in cylindrical coordinates is derived by Holman (1997) and Croft and Liliey (1977). It is

$$\frac{\partial T}{\partial t} = \alpha \left(\frac{\partial^2 T}{\partial r^2} + \frac{1}{r} \frac{\partial T}{\partial r} + \frac{1}{r^2} \frac{\partial^2 T}{\partial \phi^2} + \frac{\partial^2 T}{\partial z^2} \right) + \frac{\dot{Q}_v}{\rho c} \quad \tag{4.1}$$

where T is the temperature, t is the time, ρ is the density of the material, kg/m^3, c is the specific heat of material, J/kg°C, the quantity $\alpha = k/\rho c$ is called the thermal diffusivity of the material, m^2/s, while k is the thermal conductivity of the material, $\dot{Q}_v$ is the rate at which energy is generated per unit volume of the material, W/m^3, and r, ϕ and z are radial, circumferential and axial coordinates.

---

* In heat transfer books, τ is commonly used to represent time. In order to make the symbol consistent in this thesis t, rather than τ, is used to represent time here.

For the adsorption bed, k is the composite thermal conductivity and ρc is also a composite quantity. They are discussed below.

4.2 SOME COMPOSITE QUANTITIES OF THE COLLECTOR/DESORPTION BED

4.2.1 The Volumetric Heat Capacity ρc.

Since the quantity of ρc of gases is much lower than that of the adsorbent solid and the liquid adsorbed, it can be neglected. Therefore

$$\rho c = mc/V \approx (m_{ad}c_{ad} + m_f c_f)/V = (m_{ad}c_{ad} + xm_{ad}c_f)/V$$
$$= \rho_b(c_{ad}+xc_f) = (1 - \varepsilon)\rho_p(c_{ad}+xc_f) \tag{4.2a}$$

where ρ_b is bed density, the density based on the whole volume including the bed porosity (interpellet void), ρ_p is the particle density, and ε is the adsorption bed porosity (interpellet void fraction). For activated carbon, $\rho_p = 0.6\text{-}1.0$ g/cm^3 $((0.6\text{-}1.0)\times10^3$ kg/m$^3)$, and $\varepsilon = 0.35\text{-}0.6$. ρ_p is usually supplied by the manufacturer. If there is no data for ε, it can be determined by other quantities which are easy to measure. For example, for the activated carbon we used, with the known mass and volume, taking $\rho_p = 0.78$ g/cm^3, it was founded $\varepsilon = 0.42$.

Taking $\rho_p = 0.78\times10^3$ kg/m^3, and $\varepsilon = 0.42$, $c_{ad} = 1000$ J/kg/°C, and $c_f = 81.17$ J/mol/K $= 2536.56$ J/kg/K (Cheng and Kung, 1994), we have

$$\rho c = 452.4+1147.54x \qquad \text{kJ/ m}^3/°C) \tag{4.2b}$$

4.2.2 The Effective Thermal Conductivity of Packed Bed with Still Fluid, $k_{be,0}$

The effective thermal conductivity of packed bed can be expressed as

$$k_{be,0} = \frac{2k_g}{1-k_g/k_{pe}}\left(\frac{\ln(k_{pe}/k_g)}{1-k_g/k_{pe}} - 1\right) \tag{4.3}$$

(Mohamad et al, 1994, Rohsenow, 1998) where k_g is the thermal conductivity of the gas teeming in the interpellet voidage and k_{pe} is the effective (apparent) thermal conductivity for the porous particle.

The *effective (apparent) particle conductivity* k_{pe}. The effective particle conductivity of the adsorption particle which consists of the solid material with the conductivity k_s and the fluids teemed

in the intraparticle voidage with the effective (apparent) conductivity k_{fa}, according to Eucken (Jakob, 1958; Kaviany, 1995), can be expressed as

$$k_{pe} = k_s \left[1 - \frac{3(k_s - k_{fa})}{(k_s - k_{fa}) + (2k_s + k_{fa})/\varepsilon_p} \right] \tag{4.4}$$

where ε_p is the pellet porosity, and $\varepsilon_p = 0.5\text{-}0.6$ for activated carbon.

If the fluid in the pore is still, its effective (apparent) conductivity k_{fa} can be evaluated from consideration of the conductivity of the liquid adsorbed and the vapour teemed in the rest of the pore and the proper approximation of the shape of the pore. However, the fluid may migrate when it is heated, which increases the heat transfer rate significantly. As an approximation, the conductivity of the liquid can be taken as the effective conductivity.

Taking $k_{fa} = k_{f,\text{Methanol}} = 0.203$ W/m/K (Cheng and Kung, 1994), $k_s = 1.6$ W/m/K (Incropear and DeWitt , 1996), and $\varepsilon_p = 0.55$, $k_{pe} = 0.716$ W/m/K from Eq. (4.5).

The thermal conductivity of the gas teemed in the interpellet voidage k_g

In heating process 1-2, there is no methanol desorbed so the gas teemed in the interpellet voidage is only the pressure adjusting gas. According to the data given by Incropear and DeWitt (1996), the conductivity and viscosity of Helium, in the temperature range of the solar adsorption refrigeration system, is

$$k_{He} = (47 + 0.35T)/1000 \quad \text{W/m/}^\circ\text{C} \quad \text{and} \quad \mu_{He} = (67 + 0.44T) \times 10^{-7} \quad \text{Ns/m}^2 \tag{4.5}$$

For example, if we take the temperature range $T_1 - T_2$ as 293.15-337 K (Chapter 2), the average thermal conductivity $k_{g,1-2} = k_{He} = 0.1573$ W/m/$^\circ$C.

After the temperature reaches the desorption threshold temperature, methanol is desorbed. The heat conductivity of the gas mixture can be approximated by

$$k_{mix} = \sum \left(x_i k_i / \sum x_j \Phi_{ij} \right) \tag{4.6}$$

in which

$$\Phi_{ij} = \frac{1}{\sqrt{8}} \left(1 + \frac{M_i}{M_j} \right)^{-1/2} \left[1 + \left(\frac{\mu_i}{\mu_j} \right)^{1/2} \left(\frac{M_j}{M_i} \right)^{1/4} \right]^2 \tag{4.7}$$

where x_i, μ_i, and M_i are the mole fraction, the viscosity, and the mole weight of the ith species (Bird, et al, 1960). The mole fraction of the ith species can be determined as follows.

In this process, the partial pressure of the methanol vapour is the saturation pressure corresponding to the condenser temperature. If the condenser temperature is 35 °C, $P_{Meth,35C}$=0.2767 bar (Eq (2.4)). The partial pressure of Helium is determined as follows.

In the process of charging methanol, the evaporating temperature was maintained above 0°C (chapter 3). Taking it as 2°C, the partial pressure of methanol is the saturated pressure at this temperature (0.0457 bar). In the process of charging Helium, if the environment temperature is 20 °C and the total pressure of the system is one atmosphere, ie, 1.01325 bar, the partial pressure of helium is 0.96755 bar. At the condenser temperature of 35°C in the condensing process, the partial pressure of helium is $P_{He,35C} = P_{He,20C} \times (308.15) / (293.15) = 1.017056$ bar. The total pressure in the condensing process is 1.29376 bar.

Therefore, the mole fraction of the two species $x_{Meth} = P_{Meth}/P$=0.214, and $x_{He} = 0.786$.

For methanol, $k_{g,Meth}$=0.0157 W/m/°C (Cheng and Kung, 1994). For helium, in the temperature range 337-383.15 K (Chapter 2) the average thermal conductivity $k_{He} = 0.173$ W/m/°C from Eq. (4.5). So for the gas mixture $k_g = k_{mix} = 0.0886$ W/m/°C from Eq. (4.6).

Therefore, according to Eq. (4.3), the effective thermal conductivity of the place in the packed bed before and after the desorption threshold temperature is $k_{bc,0,1-2} \approx 0.38$ W/m/°C (in process 1-2) and $k_{bc,0,2-3} \approx 0.28$ W/m/°C (in process 2-3), respectively.

Alternatively, $k_{bc,0}/ k_g$ can be correlated by plotting it against k_s/ k_g for various void fractions by Schumann and Voss (McAdams, 1954) where k_s is the thermal conductivity of the solid particle. The results from the two approaches are coincident.

4.2.3 The Effective Thermal Conductivity of Packed Bed with Fluid Flow, $k_{bc,u}$

When a fluid flows at steady rate through the voids in the column, the equation for the effective (apparent) bed conductivity of the adsorption bed, which consists of the adsorbent porous pellet having the apparent conductivity k_{pe} and interpellet voidage teemed with gases of conductivity k_g, was given by Felix and Neill (McAdams, 1954). In SI system, it can be expressed as

$$\frac{k_{be}}{k_g} = \frac{0.3048}{D_t}\left(\frac{k_{pe}}{k_g}\right)^{0.12}\left(3.65 + 0.0106\frac{D_p u_s}{\varepsilon v}\right) \qquad (4.8)$$

for cylindrical packing flowed heated and cooled air upward through voids, where D_t is the inside diameter of tube, D_p is the diameter of particle, u_s is the superficial velocity based on the total cross section without particles respectively, v is the kinematic viscosity of fluid, and ε is the adsorption bed porosity.

The kinematic viscosity of fluid

After the temperature along the centre line of the bed reaches the desorption threshold temperature, there is methanol desorbed. The kinematic viscosity of the mixture is $v_{mix} = \mu_{mix} / \rho_{mix}$ where μ_{mix} and ρ_{mix} are the viscosity and the density of the mixture, respectively.

The viscosity of the gas mixture can be approximately by (Bird, et al, 1960)

$$\mu_{mix} = \sum \left(x_i \mu_i / \sum x_j \Phi_{ij} \right) \qquad (4.9)$$

The viscosity μ of methanol vapour at 25°C is 96.1×10^{-7} Ns/m^2 (Cheng and Kung, 1994), and the average value of μ of Helium in the temperature range 337-383.15 K (chapter 2) can be taken as $\mu_{2-3,He} = 225.433 \times 10^{-7}$ Ns/m^2 (Eq. 4.5). So the viscosity of the mixture $\mu_{mix} = 156.739 \times 10^{-7}$ Ns/m^2.

The density of the mixture which can be expressed as $\rho = \rho_{He} + \rho_{Me}$ and $\rho_i = P_i/(R_i T)$. Taking the values for P_{Me} and P_{He}, we have $\rho_{Me,35C} = 0.2767 \times 10^5 / (8134/32) / (308.15) = 0.3456$ kg/m^3, and $\rho_{He,35C} = 1.01706 \times 10^5 / (8134/4) / (308.15) = 0.1588$ kg/m^3. In the heating bed, taking the average temperature as the reference temperature, we have $\rho_i = \rho_{i,35C} \times 308.15/T_{2-3}$. If the average temperature is taken as 360.08 K, $\rho_{Me} = 0.29577$ kg/m^3, and $\rho_{He} = 0.1359$ kg/m^3, and $\rho = 0.43165$ kg/m^3.

Therefore, the kinematic viscosity of the mixture $v_{2-3} = v_{mix} = \mu_{mix} / \rho_{mix} = 363.105 \times 10^{-7}$ m^2/s.

Taking $D_t = 48.5 \times 10^{-3}$ m, $D_p = 4 \times 10^{-3}$ m, $\varepsilon = 0.42$, $k_{pe} = 0.716$ W/m/K, $k_{g,2-3} = 0.0886$ W/m/K, $v_{2-3} = 363.105 \times 10^{-7}$ m^2/s into Eq. (4.8), we have $k_{be,u=0.3} = 3.21$ W/m/K for $u_s = 0.3$ m/s.

4.3 SOLUTION APPROACHES — FINITE-DIFFERENCE FORMULATIONS FOR CYLINDRICAL REGION

Analytic Approach Vs. Numerical Approach

There are two approaches in solving the heat-conduction equations. One is analytic and the other one is numerical (Gebhart, 1993). The analytic technique (Carslaw and Jaeger, 1959) is based on

generating solutions in mathematical form. The relevant differential equations, subject to idealised boundary and initial conditions, often results in a definite solution; However, an important limitation of the analytical technique is that solutions commonly result only for very simple or idealised geometric regions and initial and boundary conditions. On the other hand, numerical methods provide a very suitable and convenient alternative. In this thesis, numerical methods are adopted.

The Finite-Difference Representation Vs. the Finite-Element Representation

There are two commonly-used numerical methods for heat transfer analysis: one is the finite-difference representation, the other is the finite-element representation. The finite-difference method (Croft and Lilley, 1977) converts the partial differential equations, the PDE, and the bounding conditions, BC, into the finite-difference equations solved at individual grid points. The finite-element method also represents the region of calculation by finite subdivisions. However, there is much flexibility in the choice of the grid in finite-element analysis. Therefore, irregular regions and complicated boundary conditions may be analysed almost as simply as very regular ones. The finite element itself comprises a group of closed associated nodal points, and interrelates all of the constituent nodal points. In our case, the geometry is simple enough to use the finite-difference representation.

Finite-Difference Formulations for Cylindrical Region

For an *internal node* at constant and uniform conductivity premise, the finite-difference equation in implicit form at time level p corresponding to Eq. (4.1) is

$$\frac{1}{(\Delta r)^2}\left[\left(1-\frac{1}{2i}\right)T_{i-1,j,k}^{p+1}+\left(1+\frac{1}{2i}\right)T_{i+1,j,k}^{p+1}-2T_{i,j,k}^{p+1}\right]+\frac{T_{i,j,k-1}^{p+1}+T_{i,j,k+1}^{p+1}-2T_{i,j,k}^{p+1}}{(\Delta z^2)}$$
$$+\frac{1}{i^2(\Delta r\Delta\phi)^2}\left(T_{i,j+1,k}^{p+1}+T_{i,j-1,k}^{p+1}-2T_{i,j,k}^{p+1}\right)+\frac{\dot{Q}_v^{p+1}{}_{i,j,k}}{k}=\frac{\left(T_{i,j,k}^{p+1}-T_{i,j,k}^{p}\right)}{\alpha\Delta t} \tag{4.10}$$
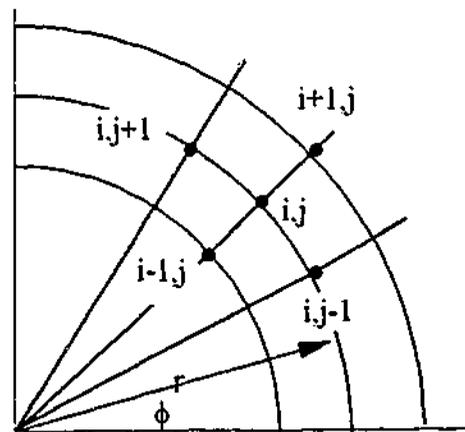

Figure 4.1 The representation of two-dimensional temperature fields in cylindrical region.

*At node* 0 (the centre line of the cylindrical bed),
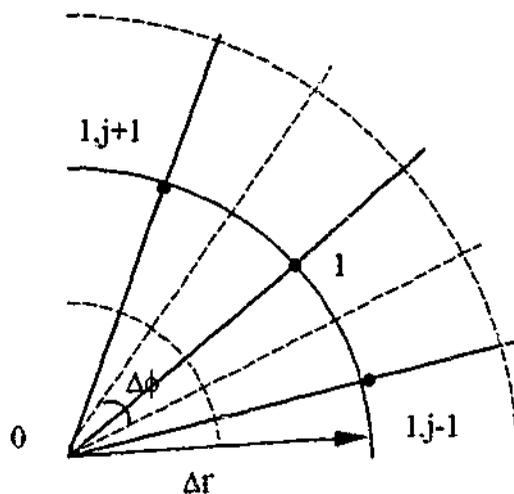
Figure 4.2 The representation of two-dimensional temperature fields in cylindrical region

and the finite-difference equation is

$$\frac{4}{\left(\Delta r\right)^2}\left(T_{1,j,k}^{p+1} - T_{0,0,k}^{p+1}\right) + \frac{T_{0,0,k-1}^{p+1} + T_{0,0,k+1}^{p+1} - 2T_{0,0,k}^{p+1}}{\left(\Delta z^2\right)} + \frac{\dot{Q}_{v,0}^{p+1}}{k} = \frac{T_{0,0,k}^{p+1} - T_{0,0,k}^{p}}{\alpha \Delta t} \qquad (4.11)$$

The surface (the boundary) and the region immediately inside it of the cylindrical geometry are shown in Fig. (4.3)
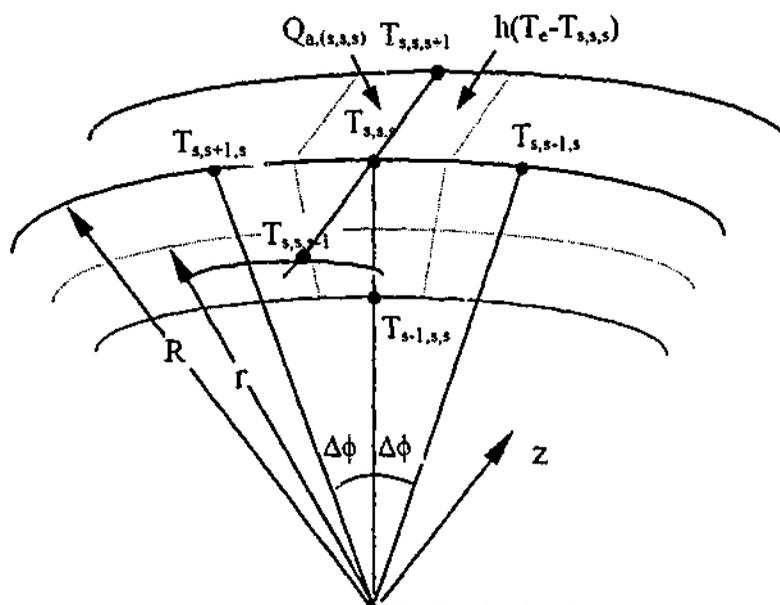
Figure 4.3 Numerical formulation at curved bounding surfaces of a cylindrical region

There are five conductive paths affecting the surface region of $T_{s,s,s}$. They are from $T_{s-1,s,s}$, $T_{s,s-1,s}$, $T_{s,s+1,s}$, $T_{s,s,s-1}$, and $T_{s,s,s+1}$. In addition, surface flux $\dot{Q}_{a,(s,s,s)}$ and convection loading at the surface are included, as $\dot{Q}_{a,(s,s,s)}R\Delta\phi\Delta z$ and $h(T_e-T_{s,s,s})R\Delta\phi\Delta z$. The distributed source flux $\dot{Q}_{v,(s,s,s)}$ arises in the volume element $R\Delta\phi\Delta z\Delta r/2$. The backward-difference energy balance for the surface point (s,s,s) is

$$\frac{kR\Delta\phi\Delta z}{\Delta r}\left(T_{s-1,s,s}^{p+1}-T_{s,s,s}^{p+1}\right)+\frac{k\Delta r\Delta z}{2R\Delta\phi}\left(T_{s,s-1,s}^{p+1}+T_{s,s+1,s}^{p+1}-T_{s,s,s}^{p+1}\right)$$

$$+\frac{kR\Delta\phi\Delta r}{2\Delta z}\left(T_{s,s,s-1}^{p+1}+T_{s,s,s+1}^{p+1}-T_{s,s,s}^{p+1}\right)+\dot{Q}_{a,(s,s,s)}^{p+1}R\Delta\phi\Delta z+hR\Delta\phi\Delta z\left(T_e^{p+1}-T_{s,s,s}^{p+1}\right) \quad (4.12)$$

$$+\frac{\dot{Q}_{v,(s,s,s)}^{p+1}R\Delta\phi\Delta z\Delta r}{2}=\frac{\rho c R\Delta\phi\Delta z\Delta r}{2\Delta t}\left(T_{s,s,s}^{p+1}-T_{s,s,s}^{p}\right)$$

4.4 HEAT TRANSFER ANALYSIS ON THE COLLECTOR/DESORPTION BED IN HEATING AND HEATING/DESORPTION PROCESSES

As mentioned above, the heating process can be divided into two steps. In the first step (from state 1 to 2), there is no adsorbate desorbed theoretically, so the heat effect is zero and the density of the pellet is approximately constant. In the second step (from state 2 to 3), the adsorbate is desorbed, so the heat effect, the changes of the density and the apparent thermal conductivity of the pellet, and the effect of convention must be taken into account.

4.4.1 The Governing Equations and Conditions

From state 1 to 2, the heat conduction equation can be simplified as

$$\frac{\partial T}{\partial t}=\alpha\left(\frac{\partial^2 T}{\partial r^2}+\frac{1}{r}\frac{\partial T}{\partial r}\right)=\frac{\alpha}{r}\frac{\partial}{\partial r}\left(r\frac{\partial T}{\partial r}\right) \quad (4.13)$$

The initial condition is

$$T(r,0)=T_{re} \quad (4.14)$$

and the boundary condition is

$$r=0, \ \frac{\partial T}{\partial r}=0 \quad (4.15a)$$

$$r=R_b, \ \dot{Q}_{a,s}=\dot{Q}_{a,0}-m_{c/g}c_{c/g}\frac{dT_{c/g}}{dt} \quad (4.15b)$$

where $m_{c/g}$, $c_{c/g}$, and $T_{c/g}$ is the mass, the specific heat and the temperature of the collector/generator.

From state 2 to 3, the heat conduction equation is

$$\frac{\partial T}{\partial t}=\alpha\left(\frac{\partial^2 T}{\partial r^2}+\frac{1}{r}\frac{\partial T}{\partial r}\right)+\frac{\dot{Q}_v}{\rho c}=\frac{\alpha}{r}\frac{\partial}{\partial r}\left(r\frac{\partial T}{\partial r}\right)+\frac{\dot{Q}_v}{\rho c} \quad (4.16)$$

and the boundary conditions are in the same form as in step 1.

The so-called heat sink

$$\dot{Q}_v = \frac{h_{de}d(m_{ad,v}x)/d\tau}{\Delta V} = (1-\varepsilon)\rho_p h_{de}\frac{dx}{dt}$$

$$= -(1-\varepsilon)\rho_p nRDx_0(A-\ln P_c)^2 T[(A-\ln P_c)T-B]^{n-1}\exp\{-D[(A-\ln P_c)T-B]^n\}\frac{dT}{dt} \tag{4.17}$$

It is difficult to get the analytic solutions for all of these equations.

4.4.2 The Numerical Solutions

Using finite-difference methods, we can get the numerical solutions for the energy equations for the two heating steps. There are two finite-difference schemes: the explicit scheme and the implicit scheme. Although the former offers computational convenience, it suffers from limitations on the selection of the increment of time and results in a very large numbers of time intervals. To reduce the amount of computation time, the latter is employed in the analysis carried out here.

To simplify the expressions of the finite-difference equations, introducing the finite-difference form of the Fourier number which is defined as

$$Fo = \alpha\Delta t /(\Delta r)^2 \tag{4.18}$$

In step 1, the finite-difference equations in implicit form are

$$(1+4Fo)T_0^{p+1} - 4FoT_1^{p+1} = T_0^p \tag{4.19}$$

$$-\left(1-\frac{1}{2i}\right)FoT_{i-1}^{p+1} + (1+2Fo)T_i^{p+1} - \left(1+\frac{1}{2i}\right)FoT_{i+1}^{p+1} = T_i^p \tag{4.20}$$

$$-2FoT_{s-1}^{p+1} + (1+2Fo)T_s^{p+1} = T_s^p + \frac{2\Delta t}{\rho c\Delta r}\dot{Q}_{a,s}^{p+1} \tag{4.21}$$

where

$$\dot{Q}_{a,s}^{p+1} = \dot{Q}_{a,0} - \frac{m_{c/g}c_{c/g}}{A}\frac{T_{c/g}^{p+1} - T_{c/g}^p}{\Delta t} = \frac{T_{c/g}^{p-1} - T_s^{p-1}}{R_c} \tag{4.22}$$

where A is the area of the contact, $A=2\pi R_b l$, and R_c is the contact thermal resistance per area. So Eq. (4.21) can be expressed as

$$-2FoT_{s-1}^{p+1} + \left[1+2Fo+2Fo\frac{\Delta r}{kR_c}\right]T_s^{p+1} - 2Fo\frac{\Delta r}{kR_c}T_{c/g}^{p+1} = T_s^p \tag{4.23}$$

From Eq (4.22), we also have

$$-\frac{A\Delta t}{A\Delta t + m_{c/g}c_{c/g}R_c}T_s^{p+1} + T_{c/g}^{p+1} = +\frac{m_{c/g}c_{c/g}R_c}{A\Delta t + m_{c/g}c_{c/g}R_c}T_{c/g}^p + \frac{A\Delta t R_c}{A\Delta t + m_{c/g}c_{c/g}R_c}\dot{Q}_{a,0} \quad (4.24)$$

Eqs. (4.19), (4.20), (4.23), and (4.24) can be used to solve temperature distribution in this heating step.

When the temperature of a place in the bed reaches the desorption threshold temperature, step 2 starts at this place. Since there is refrigerant desorbed, the properties at the point will change with the time, and when the fan runs, a further change of the properties at the point will take place. Therefore, the changing properties should be used in the evaluation for this step. To simplify the calculation, the thermal conductivity k in the following finite-difference equations and Fourier number Fo is taken as two constant values according to the temperature of the centre line of the heating bed (one is for the points where the temperature is equal to or greater than, but the temperature of the centre line is less than, the desorption threshold temperature, and the other is after the temperature of the centre line reaching the desorption threshold temperature). The finite-difference equations in this step are

$$(1+4Fo)T_0^{p+1} - 4FoT_1^{p+1} = T_0^p + \frac{(\Delta r)^2}{k}Fo\dot{Q}_{v,0}^p \quad (4.25)$$

$$-\left(1-\frac{1}{2i}\right)FoT_{i-1}^{p+1} + (1+2Fo)T_i^{p+1} - \left(1+\frac{1}{2i}\right)FoT_{i+1}^{p-1} = T_i^p + \frac{(\Delta r)^2}{k}Fo\dot{Q}_{v,i}^p \quad (4.26)$$

$$-2FoT_{s-1}^{p+1} + \left[1+2Fo+2Fo\frac{\Delta r}{kR_c}\right]T_s^{p+1} - 2Fo\frac{\Delta r}{kR_c}T_{c/g}^{p+1} = T_s^p + \frac{(\Delta r)^2}{k}Fo\dot{Q}_{v,s} \quad (4.27)$$

and

$$-\frac{A\Delta t}{A\Delta t + m_{c/g}c_{c/g}R_c}T_s^{p+1} + T_{c/g}^{p+1} = \frac{m_{c/g}c_{c/g}R_c}{A\Delta t + m_{c/g}c_{c/g}R_c}T_{c/g}^p + \frac{A\Delta t R_c}{A\Delta t + m_{c/g}c_{c/g}R_c}\dot{Q}_{a,0} \quad (4.28)$$

where

$$\dot{Q}_{v,i}^p = -(1-\varepsilon)\rho_p nRDx_0(A-\ln P_c)^2 T_i^p[(A-\ln P_c)T_i^p - B]^{n-1}$$
$$\exp\{-D[(A-\ln P_c)T_i^p - B]^n\}\frac{T_i^p - T_i^{p-1}}{\Delta t} \qquad (i=0, 1,\ldots\ldots, s\text{-}1, s) \quad (4.29)$$

To save the energy used in the heating process 1-2 so as to improve the Coefficient of the Performance (COP) of the system, the fan is switched on only when the temperature of the centre line of the bed reaches the desorption threshold temperature T_2. T_2 can be determined theoretically (chapter 2).

For example, in our case the adsorption bed, l=0.53 m and R_b=2.425×10^{-2} m. If T_e= 2°C, T_c =35°C, T_1 = 20°C, T_3 =110°C, and the activated carbon/methanol we tested is used as the working

pair. the values for the numerical analysis can be obtained. Substituting $k_{be,0.1-2} \approx 0.38$ W/m/°C (fan off in step 1-2). $k_{be,0.2-3} \approx 0.28$ W/m/°C for the points, if there is any, where the temperature is equal to or greater than, but the temperature of the centre line is less than, the desorption threshold temperature, and $k_{be,u} = 3.21$ W/m/K (fan is on after the temperature of the centre line reaching the desorption threshold temperature), $\rho c = 452 + 1147.5x$ kJ/m³/°C, $m_{c'g}c_{c'g} = 0.95 \times 460 = 437$ J/K, $\varepsilon = 0.42$, $\rho_p = 0.78 \times 10^3$ kg/m³, $\dot{Q}_{a,0} = 821 A_c l = 821 \times 2 R_b l$, $n = 1.34$, $D = 14.962 \times 10^{-5}$, $x_0 = 0.298$ kg / (kg adsorbent), $P_c = P_{Methanol, 35C} = 0.2767$ bar, and $Rc = 5 \times 10^{-2} / (k_{c'g} + k_{bed})$ into the above equations and solving them, the results are shown in Figure 4.4.
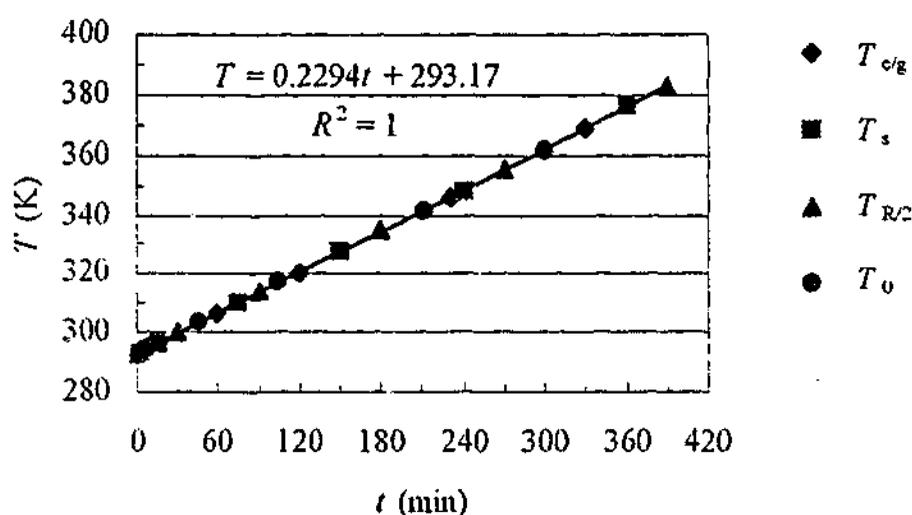

Figure 4.4 The temperature distribution of the heating processes in the bed ($L = 0.53$ m and $u_s = 0.3$ m/s). $T_{c'g}$ is the temperature of the collector/generator, T_s, T_{Rb2}, and T_0 is the temperature of the surface, the half radius, and the centre line of the bed, respectively.

From the figure, it can be seen that the temperature distribution in the bed is rather even, and no matter how complicated and different in the two heating steps, the temperature of the bed is linearly proportional to the time and the linear relationship is the same in the whole heating process (step 1 and step 2) with the constant heating flux on the collector. This relationship is useful in determining the heating time for the two heating steps.

4.5 THE THEORETICAL SOLUTIONS CONPARED TO THE EXPERIMENTAL DATA

To justify the theoretical results, it is necessary to compare them with the corresponding tested data. The theoretical and the tested temperatures with space and time in the heating processes are shown in Fig. 4.5.

It can be seen from Fig. 4.5 that the temperature distribution in the bed is really even, and the temperature of the bed is indeed linearly proportional to the time and the linearly relationship is the same in the whole heating process (step 1 and step 2) with the constant heating flux on the collector. However, the temperature of the bed is a little lower than that anticipated theoretically. The reason is that it was assumed the bed is well insulated (adiabatic) so there is no heat exchange between the bed/heating mat and the environment in the theoretical analysis, while actually there is heat lost from the bed/heating mat to the environment. Since the heat loss from the bed/heating mat may differ from one case to another, the no-heat-loss model is used preferably.
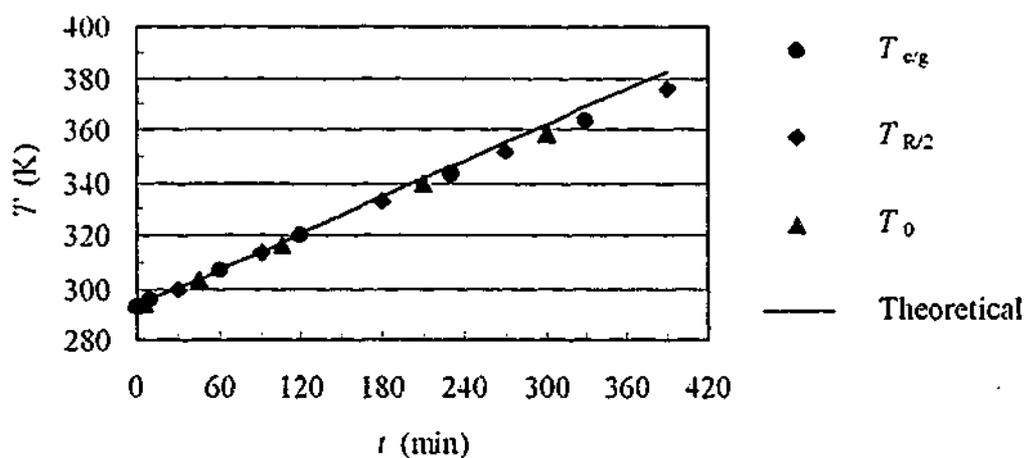
Figure 4.5 The experimental temperature distribution of the heating processes in the bed (L=0.53 m and u_s=0.3 m/s). $T_{c/g}$ is the temperature of the collector/generator, $T_{R/2}$, and T_0 is the temperature of the middle radius, and the centre line of the bed, respectively.

Further investigation shows that the intercept should be the value of the initial temperature which is taken as 293.15K in the theoretical analysis and test. So the temperature (K) – time (minute) relationship in the bed in our case can be expressed as

$$T = 0.23t + T_{initial} \qquad (4.30)$$

5

The First Law Analysis on the Solar Adsorption Refrigeration Cycle

In this chapter, the first law analysis (energy analysis) of the solar adsorption refrigeration cycle is described. The first law of thermodynamics is briefly reviewed and extended to the situation with heat generation/depletion in the system. Based on the first law, the detailed energy analysis on the heating and refrigeration processes is carried out. The Coefficient of Performance (COP) of the cycle is derived in equation and is also plotted on figures. Part of the work of this chapter has already been published (Publication 16).

5.1 CONSERVATION OF ENERGY PRINCIPLES

Energy Balance without Heat Generation/Depletion in the System

The conservation of energy for a closed system which is stationary in differential form is (Wark and Richards 1999; or Moran and Shapiro, 1995)

$$\delta Q + \delta W = dU \tag{5.1}$$

where Q and W represent heat and work interactions, respectively, and U is the internal energy of the substance. The heat transfer into the system is taken to be positive and the work done on the system is considered as positive which is the convention recommended by the international Union of Pure and Applied Chemistry (Smith et al, 1996). The symbol δ is employed to indicate that the term refers to an incremental amount of a quantity which is not a property, while d denotes the incremental change of a property.

For a control volume which remains fixed in space, the energy balance in the differential form is (Wark, 1995)

$$\delta Q + \delta W = \Sigma(h+V^2/2+gz)_e \, dm_e - \Sigma(h+V^2/2+gz)_i \, dm_i + dU_{cv} \tag{5.2}$$

where the subscripts i and e represent inlet and exit states.

Energy Balance with Heat Generation/Depletion in the System

For a control volume with heat generation or depletion, the energy balance in the differential form should be

$$\delta Q + \delta W = \Sigma(h+V^2/2+gz)_e \, dm_e - \Sigma(h+V^2/2+gz)_i \, dm_i + \delta Q' + dU_{CV} \qquad (5.3)$$

where Q' is the heat depleted (positive) or heat generated (negative).

Internal Energy and Enthalpy

For ideal gases

$$dU = m\, du = mc_v\, dT \qquad \text{and} \qquad dh = c_p\, dT \qquad (5.4)$$

For incompressible materials (liquid and solid)

$$c_v = c_p = c\,, \qquad dU = m\, du = mc\, dT\,, \qquad \text{and} \qquad dh = c\, dT + v\, dp \qquad (5.5)$$

5.2 ENERGY ANALYSIS ON PROCESSES AND THE CYCLE

5.2.1 Heating Process 1—2

In the heating process 1—2, the temperature of the adsorbent/adsorbate (eg. activated carbon/methanol) is increased from T_1 to T_2. However, there is no adsorbate (methanol) desorbed from the adsorbent (activated carbon) theoretically so the concentration in this process is constant at x_{max}. To minimise the energy used, the fan is not switched on so the pressure-adjusting gas is not circulated.

In this case, the collector and the collected space can be taken as a closed system. Since there is no work done, from the first law (Eq. 5.1), we have

$$\delta Q = dU \qquad (5.6a)$$

or

$$Q_{1-2} = \Delta U \qquad (5.6b)$$

That is to say that the heat used in this process Q_{1-2} is the increase of the internal energy of the system. The increase of the internal energy of the system is the sum of the increases of the internal energy of the solar collector/generator and the adsorbent (a), the refrigerant (b), and the pressure adjusting gas (c) (denoted with the subscript c/g, ad, r, and pr, respectively). Since there is no phase

changes in the substances being heated, the change of the internal energy is the sensible heat heating the solar collector/generator tubes, the adsorbent, the refrigerant, and the pressure adjusting gas.

a. The internal energy changes (the sensible heat) of the solar collector/generator tubes and the adsorbent

$$dU_{c/g,1-2} + dU_{ad,1-2} = (m_{c/g}c_{c/g} + m_{ad}c_{ad})dT \qquad (5.7a)$$

and

$$\Delta U_{c/g,1-2} + \Delta U_{ad,1-2} = \int_{T_1}^{T_2} (m_{c/g}c_{c/g} + m_{ad}c_{ad})dT = (m_{c/g}c_{c/g} + m_{ad}c_{ad})(T_2 - T_1) \qquad (5.7b)$$

where m and c represents mass and specific heat, respectively, and $c_{c/g}$ and c_{ad} can be taken constant in the temperature range.

The mass and the specific heat of the collector depend on the amount and the material used. In our case, $m_{c/g} = 0.95$ kg and $c_{c/g} = 460$ kJ/kg K.

The mass of the adsorbent (activated carbon pellets) in the collector pipe with radius R_b $= 2.425 \times 10^{-2}$ m, and length $L_b = 0.53$ m in our case is 0.325151 kg. Alternatively,

$$m_{ad} = \rho_p V = (1 - \varepsilon)\rho_p V_b = \pi(1 - \varepsilon)\rho_p R_b^2 L_b \qquad (5.8)$$

where ε is the fixed bed porosity and $\varepsilon = 0.35\text{-}0.6$ for activated carbon pellet bed, ρ_p is the density of the pellet and $\rho_p \approx 0.6\text{-}1.0$ g/cm^3 for activated carbon pellet.

Taking $\varepsilon = 0.42$, $\rho_p = 0.78 \times 10^{-3}$ kg/m^3, $R_b = 2.425 \times 10^{-2}$ m, and $L_b = 0.53$ m, we also have $m_{ad} = 0.325151$ kg.

b. The internal energy change (the sensible heat) of the refrigerant

$$dU_r = d(m_r u_r) = m_r c_{v,r} dT \qquad (5.9a)$$

and

$$\Delta U_{r,1-2} = \int_1^2 d(m_r u_r) = m_r \int_1^2 c_{v,r} dT \qquad (5.9b)$$

where the subscript r represents refrigerant.

The mass of the refrigerant is given by

$$m_r = m_{ad} x_{max} \qquad (5.10)$$

where x_{max} is the maximum concentration of the refrigerant in the adsorbent.

The concentration of the refrigerant adsorbed

Substituting Eq. (2.11) into Eq. (2.9b), we have

$$x = x_0 \exp\{-D[(A-\ln P)\, T-B]^n \}$$ (5.11)

where A and B can be determined by Eq. (3.15a) and Eq. (2.13a), respectively.

Hence, the maximum concentration x_{max} can be determined by

$$x_{max} = x_0 \exp\{-D[(A(T_1)-\ln P_e)\, T_1 -B(T_1)]^n \}$$ (5.12)

The specific heat of the refrigerant

Strictly speaking, the refrigerant in the adsorbent pores is in both liquid and vapour states. However, it is mainly liquid. Therefore, it is reasonable to assume that the refrigerant adsorbed is in liquid, and there is little difference between the constant-volume specific heat $c_{v,r}$ and the constant-pressure specific heat $c_{p,r}$, ie,

$$c_{v,r} = c_{p,r} = c_f$$ (5.13)

Since the refrigerant is in saturated liquid state here, the subscript r is dropped out and the subscript f is used to represent the saturated liquid refrigerant.

Specific heat is usually given by an empirical equation; one of the simplest expressions of practical value is (Smith, 1996)

$$\tilde{c}_p / \tilde{R} = \alpha + \beta T + \gamma T^2$$ (5.14a)

where $\tilde{c}_p$ is molar heat capacity at constant pressure.

The mass heat capacity at constant pressure can be expressed as

$$c_p = \tilde{c}_p / M = \alpha' + \beta T + \gamma T^2$$ (5.14b)

The *mean specific heat* for heat calculation, $\bar{c}_{1-2}$, is defined as

$$\bar{c}_{1-2} = \frac{1}{(T_2 - T_1)} \int_{T_1}^{T_2} c\, dT$$ (5.15)

$\bar{c}_{1-2}$ is usually simply expressed as $\bar{c}$ when it is not necessary to specify the temperature range. So the *mean mass heat capacity at constant pressure* $\bar{c}_p$ is calculated as

$$\bar{c}_p = \frac{\int_{T_1}^{T_2} c_p dT}{T_2 - T_1} = \frac{\int_{T_1}^{T_2} (\alpha' + \beta'T + \gamma'T^2)dT}{T_2 - T_1} = \alpha' + \beta'\frac{T_1 + T_2}{2} + \gamma'\frac{T_1^2 + T_1 T_2 + T_2^2}{3} \qquad (5.16a)$$

More often, $\bar{c}_{1-2}$ and $T_2 - T_1$ appear in the form of $\bar{c}_{1-2}$ $(T_2 - T_1)$, and

$$\bar{c}_p(T_2 - T_1) = \alpha'(T_2 - T_1) + \frac{\beta'}{2}(T_2^2 - T_1^2) + \frac{\gamma'}{3}(T_2^3 - T_1^3) \qquad (5.16b)$$

For methanol, the liquid heat capacity is (Daubert and Danner, 1984)

$$\tilde{c}_f = 107.6 - 0.3806T + 0.000979T^2 \qquad J/mol/K$$

$$175.6\,K < T < 400\,K, \quad \text{error} < 1\% \qquad (5.17a)$$

Alternatively, the heat capacity of methanol in kJ/kg/K is

$$c_f = 3.3625 - 0.01189375T + 0.0000305937T^2 \qquad kJ/kg/K \qquad (5.17b)$$

So for methanol the mean specific heat is

$$\bar{c}_{f,1-2} = 3.3625 - 0.005946875(T_1 + T_2) + 0.0000101977(T_1^2 + T_1 T_2 + T_2^2) \qquad (5.18a)$$

and

$$\bar{c}_{f,1-2}(T_2 - T_1) = 3.3625(T_2 - T_1) - 0.005946875(T_2^2 - T_1^2) + 0.0000101977(T_2^3 - T_1^3) \qquad (5.18b)$$

Hence the change of the internal energy of the refrigerant (methanol)

$$\Delta U_{r,1-2} = m_{ad} x_{max} \bar{c}_{f,1-2}(T_2 - T_1) \qquad (5.9c)$$

where x_{max} and $\bar{c}_{f,1-2}$ can be determined by Eqs. (5.12) and (5.18a), respectively.

c. The internal energy change (the sensible heat) of the pressure-adjusting gas

The pressure-adjusting gas is heated in a constant-volume process, so

$$dU_{pr} = m_{pr} c_{v,pr} dT \qquad (5.19a)$$

and

$$\Delta U_{pr,1-2} = \int_1^2 m_{pr} c_{v,pr} dT = m_{pr} c_{v,pr} (T_2 - T_1) \qquad (5.19b)$$

where $c_{v,pr}$ is the constant-volume specific heat of the pressure-adjusting gas. Since an inert gas is used as the pressure-adjusting gas, and the inert gas is in the *perfect gas* (ideal gas with constant specific heats, Kotas, 1995) state in the pressure and the temperature ranges of the refrigeration system, the specific heat is constant.

For Helium,

$$c_{p,pr} = 5.193 \text{ kJ/(kgK)} \text{ (ASHRAE, 1997)}, \quad R = 2.077 \text{ (van Wylen, 1993)},$$

$$\text{and} \quad \underline{c_{v,pr}} = c_{p,pr} - R = 3.116 \text{ kJ/(kgK)} \tag{5.20}$$

The mass of the pressure-adjusting gas is

$$m_{pr} = \frac{P_{pr}V_{pr}}{R_{pr}T} = \frac{(P_1 - P_e)V_{pr}}{R_{pr}T_1} = \frac{(P_2 - P_c)V_{pr}}{R_{pr}T_2} \tag{5.21a}$$

where V_{pr} is the volume occupied by the pressure-adjusting gas, P_{pr} is the partial pressure of the adjusting gas, P_1 is the pressure of the system at temperature T_1, P_e is the evaporator pressure which can be taken as the partial pressure of the refrigerant vapour at T_1, P_2 is the pressure of the system at temperature T_2, and P_c is the condenser pressure which can be taken as the partial pressure of the refrigerant vapour at T_2.

Since the pressure-adjusting gas is not ad⁻ʰᵉd by the adsorbent, the volume occupied by the pressure-adjusting gas is the difference between the volume of the fixed bed V_b ($=\pi R_b L_b$) and the volume occupied by the adsorbent particles V_p, ie,

$$V_{pr} = V_b - V_p = \varepsilon V_b \tag{5.22}$$

Since the amount of the gas charged could be adjusted readily before the heating process starts, state 1 is chosen for the calculation. So

$$m_{pr} = \frac{(P_1 - P_e)\varepsilon V_b}{R_{pr}T_1} \tag{5.21b}$$

(The calculation shows that compared with other terms, the internal energy change (the sensible heat) of the pressure-adjusting gas can be neglected.)

Therefore, *the total heat used in this process, $Q_{CM,1-2}$,*

$$Q_{CM,1-2} = (m_{c/g}c_{c/g} + m_{ad}c_{ad} + m_{ad}x_{max}\bar{c}_{f,1-2} + m_{pr}c_{v,pr})(T_2 - T_1) \tag{5.23}$$

where T_2, x_{max}, $\bar{c}_{f,1-2}$, m_{pr} are determined by Eq. (2.37), (5.12), (5.18a), (5.21), respectively.

5.2.2 Heating Process 2—3 (Desorption Period)

When the temperature of the adsorbent/refrigerant reaches T_2 the desorption starts. In the process 2—3 the temperature of the adsorbent/refrigerant continually increases to the maximum temperature T_3 (corresponding to the minimum concentration x_{min}). During this temperature-rising process, the refrigerant is driven off continuously but the partial pressure of the refrigerant vapour in the system remains constant at the condenser pressure P_c. To improve the condensation heat transfer, the fan has to be turned on. Thus, the mixture of the desorbed refrigerant vapour and the inert gas is forced through the bed. Taking the collector/generator as the control volume (CV), the energy balance in the differential form is

$$\delta Q = \Sigma h_e\, dm_e - \Sigma h_i\, dm_i + \delta Q^{\cdot} + dU_{cv} \qquad (5.24)$$

It can be seen that the energy balance for this process comprises the following components: (a) the change of the energy of the streams exiting and entering the CV; (b) the heat depleted; and (c) the increment of the energy of the CV. The last term consists of the increases of the internal energy of the collector/generator, the adsorbent, and the refrigerant adsorbed in the adsorbent from T_2 to T_3, (denoted with the subscript c/g, ad, and r respectively).

a. The change of the energy of the streams exiting and entering the CV

In this process, the stream exiting the CV is the mixture of the refrigerant vapour desorbed and the pressure-adjusting gas (denoted with the subscript pr). Supposing the refrigerant vapour is condensed completely in the condenser, the stream entering the CV then is the pressure-adjusting gas only. Hence

$$\Sigma h_e\, dm_e - \Sigma h_i\, dm_i = h_{r,e}\, dm_{r,e} + (h_{pr,e}\, dm_{pr,e} - h_{pr,i}\, dm_{pr,i}) \qquad (5.25)$$

ie, the change of the energy of the stream is the sum of the change of the enthalpy of the pressure-adjusting gas (the item in the parentheses) and the enthalpy leaving the CV with the refrigerant.

The change of the enthalpy of the pressure-adjusting gas

Since there is no change of the mass of the pressure-adjusting gas from the inlet to the outlet of the CV, $dm_{pr,e} = dm_{pr,i} = dm_{pr}$. The change of the enthalpy of the adjusting gas is

$$\Delta(dH)_{pr} = h_{pr,e}\, dm_{pr,e} - h_{pr,i}\, dm_{pr,i} = (h_{pr,e} - h_{pr,i})\, dm_{pr} \qquad (5.26a)$$

or in the rate format

$$\Delta \dot{H}_{pr} = (h_{pr,e} - h_{pr,i}) \dot{m}_{pr} \qquad (5.26b)$$

where $\dot{m}_{pr}$ is the mass rate of the gas passing though the CV

The *mass rate* can be determined by

$$\dot{m}_{pr} = \rho \dot{V}_{pr} = \pi R_b^2 u_s \rho \tag{5.27}$$

where ρ is the density of the gas, $\dot{V}_{pr}$ is the volume flow rate, R_b is the radius of the bed, u_s is the superficial velocity and is usually kept constant.

According to the data given by Incropera and DeWitt (1996), the thermophysical properties of helium gas varies with temperature approximately linearly in the temperature range of the flat-plate solar adsorption refrigeration system and $\rho = 0.2843 - 0.000406T$.

Assume a constant mass flow rate of the pressure-adjusting gas, the change of the enthalpy of the adjusting gas is

$$d(\Delta H_{pr}) = \dot{m}_{pr} c_{p,pr} (T_e - T_i)_{pr} dt \tag{5.28a}$$

and

$$\Delta H_{pr,2-3} = \dot{m}_{pr} c_{p,pr} \int (T_e - T_i)_{pr} dt \tag{5.28b}$$

where T_i and T_e are the temperatures of the stream flows in and out the CV, t is the time variable, and $c_{p,pr}$ is the constant pressure specific heat. For helium treated as a perfect gas, $c_{p,pr} \equiv 5.193$ kJ/kgK.

Neglecting the energy loss to the environment, the heat transferred to the gas should be equal to the energy absorbed by the gas, ie,

$$\dot{Q} = hA_{tot}(T_p - T_{pr}) = \dot{m}_{pr} c_{pr} (T_e - T_i)_{pr} \tag{5.29}$$

where h is the average heat transfer coefficient, A_{tot} is the total heating area, T_p is the temperature of the pellets and it is supposed to be the same along the axis direction in the bed (chapter 4), and T_{pr} is the temperature of the pressure-adjusting gas.

The heat transfer coefficient h

A large amount of experimental information in packed beds has been analysed to arrive at the following empirical correlation (Yoshida et al. 1962; see also Bird et al. 1960)

$$j_H = 0.91 \mathrm{Re}^{-0.51} \psi \qquad (\mathrm{Re} < 50) \tag{5.30}$$

Here

$$j_H = \frac{h_{loc}}{\rho c_p u_s} \Pr^{2/3} \quad \text{and} \quad \Re = \frac{u_s}{a \nu \psi} \tag{5.31}$$

where h_{loc} is the local heat transfer coefficient, a is the solid particle surface area per unit bed volume, ν is the viscosity, and ψ is the shape factor (ψ=0.91 for cylindric particles).

The solid particle surface area per unit bed volume a is the sum of the surface area of all pellets A_p, ie, $a = nA_p$ in which n is the number of the particles per bed volume and A_p is the surface area of a pellet.

The number of the particles

$$n = \frac{V_{p,t}}{V_p} = \frac{(1-\varepsilon)}{\pi R_p^2 L_p} = \frac{(1-\varepsilon)}{\pi R_p^2 L_p} \tag{5.32}$$

So

$$a = nA_p = \frac{(1-\varepsilon)}{\pi R_p^2 L_p}(2\pi R_p^2 + 2\pi R_p L_p) = 2(1-\varepsilon)\frac{R_p + L_p}{R_p L_p} \tag{5.33}$$

For example, in the case of ε=0.42, R_p=2×10^{-3}m and L_p=6×10^{-3}m, a=773m^2 (Eq. 5.33).

The viscosity ν and Prandtl number Pr can also be expressed as according to the data given by Incropera and DeWitt (1996), $\nu = (-109+0.77T)\times10^{-6}$ m^2/s and Pr $= 0.695-5\times10^{-5}T$.

The average heat transfer coefficient. The heat transfer coefficient changes with the temperature which changes along the bed. The local heat transfer coefficient is rather difficult to evaluate since it demands on the temperature distribution of the heated gas in the bed which is the quantity to be calculated. So the determination of the local heat transfer coefficient needs many trials. Fortunately, the change of the heat transfer coefficient with temperature is rather small, for example, according to the related equations the ratio of the heat transfer coefficients corresponding to 110°C and 35°C is about 0.95. So a local heat transfer coefficient can be used as the average heat transfer coefficient for the whole bed length, ie, $h \approx h_{loc}$.

The total heating area A_{tot}

The total heating area A_{tot} should be the sum of the surface area of pellets $A_{p,t}$ and the area of the collector exposed to the gas $A_{c/g}$, ie, $A_{tot} = A_{p,t} + A_{c/g}$.

The surface area of pellets in the bed is the sum of the surface area of all n pellets A_p

$$A_{p,t} = nA_p = aV_b = \pi a R_b^2 L_b = 2\pi(1-\varepsilon)R_b^2 L_b \frac{R_p + L_p}{R_p L_p} \tag{5.34}$$

and *the area of the collector exposed to the gas*

$$A_{c/g} \approx 2\pi R_b L_b \tag{5.35}$$

Therefore

$$A_{tot} = A_{p,t} + A_{c/g} \approx 2\pi(1-\varepsilon)R_b^2 L_b \frac{R_p + L_p}{R_p L_p} + 2\pi R_b L_b \tag{5.36}$$

For example, in our case $\varepsilon=0.42$, $R_p = 2\times10^{-3}$ m, $L_p = 6\times10^{-3}$ m, $R_b=2.425\times10^{-2}$ m, and $L_b=0.53$ m, then $A_{tot} =0.838$ m^2.

The temperature difference T_p-T_{pr}

Strictly speaking, the average temperature difference is some sort of mean temperature difference. To ensure the temperature of the exiting stream is no greater than the temperature of the heating bed[†], take the average temperature difference as

$$\Delta T \approx T_p - T_{pr,e} \tag{5.37}$$

So that

$$T_{pr,e} = \frac{\dot{m}_{pr} c_{pr} T_{pr,i} + hA_{tot} T_p}{\dot{m}_{pr} c_{pr} + hA_{tot}} \tag{5.38}$$

[†] If we take the average temperature difference as

$$T_p - T_{pr} = T_p - \frac{T_{pr,e} + T_{pr,i}}{2} \tag{a}$$

By substituting Eq (a) into Eq (6.29), we have

$$T_{pr,o} = \frac{2\dot{m}_{pr} c_{pr} T_{pr,i} + hA_{tot}(2T_p - T_{pr,i})}{2\dot{m}_{pr} c_{pr} + hA_{tot}} \tag{b}$$

Substituting the values of the parameters in the above equation, it is found that $T_{pr,o} > T_p$, an absurd result. The reasons for this dilemma may be the improper model in the calculation of the heat transfer coefficient and/or the use of contacting area (In the model, the whole surface area of the solid is used as the contacting area between the gas and the solid. For the cylindrical pellet bed, the end-to-end contact between the pellets reduces the area exposed to the gas and not all the exposed area acts as the heating area).

(Substituting the values of the parameters into the above equation, it is found that $T_{pr,e}$ approaches T_p. This result is reasonable and understandable since the contacting area of the gas and the heating particles in the bed is huge.)

Therefore

$$d(\Delta H_{pr}) \approx \frac{\dot{m}_{pr}c_{pr}hA_{tot}}{\dot{m}_{pr}c_{pr} + hA_{tot}}(T_p - T_{pr,i})dt \tag{5.28c}$$

and

$$\Delta H_{pr,2-3} \approx \frac{\dot{m}_{pr}c_{pr}hA_{tot}}{\dot{m}_{pr}c_{pr} + hA_{tot}}\int(T_p - T_{pr,i})dt \tag{5.28d}$$

For L=0.53 m and u_s =0.3 m/s, from heat transfer analysis (chapter 4), $T_p = 0.23t + T_1$, where t is the heating time in this process, in minutes. If t is in seconds

$$T_p = (0.23/60)t + T_1 \tag{5.39a}$$

There are two approaches to solve Eq. (5.28d). One is to substitute Eq. (5.39a) into Eq. (5.28d) and integrate it from the time t_2 to t_3. The other is to substitute dt in Eq. (5.28d) with dT_p and integrate it from the temperature $T_{p,2}$ to $T_{p,3}$. Since calculations of the thermal energy used in heating processes are usually based on temperature, it is preferable to use temperature as the variable, so the latter approach is used here.

Differentiating this equation and rearrange it

$$dt=(60/0.23)dT_p \tag{5.39b}$$

Substituting Eq. (5.39b) into Eq. (5.28), we have

$$d(\Delta H_{pr}) \approx \frac{60}{0.23}\frac{\dot{m}_{pr}c_{p,pr}hA_{tot}}{\dot{m}_{pr}c_{p,pr} + hA_{tot}}(T_p - T_{pr,i})dT_p \tag{5.28e}$$

and

$$\Delta H_{pr,2-3} \approx \frac{60}{0.23}\frac{\dot{m}_{pr}c_{p,pr}hA_{tot}}{\dot{m}_{pr}c_{p,pr} + hA_{tot}}[\frac{T_3^2 - T_2^2}{2} - T_{pr,i}(T_3 - T_2)] \tag{5.28f}$$

The enthalpy leaving the CV with the refrigerant $H_{r,e}$

$$dH_{r,e} = h_{r,e}dm_{r,e} \tag{5.40a}$$

The enthalpy of the unit vapour leaving the CV, $h_{r,e}$: The refrigerant leaving the CV is the vapour desorbed and it can be thought to be the saturated vapour corresponding to the liquid in the adsorbent, ie,

$$h_{r,e} = h_g = h_f + h_{fg} \tag{5.41a}$$

The *enthalpy of a saturated liquid* at temperature T, $h_f(T)$, is

$$dh = c_f dT + d(pv) \tag{5.42a}$$

So

$$h_f(T) = h_{f,0} + \int_{T_0}^{T} c_f dT + v(p - p_0) = h_{f,0} + \int_{T_0}^{T} (\alpha' + \beta T + \gamma T^2) dT + pv - p_0 v_0$$

$$= h_{f,0} + \alpha'(T - T_0) + \frac{\beta'}{2}(T^2 - T_0^2) + \frac{\gamma'}{3}(T^3 - T_0^3) + pv - p_0 v_0 \tag{5.42b}$$

$$= h_{f,0} + \overline{c}_{f,T_0-T}(T - T_0) + pv - p_0 v_0$$

where $h_{f,0}$, $\overline{c}_{f,T_0-T}$, p, and v are the enthalpy of the refrigerant at the reference state, the average specific heat of the fluid from T_0 to T, the saturation pressure of the fluid corresponding to T, and the specific volume of the saturated liquid, respectively.

The reference state used for most of the refrigerants corresponds to the international convention of 200 kJ/kg for enthalpy for the saturated liquid at 0°C (ASHRAE Fundamentals, 1997), ie, T_0 =273.15 K, and $h_{f,0}$=200 kJ/kg.

Similar to Eq. (5.18a), the average specific heat of the fluid from 273.15 K to T for methanol

$$\overline{c}_{f,273.15-T} = 3.3625 - 0.005946875(T + 273.15) + 0.0000101977(T^2 + 273.15T + 273.15^2)$$

The pressure and the specific volume of the saturated liquid can be determined by Eq. (2.4) and Eq. (2.5) for methanol. So

$$p_s v_f = [10^2 \times \exp(12.6973 - 4024.37/T - 87582.885/T^2)]/(937.911 - 0.058267T - 0.001459T^2) \text{ kJ/kg}$$

$$\tag{5.43}$$

Hence, for methanol

$$h_f(T) = 200 + \overline{c}_{f,273.15-T}(T - 273.15) + Pv - P_{0C} v_{0C} \qquad kJ/kg \tag{5.44}$$

The *enthalpy change of the liquid-vapour transformation* can be calculated by Eq. (2.19), and the saturation pressure P_s of the refrigerant is given by (Eq. (2.11). So

$$h_{fg} = R \times B \tag{5.45a}$$

where R is the gas constant. In terms of methanol R =8314/32.042 = 259.5 J/(kgK).

Substituting the value of R and the expression for B (Eq. 3.16 into Eq. 2.13a), the enthalpy of evaporation

$$h_{fg} = 259.5 \times (4024.37 + 2 \times 87582.885/T) \qquad J/(kg\ K) \qquad (5.45b)$$

The mass of the refrigerant leaving the CV: It is also reasonable to assume that the refrigerant adsorbed is in liquid and the refrigerant desorbed is in vapour. That is to say

$$m_L = m_r = m_{ad}x \qquad \text{and} \qquad m_V = m_{ad}(x_{max}-x) \qquad (5.46a)$$

and

$$dm_L = m_{ad}dx, \qquad \text{and} \qquad dm_{r,e} = dm_V = -m_{ad}dx \qquad (5.46b)$$

where subscripts L and V represent the adsorbed refrigerant liquid and the desorbed refrigerant vapour.

Therefore

$$H_{r,e} = -m_{ad}\int h_{r,e}\ dx = -m_{ad}\int(h_f + h_{fg})dx \qquad (5.40b)$$

where h_f and h_{fg} are expressed by Eq. (5.44) and (5.45b), respectively, and x is given by Eq. (2.9b).

To simplify the calculation, taking an average value for the enthalpy in Eq (5.40b), gives

$$H_{r,e} = -m_{ad}\int h_{r,e}\ dx = m_{ad}\Delta x\ \overline{h}_g = m_{ad}\Delta x(\ \overline{h}_f + \overline{h}_{fg}) \qquad (5.40c)$$

where $\Delta x = x_{max}-x_{min}$, $\overline{h}_f$ and $\overline{h}_{fg}$ are the average enthalpies of the liquid refrigerant and the average enthalpy change of the liquid-vapour transformation of the refrigerant from T_2 to T_3. They can be determined as following.

The minimum concentration: Similar to the derivation for the maximum concentration (Eq. 5.12), the minimum concentration can be determined by

$$x_{min} = x_0\,exp\{-D[(A-\ln P_c)\ T_3 - B]^n\} \qquad (5.47)$$

The average enthalpy of the liquid refrigerant $\overline{h}_{f,2-3}$ can be taken as

$$\overline{h}_{f,2-3}(T) \approx \frac{h_{f,2} + h_{f,3}}{2} \qquad (5.48)$$

For methanol

$$\overline{h}_{f,2-3} = 200 + \frac{1}{2}[\overline{c}_{f,273.15-T_2}(T_2 - 273.15) + \overline{c}_{f,273.15-T_3}(T_3 - 273.15)] + (\frac{P_2v_2 + P_3v_3}{2} - P_{0C}v_{0C}) \qquad (5.49)$$

where $\overline{c}_{f,273.15-T_2}$ and $\overline{c}_{f,273.15-T_3}$ are determined by Eq (5.18c).

The average enthalpy change of the liquid-vapour transformation of the refrigerant from T_2 to T_3 can be taken as

$$\overline{h}_{fg,2\text{-}3} = 259.5 \times [4024.37 + 87582.885(1/T_2 + 1/T_3)] \qquad \text{J/(kg K)} \tag{5.50}$$

Therefore, the enthalpy leaving the CV with the refrigerant vapour

$$H_{r,e} = m_{ad}\Delta x\{200 + \frac{1}{2}[\overline{c}_{f,0\text{-}2}(T_2 - 273.15) + \overline{c}_{f,0\text{-}3}(T_3 - 273.15)] + (\frac{P_2 v_2 + P_3 v_3}{2} - P_{0C} v_{0C}) + \overline{h}_{fg}\} \tag{5.40d}$$

b. The heat of depletion

The desorption of methanol from carbon is a heat absorption process. The heat absorbed is called heat of desorption, and denoted by subscript *de*. In a desorption process, a portion of heat is used to boil the liquid, and the rest of heat is consumed to release the vapour and so on. On the other hand, to transit a pure substance from a saturated liquid state to the corresponding saturated vapour state requires the latent heat of liquid-vapour transition. Therefore, the net heat consumed or depleted in a desorption process should be the difference of the heat of desorption and the latent heat (the enthalpy difference) of liquid-vapour transition, ie,

$$q' = h_{de} - h_{fg} \tag{5.51a}$$

or

$$Q' = \int_2^3 (h_{de} - h_g)dm_V = m_{ad}\Delta x(\overline{h}_{de} - \overline{h}_{fg}) \tag{5.52b}$$

The average enthalpy of the vapour $\overline{h}_{fg}$ can be determined in the same form as Eq. (5.50). The heat of desorption h_{de} can be taken as the heat of adsorption h_{ad} which can be calculated as follows.

Using Eq. (2.21) and Eq. (2.34), h_{ad} can be determined by

$$h_{ad} = R \times (A(T)\text{-}\ln P)\, T \tag{5.53}$$

The average heat of adsorption can be taken as

$$\overline{h}_{ad} = R(A((T_2 + T_3)/2)\text{-}\ln P_c) \times (T_2 + T_3)/2 + 0.5(R(A(T_2)\text{-}\ln P_c)T_2 + R(A(T_3)\text{-}\ln P_c)\,T_3) \tag{5.54}$$

c. The increment of the internal energy of the CV

The change of the internal energy of the solar collector/generator tubes and the adsorbent

$$\Delta U_{c/g,2\text{-}3} + \Delta U_{ad,2\text{-}3} = \int_{T_1}^{T_3} (m_{c/g}c_{c/g} + m_{ad}c_{ad})dT = (m_{c/g}c_{c/g} + m_{ad}c_{ad})(T_3 - T_2) \tag{5.55}$$

The change of the internal energy of the refrigerant

Again, the change of the internal energy of the refrigerant adsorbed in adsorbent is taken as the change of the internal energy of the refrigerant liquid. Therefore

$$\Delta U_{r,2-3} = \int_2^3 d(m_L u_f) = m_{L,3} u_{f,3} - m_{L,2} u_{f,2} \tag{5.56a}$$

According to the definition $u = h - pv$ and noticing that $x_2 = x_{max}$ and $x_3 = x_{min}$, the change of the internal energy of the refrigerant is

$$\Delta U_{r,2-3} = m_{ad} x_{min} [200 + \bar{c}_{f,0-3}(T_3 - 273.15) - P_{0C} v_{0C}] - m_{ad} x_{max} [200 + \bar{c}_{f,0-2}(T_2 - 273.15) - P_{0C} v_{0C}]$$
$$= m_{ad} x_{max} \bar{c}_{f,2-3}(T_3 - T_2) - m_{ad} \Delta x [200 + \bar{c}_{f,0-3}(T_3 - 273.15) - P_{0C} v_{0C}]$$

$$\tag{5.56b}$$

Therefore, *the total heat supplied in this process* is

$$Q_{CV,2-3} = (m_{c/g} c_{c/g} + m_{ad} c_{ad} + m_{ad} \frac{x_{max} + x_{min}}{2} \bar{c}_{f,2-3})(T_3 - T_2) + m_{ad} \frac{\Delta x}{2}(P_2 v_2 + P_3 v_3) \tag{5.57}$$
$$+ \Delta H_{pr,2-3} + m_{ad} \Delta x \bar{h}_{de}$$

The total heat supplied in the total heating process is

$$Q_{h,1-3} = Q_{CM,1-2} + Q_{CV,2-3}$$
$$= (m_{c,g} c_{c,g} + m_{ad} c_{ad} + m_{ad} x_{max} \bar{c}_{f,1-3})(T_3 - T_1) - m_{ad}(\Delta x/2) \bar{c}_{f,2-3}(T_3 - T_2) \tag{5.58}$$
$$+ m_{pr} c_{v,pr}(T_2 - T_1) + \Delta H_{pr,2-3} + m_{ad}(\Delta x/2)(P_{s,2} v_{f,2} + P_{s,3} v_{f,3}) + m_{ad} \Delta x \bar{h}_{de}$$

5.2.3 Cooling Process 3—4

From state 3 to state 4, the collector is cooled to the temperature T_4. In a theoretical cycle, the collector and the evaporator which is now charged with the condensed methanol are separated by the valve in this process (see Fig. 1.1).

5.2.4 Refrigeration Period 4—1 (Adsorption/Refrigeration Process)

After the collector being cooled to the temperature T_4, open the valve and the adsorption/refrigeration process happens.

Take the receiver and the evaporator as the control volume for which $\delta W = 0$. There is only one outlet and the vapour exiting can be taken as the saturated vapour, and the kinetic and potential

energy can be neglected (as they have been in virtually every analysis so far). With these assumptions, the energy balance Eq. (5.16) reduces to

$$\delta Q = dU_{CV} + h_{ex} dm_{ex}$$

$$= d(mu)_{CV} + h_{ex} dm_{ex} \tag{5.59a}$$

where

$$u = u_f + x (u_g - u_f) \qquad \text{and} \qquad m = m_f + x (m_g - m_f)$$

and x is the quality in the control volume.

The vapour exiting the evaporator can be regarded at the saturated state corresponding to the evaporation pressure, so $h_{ex} = h_{g,e}$. The subscript e indicates that this quantity corresponds to the evaporation temperature T_e (supposing all evaporation is at constant temperature).

Substituting the mass balance $dm_{ex} = -dm_{CV}$ into the above equation and dropping the subscript CV results in

$$\delta Q = d(mu) - h_{g,e} dm \tag{5.59b}$$

The net cooling produced during the process, $Q_{net,c}$, can be calculated by integrating the following differential equation for the heat balance in the evaporator:

$$\delta Q_{net,c} = \delta Q - (\delta Q_{rec} + \delta Q_{ev} + \delta Q_{leak}) \tag{5.60}$$

where Q_{rec} is the sensible heat cooling the receiver if applicable, Q_{ev} is the sensible heat cooling the evaporator, Q_{leak} is the heat leakage from the surroundings.

The refrigeration process can be thought to occur in two steps. Firstly, a portion of the liquid refrigerant in the receiver/evaporator evaporates and cools the receiver, evaporator and the rest of the liquid refrigerant to the designed evaporating temperature (from T_c to T_e), and then the liquid refrigerant evaporates at the evaporating pressure P_e (corresponding to the evaporating temperature T_e) until it is all evaporated and absorbs heat from the objects to be cooled (Exell, 1983).

In the first step, the temperature of the refrigerant decreases from T_c to T_e (Denoting the process as $r0$—$r1$), the heat flow into the control volume is

$$Q_{r0-r1} = \int \delta Q = \int (d(mu) - h_{g,e} dm) = (m_{r1}u_{r1} - m_{r0}u_{r0}) - (m_{r1} - m_{r0}) h_{g,e}$$

$$= (m_{r0} - m_{r1})(h_{g,e} - u_{r1}) - m_{r0}(u_{r0} - u_{r1}) \tag{5.61}$$

Since the first step happens very quickly, it is reasonable to assume that there is no heat exchange between the system and its surroundings, ie, $Q_{r0-r1} = 0$, so that

$$m_{r1} = m_{r0} \frac{h_{g,e} - u_{ro}}{h_{g,e} - u_{r1}} = m_{r0} \frac{h_{fg,e} + p_e v_e - \bar{c}_f (T_c - T_e)}{h_{fg,e} + p_e v_e} \tag{5.62}$$

Therefore, the net cooling is

$$Q_{net.c,r0-r1} = Q_{r0-r1} - (Q_{rec,r0-r1} + Q_{ev,r0-r1} + Q_{leak,r0-r1}) = 0 \tag{5.63}$$

In the second step, $T = T_e = $ constant (Denoting the process as $r1\!-\!\!-\!r2$),

$$Q_{r1-r2} = \int \delta Q = \int (d(mu) - h_{g,e} dm) = (0 - m_{r1}u_{r1}) - h_{g,e}(0 - m_{r1})$$
$$= m_{r1}(h_{g,e} - u_{r1}) \tag{5.64}$$

and

$$Q_{net.c,r1-r2} = m_{r1}(h_{g,e} - u_{r1}) - (Q_{rec,r1-r2} + Q_{ev,r1-r2} + Q_{leak,r1-r2}) \tag{5.65}$$

The net cooling of load in the whole process

$$Q_{net.c, r0-r2} = Q_{net.c,r0-r1} + Q_{net.c,r1-r2}$$
$$= m_{r0}(h_{g,e} - u_{r0}) - (Q_{rec,r0-r2} + Q_{ev,r0-r2} + Q_{leak,r0-r2}) \tag{5.66a}$$

It does not matter whether it is in the first or the second step that the receiver and the evaporator are cooled from T_c to T_e, the heat $Q_{rec,r0-r2} + Q_{ev,r0-r2}$ must equal the change in internal energy:

$$Q_{rec,r0-r2} + Q_{ev,r0-r2} = (m_{rec} c_{rec} + m_{ev} c_{ev})(T_c - T_e) \tag{5.67}$$

The mass of the refrigerant at the beginning of the evaporation is

$$m_{r0} = m_{ad}(x_{max} - x_{min}) = m_{ad}\Delta x \tag{5.68}$$

The quality in the control volume (evaporator) before the beginning of the step 1 is negligible, so

$$u_{r0} \approx u_{f,r0} = h_{f,r0} - P_{r0} v_{f,r0}$$

where P_{r0}, $v_{f,r0}$ and $h_{f,r0}$ is the pressure, the specific volume, and the specific enthalpy of the saturated liquid corresponds to the temperature T_c.

So $(h_{g,e} - u_{r0})$ may be expressed as

$$h_{e,g} - u_{r0} = h_{fg,e} - (h_{f,r0} - h_{f,e}) + P_{r0} v_{f,r0} = h_{fg,e} - (u_{f,r0} - u_{f,e}) + P_e v_{f,e}$$
$$= h_{fg,e} - \bar{c}_{r,f}(T_c - T_e) + P_e v_{f,e} \tag{5.69}$$

where c and e represents the quantity at condenser temperature and evaporator temperature respectively.

The latent heat of liquid-vapour transition at evaporator temperature can be determined by

$$h_{fg,e} = 259.5 \times [-1024.37 + 175165.77(1/T_e)] \quad J/(kg\ K) \tag{5.70}$$

Therefore, the *Net Cooling* effect (the cooling available for use) is

$$Q_{net,c} = m_{ad}\Delta x[h_{fg,e} - \overline{c}_f(T_c - T_e) + P_e v_{f,e}] - (m_{rec}c_{rec} + m_{ev}c_{ev})(T_c - T_e) - Q_{leak} \tag{5.66b}$$

If the heat leakage and the sensible heat cooling the receiver and the evaporator are neglected, the amount of the cooling calculated is called the *Gross Cooling Production*, i.e.,

$$Q_{gro,c} = m_{ad}\Delta x[h_{fg,e} - \overline{c}_f(T_c - T_e) + P_e v_{f,e}] \tag{5.71}$$

5.2.5 COP of the Ideal Refrigeration Cycle

The coefficient of performance (COP) for cooling is usually used as a criterion to evaluate the performance of a refrigeration cycle. The COP of a cycle is defined as the ratio of the amount of the energy (cooling) extracted from the cooled body to the energy transferred to the cycle to accomplish this effect. In terms of our solar adsorption refrigeration system (see Fig. 1.1), the energy in is the heat used in the two heating processes 1-2 and 2-3, and it is expressed by Eq (5.58). Corresponding to the cooling effect considered, there are two kind of COP, the net COP and the gross COP. The *Net COP* of the cycle is

$$COP_{net} = \frac{Q_{net,c}}{Q_h}$$
$$= \frac{m_{ad}\Delta x[h_{fg,e} - \overline{c}_{f,c-e}(T_c - T_e) + P_e v_{f,e}] - (m_{rec}c_{rec} + m_{ev}c_{ev})(T_c - T_e) - Q_{leak}}{(m_{c/g}c_{c/g} + m_{ad}c_{ad} + m_{ad}x_{max}\overline{c}_{f,1-3})(T_3 - T_1) - m_{ad}(\Delta x/2)\overline{c}_{f,2-3}(T_3 - T_2) + m_{pr}c_{v,pr}(T_2 - T_1)} \tag{5.72}$$
$$+ \Delta H_{pr,2-3} + m_{ad}(\Delta x/2)(P_2 v_{f,2} + P_3 v_{f,3}) + m_{ad}\Delta x\overline{h}_{de}$$

Since different refrigeration systems may have different heat capacities of receiver and evaporator and different insulation, the *Gross COP* of the cycle may be a common index in comparison of different refrigeration systems. The Gross COP of the cycle is

$$COP_{gro} = \frac{Q_{gro,c}}{Q_h}$$
$$= \frac{m_{ad}\Delta x[h_{fg,e} - \overline{c}_{f,c-e}(T_c - T_e) + P_e v_{f,e}]}{(m_{c/g}c_{c/g} + m_{ad}c_{ad} + m_{ad}x_{max}\overline{c}_{f,1-3})(T_3 - T_1) - m_{ad}(\Delta x/2)\overline{c}_{f,2-3}(T_3 - T_2) + m_{pr}c_{v,pr}(T_2 - T_1)} \tag{5.73}$$
$$+ \Delta H_{pr,2-3} + m_{ad}(\Delta x/2)(P_2 v_{f,2} + P_3 v_{f,3}) + m_{ad}\Delta x\overline{h}_{de}$$

It can be seen that for any adsorption/refrigerant pair, the value of COP is the function of the operating temperatures. For the activated carbon/methanol pair used in this research, the relationships of the gross COP and the operating temperatures (the peak temperature of the collector T_{peak}, the temperature of the collector in the morning $T_{morning}$, the condenser temperature T_c, and the evaporator temperature T_e) typically in the range of the solar refrigeration application are shown in Fig. 5.1 to 5.9, respectively (the solid mark and line). The COPs of the cycle without pressure-adjusting gas are also shown in the corresponding figures (the hollow mark and dotted line) for comparison.
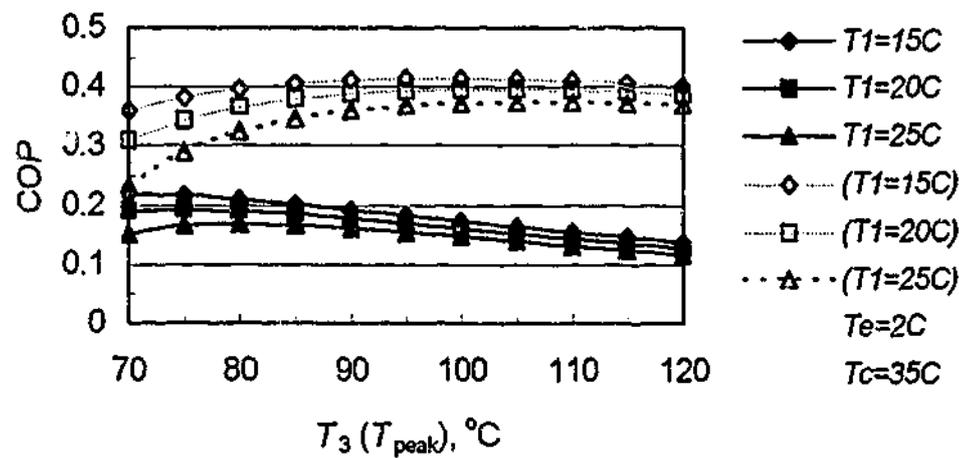
Figure 5.1 The relationship of the Coefficient of Performance (COP) and the peak temperature of the collector (T_e=2°C, T_c=35°C)
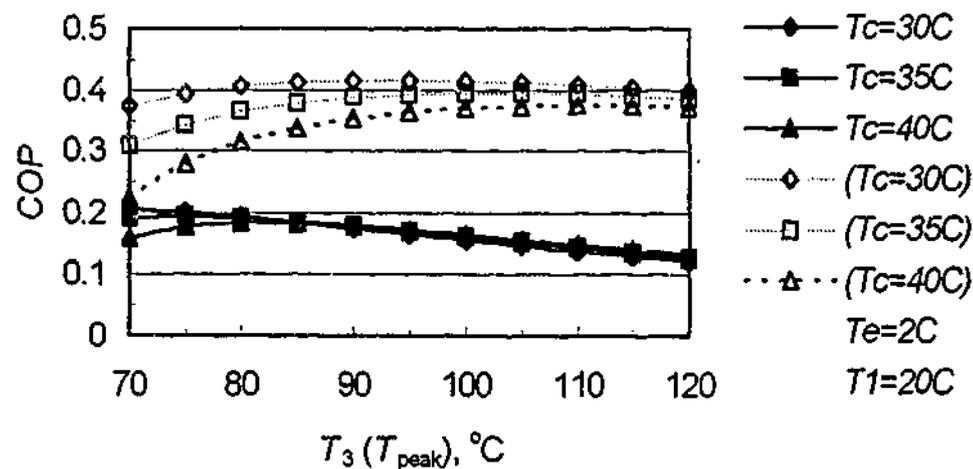
Figure 5.2 The relationship of the Coefficient of Performance (COP) and the peak temperature of the collector (T_e=2°C, T_1=20°C)
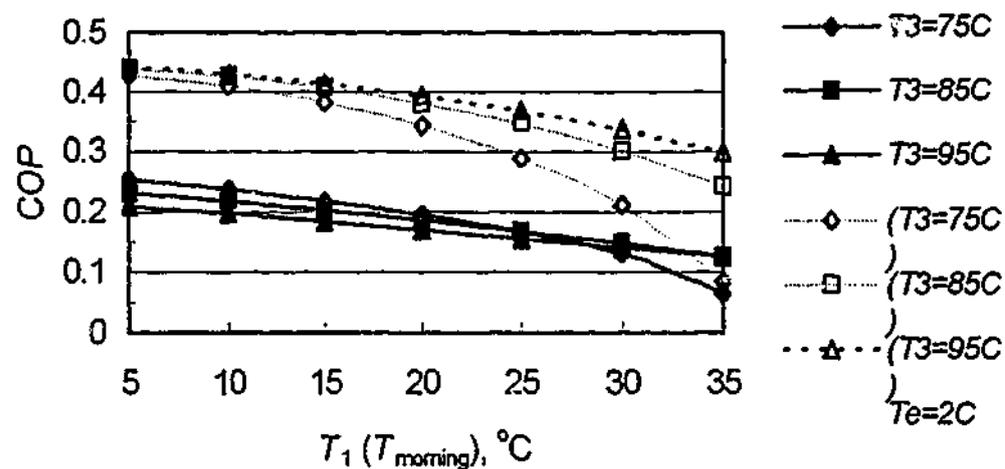
Figure 5.3 The relationship of the Coefficient of Performance (COP) and the temperature of the collector in the morning ($T_e=2°C$, $T_c=35°C$)
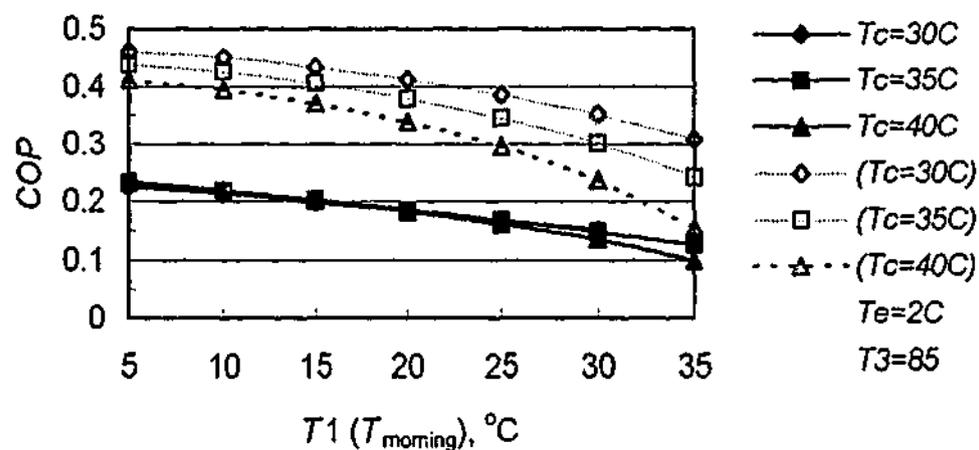
Figure 5.4 The relationship of the Coefficient of Performance (COP) and the temperature of the collector in the morning ($T_e=2°C$, $T_3=85°C$)
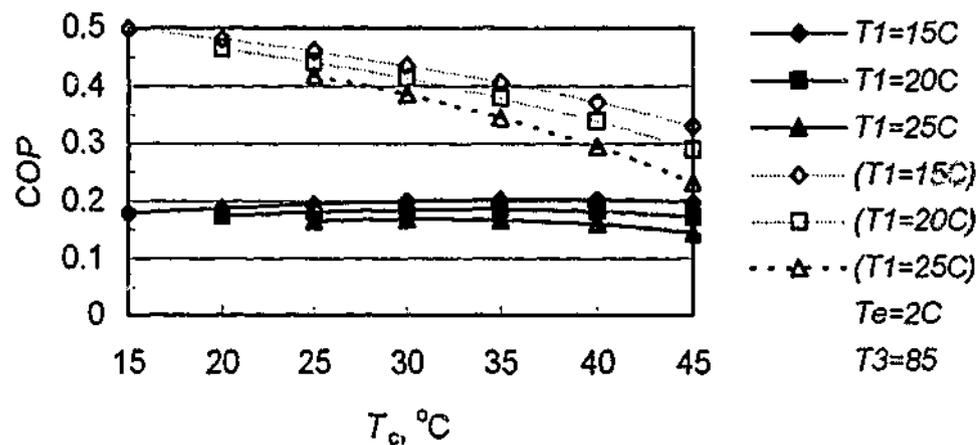
Figure 5.5 The relationship of the Coefficient of Performance (COP) and the condenser temperature ($T_e=2°C$, $T_3=85°C$)
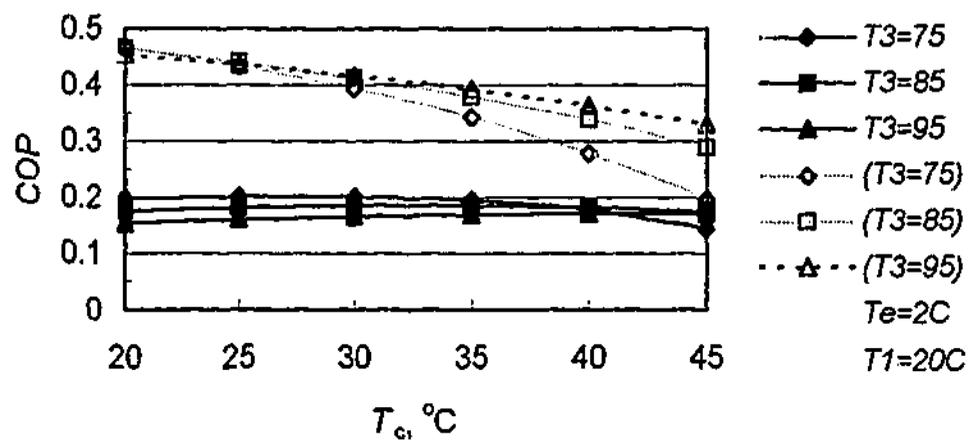
Figure 5.6 The relationship of the Coefficient of Performance (COP) and the condenser temperature (T_e=2°C, T_1=20°C)
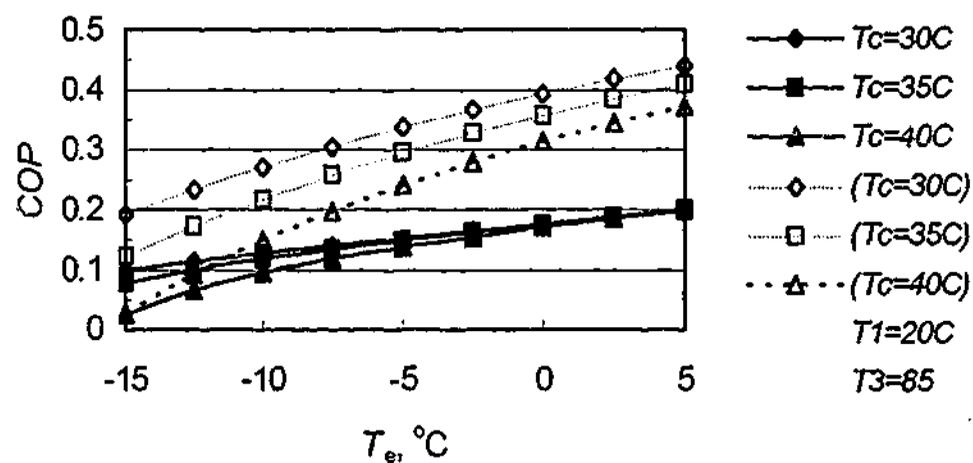
Figure 5.7 The relationship of the Coefficient of Performance (COP) and the evaporator temperature (T_1=20°C, T_3=85°C)
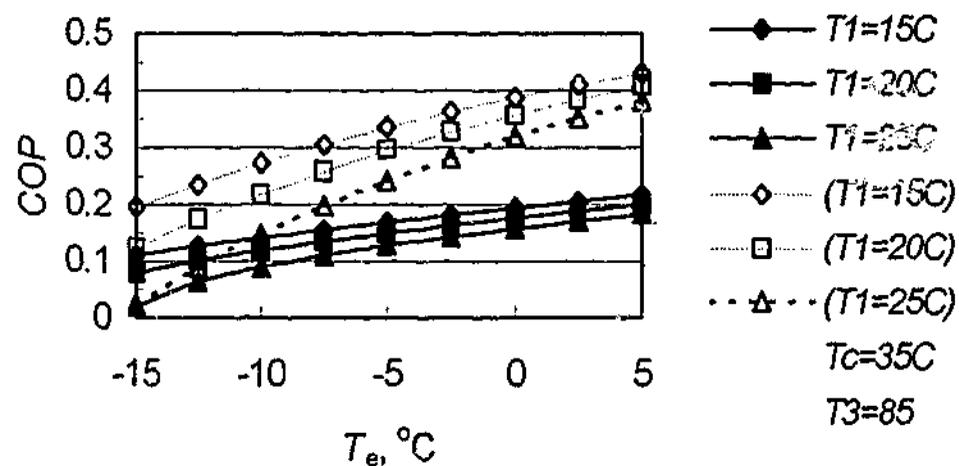
Figure 5.8 The relationship of the Coefficient of Performance (COP) and the evaporator temperature (T_c=35°C, T_3=85°C)
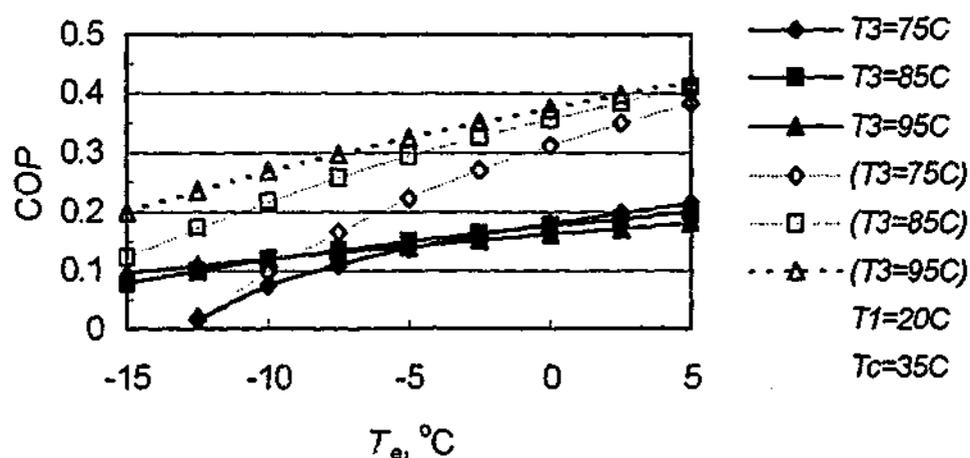
Figure 5.9 The relationship of the Coefficient of Performance (COP) and the evaporator temperature (T_1=20°C, T_c=35°C)

From the figures it can be seen that

- At a certain evaporator temperature, condenser temperature, and morning temperature, the COP of the system increases with the peak temperature of the collector, reaches a maximum, and then falls off. The lower the morning temperature, the lower the optimal peak temperature. In the typical conditions studied here, the optimal peak temperature is in the range of 70-95°C (Fig. 5.1, 5.2);

- At a certain evaporator temperature and condenser temperature, the lower the morning temperature, the higher the COP (Fig. 5.1, 5.3, 5.4, 5.5, 5.8). But the change of the COP also depends on the peak temperature. The lower the peak temperatures (eg, 75°C), the higher the COP in the low morning temperature range (eg, less than 25°C), but the COP drops sharper with the morning temperature (Fig. 5.3);

- At a certain evaporator temperature and the morning temperature, the condenser temperature has only a little impact on COP. But the impact also depends on the peak temperature. The lower the peak temperatures (eg, 75°C), the higher the COP in the low condenser temperature range (eg, less than 38°C), but after some condenser temperature (eg, 38°C), the COP drops sharper with the temperature (Fig. 5.6);

- At a certain morning temperature and condenser temperature, the higher the evaporator temperature, the higher the COP (Fig. 5.7, 5.8, 5.9). The condenser temperature has little impact on the COP in some evaporator temperature ranges (eg, 0°C), but in the evaporator temperature range less than some amount (eg, 0°C), the lower the condenser temperature, the higher the COP (Fig. 5.7). The COP of the systems with higher peak temperature (eg, 85°C) has higher value for low evaporator temperatures and then (eg, greater than -5 °C) the systems with lower peak temperature has higher COP (Fig. 5.9);

- At a certain evaporator temperature, the peak temperature, and the morning temperature, the COP of the system increases with the condenser temperature, reaches a maximum, and then falls off, but the impact of the condenser temperature is rather small (Fig. 5.4, 5.5, 5.6);

- At a certain evaporator temperature and morning temperature, the COP of the systems with lower condenser temperatures have higher COPs for some peak temperatures (eg less than 85°C), and then the systems with higher condenser temperatures have higher COPs but the difference is rather small (Fig. 5.2);

It can be deduced that for a certain climate (eg, a certain morning temperature and condenser temperature) and a certain application (eg, a specific evaporator temperature), there is an optimal peak temperature at which the COP of the system reaches a maximum. Therefore there is no need to pursue a higher peak temperature than necessary.

It can also be seen that the solar refrigeration system is suitable for low morning temperatures, and medium condenser temperatures.

The introduction of the pressure-adjusting gas into the system increases the heat consumed in the heating process, which decreases the COP. Comparing the COPs of the system with and without the pressure-adjusting gas (solid and dotted line, respectively). Some difference is very obvious. For example, the peak temperature corresponding to the maximum COP of the system with the pressure-adjusting gas is lower than that of the system without the gas. The optimal COP of the new system is about half of that the conventional system (eg, 0.21/0.415) at the same evaporator temperature (eg, 2°C), condenser temperature (eg, 30°C) and morning temperature (eg, 20°C). The difference of the COPs between the systems with and without the pressure-adjusting gas also depends on the velocity of the stream. *The most important task in this research is to eliminate the leaking problem for the vacuum system; therefore, the difference of the COPs of the systems with and without the pressure-adjusting gas is not the main concern here.* The COP of the system working around atmospheric pressure can be maximised by making it work under the optimal operation conditions as explored here, and the COP can be further improved by reducing the velocity of the stream, thus the difference of COPs between the systems with and without the pressure-adjusting gas can be reduced.

6

Adsorption Mass Transfer Analysis

From our observation, it is found that the introduction of the inert gas into the adsorption refrigeration system increases the adsorption resistance for methanol. Therefore, mass transfer analysis is the natural and necessary task of this chapter. A detailed analysis on the adsorption mechanisms is described. Based on this analysis, the rate of adsorption is evaluated by transforming and solving the macroscopic conservation equation in the adsorption bed. The experimental results are also shown in the figures for comparison. The relationship of the rate of refrigeration and the velocity is also investigated. Part of the work here has also been published (Publication 15).

6.1. ADSORPTION MASS TRANSFER ANALYSIS

Although there are huge amount of literature and a few well-established books (Ruthven, 1984, Yang, 1987, Suzuki, 1990, and Tien, 1994) on adsorption calculations, there is no model ready to be used for our application. Thus, while these well-established theories are used where it is suitable, some formulae are also derived for our application.

In a transport of adsorbate from the bulk of the fluid phase to the interior of a pellet, three mass transfer processes may be present: interpellet mass transfer, interphase mass transfer, and intrapellet mass transfer. *Interpellet mass transfer* refers to the diffusion and mixing of adsorbates in fluid occupying the space between the pellets. *Interphase mass transfer* is the transfer of adsorbate across the fluid-pellet interface. *Intrapellet mass transfer* refers to the diffusion of adsorbates within the pellet. Intrapellet mass transfer often takes place simultaneously with adsorption.

Adsorption of adsorbate from the solution phase onto the adsorption site, in most cases, occurs much faster than the various transport steps and can therefore be ignored when formulating the overall rate expression.

6.1.1 The Macroscopic Conservation Equations in the Adsorption Bed

Adsorption in our case is one-dimensional mode with fluid stream flowing along the direction of the bed's axis. A small element of the bed, as sketched in Fig. 6.1, is taken as the control volume to be analysed.
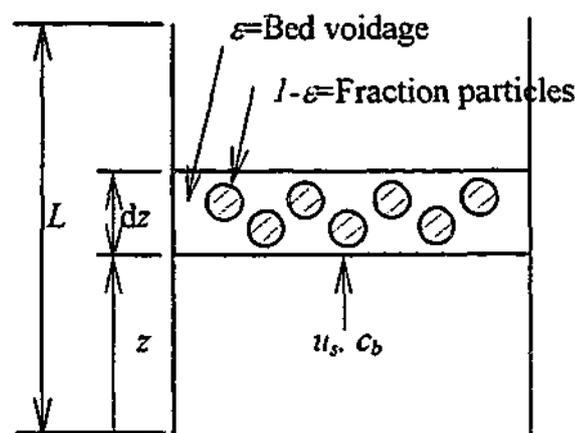
Figure 6.1 Control volume (element) of the bed

The rate of accumulation in the fluid and in the solid is the difference between input and output flows. Since the flow is a plug flow, the radial dispersion is ignorable. The mass balance is

$$-\varepsilon D_z \frac{\partial^2 c}{\partial z^2} + \varepsilon \frac{\partial c}{\partial t} + (1-\varepsilon)\rho_p \frac{\partial \bar{q}}{\partial t} = u_s c - \left(u_s c + \frac{\partial(u_s c)}{\partial z}\right)$$ (6.1a)

or

$$-\varepsilon D_z \frac{\partial^2 c}{\partial z^2} + \frac{\partial(u_s c)}{\partial z} + \varepsilon \frac{\partial c}{\partial t} + (1-\varepsilon)\rho_p \frac{\partial \bar{q}}{\partial t} = 0$$ (6.1b)

where c is the solution concentration for liquid adsorption and partial pressure for gas adsorption, t and z is the independent variables for time, and axial distance, respectively, u_s is the superficial velocity, ε is the fixed bed porosity (interpellet void fraction), and ε=0.35-0.6 for activated carbon pellet bed, D_z is the axial dispersion coefficient, and is based on the void cross section, $\bar{q}$ is the average adsorbed-phase concentration (on a mass basis), ρ_p is the density of the pellet and for activated carbon pellet, $\rho_p \approx 0.6$-1.0 g/cm^3.

The superficial velocity u_s is not strictly constant because of adsorption. However, for systems with adsorbate in trace amount such as in our case the removal of adsorbate from the fluid stream by adsorption has a very small effect on u_s, so u_s may be regarded as constant. For a plug flow in our case, it is also reasonable to assume that there is no dispersion[†]. So the mass balance equation can be simplified as

---

[†] In certain fixed-bed adsorption cases, axial dispersion needs to be considered. It is generally recognised that axial dispersion is caused by both molecular diffusion and turbulent mixing. As an approximation, it may be expressed as

$$D_z = \gamma_1 D_M + \gamma_2 d_p u_s / \varepsilon$$ (a)

$$\frac{\partial c}{\partial t}+u_s\frac{\partial c}{\partial z}+\frac{1-\varepsilon}{\varepsilon}\rho_p\frac{\partial \widetilde{q}}{\partial t}=0 \tag{6.2}$$

Neglecting the accumulation term for the fluid, Eq. (6.5) can be further simplified as

$$\frac{\partial c}{\partial z}+\frac{1-\varepsilon}{\varepsilon u_s}\rho_p\frac{\partial \widetilde{q}}{\partial t}=0 \tag{6.3}$$

The transport of the adsorbate species from the bulk of the fluid phase to the external surface of adsorbent pellets constitutes an important step in the overall uptake process. For single-species adsorption, the interphase mass transfer rate may be expressed as

$$\frac{\partial \bar{q}}{\partial t}=k_f a\left(c_b-c_s\right)=\frac{k_f A_p}{\rho_p V_p}\left(c_b-c_s\right) \tag{6.4}$$

where c_b and c_s is the adsorbate concentration in the bulk of fluid and that at the fluid-pellet interface (the pellet surface), A_p is the surface area of a pellet, V_p is the volume of a pellet, a is the specific

---

where γ_1 and γ_2 are two constants, D_M and d_p are molecular diffusivity in the bulk phase and the pellet diameter, respectively.

After substituting appropriate correlations for γ_1 and γ_2, the above equation becomes

$$\frac{1}{Pe}=\frac{A_1}{Re\,Sc}+\frac{1}{\left(Pe_z\right)_\infty}\frac{1}{1+A_2\,/\left(Re\,Sc\right)} \tag{b}$$

where A_1 and A_2 are constants, $(Pe_z)_\infty$ is the limiting value of Pe_z at large value of Re, and Pe_z, Re, and Sc are Peclet number for axial dispersion, Reynolds number, and Schmidt number, respectively, and they are defined as

$$Pe_z=\frac{d_p\left(u_s\,/\,\varepsilon\right)}{D_z},\qquad Re=\frac{u_s d_p}{\nu},\qquad \text{and}\qquad Sc=\frac{\nu}{D_M}$$

and where ν is the kinematic viscosity

Several investigators use Eq. (b) to correlate axial dispersion results. The correlation proposed by Wen and Fan (1975) gives A_1=0.3, A_2=3.8 and $(Pe_z)_\infty$=2.0 for pellet diameter great than and equal to 0.3 cm. That is

$$\frac{1}{Pe_z}=\frac{0.3}{Re\,Sc}+\frac{0.5}{1+3.8\,/\left(Re\,Sc\right)} \tag{c}$$

for $0.008<Re<400$ and $0.28<Sc<2.2$.

surface area (area per unit mass of adsorbent), $F_p/(\rho_p V_p)$, and k_f is the interphase (or external) mass transfer coefficient.

To simplify the solvation for the adsorbate uptake rate, the so-called lumped parameter model has been developed. It is postulated that the uptake rate of adsorbate by a pellet is linearly proportional to a driving force, defined as the difference between the surface and the average adsorbed phase concentrations. Mathematically

$$\frac{d\bar{q}}{dt} = k_p \left(q_s - \bar{q} \right) \tag{6.5}$$

where k_p is the so-called particle-phase transfer coefficient, and q_s is the adsorbed-phase concentration at the exterior surface of the pellet.

The mechanism of transfer of adsorbate to the solid includes diffusion through the fluid film around the particle and diffusion through the pores to internal adsorption sites. So the adsorbate uptake rate per pellet is given as

$$\rho_p V_p \frac{\partial \bar{q}}{\partial t} = k_f A_p (c_b - c_s) = \rho_p V_p k_p (q_s - \bar{q}) \tag{6.6}$$
$$= A_p k_{of} (c_b - c^*) = \rho_p V_p k_{op} (q^* - \bar{q})$$

where $c*$ is the value in equilibrium with $\bar{q}$ and $q*$ is with c_b, k_{of} and k_{op} is the overall transfer coefficient with c_b-c* and $q*-\bar{q}$ as the respective overall driving forces.

For the linear isotherm case, k_{of} and k_{op} are defined as (Tien, 1994)

$$\frac{1}{k_{of}} = \frac{1}{k_f} + \frac{A_p c_{in}}{\rho_p V_p q_{ref}} \frac{1}{k_p} \tag{6.7}$$

and

$$\frac{1}{k_{op}} = \frac{\rho_p V_p q_{ref}}{A_p c_{in}} \frac{1}{k_f} + \frac{1}{k_p} \tag{6.8}$$

where c_{in} is the concentration in the feed to adsorber, and $q_{ref} = f(c_{in})$.

The next step is the determination of the quantities related with k_{of} and k_{op}

6.1.2 The Isotherm Expression $q = f(c)$

Replacing w by q in Eq. (2.9a) and also expressing the isothermal expression in Henry's equation form, we have

$$q_{ref} = q_0 exp\{-D[T\ln(P_s/P_e)]^n\} = K(P_{Methanol}/P_{tot}) = Kc_{in} \qquad (6.9)$$

where K is Henry's constant.

For the activated carbon and methanol pair used here, $q_0 = 0.298343$, $n = 1.34$, $D = 14.962 \times 10^{-5}$. Taking $T = 303.15$ K, $P_s = P_{s(30C)} = 2.16 \times 10^4$ Pa, $P_{Methanol} = P_e = P_{s(2C)} = 4.57 \times 10^3$ Pa, and $P_{tot} = 1.01325 \times 10^5$ Pa, we get $q_{ref} = 0.16842$, $c_{in} = 0.45103$ and $K = 3.73413$.

6.1.3 The Interphase (or External) Mass Transfer Coefficient k_f

The equation for the interphase (or external) mass transfer coefficient k_f

The magnitude of k_f depends on the flow conditions around the pellet. Numerous investigators have measured the mass transfer in fixed beds and have established correlations for their results. The mass transfer results are usually correlated in terms of the Sherwood number Sh or the j factor j_M. The j_M is defined as (Tien, 1994)

$$j_M = \left(\frac{k_f}{u_s}\right)\left(\frac{v}{D_M}\right)^{2/3} \qquad (6.10)$$

where v is the kinematic viscosity and D_M is the adsorbate bulk-phase diffusivity (molecular diffusivity).

Neglecting the dispersion effect, the j factor j_M can also be obtained from the following equation

$$j_M = \frac{0.458}{\varepsilon} Re^{-0.407} \qquad \text{(for } Re = \frac{u_s d_p}{v} > 10\text{)} \qquad (6.11)$$

where Re is the Reynolds number, and d_p is particle diameter.

Equating eqs. (6.10) and (6.11), we have

$$k_f = 0.458 \varepsilon^{-1} d_p^{-0.407} v^{-0.26} D_M^{0.667} u_s^{0.593} \qquad (6.12)$$

The kinematic viscosity of the mixture

Using the same approach as in chapter 4, it is determined that the kinematic viscosity of the mixture at the bed temperature 30°C $v = 856.0787 \times 10^{-7}$ m²/s.

The molecular diffusivity D_M

The molecular diffusivity for a binary gas mixture can be estimated by the familiar Chapman-Enskog equation (Satterfield and Sherwood, 1963)

$$D_M = 0.0018583 \frac{T^{3/2}(1/M_A + 1/M_B)^{1/2}}{P\sigma_{AB}^2 \Omega_{AB}} \qquad cm^2/s \qquad (6.13)$$

where T is the temperature, K, M_A and M_B is the molecular weights of the two species, P is the total pressure, atm, $\sigma_{AB} = (\sigma_A + \sigma_B)/2$, the collusion diameter from the Lennard-Jones potential, in Angstroms, Ω_{AB} is the collusion integral, a function of $k_B T/\varepsilon_{AB}$ where k_B is Boltzmann's constant and $\varepsilon_{AB} = (\varepsilon_A \varepsilon_B)^{1/2}$, the Lennard-Jones force constant.

For methanol (species A) and Helium (species B) system, M_A=32.042 and M_B=4.0026. According to Satterfield and Sherwood (1963), $\varepsilon_A/k_B = 507$, $\varepsilon_B/k_B = 10.22$, $\sigma_A = 3.585$, and $\sigma_B = 2.576$.

Taking $T = 303.15$K, we have $k_B T/\varepsilon_{AB} = k_B T/\sqrt{\varepsilon_A \varepsilon_B} = 4.211$, $\Omega_{AB} = 0.8689$, and $\sigma_{AB} = (\sigma_A + \sigma_B)/2 = 3.081$. Assuming P=1atm, therefore

$$D_M = 0.0018583 \frac{303.15^{3/2}(1/32.042 + 1/4.0026)^{1/2}}{3.081^2 0.8689} = 0.63043 \ (cm^2/s)$$

Taking $\varepsilon = 0.42$, $d_p = 4\times10^{-3}$ m, $v = 856.0787\times10^{-7}$ m^2/s, and $D_M = 0.63043\times10^{-4}$ m^2/s, we have

$$k_f = 0.18599 u_s^{0.593} \qquad (6.14)$$

6.1.4 The Particle-phase Transfer Coefficient k_p

The equation for the particle-phase transfer coefficient k_p

It was postulated that the uptake rate of adsorbate by a pellet is described by Eq. (6.5), so the average adsorbed-phase concentration of the pellet

$$\bar{q} = \frac{1}{V_p} \int_{V_p} q dV \qquad (6.15)$$

For a cylindrical pellet

$$\bar{q} = \frac{2}{R_p^2} \int_0^{R_p} q r dr \qquad (6.16a)$$

where R_p is the radius of the pellet, and r is the radial distance from the centre of the pellet.

Several earlier investigators have independently employed expression similar to Eq. (6.5), but Glueckauf (1955) is commonly credited with providing a theoretical basis for this rate expression. Glueckauf also obtained a relationship between k_p and D_e. However, Glueckauf's derivation is cumbersome. Rice(1982) assumed that the adsorbed phase concentration profile is parabolic. For a pellet

$$V_p \frac{d\bar{q}}{dt} = D_e A_p \left(\frac{\partial q}{\partial r} \right)_{r=R_p} \tag{6.17}$$

where D_e is the effective intrapellet diffusivity.

If the adsorbed phase concentration profile is assumed parabolic

$$q = a_0 + a_2 r^2 \tag{6.18}$$

where a_0 and a_2 are functions of time. The surface concentration and the surface-concentration gradient are

$$q_s = a_0 + a_2 R_p^2 \tag{6.19a}$$

and

$$\left(\frac{dq}{dr} \right)_{r=R_p} = 2a_2 R_p \tag{6.19b}$$

The average concentration $\bar{q}$ can be found by substituting Eq. (6.18) into Eq. (6.16a)

$$\bar{q} = \frac{2}{R_p^2} \int_0^{R_p} qr\,dr = a_0 + \frac{1}{2} a_2 R_p^2 \tag{6.16b}$$

Therefore

$$q_s - \bar{q} = \frac{1}{2} a_2 R_p^2 \tag{6.20}$$

Comparing Eq. (6.19) with (6.20), we have

$$\left(\frac{dq}{dr} \right)_{r=R_p} = \frac{4}{R_p} (q_s - \bar{q}) \tag{6.21}$$

Substituting Eq. (6.21) into Eq. (6.16)

$$\frac{d\bar{q}}{dt} = \frac{A_p}{V_p} D_e \left(\frac{\partial q}{\partial r} \right)_{r=R_p} = \frac{4A_p}{R_p V_p} D_e (q_s - \bar{q}) \tag{6.22}$$

Comparing Eq. (6.5) with Eq. (6.22), it can be seen that

$$k_p = \frac{4A_p}{R_p V_p} D_e$$

$$= \frac{8(1+\alpha)D_e}{\alpha R_r^2} \quad (for \quad a \quad cylindrical \quad pellet) \tag{6.23}$$

where α is the the ratio of the length of the pellet to the radius of it, $\alpha = l/R_p$. In our case $l = 6$ mm and $R_p = 2$ mm, so $\alpha = 3$.

The effective intrapellet diffusivity D_e

The effective intrapellet diffusivity D_e is defined as

$$D_e = \frac{D_p}{f'(c)} \frac{1}{\rho_p} + D_s \tag{6.24}$$

where D_p is the pore diffusivity, and D_s is the surface diffusivity.

The pore diffusion D_p

The pore diffusion in the fluid phase results from collisions among molecules (molecular diffusion) and with pore surfaces (Knudsen diffusion). In some cases, both diffusions may occur simultaneously. The pore diffusivity D_p in Eq. (10) should be determined as

$$\frac{1}{D_p} = \frac{1}{D_{pM}} + \frac{1}{D_K} \tag{6.25}$$

where D_{pM} and D_K is the molecular diffusivity and Knudsen diffusivity.

The molecular diffusion D_{pM}. For the collisions among molecules, the diffusion occurs in the zigzag and randomly arranged paths, and the commonly accepted expression for D_{pM} is

$$D_{pM} = \varepsilon_p D_M / \tau \tag{6.26}$$

where ε_p is the pellet porosity which denotes that diffusion occurs only in the pore space, $\varepsilon_p \approx 0.5$-$0.6$ for activated carbon, τ is known as the tortuosity factor to account for the fact that diffusion takes place zigzag-wise rather than along the radial direction. For activated carbon the value of τ is quoted to vary from 5-65 (Yang 1987). Since the precise value of τ is unknown, Eq. (6.12) can only be used to provide a crude estimate of D_{pM}. Taking $\varepsilon_p = 0.55$, $\tau = 35$, and $D_M = 0.63043$ into Eq. (6.27) we get $D_{pM} = 0.0099$ cm^2/s.

Knudsen diffusion D_K: When the pore diameter becomes small, collision between the fluid molecules and the pore wall become increasingly important. In a very small pore, collisions with the pore surface dominate, resulting in a different type of diffusion mechanism, known as Knudsen diffusion. The relative importance of molecular diffusion and Knudsen diffusion is determined by the ratio of the pore diameter and the mean free path of the fluid molecules. The mean free path is evaluated by following expression

$$Mean \quad free \quad path = \frac{1}{\sqrt{2}n\pi\sigma^2}$$

where n is the gas number density in molecules/volume, σ is the collision diameter which can be calculated from transport properties or the second virial coefficient.

Generally speaking, when the pore diameter is greater than ten times the mean free path, molecular diffusion prevails; Knudsen diffusion may be assumed when the mean free path is less than ten times the pore diameter.

The Knudsen diffusivity D_K is given by

$$D_K = 9700 r_p (T/M)^{1/2} \tag{6.27}$$

where r_p is the mean pore radius, cm, $r_p=20\times10^{-8}$—50×10^{-8} cm for activated carbon, M is the molecular weight of diffusion species, T is the temperature, K, D_K is in cm^2/s. Taking $r_p=35\times10^{-8}$ cm, $T=303.15$ K, and $M=32.042$ into Eq. (5.11), we have $D_K=0.01044$ cm^2/s.

When the mean free path is not known, Knudsen diffusion should be taken into account.

It can be seen that in our case, molecular diffusion and Knudsen diffusion have almost the same value, so both of them should be considered. Therefore

$$\frac{1}{D_p} = \frac{1}{0.0099} + \frac{1}{0.01044} = 196.7717 \quad \text{or} \quad D_p = 0.0051 \text{ cm}^2/\text{s}.$$

The surface diffusivity D_s

The surface diffusivity characterises surface diffusion which is known to vary with both temperature and the extent of surface coverage (or q). A general correlation of D_s for gas adsorption was developed by Sladek et al. (1974). This correlation relates D_s with the parameter h_{ad}/mRT where h_{ad} is the heat of adsorption and m is an integer with a value of 1,2,3, depending on the nature of the

bond between the adsorbate molecules and the adsorption site as well as the substrate material. For a polar adsorbate and a solid conductor, $m=2$.

In our case, $h_{ad}/mRT=b/2T=(A-\ln P_e)/2$. Taking $A=13.65$ ($30°C$, chapter 3) and $P_e = 0.0457$ bar ($2°C$, chapter 3) into the above equation, we have $h_{ad}/mRT=7.368$. From the figure given by Gilliland et al (Tien, 1994), we can find that

$$\text{Log}D_s = -3.388, \quad \text{so} \quad D_s = 0.000409 \text{ cm}^2/\text{s}$$

The derivative of the isotherm expression $f'(c)$

From Eq. (6.9), we obtain

$$f'(c) = q'(p) = q_0 nD \, P_s \, T^n [\ln(P_s/P)]^{n-1} \, exp\{-D[T\ln(P_s/P)]^n\}/P \tag{6.28}$$

For the activated carbon and methanol pair used here, $q_0 = 0.298343$, $n = 1.34$, $D = 14.962 \times 10^{-5}$. Taking $T=303.15K$, $P_s=P_{s(30C)}=2.16\times10^4$Pa, and $P=P_e=P_{s(2C)}=4.57\times10^3$Pa, we get $f'(c) = 0.393$.

Substituting $D_p = 0.0051$, $D_s = 0.000409$, $f'(c) = 0.393$, and $\rho_p = 0.78\times10^3$ kg/m³ into Eq. (6.24), we have $D_e = 0.000426$ cm²/s.

6.1.5 The Equations of the Overall Transfer Coefficient k_{of} and k_{op} for the Cylindrical Pellet

Substituting Eq. (6.23) into (6.8), for a cylindrical pellet, we have

$$\frac{1}{k_{of}} = \frac{1}{k_f} + \frac{R_p c_{in}}{4\rho_p q_{ref} D_e} \tag{6.29a}$$

and

$$\frac{1}{k_{op}} = \frac{\alpha R_p}{2(1+\alpha)}(\frac{\rho_p q_{ref}}{c_{in}}\frac{1}{k_f} + \frac{R_p}{4D_e}) \tag{6.30a}$$

For our case, taking $R_p = 2\times10^{-3}$ m, $\alpha = 2$, $\rho_p = 0.78\times10^3$ kg/m³, $c_{in} = 0.45103$, $q_{ref} = 0.16842$, $D_e = 0.000426$ cm²/s, and $k_f = 0.18599u_s^{0.593}$ into Eq. (6.29a) and (6.30a), we obtain

$$k_{of} = \frac{0.18599u_s^{0.593}}{1+0.74965u_s^{0.593}} \tag{6.29b}$$

and

$$k_{op} = \frac{0.09578u_s^{0.593}}{1+0.74965u_s^{0.593}} \tag{6.30b}$$

6.2 APPLICATION

6.2.1 The Maximum Velocity of the Stream

Substituting eq. (6.6) into eq. (6.3), we have

$$\frac{\partial c}{\partial z} + \frac{(1-\varepsilon)A_p}{\varepsilon u_s V_p} k_{of} \left(c_b - c^*\right) = 0 \tag{6.31}$$

Assuming $c^* = \beta c_b$ (where β is a constant), we get

$$\frac{\partial c}{\partial z} + \frac{(1-\varepsilon)A_p}{\varepsilon u_s V_p} k_{of} (1-\beta)c_b = 0 \tag{6.32}$$

So at the end of the bed where $z=L$, the concentration

$$\ln\frac{c}{c_{in}} = -\frac{(1-\varepsilon)A_p}{\varepsilon u_s V_p} k_{of} (1-\beta)L \tag{6.33}$$

The value of β is related with k_{of}. When k_{of} approaches 0, β approaches 0; and when k_{of} approaches infinite, β approaches unity. If β is taken as

$$\beta = 1 - \exp(-k_{of}) \tag{6.34}$$

and to make the exit c no more than $0.05c_{in}$, ie, $\ln(c/c_{in}) \leq -3$, the length of the bed L must be

$$L \geq \frac{3\varepsilon V_p u_s}{(1-\varepsilon)A_p k_{of}} \exp(k_{of}) \tag{6.35}$$

or, the velocity of the stream for a fixed bed length

$$u_s \leq \frac{(1-\varepsilon)A_p k_{of} \exp(-k_{of})}{3\varepsilon V_p} L \tag{6.36}$$

Eq. (6.35) is preferable here since it is in the explicit form. Therefore, the relationship of $u_{s,max}$ and L can be easily obtained by diverting the relationship of L_{min} and u_s obtained from Eq. (6.35) and it is shown in Fig. 6.2 for the case of $\varepsilon = 0.42$ and $V_p / A_p = 0.75 \times 10^{-3}$ ($R_p=2\times10^{-3}$ m and $\alpha=3$).

From Fig. 6.2, it can be seen that the maximum allowable velocity corresponding to the length of the adsorption bed is rather high. In our application the velocity does not need to be that high (see also the following analysis), so there is no worry about the upper velocity limit.
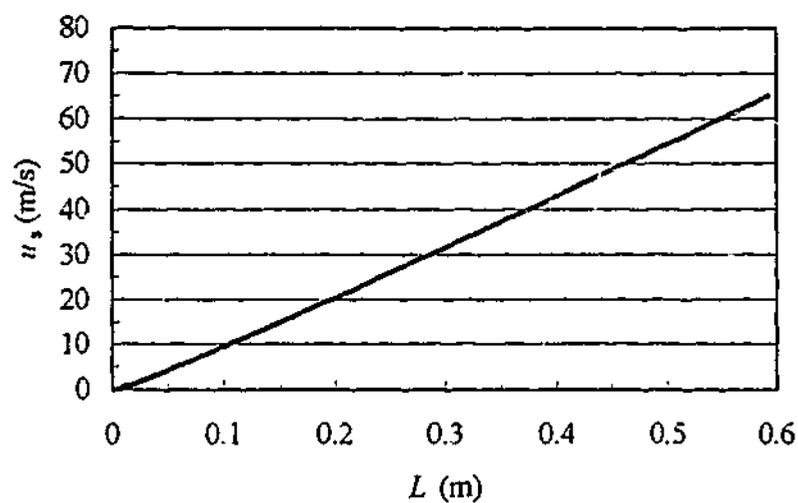
Figure 6.2 The relationship of u_s and L

6.2.2 The Rate of the Adsorption

Here we are also interested in the rate of the amount of the adsorbate adsorbed in a certain amount adsorbent. Assume the equilibrium isotherm is described by Henry's law, i.e.

$$q^* = Kc_b \tag{6.37}$$

where K is the Henry's law constant.

Rewrite Henry's equation as

$$c_b = \frac{1}{K}q^* \tag{6.38}$$

Thus, we have

$$\frac{\partial c_b}{\partial z} = \frac{1}{K}\frac{\partial q^*}{\partial z} \tag{6.39}$$

From Eq. (6.6), we have

$$q^* = \frac{1}{k_{op}}\frac{\partial \bar{q}}{\partial t} + \bar{q} \tag{6.40}$$

Substituting Eq. (6.39) into Eq. (6.40), we get

$$\frac{\partial c_b}{\partial z} = \frac{1}{Kk_{op}}\frac{\partial^2 \bar{q}}{\partial z \partial t} + \frac{1}{K}\frac{\partial \bar{q}}{\partial z} \tag{6.41}$$

Substituting Eq. (6.41) into Eq. (6.3), after rearrangment, we have

$$\frac{\partial^2 \bar{q}}{\partial z \partial t} + k_{op}\frac{\partial \bar{q}}{\partial z} + \frac{(1-\varepsilon)}{\varepsilon u_s}\rho_p Kk_{op}\frac{\partial \bar{q}}{\partial t} = 0 \tag{6.42}$$

The initial and boundary conditions are

$$\bar{q} = 0, \quad \text{at } z > 0 \ (0 \le z \le L), \, t \le 0$$

$$c_b = c_{in} \text{ so } q^* = q_{ref} = Kc_{in}, \quad \text{at } z = 0, \, t > 0 \tag{6.43}$$

From Eq.6.6, we have

$$\frac{d\bar{q}}{dt} = -k_{op}(\bar{q} - q^*) \tag{6.44}$$

The solution of Eq. 6.44 (at $z = 0$) is

$$\bar{q} - q^* = -q_{ref} \exp(-k_{op}t) \tag{6.45}$$

So the initial and boundary conditions in Eq. (6.43) are

$$\bar{q} = 0, \quad \text{at } z > 0, \, t \le 0$$

$$\bar{q} = q_{ref}\left(1 - \exp(-k_{op}t)\right) \quad \text{at } z = 0, \, t > 0 \tag{6.46}$$

Supposing $\bar{q}(z,t) = \bar{q}(z)\bar{q}(t)$ and substituting it and $\bar{q}(t) = q_{ref}\left(1 - \exp(-k_{op}t)\right)$ into Eq. (6.42), the solution is

$$\bar{q}(z,t) = q_{ref}\left[1 - \exp(-k_{op}t)\right]\exp\left[-\frac{1-\varepsilon}{\varepsilon u_s}\rho_p Kk_{op}z\exp(-k_{op}t)\right] \text{ mol/kg adsorbent} \tag{6.47}$$

For the small element shown in Fig. 6.1, the amount of adsorption is

$$\delta Q(z,t) = \bar{q}(z,t)dm_p = \bar{q}(z,t)n\rho_p V_p = \bar{q}(z,t)(1-\varepsilon)\pi R_b^2 \rho_p dz \tag{6.48}$$

where $\delta Q(z,t)$ is the amount of adsorption in the small element dz, dm_p is the mass of adsorbent in the small element dz, n is the number of the pellet, V_p is the volume of a pellet, R_b is the radius of the adsorption bed and $R_b = 2.425 \times 10^{-2}$ m.

Therefore, for the whole bed,

$$Q(t) = \int_0^L \delta Q(z,t)$$

$$= \frac{q_{ref}\pi R_b^2 \varepsilon u_s}{Kk_{op}}\left[1 - \exp(-k_{op}t)\right]\left\{1 - \exp\left[-\frac{1-\varepsilon}{\varepsilon u_s}\rho_p Kk_{op}L\exp(-k_{op}t)\right]\right\}\Big/\exp(-k_{op}t) \tag{6.49a}$$

Substituting values into the above equation, for our case

$$Q(t) = 3.5 \times 10^{-5}\frac{u_s}{k_{op}}\left[1 - \exp(-k_{op}t)\right]\left\{1 - \exp\left[-4.0222 \times 10^3 L(k_{op}/u_s)\exp(-k_{op}t)\right]\right\}\Big/\exp(-k_{op}t)$$

$$\tag{6.49b}$$

The rate of adsorption

$$\dot{Q}(t) = \frac{q_{ref}\pi R_b^2 \varepsilon}{K} \frac{u_s}{\exp(-k_{op}t)}$$

$$\left\{1 - \exp\left[-\frac{1-\varepsilon}{\varepsilon u_s}\rho_p K k_{op} L \exp(-k_{op}t)\right]\left[1 + \frac{1-\varepsilon}{\varepsilon u_s}\rho_p K k_{op} L \exp(-k_{op}t)\left(1 - \exp(-k_{op}t)\right)\right]\right\} \quad (6.50a)$$

For our case

$$\dot{Q}(t) = 3.5 \times 10^{-5} u_s \exp(k_{op}t)\left\{\begin{array}{l}1 - \exp\left[-4.0222 \times 10^3 (k_{op}/u_s)L \exp(-k_{op}t)\right] \\ \left[1 + 4.0222 \times 10^3 (k_{op}/u_s)L \exp(-k_{op}t)\left(1 - \exp(-k_{op}t)\right)\right]\end{array}\right\} \quad (6.50b)$$

The amount of adsorption and the rate of the adsorption are shown in Fig. 6.3 and 6.4, respectively.

(a)

(b)
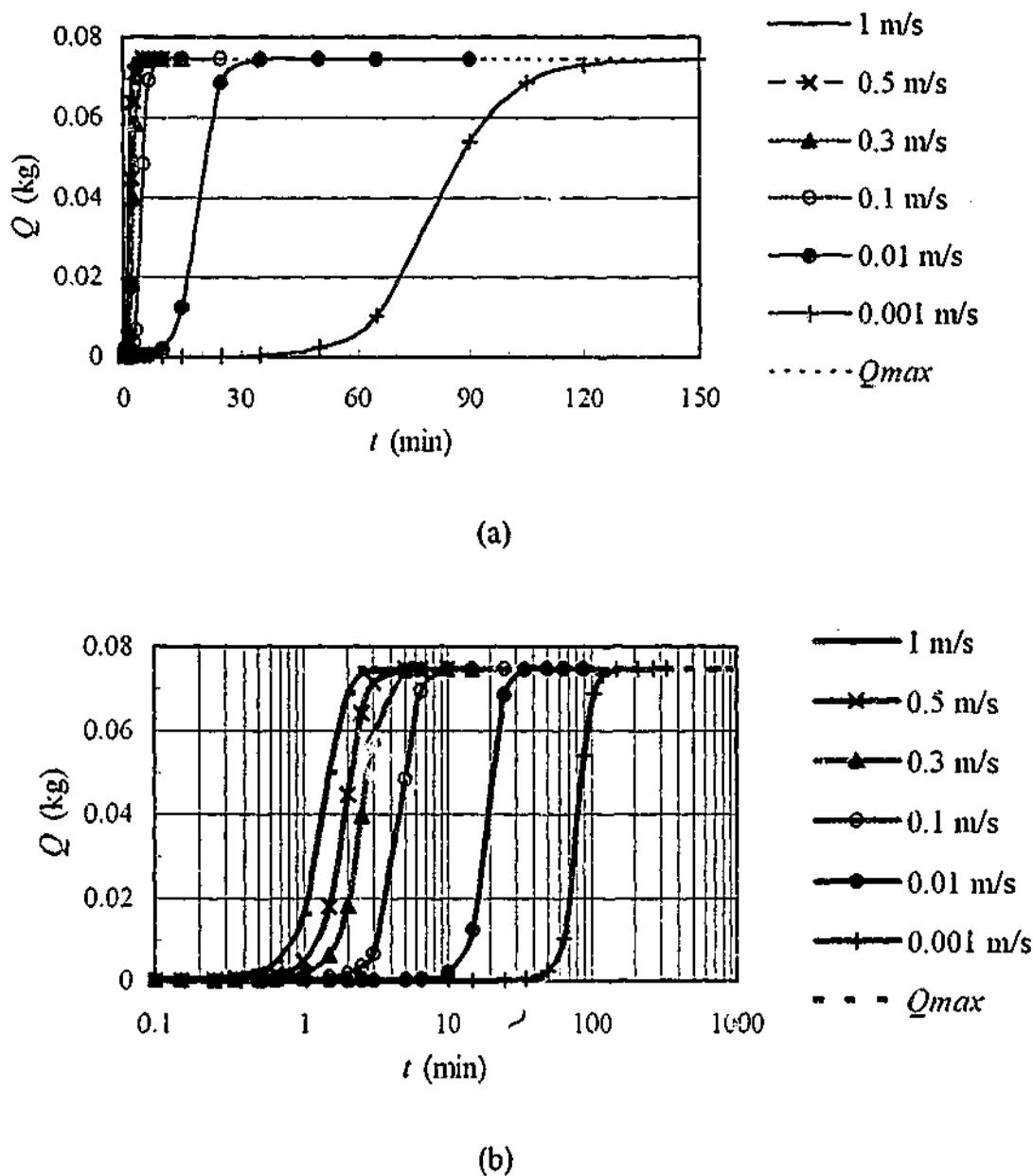
Figure 6.3 The relationship of the amount of adsorption and velocity and time

(a)

(b)
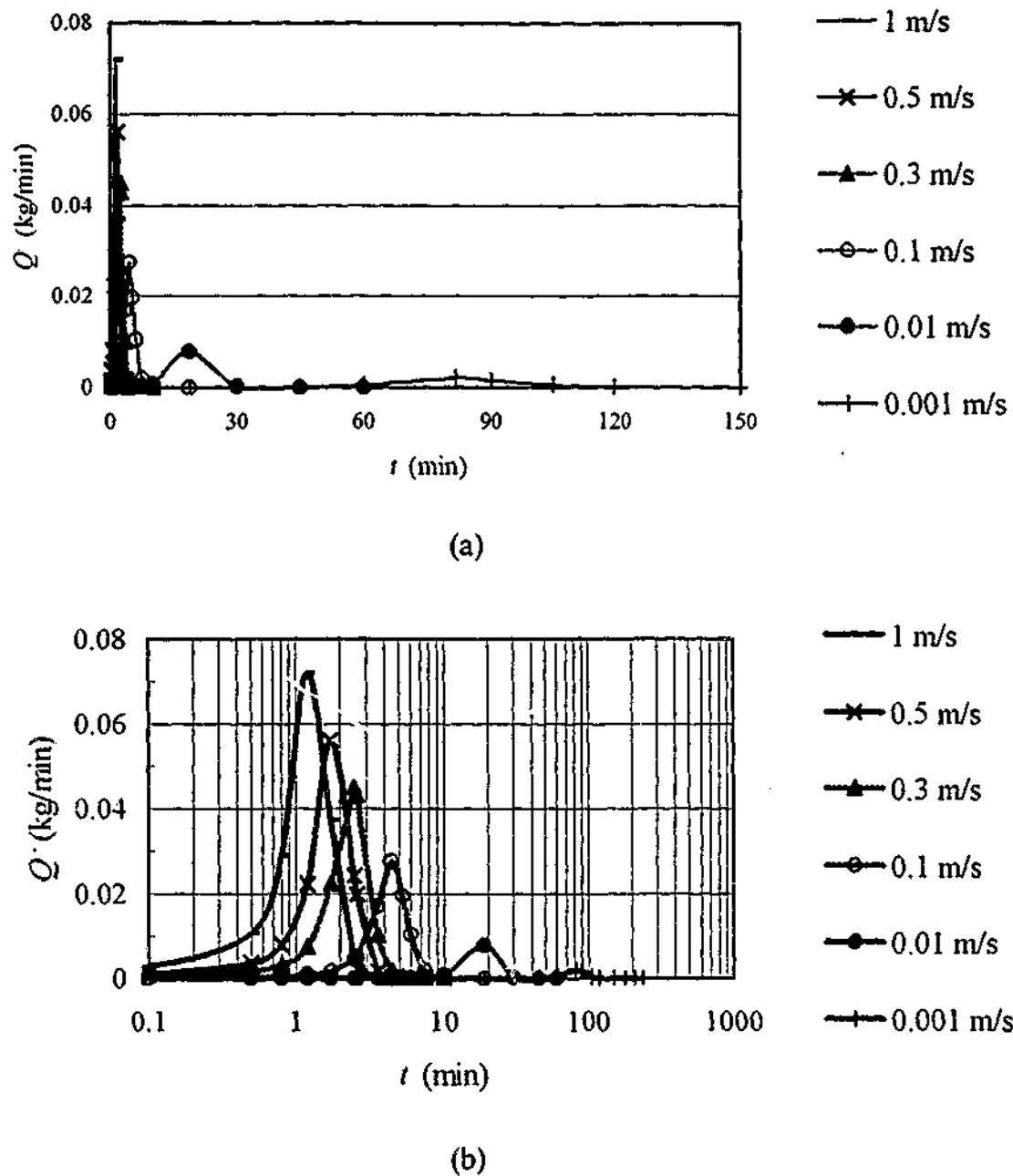
Figure 6.4 The relationship of the rate of adsorption and velocity and time

It can be seen that the higher the velocity, the quicker the adsorption takes place. For a certain velocity, the rate of adsorption increases first and then decreases. The higher the velocity, the higher the peak value of the rate of adsorption and the earlier the peak occurs.

6.3 THE THEORETICAL RESULTS COMPARED TO THE EXPERIMENTAL DATA

To justify the theory developed here, it is necessary to compare the theoretical results with the test data. Of primary interest is the adsorption rate in the adsorption/refrigeration process. This process starts from the amount adsorbed $m_{ad}x_{min}$ and stops at $m_{ad}x_{max}$. Fig. 6.5 shows such an adsorption range. The theoretical and experimental relationship of adsorption amount and the time, and rate of adsorption and the time in the adsorption range is shown in Fig. 6.6 and 6.7, respectively.
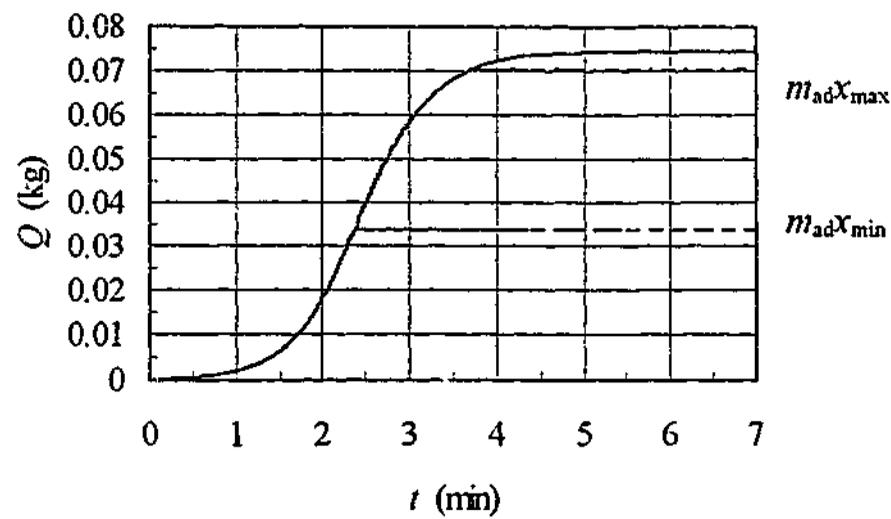
Figure 6.5 The adsorption range in an adsorption/refrigeration process (T_1=20°C, T_3=85°C, T_e=2°C, T_c=35°C, and u_s=0.3 m/s)
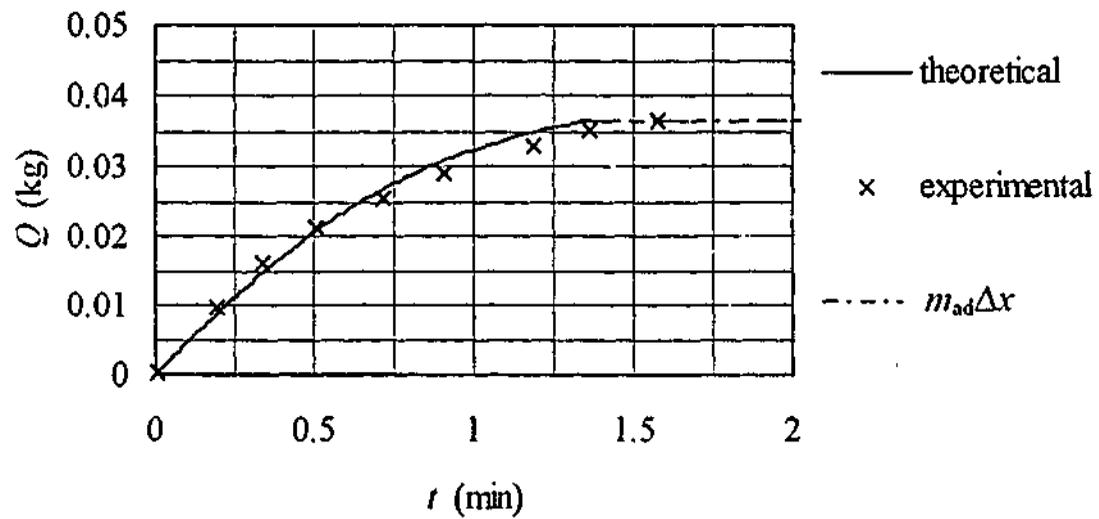
Figure 6.6 The theoretical and experimental relationship of adsorption amount and the time in the adsorption range
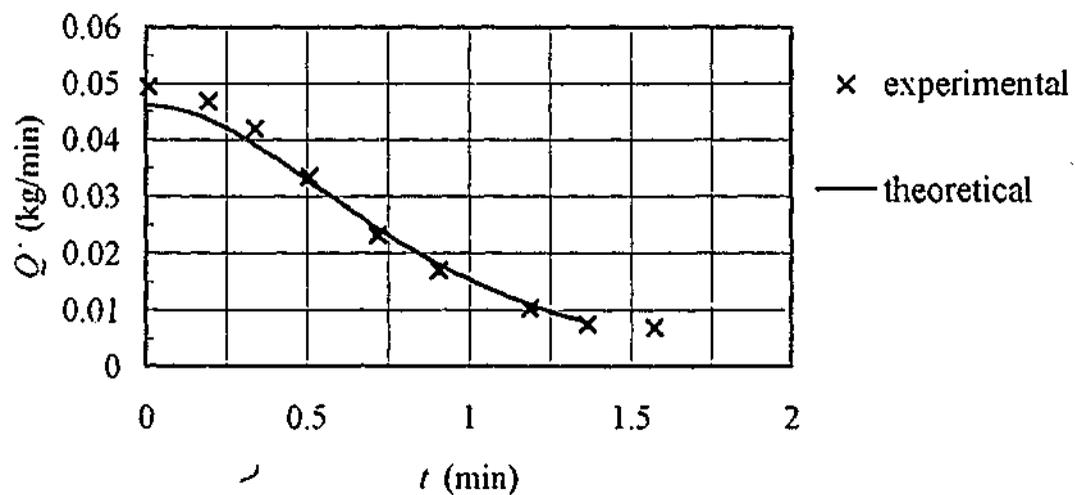
Figure 6.7 The theoretical and experimental relationship of the rate of adsorption and the time in the adsorption range

It can be seen from Fig. 6.6 and 6.7, the theoretical results agree with the experimental data although there is a little derivation. This derivation can be explained as follows. The theoretical calculation is based on the isothermal adsorption model and the temperature of the bed is assumed as 30°C. In the experiment, the bed is left to cool to a temperature just above ambient before the adsorption process starts. Therefore, at the beginnings of the adsorption, the real adsorption rates are a little higher than the theoretical values. With the adsorption proceeding, the temperature of the bed rises, and will be over 30°C, so the real adsorption rates are a little less than the theoretical values in this phase.

6.4 THE SUPERFICIAL VELOCITY AND THE RATE OF COOLING

With the rate of adsorption, the rate of cooling can be decided as

$$\dot{Q}_c = \dot{Q}(t)h_{fg} \tag{6.51}$$

which is shown in Fig. 6.5.

In practical cases, the heat leak is inevitable. Obviously only when $\dot{Q}_c > \dot{Q}_{leak}$ will there be net cooling effect.

(a)

(b)
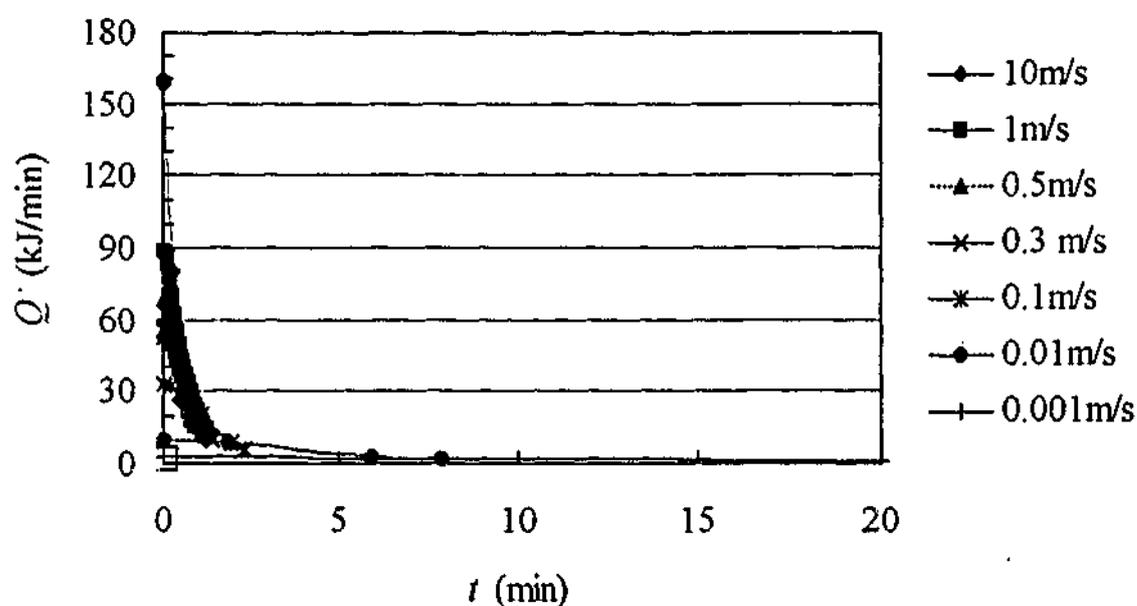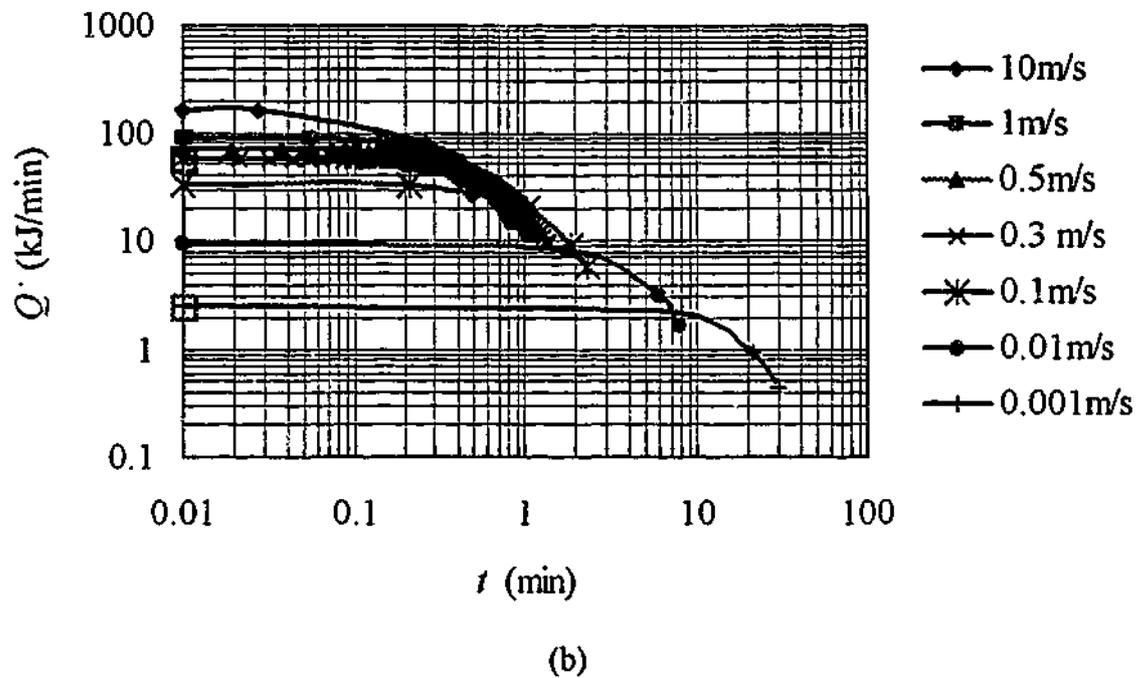
Figure. 6.8 The relationship of the rate of adsorption and velocity and time

For different evaporators, the rates of heat leakage may be different. In the condition that there is at least some cooling effect available in the next morning, ie, the heat lost due to the heat leakage in the refrigerating and storing period (which is assumed from 22:00 to 6:00, ie, 8 hours) is less than the cooling generated in the refrigeration period, the maximum allowable heat leakage rate is

$$\dot{Q}_{leak} = Q_{gro,c} /(8 \times 60) \qquad kJ \ / \min$$

In a typical condition (T_1=20°C, T_e=2°C, T_c=35°C, and T_3=85°C), the gross cooling effect is 41.1337 kJ (chapter 5), so the rate of heat leakage is 0.086 kJ/min. From Fig. 6.8, it can be seen that in the range of the amount of adsorption (0 to $m_{ad}(x_{max}- x_{min})$), the adsorption rate is greater than that required when the velocity equal to, and greater than, 0.001 m/s. Since the higher the velocity, the more heat is needed in the heating/desorption process (assuming that the fan runs at the same velocity in evaporating/cooling and heating/desorption processes); On the other hand, the lower the velocity used, the heavier the thermal insulation of the evaporator required. Since the insulation layer can not be too thick, the value of the lowest allowable velocity is limited. In our experimental rig, the evaporator could not be insulated, so the heat leakage rate is high and a high velocity is needed to produce net cooling effect. At the velocity of 0.3 m/s, frostwork at the surface of the evaporator could be observed. That is why the velocity of 0.3 m/s was taken in the research. Therefore, the lowest velocity which is determined by the condition of the thermal insulation of the evaporator can be adopted in the design for the prototype for such applications.

7

Exergy (Availability) Analysis of the Adsorption Refrigeration System

The first law analysis of thermodynamics studied in chapter 5 deals with the *quantity* of energy. Energy has also *quality*. In a complete and advanced analysis on an energy system, the *quality* of energy should also be analysed. *Exergy* analysis is a powerful tool for the efficient use of energy resources and the optimisation of energy systems. In this chapter, exergy analysis of the solar adsorption refrigeration system is described. Firstly, the exergy associated with different energy forms is comprehensively reviewed and the exergy for mixtures and the *Irreversibility* (exergy destruction) are developed. Then the detailed exergy analysis of the processes of the cycle and the whole cycle are carried out, and yields the numerical results. Since a detailed exergy analysis for adsorption refrigeration system has not been reported, the methodology of the analysis presented here is new. Part of the work in this chapter has already been published (Publication 17).

7.1 EXERGY

Thermodynamic availability or *exergy*[†] is the maximum work that can be obtained from a given form of energy using the environmental parameters as the reference state. If a system reaches the final state which is in mechanical and thermal equilibrium with the environment ($P=P_0$, $T=T_0$), the final state is called the *restricted dead state* of the system or the *environment state* (it is restricted in the sense that the chemical equilibrium with the environment is not considered), and the maximum work extractable from the system and the environment is called the *thermomechanical (physical) availability* or *thermomechanical (physical) exergy* to reinforce the observation that the exergy is released as the system and the environment reach thermal and mechanical equilibrium only. If a system comes also to chemical equilibrium with the environment but does not react chemically with the environment ($P=P_0$, $T=T_0$, $\mu_k =\mu^0_k$), the equilibrium is called the *unrestricted equilibrium*. The state at this equilibrium (with the environment) is called the *dead state*, and the maximum work obtainable in such process is called the *total exergy (availability)* (Bejan,1997, Kotas, 1995, Moran, 1989, Wark, 1995).

7.1.1 Exergy of a Closed System — Restricted Dead State

For a control mass, the exergy is defined as (Bejan,1997, Moran, 1989, Wark, 1995)

[†] Occasionally, thermodynamic availability and exergy are defined differently (Winterbone, 1997).

$$E_{x,nf}^{tm} = (E - U_0) + P_0(V - V_0) - T_0(S - S_0)^\dagger \qquad (7.1a)$$

where E_x is used identically to denote exergy for all situations. The superscript *tm* represents the exergy is the thermomechanical exergy, and the subscript *nf* represents the exergy is for the nonflow processes. Symbols E $(=U+KE+PE)$. V, and S denote the energy, volume, and entropy of the control mass at the given state respectively and U_0, V_0, and S_0 are the same properties when the control mass is at rest at the dead state.

The specific availability on a mass basis is

$$e_{x,nf}^{tm} = (u - u_0) + P_0(v - v_0) - T_0(s - s_0) + V^2/2 + gz \qquad (7.1b)$$

where V is the velocity.

The change in the availability between two states of a closed system is

$$\Delta E_{x,nf}^{tm} = (U_2 - U_1) + P_0(V_2 - V_1) - T_0(S_2 - S_1) + \Delta KE + \Delta PE \qquad (7.2)$$

7.1.2 Flow Exergy — Restricted Dead State

The availability for a stream or flow on a unit basis the flow exergy is defined as (Bejan, 1997, Moran, 1989, Wark, 1995)

$$e_{x,f}^{tm} = (h - h_0) - T_0(s - s_0) + V^2/2 + gz \qquad (7.3a)$$

where the subscript f represents the exergy is for the flow processes, h and s represent the specific enthalpy and entropy, respectively.

Eq. (7.3a) can also be rewritten as

$$e_{x,f}^{tm} = (h + V^2/2 + gz - T_0s) - (h_0 - T_0s_0) = b - b_0 \qquad (7.3b)$$

where b is called the *stream availability (exergy) parameter* (Wark, 1995) and is defined as

$$b = h + V^2/2 + gz - T_0s \qquad (7.4)$$

The change in the availability between two states of an open system is

$$\Delta e_{x,f}^{tm} = (h_2 - h_1) - T_0(s_2 - s_1) + (V_2^2 - V_1^2)/2 + g(z_2 - z_1) \qquad (7.5)$$

[†] Sometimes, the kinetic and potential-energy terms are excluded from the definition of availability (Howell and Buckius, 1992, Kotas, 1995)

7.1.3 Exergy of a Closed System — Unrestricted Dead State (the Total Exergy)

For a control mass, the *Total Exergy* is defined as (Bejan, 1997, Moran, 1989, Wark, 1995)

$$E_{x,nf}^{tot} = E + P_0 V - T_0 S - \sum N_i \mu_i^0 \qquad (7.6a)$$

or

$$e_{x,nf}^{tot} = e + P_0 v - T_0 s - \sum x_i \mu_i^0 \qquad (7.6b)$$

where the superscript *tot* represents the exergy is the total exergy, N_i ($i = 1, ..., n$) and x_i is the number of moles of substance i in the mixture and the mole fraction of the substance respectively, and μ_i^0 is the *chemical potential* of substance i in the unrestricted or environment dead state.

The change in the availability between two states of a closed system is

$$\Delta E_{x,nf}^{tot} = (U_2 - U_1) + P_0(V_2 - V_1) - T_0(S_2 - S_1) + \Delta KE + \Delta PE - (\sum_2 N_i \mu_i^0 - \sum_1 N_i \mu_i^0) \qquad (7.7)$$

The *chemical potential* of substance i in the mixture is defined as (Bejan, 1997; Kotas, 1995; Moran, 1989; Smith, et al. 1996; Wark, 1995)

$$\mu_i = \left(\frac{\partial G}{\partial N_i} \right)_{P,T,N_j} \qquad (7.8)$$

where G is the Gibbs function.

Euler's equation in thermodynamics (Hsieh, 1975; Smith et al 1996) is

$$U = TS - PV + \sum N_i \mu_i \qquad (7.9)$$

Using Euler's equation at the restricted dead state, we have

$$U_0 = T_0 S_0 - P_0 V_0 + \sum N_i \mu_{i0} \qquad (7.10)$$

where μ_{i0} is the chemical potential of substance i within the mixture at restricted dead state.

Therefore, the *thermomechanical* exergy

$$E_{x,nf}^{tm} = (E - U_0) + P_0(V - V_0) - T_0(S - S_0) = E + P_0 V - T_0 S - (U_0 + P_0 V_0 - T_0 S_0)$$
$$= E + P_0 V - T_0 S - \sum N_i \mu_{i0} \qquad (7.11)$$

By comparing Eq. (7.6) with the exergy as the control mass passes from a given state to the restricted dead state, ie, the thermomechanical exergy (Eq. (7.11)), Eq (7.6) can be written as

$$E_{x,nf}^{tot} = E + P_0 V - T_0 S - \sum N_i \mu_{i0} + \sum N_i (\mu_{i0} - \mu_i^0)$$
$$= E_{x,nf}^{tm} + \sum N_i (\mu_{i0} - \mu_i^0) \qquad (7.12a)$$

or

$$e_{x,nf}^{tot} = e_{x,nf}^{tm} + \sum x_i (\mu_{i0} - \mu_i^0) \qquad (7.12b)$$

where $\sum N_i(\mu_{i0} - \mu_i^0)$ is defined as the nonflow *chemical exergy*, $E_{x,nf}^{ch}$ (Bejan,1997, Kotas, 1995, Moran, 1989, Wark, 1995), i.e.,

$$E_{x,nf}^{ch} = \sum N_i (\mu_{i0} - \mu_i^0) \qquad (7.13)$$

From Eq (7.12) it can be seen that that the total exergy of a control mass can be written as the sum of two contributions - the thermomechanical exergy and the chemical exergy. The first is the maximum work the control mass does as it is brought by means of ideal processes from its initial state to a condition of thermal and mechanical equilibrium with the environment, eg, to the restricted dead state. For clarity, the thermomechanical exergy is denoted by the superscript *tm* throughout this thesis. The second is the maximum work released as the control mass be brought into chemical equilibrium with the environment while the temperature and pressure before and after this process are fixed at T_0 and P_0 respectively.

7.1.4 Flow Exergy — Unrestricted Dead State (the Total Exergy)

The Total Exergy for a stream or flow on a unit basis is defined as (Bejan, 1997, Moran, 1989, Wark, 1995)

$$e_{x,f}^{tot} = h - T_0 s - \sum x_i \mu_i^0 \qquad (7.14)$$

where x_i is the mole fraction of substance i in the mixture, h and s is the molal enthalpy and entropy, respectively, of the mixture. The kinetic and potential energy terms are not shown.

The change in the availability between two states of a control volume is

$$\Delta e_{x,f}^{tot} = (h_2 - h_1) - T_0 (s_2 - s_1) - (\sum_2 x_i \mu_i^0 - \sum_1 x_i \mu_i^0) \qquad (7.15)$$

The molal enthalpy and entropy of the mixture are defined as

$$h = \Sigma x_i \bar{h_i} \qquad \text{and} \qquad s = \Sigma x_i \bar{s_i} \qquad (7.16)$$

The "overbar" signifies the partial molal properties (Wark, 1995). For the ith component in a mixture, the partial molal property is (Smith, et al. 1996, Wark, 1995)

$$\bar{y}_i = \left(\frac{\partial Y}{\partial N_i}\right)_{P,T,N_j} \tag{7.17}$$

Eq. (7.14) can be rewritten as (Bejan,1997, Moran, 1989, Wark, 1995)

$$e_{x,f}^{tot} = (h - h_0) - T_0(s - s_0) + \sum x_i(\mu_{i0} - \mu_i^0) \tag{7.18a}$$

Again, it is helpful to compare this expression with the exergy delivered as the stream reaches the restricted dead state, ie the thermomechanical exergy in Eq. (7.3).

Hence, Eq. (7.18a) can be expressed as

$$\begin{aligned} e_{x,f}^{tot} &= e_{x,f}^{tm} + \sum x_i(\mu_{i0} - \mu_i^0) \\ &= e_{x,f}^{tm} + e_{x,f}^{ch} \end{aligned} \tag{7.18b}$$

This equation shows that the total flow exergy can be viewed as the sum of the thermomechanical (or physical) flow exergy and the chemical exergy defined by Eq. (7.13).

The chemical exergy can be expressed as (Zhu, 1988)

$$e_x^{ch} = RT_0 \sum x_i \ln \frac{a_{i0}}{a_i^0} \tag{7.19}$$

where a_{i0} and a_i^0 is the *activity* of substance i within the mixture at restricted dead state and the activity of substance i in the unrestricted or environment dead state respectively.

7.1.5 The Exergy of Mixtures

The general exergy equation for mixtures can be expressed as

$$e_x(T, P) = \Sigma x_i e_{xi}(T, P_i) \tag{7.20}$$

or

$$e_x(T, P) = \Sigma x_i \, \bar{e}_{xi}(T, P) \tag{7.21}$$

where e_{xi} is the exergy of ith component and is evaluated at the T and its partial pressure P_i, $\bar{e}_{xi}(T, P)$ again is the partial molal exergy of ith component.

The author (You et al, 1993a, 1993b) from the approach of *solution thermodynamics* (Hsieh, 1975, Smith and van Ness, 1987) introduced the concept of the *Exergy Change of Mixing* which is defined as

$$\Delta E_{x,mix} = E_x - \sum N_i e_{xi}(T,P) = \sum N_i (\bar{e}_i - e_{xi}(T,P)) \tag{7.22a}$$

or

$$\Delta e_{x,mix} = e_x - \sum x_i e_{xi}(T,P) = \sum x_i (\bar{e}_i - e_{xi}(T,P)) \tag{7.22b}$$

where E_x (e_x) is the exergy of the mixture, $\bar{e}_i$ is the partial molar exergy of component i, and $e_{xi}(T,P)$ is the molar exergy of the component. For all pure species, $e_{xi}(T,P)$ is evaluated at the same T and P which is simple to calculate. The calculation of formulas for the Exergy Change of Mixing were derived as (You et al, 1993a, 1993b)

$$\Delta e_{x,mix}^{tm} = -RT(1-\frac{T_0}{T})\sum x_i (\frac{\partial \ln a_i}{\partial \ln T})_{P,x} + RT_0 \sum x_i \ln a_i \qquad \text{(for restricted dead state)} \tag{7.23}$$
$$= (1-\frac{T_0}{T})\Delta h_{mix} + RT_0 \sum x_i \ln a_i$$

and

$$\Delta e_{x,mix}^{tot} = (1-\frac{T_0}{T})\Delta h_{mix} + RT_0 \sum x_i \ln \frac{a_i}{a_i^0} \qquad \text{(for unrestricted dead state)} \tag{7.24}$$

where

$$\Delta h_{mix} = -RT \sum x_i (\frac{\partial \ln a_i}{\partial \ln T})_{P,x} \tag{7.25}$$

is defined as the *Enthalpy Change of Mixing* (Hsieh, 1975, Smith, 1987).

The meanings of activity can be summarised as

1. Pure ideal gas	$a = P$	Pressure
2. The ith component in an ideal gas mixture	$a_i = P_i$	Partial pressure of species i
3. Pure real gas	$a = f$	Fugacity
4. The ith component in a real gas mixture	$a_i = \hat{f}_i$	Fugacity of species i
5. The ith component in an ideal solution	$a_i = x_i$	Mole fraction of species i
8. The ith component in a dilute solution	$a_i = x_i$	Mole fraction of species i
7. The ith component in a non-ideal solution	$a_i = \gamma_i x_i$	(γ_i is the activity coefficient)
8. Pure liquid	$a = x = 1$	Mole fraction (=1)
9. Pure solid	$a = x = 1$	Mole fraction (=1)

Eq (7.23) and (7.24) have explicit meanings. The first term in the right side of both equations reflects the effect of the enthalpy change of mixing (*Heat Effect*) Δh_{mix} on the mixture's exergy. The second term in the right side of Eq (7.23) and (7.24) reflects the effect of the diffusion of the

components on the mixture's exergy and were called *Diffusion Exergy* (You et al, 1993a, 1993b). The so-called Diffusion Exergy can be called chemical exergy in general.

The *exergy of a mixture* can be calculated by

$$e_x = \Sigma x_i e_{xi}(T, P) + \Delta e_{x,mix}$$ (7.26a)

or

$$E_x = \Sigma N_i e_{xi}(T, P) + \Delta E_{x,mix}$$ (7.26b)

It can be seen that You's approach in calculating the exergy for mixtures is simple and helpful for understanding the components of exergy.

As a specific example, You et al (1993a, 1993b, 1993c) derived the exergy for moist air from this approach and carried out the exergy analysis on a heat pump drying system.

7.1.6 The Exergy Transfer Accompanying Heat

The availability transfer accompanying heat is

$$E_{xQ} = \int_1^2 (1 - \frac{T_0}{T}) \delta Q$$ (7.27)

where T is the temperature of the heat source.

If the temperature of the heat source is lower than the temperature of the environment, the availability transfer accompanying the heat is

$$E_{xQ} = \int_1^2 (\frac{T_0}{T} - 1) \delta Q$$ (7.28)

7.1.7 The Exergy Transfer Accompanying Work

The exergy of a system is the difference of the maximum amount of work that can be derived from the system ($-W$) and the work done on the environment $P_0(V_2-V_1)$ (Wark, 1995), ie,

$$E_{xW} = -W - P_0(V_2-V_1)$$ (7.29)

If there were no change in the system volume during the process, the transfer of exergy accompanying work would equal the work of the system.

7.1.8 The Quality of Solar Irradiance

The quality of the solar irradiance (Winter et al, 1991) is given by

$$\eta(f) \approx 1 - \frac{4}{3}\frac{T_0}{T_s}(1 - 0.28\ln f) \tag{7.30}$$

where f is the dilution factor.

For a standard spectrum with $f=1.3\times10^{-5}$, taking $T_s=5,777$ K and $T_0=298$ K into Eq.(7.30), $\eta(f) \approx 0.717$.

The exergy of solar radiation

$$E_{x,Q_s} = \eta(f)Q_s \tag{7.31}$$

7.1.9 The Irreversibility I (The Exergy Loss)

Unlike energy, availability is not conserved. It is destroyed by irreversibility. The irreversible destruction of availability, or the *irreversibility*, (denoted by I) is defined as

$$\dot{I}_{CV} = \dot{W}_{act} - \dot{W}_{rev} = \dot{W}_{act,u} - \dot{W}_{rev,u} = T_0\dot{\sigma}_{CV} \qquad \text{(for a control volume)} \tag{7.32}$$

$$I_{CM} = W_{act} - W_{rev} = W_{act,u} - W_{rev,u} = T_0\sigma_{CM} \qquad \text{(for a control mass)} \tag{7.33}$$

and

$$\dot{I}_{tot} = \dot{W}_{act} - \dot{W}_{rev} = T_0\dot{\sigma}_{tot} \qquad \text{(for a control volume and the environment)} \tag{7.34}$$

where the subscript *act* and the *rev* represent the actual and the reversible process between the same end states, the subscript u represents the useful work, and σ represents the *entropy production* or *entropy generation*.

The irreversibility of a process can be evaluated from the availability equation which can be accomplished by considering the first and the second law together.

The conservation of energy equation for a general control volume process is (Wark, 1995)

$$\sum \dot{Q}_i + \dot{W}_{net} + \sum_{in}(h + \frac{V^2}{2} + gz)\dot{m} - \sum_{out}(h + \frac{V^2}{2} + gz)\dot{m} = \frac{dE_{CV}}{dt} \tag{7.35}$$

The work we are interested here is the *useful* work. Since the work done against the atmosphere is not available for other useful purposes, it must be eliminated. That is

$$\dot{W}_{net,u} = \dot{W}_{net} + P_0(\frac{dV}{dt})_{cr} \tag{7.36}$$

The second law (entropy equation) is (Moran, 1996)

$$\dot{\sigma}_{cr} = \frac{dS_{cr}}{dt} + \sum_{out}\dot{m}s - \sum_{in}\dot{m}s - \sum\frac{\dot{Q}_i}{T_i} \tag{7.37}$$

Multiplying the second law Eq. (7.37) by the environment temperature T_0 and subtracting the resulting equation from the first law Eq. (7.35) and also substituting Eq. (7.36) yield

$$\dot{I}_{cr} = T_0\dot{\sigma}_{cr} = \sum\dot{Q}_i(1-\frac{T_0}{T_i}) + \dot{W}_{net,u}$$
$$-[\sum_{out}(h+\frac{V^2}{2}+gz-T_0s)\dot{m} - \sum_{in}(h+\frac{V^2}{2}+gz-T_0s)\dot{m}] - \frac{d(E+P_0V-T_0S)_{cr}}{dt} \tag{7.38a}$$

Substituting Eq. (7.4) into Eq. (7.38a), we have

$$\dot{I}_{cr} = \sum\dot{Q}_i(1-\frac{T_0}{T_i}) + \dot{W}_{net,u} - (\sum_{out}b\dot{m} - \sum_{in}b\dot{m}) - \frac{d(E+P_0V-T_0S)_{cr}}{dt} \tag{7.38b}$$

The first and the second terms in the right side of Eq. (7.38b) is in the form of availability, while the third and the forth terms are not in the form of availability. The next step is to express each term in the right side in the form of exergy.

If the control volume is in equilibrium with the environment (T_0, P_0), there is no net heat and work interaction, and there is no irreversibility. Since there is mass entering and leaving the CV, although its intensive properties keep constant, its extensive properties may change with time. Eq. (7.38a) reduces to be

$$\frac{d(U_0+P_0V_0-T_0S_0)_{cr}}{dt} = \sum_{in}(h_0-T_0s_0)\dot{m} - \sum_{out}(h_0-T_0s_0)\dot{m} \tag{7.39}$$

Alternatively, for a control mass, at time t, and a later time $t+\Delta t$,

$$(U_0+P_0V_0-T_0S_0)_{CM,t} = (U_0+P_0V_0-T_0S_0)_{CV,t} + \sum_{in}(u_0+P_0v_0-T_0s_0)\delta m \tag{7.40}$$

and

$$(U_0+P_0V_0-T_0S_0)_{CM,t+\Delta t} = (U_0+P_0V_0-T_0S_0)_{CV,t+\Delta t} + \sum_{out}(u_0+P_0v_0-T_0s_0)\delta m \tag{7.41}$$

Subtracting Eq. (7.41) from (7.40), substituting the relationship $h_0=u_0+P_0v_0$, dividing each term by Δt, and taking the limit as Δt approaches zero, we have

$$\frac{d(U_0 + P_0V_0 - T_0S_0)_{CM}}{dt} = \frac{d(U_0 + P_0V_0 - T_0S_0)_{CV}}{dt} - [\sum_{in}(h_0 - T_0s_0)\dot{m} - \sum_{out}(h_0 - T_0s_0)\dot{m}] \quad (7.42)$$

The left term is zero (a control mass in equilibrium with the environment, both its intensive properties and extensive properties do not change with time), so we get the Eq. (7.39).

Or more directly

$$\frac{d(U_0 + P_0V_0 - T_0S_0)_{CV}}{dt} = \frac{dm(u_0 + P_0v_0 - T_0s_0)_{CV}}{dt} = (\sum_{in}\dot{m} - \sum_{out}\dot{m})(h_0 - T_0s_0)$$
$$= \sum_{in}(h_0 - T_0s_0)\dot{m} - \sum_{out}(h_0 - T_0s_0)\dot{m} \quad (7.43)$$

Subtracting Eq. (7.43) from (7.38), and substituting Eq. (7.1a) and Eq. (7.3) into it, we have

$$\dot{I}_{CV} = \sum_j (1 - \frac{T_0}{T_i})\dot{Q}_i + \dot{E}_{xW} - (\sum_{out}e_{x,f}\dot{m} - \sum_{in}e_{x,f}\dot{m}) - \frac{dE_{x,CV}}{dt} \quad (7.38c)$$

It can be seen that the rate of irreversibly in a control volume is the difference of the rate of availability transfer associated with the heat, work, and mass transfer at the control surface, as well as the rate of availability change in the control volume.

The evaluation of the availability transfer accompanying heat in the Eq. (7.38) requires knowledge of Q_i at a portion of the control surface at temperature T_i. However, the value of Q_i and T_i may be not known at every position on the control surface. On the other hand, in some cases, not only the control volume but also the reservoirs with which it interacts should be considered. By choosing a system which includes the control volume and the environment and any other thermal reservoirs which interacts, the calculation of Q_i and T_i can be avoided. In these cases, the total heat transfer rate can be expressed as the heat-transfer rates associated with the environment at T_0 and those reservoirs at T_j. That is

$$\dot{Q} = \sum \dot{Q}_i = \dot{Q}_0 + \sum \dot{Q}_j \quad (7.44)$$

By substituting Eq (7.44) into Eq (7.35), we have

$$\dot{Q}_0 + \sum \dot{Q}_j + \dot{W}_{net} + \sum_{in}(h + \frac{V^2}{2} + gz)\dot{m} - \sum_{out}(h + \frac{V^2}{2} + gz)\dot{m} = \frac{dE_{CV}}{dt} \quad (7.45)$$

By this way, not only the control volume but also the reservoirs with which it interacts are considered. Hence, the form of the entropy equation here is

$$\dot{\sigma}_{tot} = \dot{\sigma}_{CV} + \dot{\sigma}_Q = \frac{dS_{CV}}{dt} + \sum_{out} \dot{m}s - \sum_{in} \dot{m}s - \frac{\dot{Q}_0}{T_0} - \sum \frac{\dot{Q}_j}{T_j} \qquad (7.46)$$

Eliminating Q_0 between Eq.(7.45) and (7.46), the result is

$$\dot{I}_{tot} = T_0\dot{\sigma}_{tot} = \sum \dot{Q}_j(1 - \frac{T_0}{T_j}) + \dot{W}_{net,u}$$

$$-[\sum_{out}(h + \frac{V^2}{2} + gz - T_0s)\dot{m} - \sum_{in}(h + \frac{V^2}{2} + gz - T_0s)\dot{m}] - \frac{d(E + P_0V - T_0S)_{CV}}{dt} \qquad (7.47a)$$

where the direction of the Q_i is relative to the control surface. Similar to Eq. (7.38), Eq. (7.47a) can be expressed as

$$\dot{I}_{tot} = \sum(1 - \frac{T_0}{T_j})\dot{Q}_j + \dot{E}_{xW} - (\sum_{out} e_{x,f}\dot{m} - \sum_{in} e_{x,f}\dot{m}) - \frac{dE_{x,CV}}{dt} \qquad (7.47b)$$

Although Eq. (7.38c) and (7.47b) have a similar format, their usage is quite different. Eq. (7.38c) applies solely to the control volume of interest. On the other hand, Eq (7.47b) applies to the control volume and the reservoirs with which it interacts.

Although the derivation of irreversibility was done only for the thermomechanical exergy, the equations are easily to extend to the total exergy.

7.2 EXERGY ANALYSIS OF THE ADSORPTION REFRIGERATION SYSTEM

In our refrigeration system, we use methanol as the refrigerant, activated carbon as the adsorbent, and Helium as the pressure-adjusting agent. Although the pure liquid methanol and the pure solid activated carbon can be taken as the dead states for the liquid methanol and activated carbon, there is no definite dead state for methanol vapour and Helium. Hence, the restricted dead state is chosen as the dead state when evaluating the exergy of the substance.

7.2.1 Heating Process 1—2

In this process, the fan is off. The heat is used to increase the internal energy (temperature) of the collector/generator, of the adsorbent/refrigerant (eg. carbon/methanol), and of the pressure-adjusting gas. In this case, the collector and the collected space can be taken as a closed system. In our case, $P \approx P_0$. For $T > T_0$, the exergy of the control mass according to Eq. (7.26), (7.1), and (7.23) is

$$E_{x,nf} = (U - U_0) - T_0(S - S_0) + N(1 - T_o/T)\Delta\tilde{h}_{mix} + NRT_0\sum x_i \ln a_i \qquad (7.48)$$

Since in our case $P \approx P_0$, similar to Eq. (5.23)

$$U - U_0 = \sum m_i (u - u_0)_i = (m_{c/g} c_{c/g} + m_{ad} c_{ad} + m_{ad} x_{max} \overline{c}_{f,T_0-T} + m_{pr} c_{pr})(T - T_0) \tag{7.49}$$

and

$$S - S_0 = \int \frac{\delta Q}{T} = \int \frac{dU}{T} = (m_{c/g} c_{c/g} + m_{ad} c_{ad} + m_{ad} x_{max} \overline{c}_{f,S,T_0-T} + m_{pr} c_{pr}) \ln \frac{T}{T_0} \tag{7.50}$$

where $\overline{c}_{f,S}$ is the mean heat capacity and is calculated as

$$\overline{c}_S = \frac{\int_{T_1}^{T_2} \frac{c}{T} dT}{\ln(T_2/T_1)} = \frac{\int_{T_1}^{T_2} (\frac{\alpha'}{T} + \beta' + \gamma T) dT}{\ln(T_2/T_1)} = \alpha' + \beta' \frac{(T_2 - T_1)}{\ln(T_2/T_1)} + \frac{\gamma'}{2} \frac{(T_2^2 - T_1^2)}{\ln(T_2/T_1)} \tag{7.51}$$

For methanol, the specific heat capacity is given by Eq. (5.17b). So

$$\overline{c}_S = 3.3625 - 0.01189375 \frac{(T_2 - T_1)}{\ln(T_2/T_1)} + 0.0000152965 \frac{(T_2^2 - T_1^2)}{\ln(T_2/T_1)} \tag{7.52}$$

The heat of mixing $\Delta \widetilde{h}_{mix}$ is the adsorption heat h_{ad} here. Since the adsorption heat h_{ad} here is based on the amount (weight) of the refrigerant (eg. methanol),

$$N(1 - \frac{T_0}{T}) \Delta \widetilde{h}_{mix} = m_r (1 - \frac{T_0}{T}) h_{ad} = m_{ad} x (1 - \frac{T_0}{T}) h_{ad} \tag{7.53}$$

The last term in Eq. (7.48) can be determined as following. The definition of the heat of mixing (Eq. (7.25)) can be written as

$$\sum x_i (\frac{\partial \ln a_i}{\partial \ln T})_{P,x} = -\frac{\Delta \widetilde{h}_{mix}}{RT}, \quad \int \left(\sum x_i (\frac{\partial \ln a_i}{\partial \ln T})_{P,x} \right) d \ln T = -\int \frac{\Delta \widetilde{h}_{mix}}{RT} d \ln T$$

and
$$\sum x_i \ln a_i = \frac{\Delta \widetilde{h}_{mix}}{RT} + f(x) \tag{7.54}$$

For an ideal solution, $a_i = x_i$ and $\Delta h_{mix} = 0$, so $f(x) = \sum x_i \ln x_i$. Therefore

$$\sum x_i \ln a_i = \frac{\Delta \widetilde{h}_{mix}}{RT} + \sum x_i \ln x_i \tag{7.55}$$

and

$$N(1 - \frac{T_0}{T}) \Delta \widetilde{h}_{mix} + NRT_0 \sum x_i \ln a_i = N \Delta \widetilde{h}_{mix} + NRT_0 \sum x_i \ln x_i \tag{7.56}$$
$$= m_{ad} x h_{ad} + m_{ad} x R_r T_0 \sum x_i \ln x_i$$

where R_r is the gas constant for the refrigerant.

The exergy change of the control mass from state 1 to 2 for $T_2 > T_1 > T_0$ is

$$\Delta E_{x,nf,1-2} = \Delta U_{1-2} - T_0 \Delta S_{1-2} + N\left[(1 - \frac{T_0}{T_2})\Delta h_{mix,2} - (1 - \frac{T_0}{T_1})\Delta h_{mix,1}\right] \tag{7.57a}$$
$$+ NRT_0\left[\sum (x_i \ln a_i)_2 - \sum (x_i \ln a_i)_1\right]$$

Here

$$\Delta U_{1-2} = \sum m \Delta u_i = (m_{c/g}c_{c/g} + m_{ad}c_{ad} + m_{ad}x_{max}\bar{c}_{f,1-2} + m_{pr}c_{pr})(T_2 - T_1)$$

$$\Delta S_{1-2} = \int \frac{\delta Q}{T} = \int \frac{dU}{T} = (m_{c/g}c_{c/g} + m_{ad}c_{ad} + m_{ad}x_{max}\bar{c}_{f,S,1-2} + m_{pr}c_{pr})\ln \frac{T_2}{T_1}$$

and

$$N\left[(1 - \frac{T_0}{T_2})\Delta \tilde{h}_{mix,2} - (1 - \frac{T_0}{T_1})\Delta \tilde{h}_{mix,1}\right] + NRT_0\left[\sum (x_i \ln a_i)_2 - \sum (x_i \ln a_i)_1\right]$$
$$= m_{ad}x_{max}(h_{ad,2} - h_{ad,1}) + m_{ad}x_{max}R_rT_0\left[\sum (x_i \ln x_i)_2 - \sum (x_i \ln x_i)_1\right]$$

Therefore, the exergy change of the control mass for $T_2 > T_1 > T_0$ is

$$\Delta E_{x,1-2} = (m_{c/g}c_{c/g} + m_{ad}c_{ad} + m_{pr}c_{pr} + m_{ad}x_{max}\bar{c}_{f,1-2})(T_2 - T_1)$$
$$- (m_{c/g}c_{c/g} + m_{ad}c_{ad} + m_{pr}c_{pr} + m_{ad}x_{max}\bar{c}_{f,S,1-2})T_0 \ln \frac{T_2}{T_1} \tag{7.57b}$$
$$+ m_{ad}x_{max}(h_{ad,2} - h_{ad,1}) + m_{ad}x_{max}R_rT_0\left[\sum (x_i \ln x_i)_2 - \sum (x_i \ln x_i)_1\right]$$

For $T < T_0$, the exergy function E_x' [†] of the control mass is

$$E_{x,nf}' = (U_0 - U) - T_0(S_0 - S) + N(1 - T_o/T)\Delta \tilde{h}_{mix} + NRT_0\sum x_i \ln a_i \tag{7.58}$$
$$= -[(U - U_0) - T_0(S - S_0)] - N(T_o/T - 1)\Delta \tilde{h}_{mix} + NRT_0\sum x_i \ln a_i$$

The exergy change of the control mass from state 1 to 2 for $T_1 < T_0 < T_2$ is

$$\Delta E_{x,nf,1-2}' = E_{x,nf,2} - E_{x,nf,1}' = \Delta U_{0-1} - T_0\Delta S_{0-1} + \Delta U_{0-2} - T_0\Delta S_{0-2}$$
$$+ N\left[(1 - \frac{T_0}{T_2})\Delta \tilde{h}_{mix,2} - (1 - \frac{T_0}{T_1})\Delta \tilde{h}_{mix,1}\right] + NRT_0\left[\sum (x_i \ln a_i)_2 - \sum (x_i \ln a_i)_1\right] \tag{7.59a}$$

Here

$$\Delta U_{0-1} = \sum m \Delta u_i = (m_{c/g}c_{c/g} + m_{ad}c_{ad} + m_{ad}x_{max}\bar{c}_{f,0-1} + m_{pr}c_{pr})(T_1 - T_0)$$

[†] The exergy E_x is always positive while the exergy function E_x' introduced here may be either positive or negative. The relationship of the two parameters is $E_x = |E_x'|$. From the figures right, we can see that $E_{x,2} - E_{x,1}$ is the net exergy change between two states. When we need to calculate the exergy change experienced between two states when $E_{x,1}' < 0 < E_{x,2}$, it is $E_{x,2} - E_{x,1}'$ rather than $E_{x,2} - E_{x,1}$.
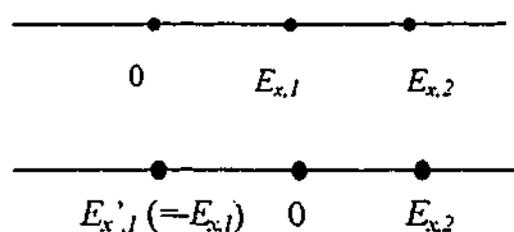
$$\Delta U_{0-2} = \sum m \Delta u_i = (m_{c/g}c_{c/g} + m_{ad}c_{ad} + m_{ad}x_{max}\overline{c}_{f,0-2} + m_{pr}c_{pr})(T_2 - T_0)$$

$$\Delta S_{0-1} = \int \frac{\delta Q}{T} = \int \frac{dU}{T} = (m_{c/g}c_{c/g} + m_{ad}c_{ad} + m_{ad}x_{max}\overline{c}_{f,S,0-1} + m_{pr}c_{pr}) \ln \frac{T_1}{T_0}$$

$$\Delta S_{0-2} = \int \frac{\delta Q}{T} = \int \frac{dU}{T} = (m_{c/g}c_{c/g} + m_{ad}c_{ad} + m_{ad}x_{max}\overline{c}_{f,S,0-2} + m_{pr}c_{pr}) \ln \frac{T_2}{T_0}$$

and

$$N\left[(1-\frac{T_0}{T_2})\Delta\widetilde{h}_{mix,2} - (1-\frac{T_0}{T_1})\Delta\widetilde{h}_{mix,1}\right] + NRT_0\left[\sum(x_i \ln a_i)_2 - \sum(x_i \ln a_i)_1\right]$$

$$= m_{ad}x_{max}(h_{ad,2} - h_{ad,1}) + m_{ad}x_{max}R_rT_0\left[\sum(x_i \ln x_i)_2 - \sum(x_i \ln x_i)_1\right]$$

Therefore, the exergy change of the control mass for $T_1 < T_0 < T_2$ is

$$
\begin{aligned}
\Delta E'_{x,1-2} &= (m_{c/g}c_{c/g} + m_{ad}c_{ad} + m_{pr}c_{pr})(T_1 + T_2 - 2T_0) + m_{ad}x_{max}[\overline{c}_{f,0-1}(T_1 - T_0) \\
&\quad + \overline{c}_{f,0-2}(T_2 - T_0)] - (m_{c/g}c_{c/g} + m_{ad}c_{ad} + m_{pr}c_{pr})T_0 \ln \frac{T_1 T_2}{T_0^2} \\
&\quad + m_{ad}x_{max}T_0(\overline{c}_{f,S,0-1} \ln \frac{T_1}{T_0} + \overline{c}_{f,S,0-2} \ln \frac{T_2}{T_0}) + m_{ad}x_{max}(h_{ad,2} - h_{ad,1}) \\
&\quad + m_{ad}x_{max}R_rT_0[\sum(x_i \ln x_i)_2 - \sum(x_i \ln x_i)_1]
\end{aligned}
\tag{7.59b}
$$

For this process, we have derived Eq. (5.23), hence the exergy used in this process

$$E_{x,Q} = \eta(f)(m_{c/g}c_{c/g} + m_{ad}c_{ad} + m_{ad}x_{max}\overline{c}_{f,1-2} + m_{pr}c_{pr})(T_2 - T_1) \tag{7.60}$$

The irreversibility of the process is

$$i = \sum \dot{E}_{x,Q_i} - \frac{d(E + P_0 V - T_0 S)_{CV}}{dt} \tag{7.61a}$$

and

$$I_{1-2} = E_{x,Q_i,1-2} - \Delta E_{x,1-2} \qquad \text{or} \qquad I_{1-2} = E_{x,Q_i,1-2} - \Delta E'_{x,1-2} \tag{7.61b}$$

7.2.2 Heating Process 2—3 (Desorption Period)

From state 2 to state 3 is the heating/desorption process. Taking the collector/generator as the control volume (CV), the exergy change of the control volume is the sum of the exergy change of the streams and the exergy change of the contents in the CV, ie,

$$\Delta E_{x,2-3} = \underbrace{\int \dot{E}_{x,f,out}dt - \int \dot{E}_{x,f,in}dt}_{a} + \underbrace{\Delta E_{x,CV}}_{b} \tag{7.62}$$

a. The exergy change of the streams

The stream entering the CV with the temperature T_{in} can be taken as the pressure-adjusting gas alone, so the exergy carried by the entering stream

$$\dot{E}_{x,f,in} = \dot{m}_{pr}[(h_{pr,in} - h_{pr,0}) - T_0(s_{pr,in} - s_{pr,0})]$$
$$= \dot{m}_{pr}c_{p,pr}(T_{in} - T_0 - T_0 \ln\frac{T_{in}}{T_0})$$

(7.63)

The stream exiting the CV with the temperature T_{out} is the mixture of the pressure-adjusting gas and the desorbed refrigerant vapour. Strictly speaking, the pressure-adjusting gas and the desorbed refrigerant vapour are not in the same temperature initially. In determining the exiting temperature, the mixture can be regarded as an ideal solution. The exergy carried by the mixture can be calculated by Eq. (7.26) as

$$\dot{E}_{x,f,ex} = (\dot{N}_{pr}\tilde{c}_{p,pr} + \dot{N}_r\tilde{\bar{c}}_g)(T_{out} - T_0) - (\dot{N}_{pr}\tilde{c}_{p,pr} + \dot{N}_r\tilde{\bar{c}}_{g,s})T_0 \ln\frac{T_{out}}{T_0} + RT_0(\dot{N}_{pr}\ln x_{pr} + \dot{N}_r\ln x_r)$$
$$= (\dot{m}_{pr}c_{p,pr} + \dot{m}_r\bar{c}_g)(T_{out} - T_0) - (\dot{m}_{pr}c_{p,pr} + \dot{m}_r\bar{c}_{g,s})T_0 \ln\frac{T_{out}}{T_0} + \dot{m}_{pr}R_{pr}T_0(\ln x_{pr} + \frac{x_r}{x_{pr}}\ln x_r)$$

(7.64)

Here

$$T_{out} = \frac{\dot{m}_{pr}c_{p,pr}T_{pr,out} + \dot{m}_r c_{p,r}T_r}{\dot{m}_{pr}c_{p,pr} + \dot{m}_r c_{p,r}}$$

(7.65)

The specific heat for methanol gas (Daubert and Danner, 1984) is (rewritten in kJ/kg/K)

$$c_g = 1.19181 + 3.25323 / e^{2186.7/T^{1.1628}} \quad \text{kJ/kg/K}$$

(7.66)

The temperature of the desorbed refrigerant vapour T_r can be taken as the temperature of the bed T_p while the temperature of the pressure-adjusting gas is estimated by Eq (5.38). So

$$T_{out} = \frac{(\dot{m}_{pr}c_{p,pr})^2 T_{pr,i} + [\dot{m}_{pr}c_{p,pr}\dot{m}_r c_{p,r} + (\dot{m}_{pr}c_{p,pr} + \dot{m}_r c_{p,r})hA_{tot}]T_p}{(\dot{m}_{pr}c_{p,pr} + \dot{m}_r c_{p,r})(\dot{m}_{pr}c_{p,pr} + hA_{tot})}$$

(7.67)

The mass flow rate of the desorbed refrigeration vapour may depend on the heating time. To simplify the calculation, the following average value may be taken in calculation

$$\dot{m}_r = m_{ad}\frac{dx}{dt} \approx m_{ad}\frac{\Delta x}{t_{2-3}}$$

(7.68)

From heat transfer analysis (chapter 4), it was found that $T_p = kt + c$. Hence

$$\dot{m}_r \approx m_{ad}k\Delta x / (T_3 - T_2)$$

(7.69)

Since $\dot{m}_{pr}c_{pr}$ and $\dot{m}_r c_r$ in our case is so small compared with hA_{tot} that $(\dot{m}_{pr}c_{pr})^2$ and $(\dot{m}_{pr}c_{pr})(\dot{m}_r c_r)$ can be neglected. Hence

$$T_{out} \approx T_p \tag{7.70}$$

which is in agreement with the outcome of the analysis in chapter 4 that the temperature of the fixed bed can be taken as the temperature of the exiting stream $T_{pr,e} \approx T_p$.

With a fixed mass flow rate of the pressure-adjusting gas, the exergy change of the streams (the first term in the right side of Eq. 7.62, a)

$$a = \int \dot{E}_{x,f,out} dt - \int \dot{E}_{x,f,in} dt \approx \int [\dot{m}_{pr}c_{p,pr}(T_p - T_{pr,i} - T_0 \ln \frac{T_p}{T_{pr,i}}) + \dot{m}_r \bar{c}_g (T_p - T_0) - \dot{m}_r \bar{c}_{g,s} T_0 \ln \frac{T_p}{T_0}]dt$$
$$+ \dot{m}_{pr}R_{pr}T_0(\ln x_{pr} + \frac{x_r}{x_{pr}}\ln x_r)t_{2-3}$$

$$\tag{7.71a}$$

Substituting the relationship $dt = 1/k \cdot dT_p$ into the above equation, we have

$$a \approx \frac{\dot{m}_{pr}c_{p,pr}}{k}[\frac{T_3^2 - T_2^2}{2} - (T_{pr,i} - T_0)(T_3 - T_2) - T_0(T_3 \ln \frac{T_3}{T_{pr,i}} - T_2 \ln \frac{T_2}{T_{pr,i}})]$$
$$+ m_{ad}\Delta x \bar{c}_{g,2-3}(\frac{T_3 + T_2}{2} - T_0) - \frac{m_{ad}\Delta x \bar{c}_{g,s,2-3}}{T_3 - T_2}T_0[T_3(\ln \frac{T_3}{T_0} - 1) - T_2(\ln \frac{T_2}{T_0} - 1)] \tag{7.71b}$$
$$+ \frac{\dot{m}_{pr}R_{pr}T_0}{k}(\ln x_{pr} + \frac{x_r}{x_{pr}}\ln x_r)(T_3 - T_2)$$

b. The exergy change of the contents in the CV

Similar to the process 1-2, the exergy change of the contents in the CV (the second term in the right side of Eq. 7.62, b) can be written as

$$b = \Delta E_{x,nf,2-3} \approx \{(m_{c/g}c_{c/g} + m_{ad}c_{ad} + m_{ad}x_{max}\bar{c}_{f,2-3})(T_3 - T_2) - m_{ad}\Delta x[200 + \bar{c}_{f,0-3}(T_3 - 273.15) - p_{0C}v_{0C}]\}(1 - \frac{T_0}{T_3 - T_2}\ln \frac{T_3}{T_2}) \tag{7.72}$$
$$+ m_{ad}x_{min}h_{ad,3} - m_{ad}x_{max}h_{ad,2} + m_{ad}RT_0[x_{min}\sum(x_i \ln x_i)_3 - x_{max}\sum(x_i \ln x_i)_2]$$

Therefore, the total exergy change of the CV is

$$\Delta E_{x,2-3} = \{[m_{c/g}c_{c/g} + m_{ad}c_{ad} + m_{ad}x_{max}\bar{c}_{f,2-3}(T_3 - T_2)$$
$$- m_{ad}\Delta x[200 + \bar{c}_{f,0-3}(T_3 - 273.15) - p_{0C}v_{f,0C}]\}(1 - \frac{T_0}{T_3 - T_2}\ln\frac{T_3}{T_2})$$
$$+ [\frac{\dot{m}_{pr}c_{p,pr}}{k}(\frac{T_3 + T_2}{2} - T_{pr,i} + T_0) + \frac{\dot{m}_{pr}R_{pr}T_0}{k}(\ln x_{pr} + \frac{x_r}{x_{pr}}\ln x_r)](T_3 - T_2) \tag{7.73}$$
$$- \frac{\dot{m}_{pr}c_{p,pr}}{k}T_0(T_3\ln\frac{T_3}{T_{pr,i}} - T_2\ln\frac{T_2}{T_{pr,i}}) + m_{ad}\Delta x\bar{c}_{g,2-3}(\frac{T_3 + T_2}{2} - T_0)$$
$$- \frac{m_{ad}\Delta x\bar{c}_{g,s,2-3}}{T_3 - T_2}T_0[T_3\ln\frac{T_3}{T_0} - T_2\ln\frac{T_2}{T_0} - (T_3 - T_2)] + m_{ad}x_{min}h_{ad,3} - m_{ad}x_{max}h_{ad,2}$$
$$+ m_{ad}RT_0[x_{min}\sum(x_i\ln x_i)_3 - x_{max}\sum(x_i\ln x_i)_2]$$

In this process, we have derived (Eq. 5.57)

$$Q_{2-3} \approx [(m_{c/g}c_{c/g} + m_{ad}c_{ad} + m_{ad}\frac{x_{max} + x_{min}}{2}\bar{c}_{f,2-3}](T_3 - T_2) + m_{ad}\frac{\Delta x}{2}(P_2v_{f,2} + P_3v_{f,3})$$
$$+ \Delta H_{pr,2-3} + m_{ad}\Delta x\bar{h}_{de}$$

So the exergy used in this process (for solar energy)

$$E_{x,Q,2-3} = \eta(f)Q_{2-3} \tag{7.74}$$

The irreversibility of the process according to Eq. (7. 42) is

$$\dot{I} = \sum\dot{E}_{x,Q_i} - [\sum_{out}(h - T_0s)\dot{m} - \sum_{in}(h - T_0s)\dot{m}] - \frac{d(E + P_0V - T_0S)_{cv}}{dt} \tag{7.75a}$$

and

$$I_{2-3} = E_{x,Q,2-3} - \Delta E_{x,2-3} \tag{7.75b}$$

7.2.3 Cooling Process 3—4

In this process, the collector is cooled by the environment. There is no heat consumption or refrigeration effect, so there is no need to conduct an exergy analysis for this process.

7.2.4 Refrigeration Period 4—1 (Adsorption Process)

As stated in chapter 5, this process can be thought to occur in two steps. Firstly, a portion of the liquid refrigerant in the receiver (if applicable) and evaporator evaporates and cools the refrigerant-self from T_c to the designed evaporating temperature T_e (flashing step). Then the liquid refrigerant evaporates at the evaporating pressure P_e (corresponding to the evaporating temperature T_e) until it is all evaporated and absorbs heat from the objects to be cooled (refrigeration step).

In the first step, the exergy released by the refrigerant vaporisation

$$E_{x,Q,r0-r1} = \int (\frac{T_0}{T_e} - 1)d(mh) = (m_{r0} - m_{r1})h_{fg}(\frac{T_0}{T_e} - 1) \qquad (7.76a)$$

The heat flow into the control volume in the first step was given by Eq. (6.61). Since the first step happens very quickly, it is reasonable to assume that there is no heat exchange between the system and its surroundings, ie, $Q_{r0-r1} = 0$,

$$m_{r1} = m_{r0}\frac{h_{g,e} - u_{r0}}{h_{g,e} - u_{r1}} = m_{r0}\frac{h_{fg,e} + p_e v_e - \overline{c}_f(T_c - T_e)}{h_{fg,e} + p_e v_e} \qquad (7.77)$$

The exergy loss according to Eq (7.38) or (7.47)

$$I = -\sum_{out}(h - T_0 s)\dot{m} - \frac{d(U + P_0 V - T_0 S)_{CV}}{dt} \qquad (7.78a)$$

and

$$\begin{aligned} I_{r0-r1} &= -(m_{r0} - m_{r1})(h_{g,e} - T_0 s_{g,e}) - [m_{r1}(u_{r1} + P_0 v_{r1} - T_0 s_{r1}) - m_{r0}(u_{r0} + P_0 v_{r0} - T_0 s_{r0})] \\ &= (m_{r0} - m_{r1})h_{fg,e}(\frac{T_0}{T_e} - 1) - m_{r0}[u_{f,e} - u_{f,c} - T_0(s_{f,e} - s_{f,c})] \\ &\quad + m_{r0}(P_0 v_{f,c} - P_e v_{f,e}) - m_{r1}(P_0 - P_e)v_{f,e} \end{aligned} \qquad (7.78b)$$

In the second step, the exergy released by the refrigerant vaporisation

$$E_{x,rels,r1-r2} = \int (\frac{T_0}{T_e} - 1)d(mh) = m_{r1}h_{fg}(\frac{T_0}{T_e} - 1) \qquad (7.79)$$

The heat exchange consists of the cooling of the substance to be cooled, the heat leakage, and maybe the cooling of the receiver and the evaporator. If the cooling chamber is well insulated so the heat leakage can be neglected, and all the items of material are cooled from T_c to T_e. If $T_e < T_c \leq T_0$, the gross exergy gain is

$$\begin{aligned} \Delta E_{x,gain,gro} &= \sum m[\overline{c}(T_e - T_c) - \overline{c}_r T_0 \ln \frac{T_e}{T_c}] \approx \sum mc(T_e - T_c - T_0 \ln \frac{T_e}{T_c}) \\ &= \sum mc(T_e - T_c - T_0 \ln \frac{T_e}{T_c}) \qquad (for \quad c \neq f(T)) \end{aligned} \qquad (7.80a)$$

Here

$$\sum m\overline{c}(T_c - T_e) = m_{r1}h_{fg,e} \qquad (7.81)$$

So the gross exergy gain is

$$\Delta E_{x,gain,gro} \cong m_{r1}h_{fg,e}(\frac{T_0}{T_c - T_e}\ln\frac{T_c}{T_e} - 1) \qquad (7.80b)$$

The net exergy gain is

$$\Delta E_{x,gain,net} = m_c[\bar{c}_c(T_e - T_c) - \bar{c}_{c,s}T_0 \ln\frac{T_e}{T_c}]$$

$$= m_c c_c(T_e - T_c - T_0 \ln\frac{T_e}{T_c}) \qquad (for \quad c \neq f(T)) \tag{7.82}$$

If $T_e < T_0 \leq T_c$, the gross exergy gain is

$$\Delta E'_{x,gain,gro} = E_{x,c} - E'_{x,e} = \sum m[\bar{c}(T_e + T_c - 2T_0) - \bar{c}_s T_0 \ln\frac{T_e T_c}{T_0^2}]$$

$$= \sum mc(T_e + T_c - 2T_0 - T_0 \ln\frac{T_e T_c}{T_0^2}) \qquad (for \quad c \neq f(T)) \tag{7.83a}$$

Substituting Eq.(7.80) into the above equation, the gross exergy gain is

$$\Delta E'_{x,gain,gro} \cong \frac{m_{r1}h_{fg,e}}{T_c - T_e}(T_e + T_c - 2T_0 - T_0 \ln\frac{T_e T_c}{T_0^2}) \tag{7.83b}$$

The net exergy gain is

$$\Delta E'_{x,gain,net} = m_c[\bar{c}_c(T_e + T_c - 2T_0) - \bar{c}_{c,s}T_0 \ln\frac{T_e T_c}{T_0^2}]$$

$$= m_c c_c(T_e + T_c - 2T_0 - T_0 \ln\frac{T_e T_c}{T_0^2}) \qquad (for \quad c \neq f(T)) \tag{7.84}$$

The exergy loss according to Eq (7.47) is

$$i = \sum \dot{E}_{x,Q_j} - (h - T_0 s)_{out}\dot{m}_{out} - \frac{d(E + P_0 V - T_0 S)_{cv}}{dt} \tag{7.85a}$$

Therefore, the exergy loss according to Eq (7.47) is

$$I_{r1-r2} = -E_{x,gain,r1-r2} - m_{r1}(h - T_0 s)_{out} + m_{r1}(u_{r1} + P_0 v_{r1} - T_0 s_{r1})$$

$$= -E_{x,grain,r1-r2} - m_{r1}h_{fg,e}(1 - T_0/T_e) + m_{r1}(P_0 - P_e)v_{f,e} \tag{7.85b}$$

or

$$I'_{r1-r2} = -E'_{x,gain,r1-r2} - m_{r1}(h - T_0 s)_{out} + m_{r1}(u_{r1} + P_0 v_{r1} - T_0 s_{r1})$$

$$= -E'_{x,grain,r1-r2} - m_{r1}h_{fg,e}(1 - T_0/T_e) + m_{r1}(P_0 - P_e)v_{f,e} \tag{7.85b}$$

7.2.5 The Relative Exergy Loss and Exergetic Efficiency for Processes and Cycle

The Exergy Efficiency of the whole cycle is used here to evaluate the performance of a refrigeration system. In terms of the solar adsorption refrigeration system, the ideal cycle consists of four processes (see Fig. 1.1).

For the whole cycle, the exergy used is the sum of the heat used in process 1-2 and 2-3

$$E_{x,used,cyc} = \eta(f)Q_{1-3} \qquad (7.86)$$

The exergy gain in the whole cycle is the exergy transferred to the products to be cooled. Since different refrigeration system may have different heat capacities of receiver and evaporator and different insulation, the gross exergetic efficiency of the cycle may be a common index for comparison of different refrigeration systems. The gross (also the maximal) exergy gain is expressed by Eq. (7.80b) or (7.83b).

The exergy loss of the cycle

$$I_{cycle} = E_{x,Q,cyc} - E_{x,gain,cyc} \qquad \text{or} \qquad I'_{cycle} = E_{x,Q,cyc} - E'_{x,gain,cyc} \qquad (7.87)$$

The relative exergy loss

$$i_i = I_i / I_{cyc} \qquad (7.88)$$

The exergy efficiency ε is defined as the ratio of the exergy gain to the exergy used, ie,

$$\varepsilon_i = \Delta E_{x,gain,i} / E_{x,used,i} = 1 - I_i / E_{x,used,i} \qquad \text{and} \qquad \varepsilon = E_{x,gain,cyc} / E_{x,used,cyc} \qquad (7.89)$$

By this way, the exergy loss, the relative exergy loss, and the exergy efficiency for each process (component) and the whole cycle (system) can be evaluated. This evaluation is essential in revealing the parts which degrade the performance of the whole system, and in comparing the performance for different systems rationally. The exergy efficiencies of the cycle are shown in Fig. 7.1 to 7.9.
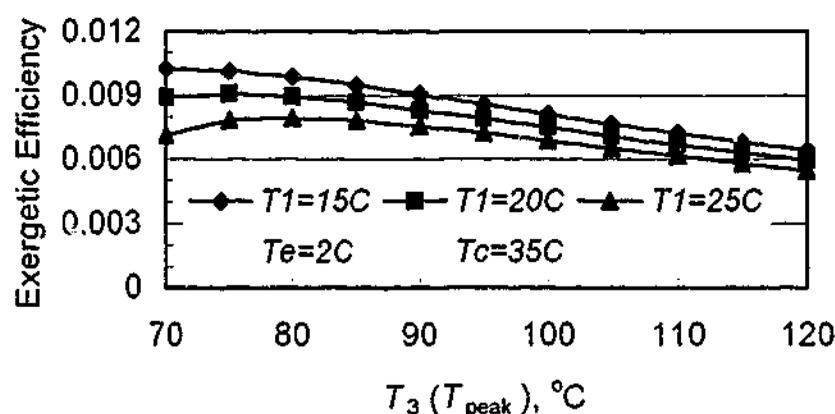
Figure 7.1 The relationship of the exergetic efficiency and the peak temperature of the collector
($T_e=2°C$, $T_c=35°C$)
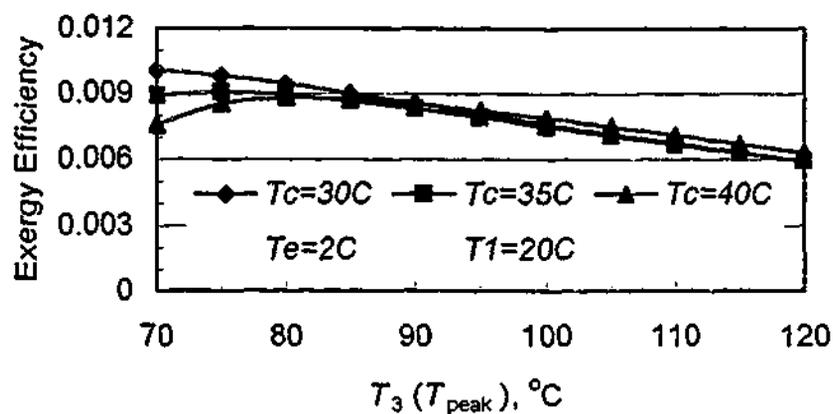
Figure 7.2 The relationship of the exergetic efficiency and the peak temperature of the collector (T_e=2°C, T_1=20°C)
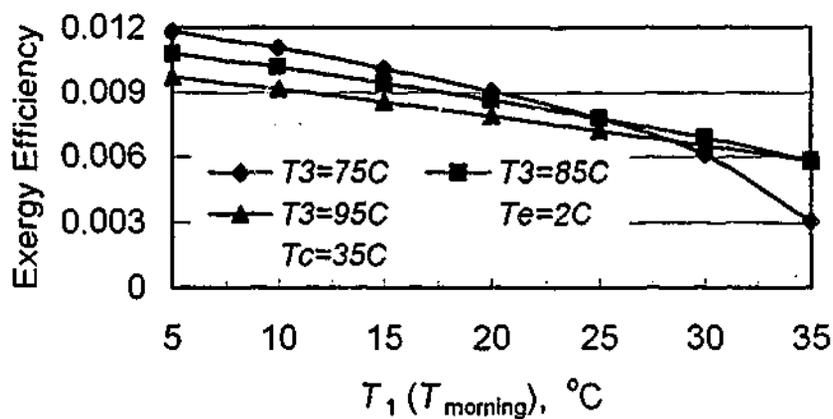
Figure 7.3 The relationship of the exergetic efficiency and the temperature of the collector in the morning (T_e=2°C, T_c=35°C)
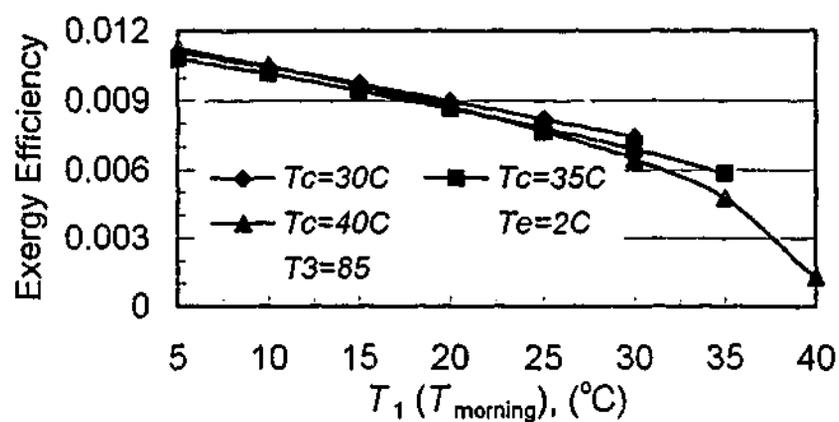
Figure 7.4 The relationship of the exergetic efficiency and the temperature of the collector in the morning (T_e=2°C, T_3=85°C)
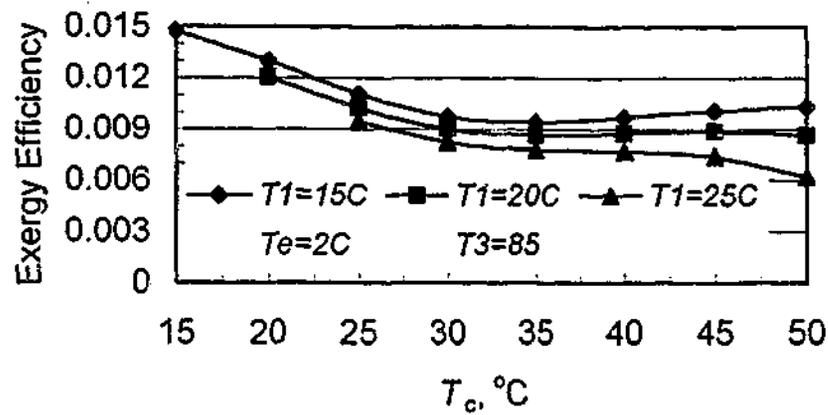
Figure 7.5 The relationship of the exergetic efficiency and the condenser temperature (T_e=2°C, T_3=85°C)
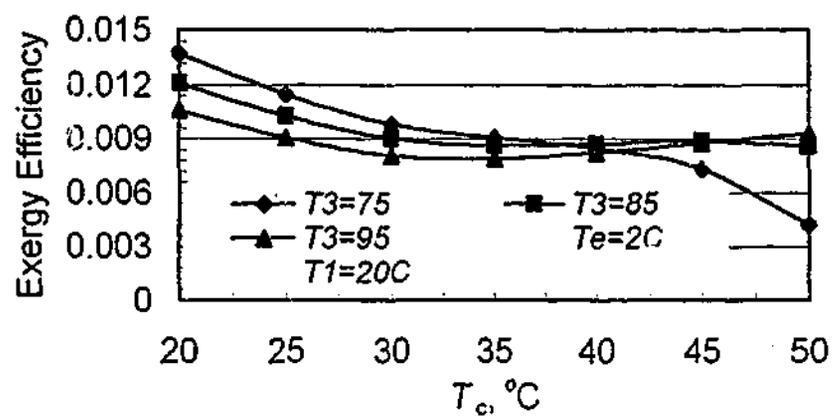
Figure 7.6 The relationship of the exergetic efficiency and the condenser temperature (T_e=2°C, T_1=20°C)
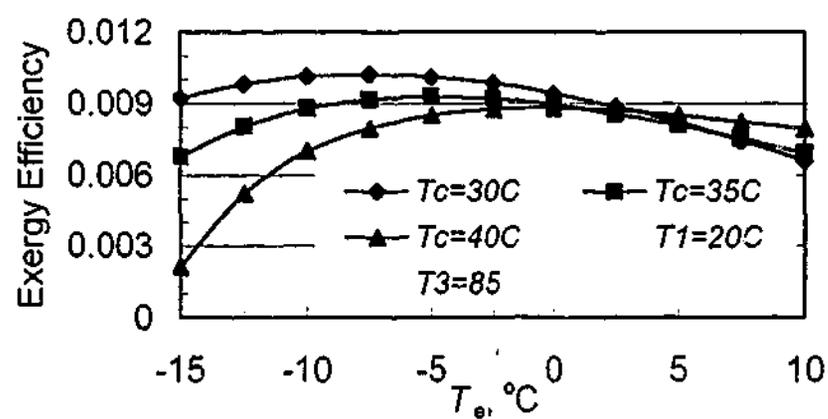
Figure 7.7 The relationship of the exergetic efficiency and the evaporator temperature (T_1=20°C, T_3=85°C)
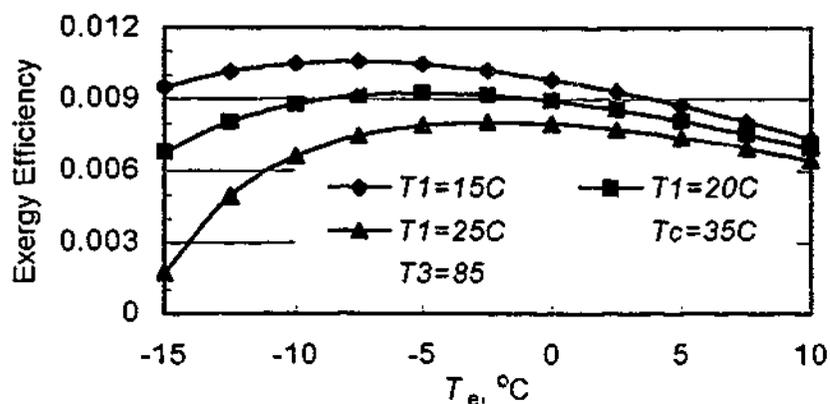
Figure 7.8 The relationship of the exergetic efficiency and the evaporator temperature (T_c=35°C, T_3=85°C)
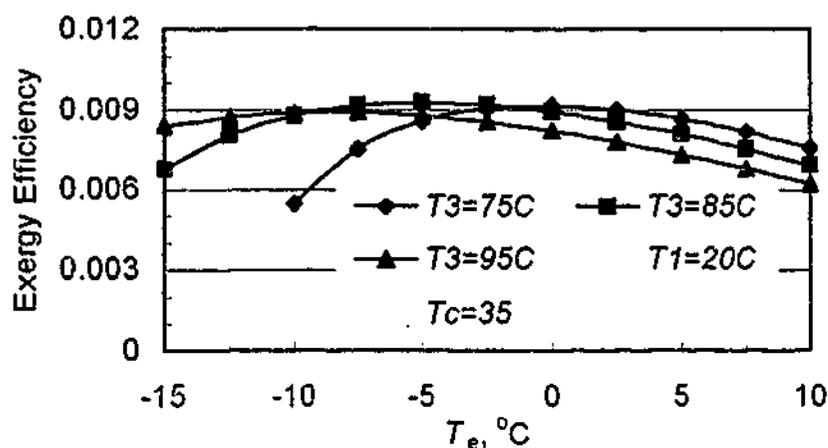
Figure 7.9 The relationship of the exergetic efficiency and the evaporator temperature (T_1=20°C, T_c=35°C)

From the Figures it can be seen that the exergetic efficiency of the system shows the same general trends as the COP but with some exceptions. They are described and explained below.

- At a certain evaporator temperature, condenser temperature, and morning temperature, the exergetic efficiency of the system increases with the peak temperature of the collector, reaches a maximum, and then falls off. The lower the morning temperature, the lower the optimal peak temperature. In the typical conditions studied here, the optimal peak temperature is also in the range of 70-95°C (Fig. 7.1, 7.2);

- At a certain evaporator temperature and condenser temperature, the lower the morning temperature, the higher the exergetic efficiency (Fig. 7.1, 7.3, 7.4, 7.5, 7.8). But the change of the exergetic efficiency also depends on the peak temperature. The lower the peak temperatures (eg, 75°C), the higher the exergetic efficiency in the low morning temperature range (eg, less than 25°C), but the exergetic efficiency drops sharper with the morning temperature (Fig. 7.3);

- The exergetic efficiency, in general, decreases with condenser temperature, but the change depends on other operating temperatures. For the cases of low peak temperature (eg, 75°C) or high morning temperature (eg, 25°C), the exergetic efficiency decreases all along. For the cases of high peak temperature (eg, 85°C) and low morning temperature (20°C), the exergetic efficiency decreases and then increases slightly, but it will decrease finally (Fig. 7.5, 7.6).

It can also be deduced that for a certain climate (eg, morning temperature and condenser temperature) and a certain application (eg, evaporator temperature), there is an optimal peak temperature at which the exergetic efficiency of the solar adsorption refrigeration system reaches a maximum. This temperature is in the range of the flat-plate collector achieving.

The introduction of the pressure-adjusting gas into the system also results in the decrease of exergetic efficiency. The difference of the exergetic efficiency of the systems with and without the pressure-adjusting gas can be reduced by further work and it is beyond the scope of this thesis.

The exergy analysis can further evaluate the quality efficiency of the components (processes) of the system. For example, the relative exergy losses for the system in some operation conditions are shown in figure 7.10 to 7.13.

(a)

(b)
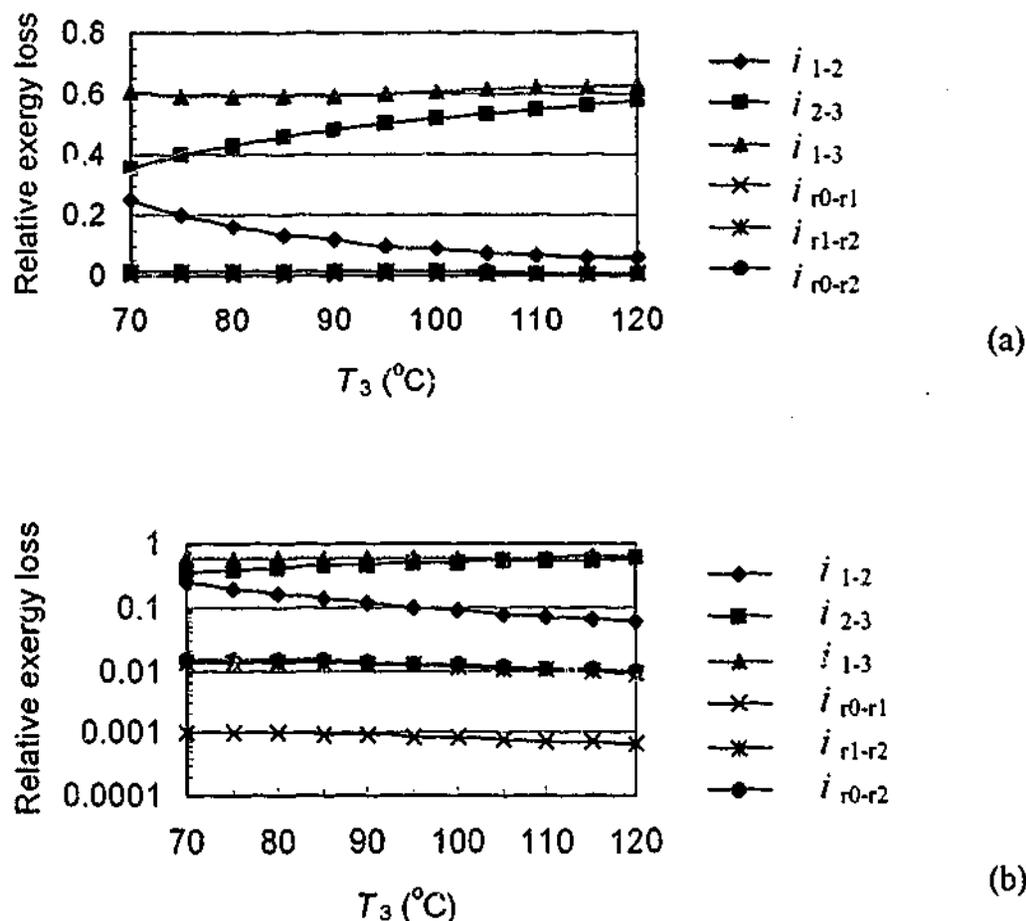
Figure 7.10 The relative exergy loss vs. the peak temperature of the collector (T_e=2°C, T_1=20°C, T_c=35°C)
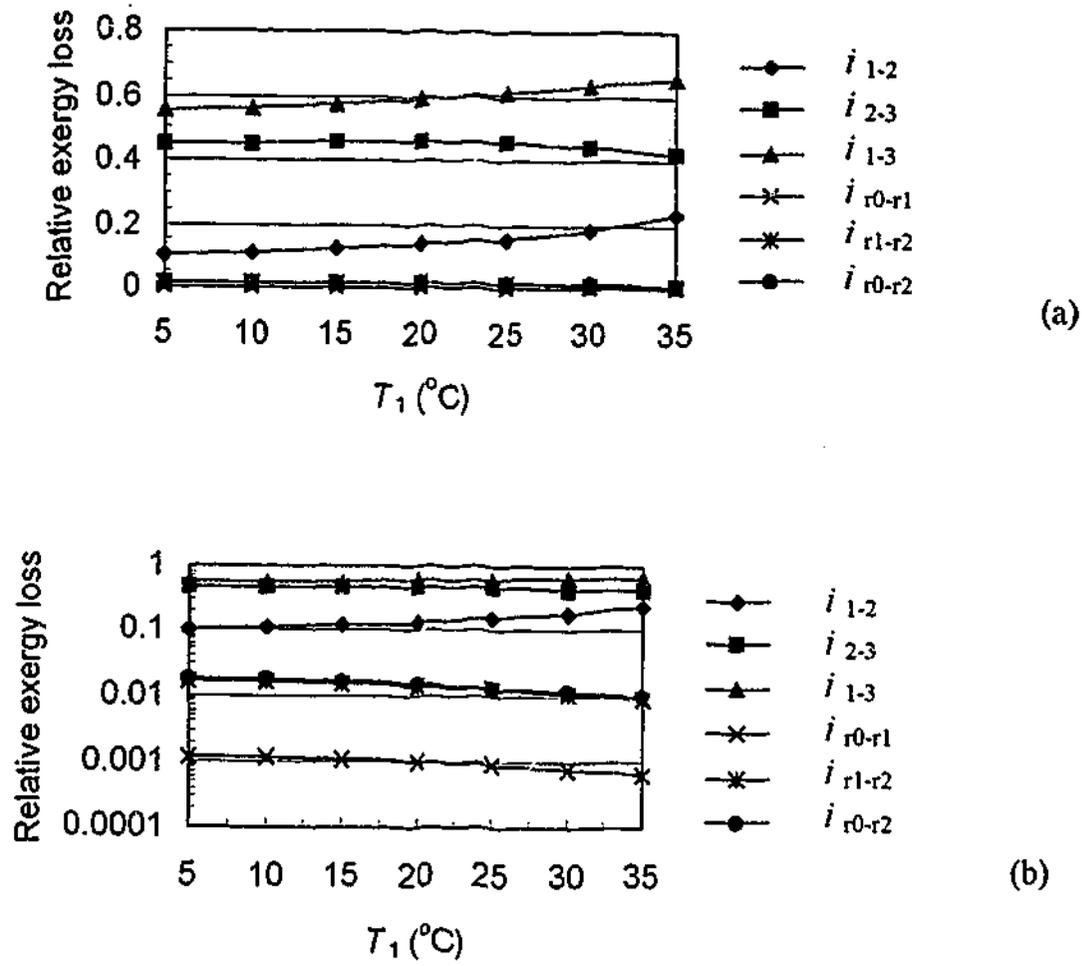
Figure 7.11 The relative exergy loss vs. the morning temperature (T_e=2°C, T_c=35°C, T_3=85°C)
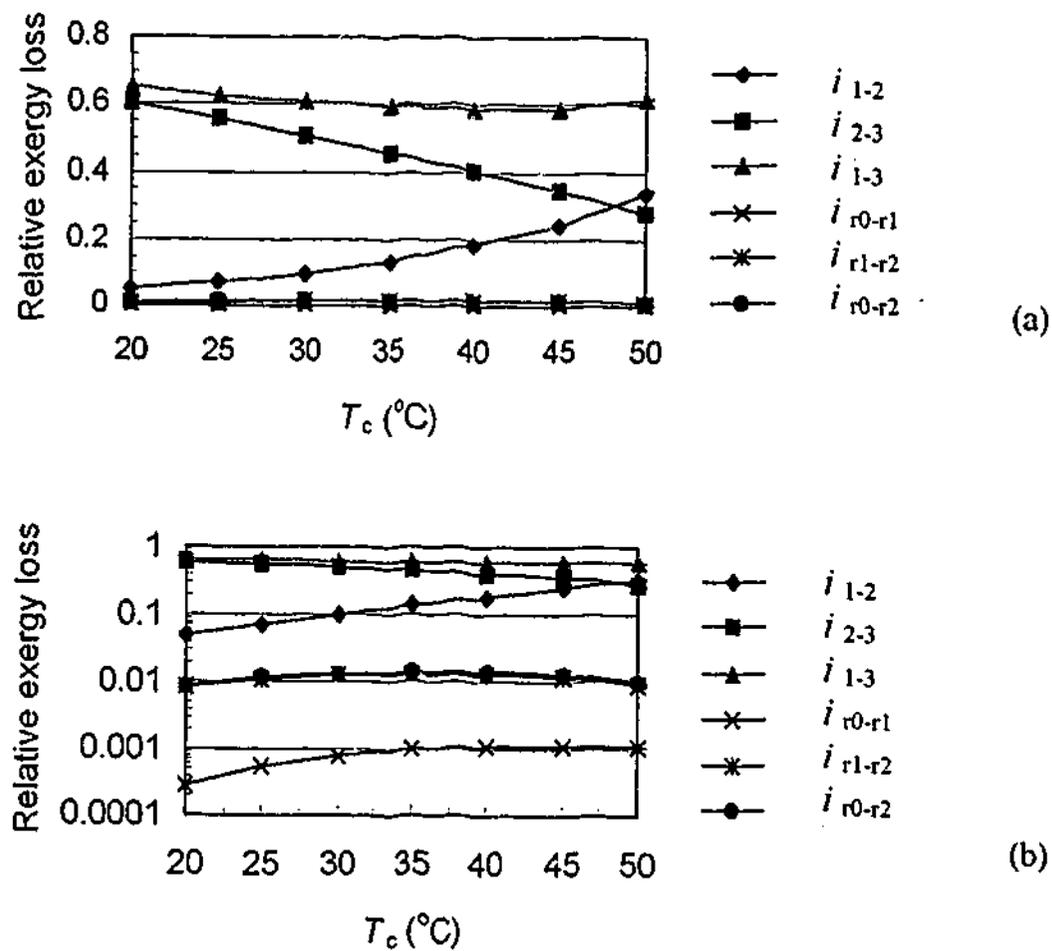
Figure 7.12 The relative exergy loss vs. the condenser temperature (T_e=2°C, f_1=20°C, T_3=85°C)
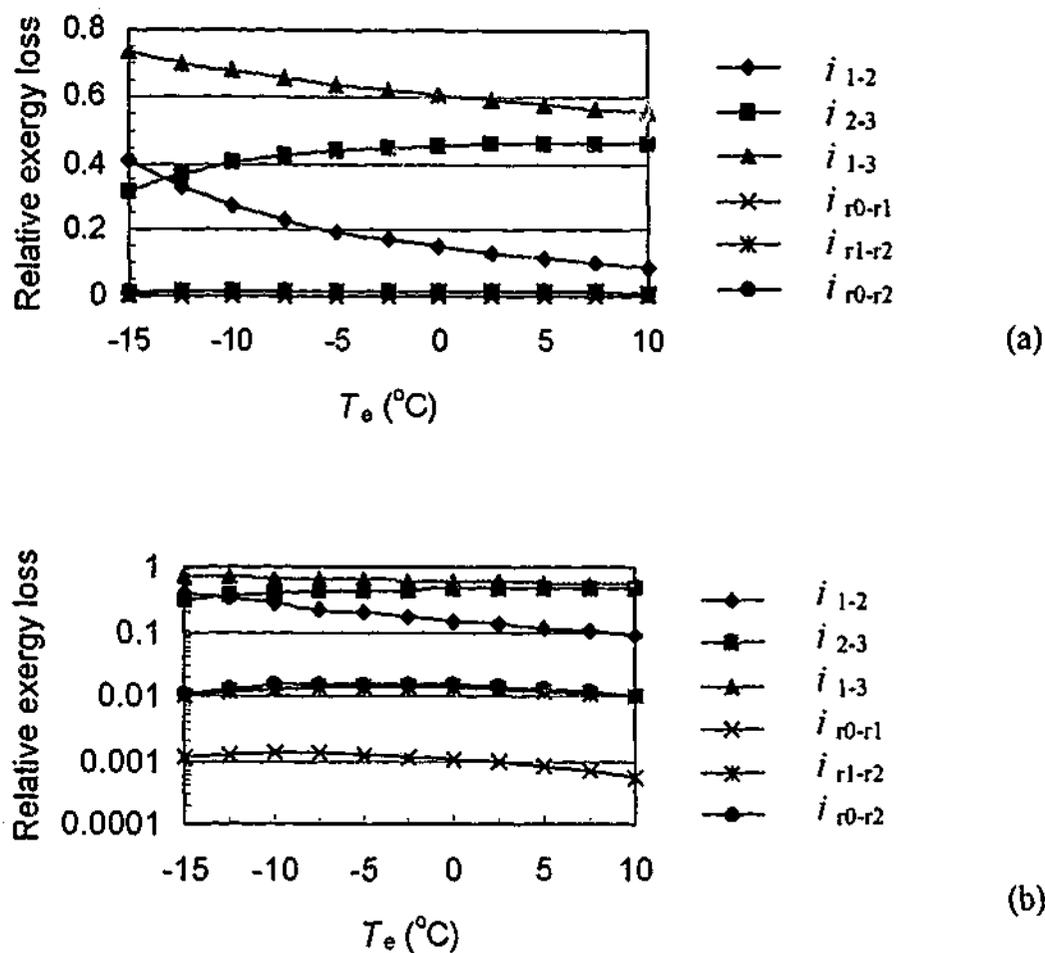
Figure 7.13 The relative exergy loss vs. the evaporator temperature (T_1=20°C, T_c=35°C, T_3=85°C) ·

From Fig. 7.10 to 7.13, it can be seen that

- At the same conditions, the maximum relative exergy loss occurs in the heating process 1-3. The relative exergy loss in the flashing step $r0$-$r1$ can be neglected.

- As the peak temperature increases, the relative exergy loss in heating process 1-2 decreases while that in heating process 2-3 increases, and the total relative exergy loss in the heating process 1-3 decreases slightly at first and then increases slightly. The minimum relative exergy loss in heating process 1-3 happens in the temperature range of 75-95°C. The relative exergy loss in refrigerating process $r0$-$r2$ decreases slightly, but it is almost a constant in a wide peak temperature range.

- As the morning temperature increases, the relative exergy loss in heating process 1-2 increases while that in heating process 2-3 decreases, and the total relative exergy loss in the heating process 1-3 increases monotonically. The relative exergy loss in refrigerating process $r0$-$r2$ decreases slightly.

- As the condenser temperature increases, the relative exergy loss in heating process 1-2 increases greatly while that in heating process 2-3 decreases greatly, and the total relative exergy loss in the heating process 1-3 decreases first and then increases. The minimum relative

exergy loss in heating process 1-3 happens in the temperature range of 35-45°C. The relative exergy loss in refrigerating process $r0$-$r2$ increases slightly at first and then decreases slightly.

- As the evaporator temperature increases, the relative exergy loss in heating process 1-2 decreases greatly while that in heating process 2-3 increases greatly first and gently and gently then, and the total relative exergy loss in the heating process 1-3 decreases greatly. The relative exergy loss in refrigerating process $r0$-$r2$ increases slight first and then decreases slightly.

It can be seen that the exergy analysis can reveal the 'weakest link' of the system. In our case, the maximum relative exergy loss occurs in the heating process 1-3. If we want to improve the exergetic efficiency of the system, it is far more effective to improve the heating processes, such as by making the system working at a suitable peak temperature and reducing the velocity of the pressure-adjusting gas circulated rather than to improve the refrigerating process.

It should also be pointed out that although the exergy analysis yields some of the same conclusions as does the COP, the exergy analysis cannot take the place of the energy analysis. Since the evaluation of the exergy for the substance at a certain state is based on some kind of datum, in some cases, the results from the exergy analysis may be specious. For example, in our case, as the evaporator temperature T_e approaches the environment temperature T_0 ($T_e < T_0$), the COP of the system increases while the exergetic efficiency of the system decreases (Fig. 7.7, 7.8, 7.9). So if only the exergy analysis is conducted, some information may be interpreted wrongly. Therefore, the energy analysis and the exergy analysis are supplementary and compensatory to each other.

8

The Simulation of the Performance of the Refrigeration Cycle Powered by Solar Radiation

The previous work is on the indoor experiment rig which is heated by a constant heat flux. For a solar powered system, the heat flux is always changing. In this chapter, performance of the refrigeration cycle powered by solar radiation in a clear day is simulated. To do so, the solar radiation (in our case for the Southern hemisphere) is determined, and then the useful heat gained by the collector pipe and the temperature of the pipe are evaluated. Based on this information, the performance of the refrigeration cycle powered by solar radiation is simulated, and the simulation can describe the performance of the system powered by solar energy more objectively.

8.1 SOLAR RADIATION

Solar energy approaches the earth as electromagnetic radiation. The total solar radiation $I_{t\theta}$ of a terrestrial surface of any orientation and tilt with an incident angle θ_i is the sum of the direct component $I_{dir} \cos \theta$ plus the diffuse component I_{dif} coming from the sky plus the radiation reflected from the ground or the adjacent objects which may reach the surface I_r (ASHRAE, 1995):

$$I_{t\theta} = I_{dir} \cos \theta + I_{dif} + I_r \qquad (8.1)$$

The Direct Irradiance

The direct irradiance I_{dir} at normal incidence can be calculated from the extraterrestrial irradiance I_0 and the zenith angle θ_s by a correlation (Hottel, 1976):

$$I_{dir} = I_0 \left[a_0 + a_1 \exp(-k/\cos \theta_s) \right] \qquad (8.2)$$

The coefficients a_0, a_1, and k depend on the altitude above sea level A. For 23-km visibility and midlatitude summer (Hottel, 1976)

$$a_0 = 0.97 \left[0.4237 - 0.00821(6-A)^2 \right]; \; a_1 = 0.99 \left[0.5055 + 0.00595(6.5-A)^2 \right]$$

and $\qquad k = 1.02 \left[0.2711 + 0.01858(2.5-A)^2 \right] \qquad (8.3)$

The extraterrestrial irradiance I_0 can be determined by (Kreider and Rabl, 1994)

$$I_0 = 1373\left(1 + 0.033\cos\frac{360^0 n}{365.25}\right) \qquad W/m^2 \qquad (8.4)$$

with n = day of year (= 1 for January 1).

The zenith angle θ_s is the angle between the normal of the earth surface at point P and the line from P to the sun, and for any latitude λ and any time of day and year

$$\cos\theta_s = \cos\lambda\cos\delta\cos\omega + \sin\lambda\sin\delta \qquad (8.5)$$

where ω is the solar hour angle and δ is solar declination (the angle between the earth-sun line and the earth's equatorial plane).

The solar hour angle

$$\omega = \text{(number of hours from solar noon) } 15^\circ = (t_{as} - 12\text{ h}) \times 360^\circ/24\text{ h} \qquad (8.6)$$

where t_{as} is the apparent solar time.

The solar declination

$$\delta = \pm 23.45^\circ \sin\frac{360^0(n + 284)}{365} \qquad (8.7)$$

where "+" and "-" are for the northern and the southern hemisphere, respectively

Solar time (t_{as}) generally differs from local standard time (t_{ls}) or day saving time (t_{ds}). The t_{as} can be determined by (Kreider and Rabl, 1994)

$$t_{as} = t_{ls} + E_t + (4\text{ min}) (L_{st} - L_{loc}) \qquad (8.8)$$

where E_t is the equation of time which is defined as the difference between solar noon and noon of local civil time; L_{st} is the longitude of the standard time meridian; and L_{loc} is the local longitude. *The equation of time E_t* can be approximated by

$$E_t = 9.87\sin 2B - 7.53\cos B - 1.5\sin B \qquad \text{min} \qquad (8.9)$$

with

$$B = 360^\circ(n-81)/364 \qquad \text{for the } n\text{th day of year for north hemisphere,}$$

and $\qquad B = 360^\circ(n-263)/364 \qquad$ for the nth day of year for south hemisphere $\qquad (8.10)$

The Incident Angle

The incident angle θ of the sun on the plane (angle between normal of plane and line to sun) (Kreider and Rabl, 1994)

$$\cos \theta = \sin \theta_s \sin \theta_p \cos \phi + \cos \theta_s \cos \theta_p \tag{8.11}$$

where θ_p is the tilt angle of the plane (measured from the horizontal), ϕ is the plane-solar azimuth. For plane facing east of south, $\phi = \phi_s - \phi_p$ in the morning and $\phi = \phi_s + \phi_p$ in the afternoon. For plane facing west of south, $\phi = \phi_s + \phi_p$ in the morning and $\phi = \phi_s - \phi_p$ in the afternoon here ϕ_s is the solar azimuth and ϕ_p is the azimuth of the plane. For south-facing surface, $\phi_p = 0$.

The solar azimuth (ASHRAE, 1995)

$$\cos \phi_s = (\cos \theta_s \sin \lambda - \sin \delta)/(\sin \theta_s \cos \lambda) \tag{8.12}$$

The Diffuse Radiation

The amount of diffuse radiation for a surface with a tilt angle θ_p, I_{dif}

$$I_{dif} = I_{dif, hor} (1+\cos \theta_p)/2 \tag{8.13}$$

where $I_{dif, hor}$ is the diffuse radiation on a horizontal surface and it can be estimated by (Liu and Jordan, 1960)

$$I_{dif, hor} = (0.2711\, I_0 - 0.2939\, I_{dir}) \cos \theta_s \tag{8.14}$$

The Reflected Radiation

$$I_r = (I_{dir} \cos \theta_s + I_{dif, hor}) \rho_g (1 - \cos \theta_p)/2 \tag{8.15}$$

where ρ_g is the reflectivity of the ground, usually 0.2 without snow (Kreider and Rabl, 1994). Typical data for the most common surfaces are given by Hunn and Calafell (1977) and Threlkeld (1970).

The theoretical total solar radiation at the Gippsland Campus, Monash University, is calculated and shown in Fig. 8.1.

8.2 COLLECTOR PERFORMANCE

The useful heat gained by collector may be evaluated by (ASHRAE 1977)

$$Q_u = I_{t\theta} (\tau\alpha)_\theta A_{pro} - U_L A_p (t - t_a)$$ (8.16)

where $(\tau\alpha)_\theta$ is the transmissivity τ of cover times absorptivity α of the collector pipe at prevailing incident angle θ, A_{pro}, A_p is the projected area and the area of the collector pipe, respectively, U_L is the heat loss coefficient, and t and t_a is the temperature of the collector and the atmosphere, respectively.

The transmissivity - absorptivity product

According to Duffie and Beckman (1991)

$$(\tau\alpha)_\theta = \frac{\tau\alpha}{1 - (1 - \alpha)\rho_d}$$ (8.17)

where τ is the transmissivity of the cover, α is the absorptivity of the collector tube, and ρ_d is the diffuse reflectivity. For flat black paint $\alpha = 0.96$ (ASHRAE, 1995) and the value of α can be assumed independent of direction for the cylindrical tube. The diffuse reflectivity $\rho_d = 0.16$, 0.24, 0.29, and 0.32 for one, two, three and four glass cover systems, respectively.

The transmissivity of the cover, τ, can be determined by (Duffie and Beckman, 1974)

$$\tau = \tau_r \tau_a$$ (8.18)

where τ_r is the transmissivity of the cover neglecting absorption, and τ_a is the transmissivity considering only absorption.

The transmissivity of the cover neglecting absorption

$$\tau_r = \frac{(1 - \rho)}{1 + (2n - 1)\rho}$$ (8.19)

where n is the number of the covers, and

$$\rho = 0.5\left[\frac{\sin^2(\theta' - \theta)}{\sin^2(\theta' + \theta)} + \frac{\tan^2(\theta' - \theta)}{\tan^2(\theta' + \theta)}\right]$$ (8.20)

where θ and θ' are the angles of incidence and refraction, respectively. The angles of refraction

$$\theta' = \arcsin\left[\frac{\sin(\theta)}{n_2}\right]$$ (8.21)

where n_2 is the index of refraction of glass, and the average index of refraction of glass for the solar spectrum is 1.526 (Duffie and Beckman, 1974).

The transmissivity considering only absorption

$$\tau_a = e^{-KL} \tag{8.22}$$

where K is the extinction coefficient, and L is the actual path of the radiation through the medium. The extinction coefficient K is assumed to be a constant in the solar spectrum, and the value of K varies from about 0.04/cm for "water white" glass to about 0.32/cm for poor (greenish cast of edge) glass. The usual nominal thicknesses of glass are 2.4, 3, 5, 5.5, 6, and 13 mm (ASHRAE, 1997).

The Temperature of the Atmosphere

Assuming that the lowest temperature appears at 6:00 am, and the peak temperature appears at 3:00 pm (15:00), the temperature of the atmosphere T_a can be expressed as

$$T_a = T_{a,min} + \left(T_{a,max} - T_{a,min}\right)\sin[(t-6)*10)] \qquad (t \le 15)$$

and $\qquad T_a = T_{a,min} + \left(T_{a,max} - T_{a,min}\right)\cos[(t-15)*10)] \qquad (t>15) \tag{8.23}$

The Product of Heat Loss Coefficient and the Surface Area $U_L A_p$

The heat loss of the pipe can be decomposed as the heat loss of the top half of the pipes and that of the lower half (back) of the pipes.

The top heat loss coefficient U_t (including convective and radiation loss) is calculated with the equation developed by Klien (1975) and discussed by Duffie and Beckmann (1991)

$$U_t = \left\{ \frac{N}{\dfrac{C}{T_{p,m}}\left[\dfrac{T_{p,m}-T_a}{N+f}\right]^e} + \frac{1}{h_w} \right\}^{-1} + \frac{\sigma(T_{p,m}+T_a)(T_{p,m}^2+T_a^2)}{(\varepsilon_{p,t}+0.0059lh_w)^{-1}+(2N+f-1+0.133\varepsilon_{p,t})/\varepsilon_g - N} \tag{8.24}$$

where $T_{p,m}$ is the temperature of the collector pipe, $f = (1+0.089h_w-0.1166h_w\varepsilon_p)(1+0.07866N)$, $e=0.43(1-100/T_{p,m})$, $C=520(1-0.000051\theta_p^2)$, θ_p is the tilt angle, $\varepsilon_{p,t}$ and ε_g is the emissivity of top part of the collector pipe and glass cover, N is the number of the glazing ($N=1$ in our case), h_w ($=2.8+3.0V$) is the wind heat transfer coefficient and V is the outdoor wind velocity.

The above equation is developed to fit the graphs for U_t for the flat absorbing surface. However, in our case, the absorbing surface is the surface of the collector tubes and it is not in the same area as the cover. So Eq. (8.24) needs to be adapted as

$$U_t A_p = \left\{ \frac{N}{\frac{C}{T_{p,m}} \left[\frac{T_{p,m} - T_a}{N+f} \right]^e} + \frac{1}{h_w} \right\}^{-1} A_c + \frac{\sigma(T_{p,m} + T_a)(T_{p,m}^2 + T_a^2)}{(\varepsilon_{p,t} + 0.00591 h_w)^{-1} + (2N + f - 1 + 0.133\varepsilon_{p,t})/\varepsilon_g - N} A_p$$

$$(8.24^*)$$

where A_p and A_c is the area of the absorbing pipe (at most half of the whole pipe) and that of the cover, respectively.

The back heat loss coefficient from the collector pipe to the casing is the sum of the convective heat loss coefficient $h_{b,c}$ and the radiation heat loss coefficient $h_{b,r}$, ie,

$$h_b = h_{b,c} + h_{b,r} \tag{8.25}$$

The back convective heat loss coefficient (Arnold et al., 1976; see also Bejan, 1984; Rohsenow, 1998)

$$h_{b,c} = Nu(\theta_p)k_{air}/L \tag{8.26}$$

where k_{air} is the heat conductivity of the air, L is the distance of the two "plate". The Nusselt number

$$Nu(\theta_p) = 1 + (Nu(90°) - 1)\sin(180 - \theta_p)$$
$$\text{and} \qquad Nu(90°) = 0.364 \ (L/H)Ra_H^{\frac{1}{4}} \tag{8.27}$$

here H is the length of the plate in the inclined direction. The Rayleigh number is defined

$$Ra_H = (g\beta H^3 T)/(\alpha v) \tag{8.28}$$

where β is the volume coefficient of expansion and $\beta = 1/T_f$, α is the thermal diffusivity, and v is the kinematic viscosity. Based on the data given by Incropera and Dewitt (1994),

$$k = (0.075T_f + 3.8) \times 10^{-3} \ \text{W/m°C}, \qquad \alpha = (0.158T_f - 24.9) \times 10^{-6} \ \text{m}^2/\text{s},$$
$$\text{and} \qquad v = (0.1052T_f - 15.67) \times 10^{-6} \ \text{m}^2/\text{s} \tag{8.29}$$

The radiative heat transfer coefficient from the lower-half of the tube to the casing is

$$h_{b,r} = \frac{\sigma(T_p + T_b)(T_p^2 + T_b^2)}{(1 - \varepsilon_{p,b})/\varepsilon_{p,b} + 1/F_{pb} + A_p(1 - \varepsilon_b)/(A_b \varepsilon_b)} \tag{8.30}$$

where T_b is the temperature of the back casing, $\varepsilon_{p,j}$ and ε_b is the emissivity of the bottom of the collector pipe and the back casing, A_p and A_b are the areas of the lower part of the pipe (half pipe) and the back casing, respectively, and F_{pb} is the radiation shape factor from surface p (pipe) to surface b (back casing). (The radiation shape factor is defined as the fraction of radiant energy leaving one surface which strikes a second surface directly, both surface assumed to be emitting energy diffusely. Detailed definitions and analysis on thermal radiation see Siegel and Howell 1981.) In order to reduce the radiation heat loss, the collector pipe is not painted black or covered by an adsorbing film, so the emissivity of the lower part of the pipe is not the same as the top part. The pipe is usually made of stainless steel, and the back casing is usually made of aluminium sheet. For the typical stainless steel, $\varepsilon = 0.22$ and for the heavily oxidized aluminium, $\varepsilon = 0.2\text{-}0.31$ (Holman, 1997). The radiation shape factor $F_{pb} = F_{bp} (A_b /A_p) = F_{bp} (A_b /A_p) = 2/\pi$ for the cylindric pipes contacting closely and neglecting the edge effect.

8.3 SIMULATION OF THE PERFORMANCE OF THE ADSORPTION EFRIGERATION CYCLE POWERED BY SOLAR RADIATION

8.3.1 The Temperature of the Collector and the Useful Heat Gained by the Collector

The useful heat gained by collector depends also on the temperature of the collector pipe. By replacing the constant heat flux with the variable heat flux in the equations in chapter 4, the temperature change of the collector pipe, and the useful heat gained by collector can be evaluated. The results for our case are illustrated in Fig. 8.1 and 8.2, respectively. The total solar radiation I_t is also shown in Fig. 8.1.
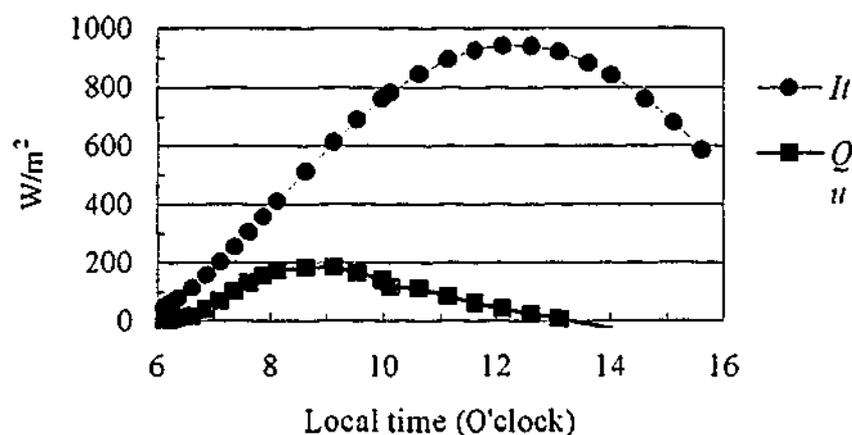

Figure 8.1 The total solar radiation I_t and the useful heat Q_u gained by the collector (January 21, Gippsland, $V=5$ m/s, $\theta_p=30°$, one-glass cover, 2.4 mm thick, $\varepsilon_{p,t} = 0.96$, $\varepsilon_g =0.88$, $\varepsilon_{p,b}=0.22$, $\varepsilon_b =0.216$, $D_i =0.0506$ mm, $L=0.05$ m, and $H=0.53$ m)
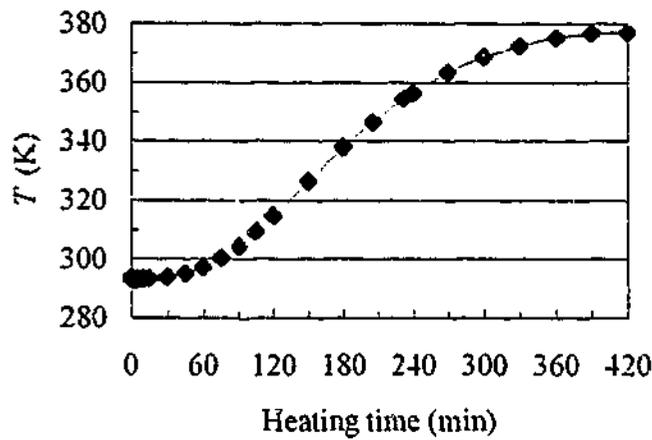
Figure 8.2 The temperature of the solar collector tube (T_e=2°C, T_l=20°C)

The ratio of the useful heat to the solar radiation is called the efficiency of the collector, and it is evaluated and shown in Fig. 8.3 for our case.
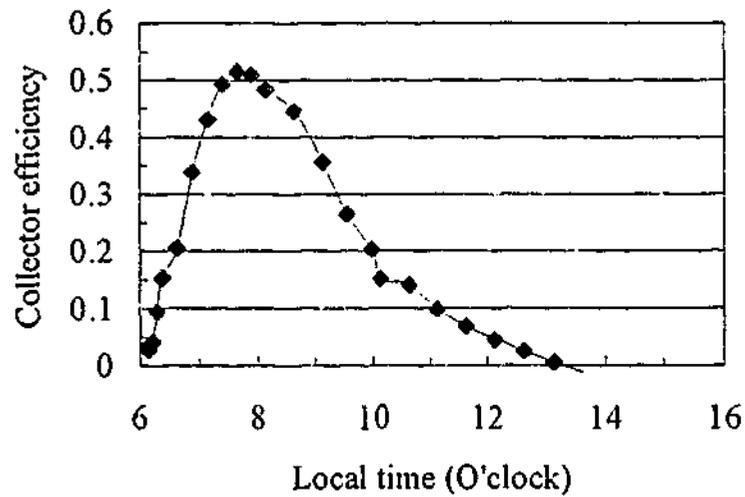

Figure 8.3 The efficiency of the solar collector (January 21, Gippsland, V=5 m/s, θ_p=30°, one-glass cover, 2.4 mm thick, $\varepsilon_{p,t}$ = 0.96, ε_g = 0.88, $\varepsilon_{p,b}$= 0.22, ε_b = 0.216, D_i =0.0506 mm, L=0.05 m, and H=0.53 m)

From the figures, it can be seen that the solar radiation, the temperature of the pipe, the useful heat, and the efficiency of the collector all initially increases with time and then decrease. After the temperature reaches its maximum, the heat loss is greater than the heat gain, so the temperature will decrease then. The efficiency of the collector changes with the time (Fig. 8.3).

8.3.2 The Simulation of COP

To simulate the performance of the adsorption refrigeration cycle powered by the solar radiation, it is necessary to correlate the temperature of the collector pipe and the heating time. The investigation of the Fig. 8.2 results in the following regression expressions (the relationship of the heating time t and the temperature T):

$$t = \frac{410}{\pi}\cos^{-1}(\frac{346.56 - T}{53.41}) \qquad (T \leq 346.56 \text{ K}) \qquad (8.31a)$$

$$t = 205 + \frac{430}{\pi}\sin^{-1}(\frac{T - 346.56}{30.58}) \qquad (346.56 < T < 377.14\text{K}) \qquad (8.31b)$$

and

$$t = 420 + \frac{430}{\pi} + \sin^{-1}(\frac{T - 377.14}{30.58}) \qquad (T \geq 3377.14 \text{ K}) \qquad (8.31c)$$

Substituting these relationships (Eq. 8.31) into Eq. (5.28d), the enthalpy change of the pressure adjusting gas

$$\Delta H_{pr,2-3} \approx \frac{\dot{m}_{pr}c_{pr}hA_{tot}}{\dot{m}_{pr}c_{pr} + hA_{tot}}\left[60(346.56 - T_c)(t_3 - t_2) + 53.41\frac{410}{\pi}\left(\sin(\frac{\pi}{410}t_3) - \sin(\frac{\pi}{410}t_2)\right)\right]$$

$$(T \leq 346.56 \text{ K}) \qquad (8.32a)$$

$$\Delta H_{pr,2-3} \approx \frac{\dot{m}_{pr}c_{pr}hA_{tot}}{\dot{m}_{pr}c_{pr} + hA_{tot}}\left[\begin{array}{l}60(346.56 - T_c)(205 - t_2) + \frac{53.41 \times 410}{\pi}\left(\sin(\frac{\pi}{410}t_3) - \sin(\frac{205\pi}{410})\right)\\ + 60(346.56 - T_c)(t_3 - 205) + \frac{30.58 \times 430}{\pi}\left(1 - \cos(\frac{\pi(t_3 - 205)}{430})\right)\end{array}\right]$$

$$(346.56 < T < 377.14\text{K}) \qquad (8.32b)$$

and

$$\Delta H_{pr,2-3} \approx \frac{\dot{m}_{pr}c_{pr}hA_{tot}}{\dot{m}_{pr}c_{pr} + hA_{tot}}\left[\begin{array}{l}60(346.56 - T_c)(205 - t_2) + \frac{53.41 \times 410}{\pi}\left(\sin(\frac{\pi}{410}t_3) - \sin(\frac{205\pi}{410})\right)\\ + 60 \times 215 \times (346.56 - T_c) + \frac{30.58 \times 430}{\pi}\left(1 - \cos(\frac{215\pi}{430})\right)\\ + 60(346.56 - T_c)(t_3 - 420) + \frac{30.58 \times 430}{\pi}\left(1 - \cos(\frac{\pi(t_3 - 420)}{430})\right)\end{array}\right]$$

$$(T \geq 3377.14 \text{ K}) \qquad (8.32c)$$

Other items in the COP formula (Eq. 5.73) can be evaluated by the same equations presented in chapter 5. Substituting Eq. (8.32) and other related equations into Eq. (5.73), the coefficient of performance (COP) of the adsorption refrigeration cycle powered by the solar radiation can be evaluated now. The results are shown in Fig. 8.4 to 8.12. The COP of the system without pressure-adjusting gas is also shown in the figures in hollow mark and dotted line.
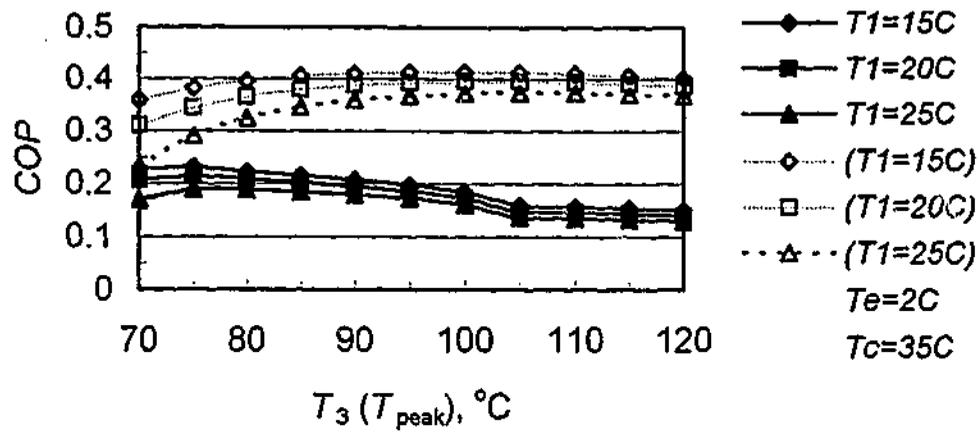
Figure 8.4 The relationship of the Coefficient of Performance (COP) and the peak temperature of the collector (T_e=2°C, T_c=35°C)
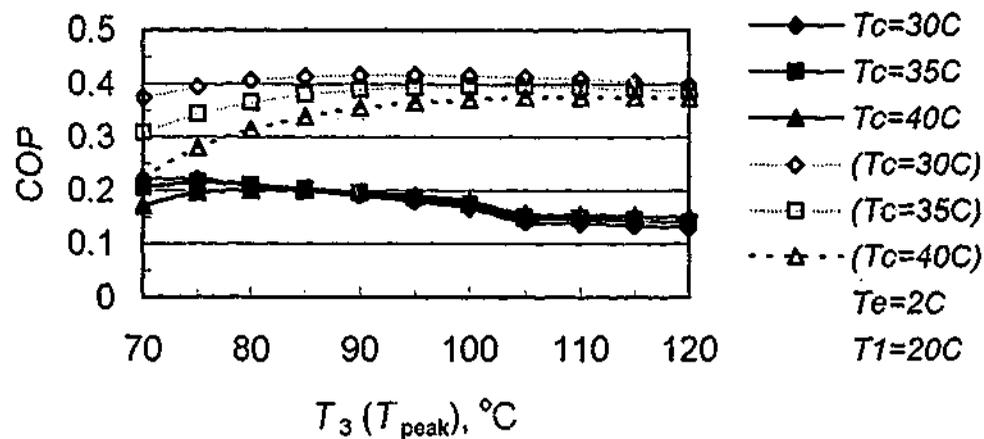
**Figure 8.5** The relationship of the Coefficient of Performance (COP) and the peak temperature of the collector (T_e=2°C, T_1=20°C)
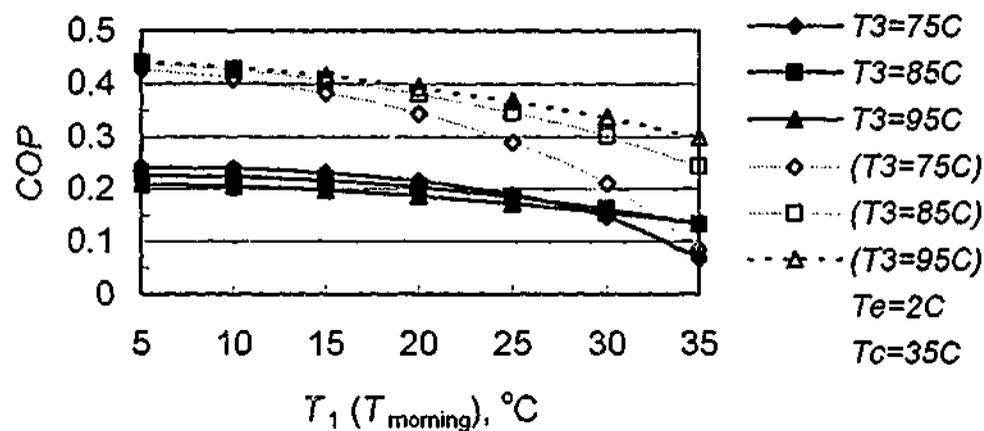

Figure 8.6 The relationship of the Coefficient of Performance (COP) and the temperature of the collector in the morning (T_e=2°C, T_c=35°C)
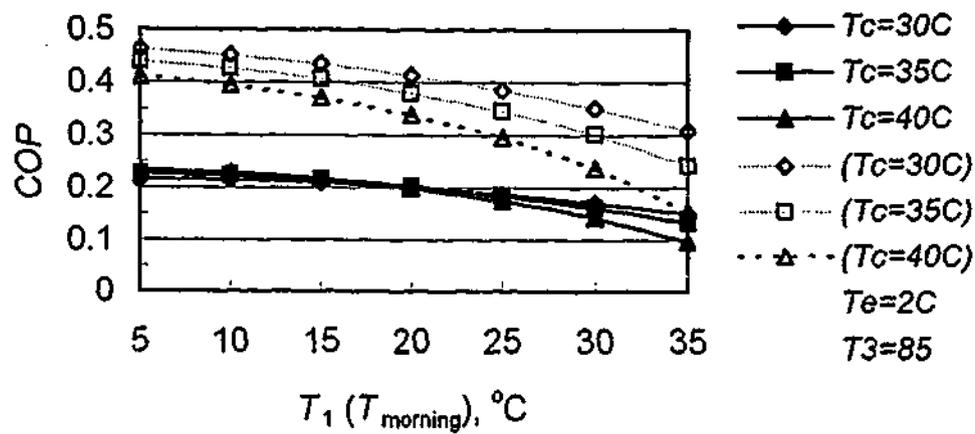
Figure 8.7 The relationship of the Coefficient of Performance (COP) and the temperature of the collector in the morning (T_e=2°C, T_3=85°C)
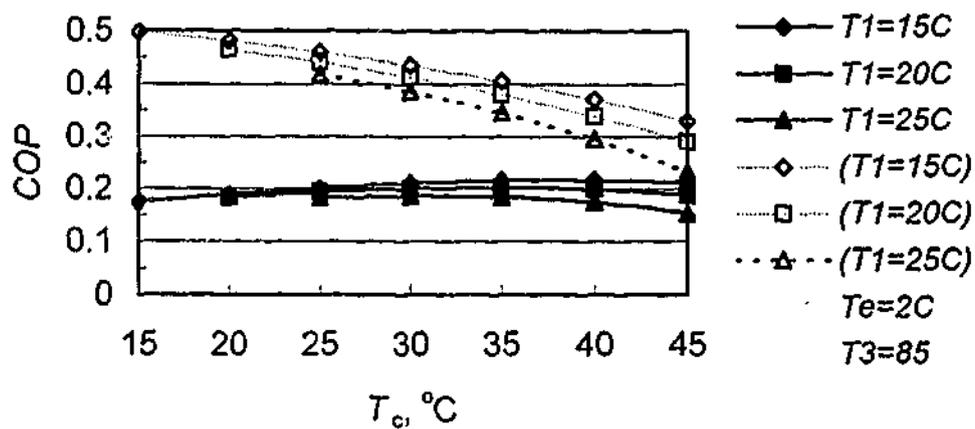
**Figure 8.8** The relationship of the Coefficient of Performance (COP) and the condenser temperature (T_e=2°C, T_3=85°C)
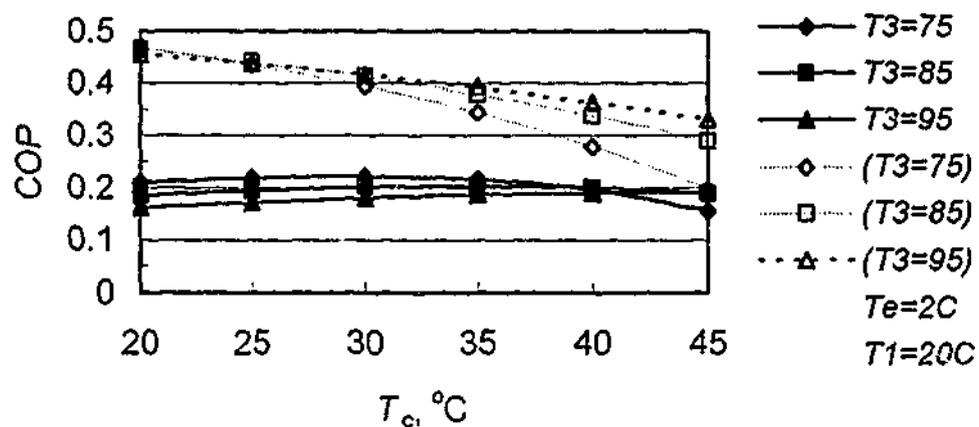
Figure 8.9 The relationship of the Coefficient of Performance (COP) and the condenser temperature (T_e=2°C, T_1=20°C)
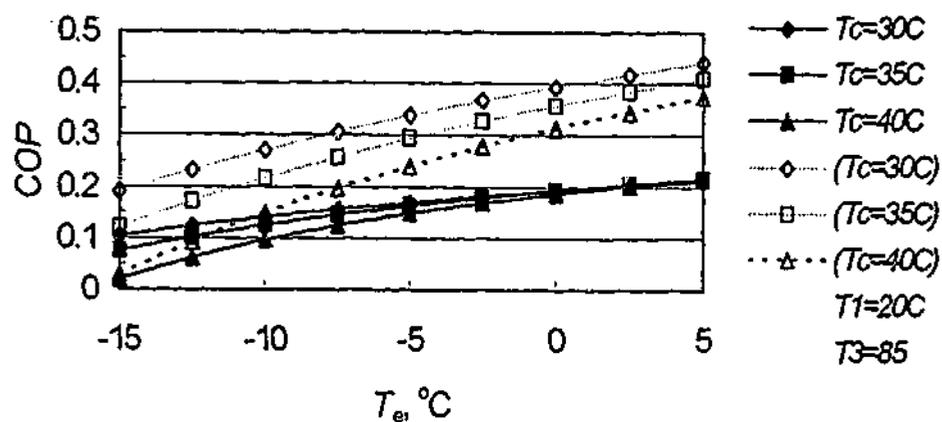
**Figure 8.10** The relationship of the Coefficient of Performance (COP) and the evaporator temperature (T_1=20°C. T_3=85°C)
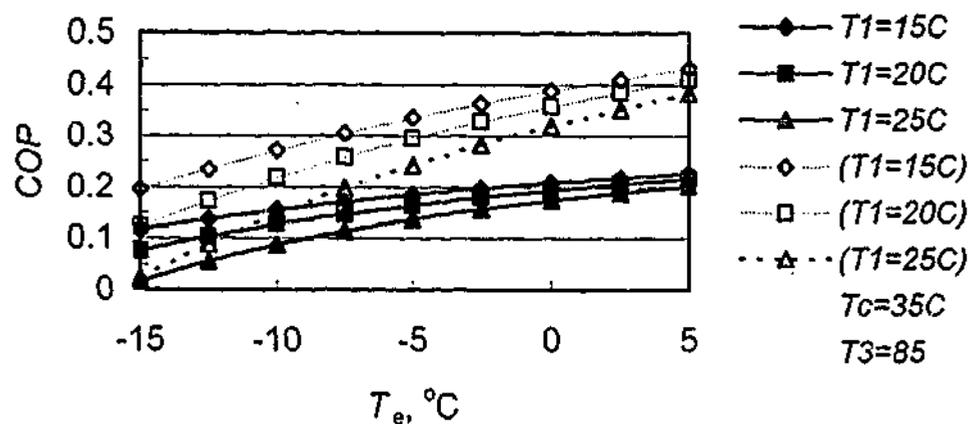
Figure 8.11 The relationship of the Coefficient of Performance (COP) and the evaporator temperature (T_c=35°C, T_3=85°C)
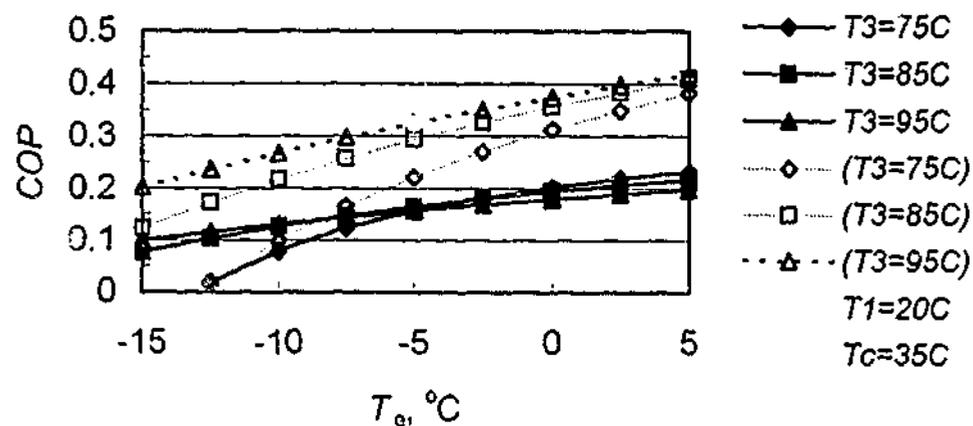
**Figure 8.12** The relationship of the Coefficient of Performance (COP) and the evaporator temperature (T_1=20°C, T_c=35°C)

From the figures, it can be seen that the COP of the system has similar trends as shown in chapter 5. The COP decreases markedly away the peak temperature of 110°C (Fig. 8.4 and 8.5).

8.3.3 The Simulation of the Exergetic Efficiency

Substituting Eq. (8.31) into Eq. (7.71a), the exergetic efficiency of the adsorption refrigeration cycle powered by solar radiation can be evaluated and it is shown in Fig. 8.13 to 8.21
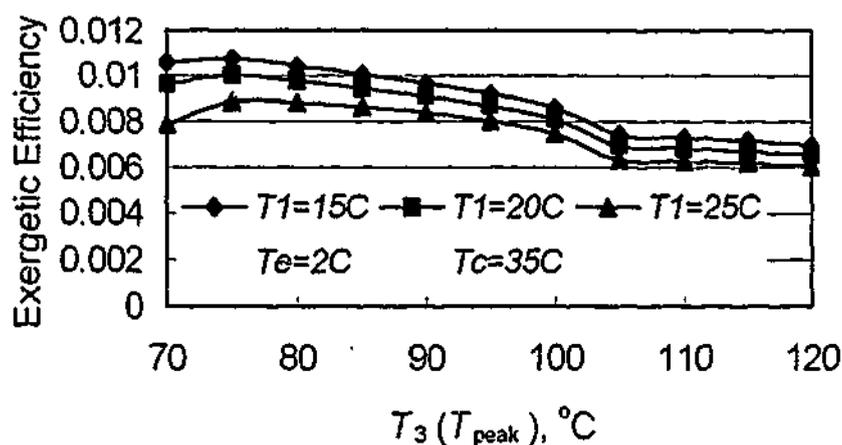

Figure 8.13 The relationship of the exergetic efficiency and the peak temperature of the collector (T_e=2°C, T_c=35°C)
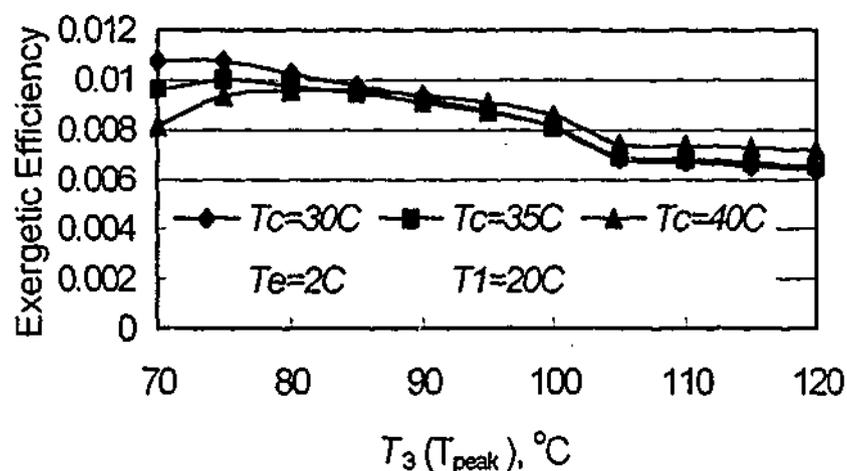
**Figure 8.14** The relationship of the exergetic efficiency and the peak temperature of the collector (T_e=2°C, T_1=20°C)
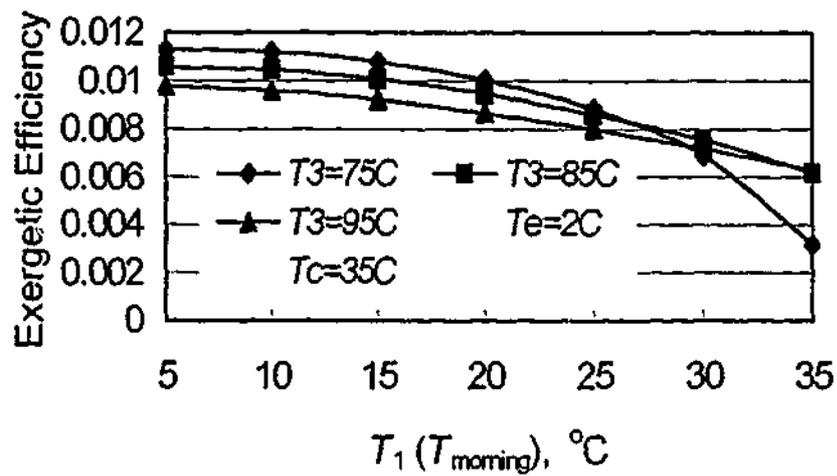
**Figure 8.15** The relationship of the exergetic efficiency and the temperature of the collector in the morning (T_e=2°C, T_c=35°C)
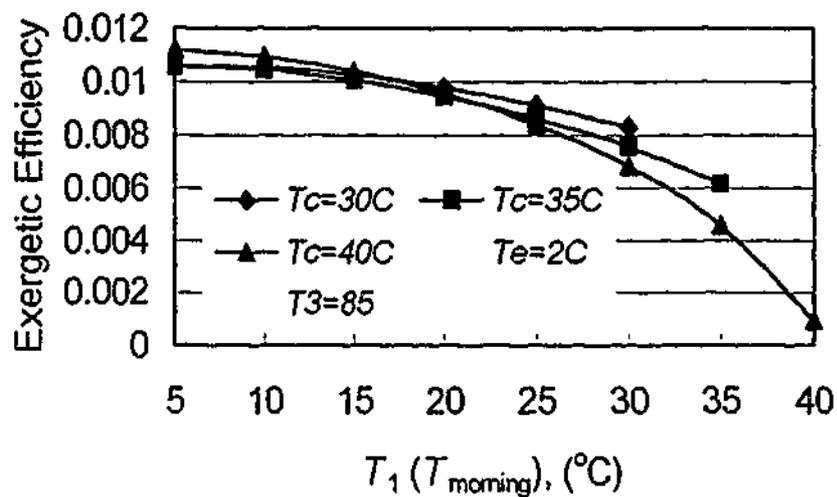
**Figure 8.16** The relationship of the exergetic efficiency and the temperature of the collector in the morning (T_e=2°C, T_3=85°C)
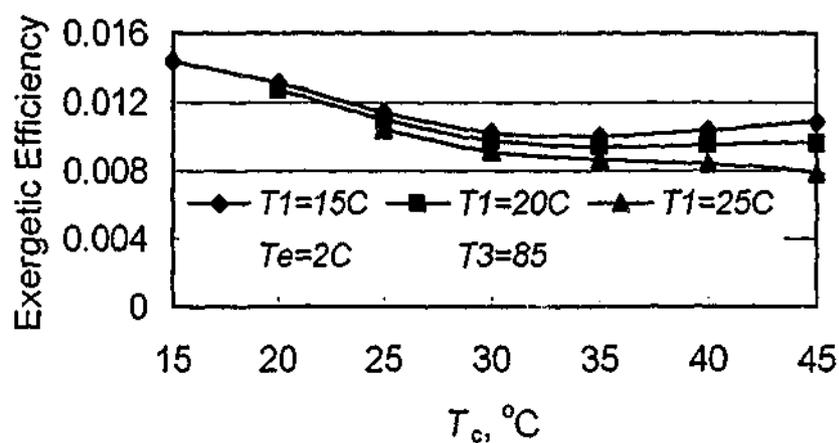
Figure 8.17 The relationship of the exergetic efficiency and the condenser temperature (T_e=2°C, T_3=85°C)
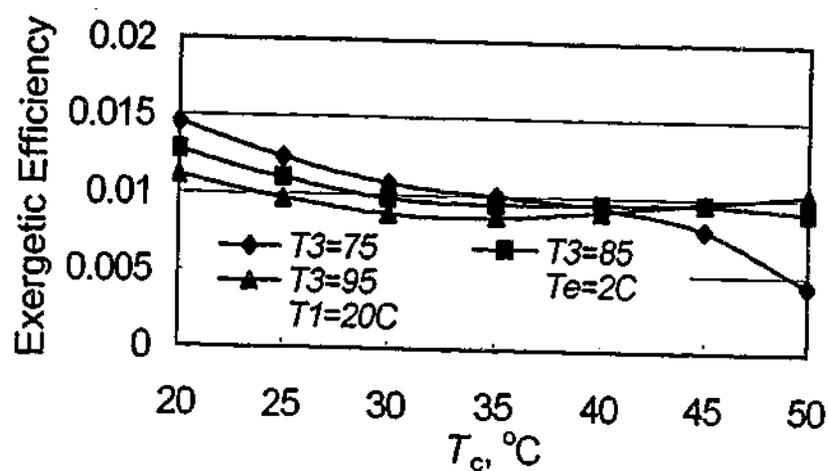
Figure 8.18 The relationship of the exergetic efficiency and the condenser temperature (T_e=2°C, T_1=20°C)
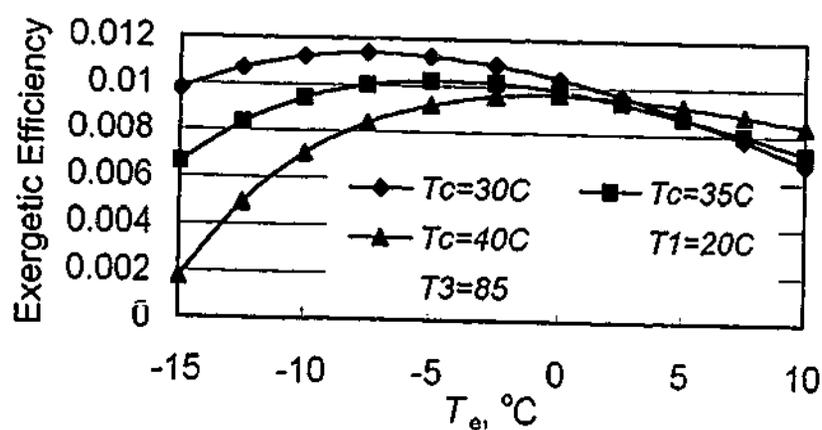
Figure 8.19 The relationship of the exergetic efficiency and the evaporator temperature (T_1=20°C, T_3=85°C)
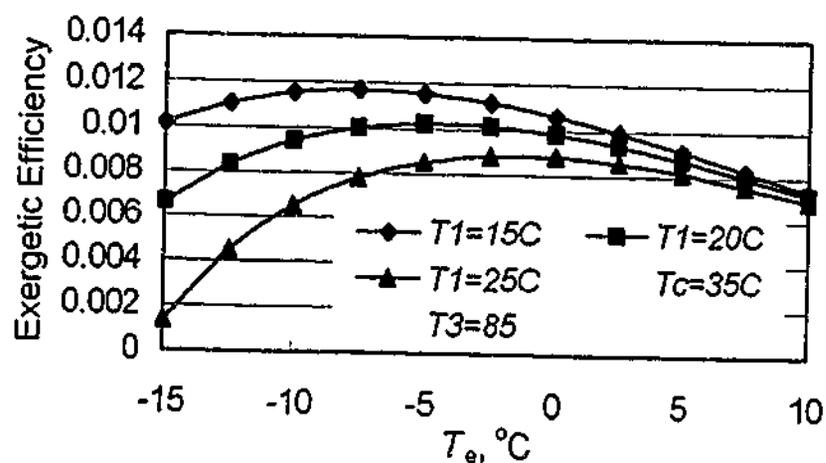
**Figure 8.20** The relationship of the exergetic efficiency and the evaporator temperature (T_e=35°C, T_3=85°C)
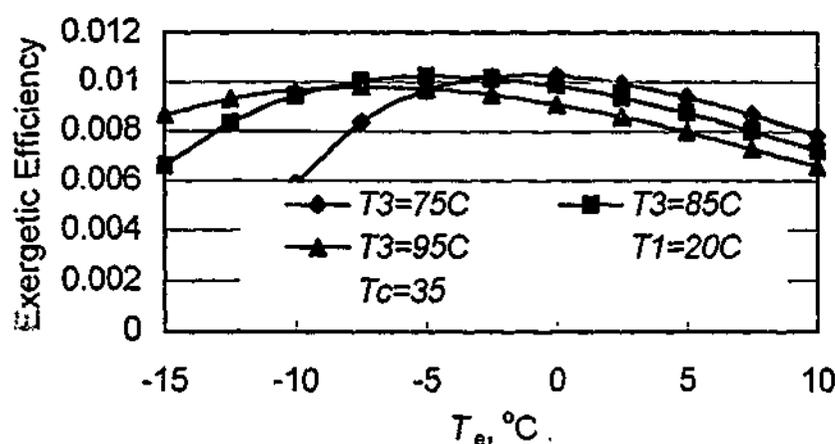
Figure 8.21 The relationship of the exergetic efficiency and the evaporator temperature (T_1=20°C, T_c=35°C)

From the figures, it can be seen that similar to COP, the exergetic efficiency of the system has similar trends found in chapter 7. The exergetic efficiency of the system changes wave-shapely with the peak temperature (Fig. 8.13 and 8.14). At the same peak temperature, the exergetic efficiency of the system is in the same trend with and almost the same amount as that in chapter 7.

8.4 THE SUMMARY OF USEFUL FORMULA

This thesis presented a comprehensive study on the solar adsorption refrigeration system. To facilitate the evaluation and simulation for the performance of the solar adsorption refrigeration system, some useful formulae are indexed here.

Some of the thermophysical properties of methanol, the adsorption property and the key thermodynamic properties of the adsorbent/methanol are determined in chapter 2. The saturated vapour pressure of methanol is determined by Eq. (2.4), or (2.1) and (2.2). The saturated density of methanol liquid is determined by Eq. (2.3) or (2.5). The P-T-x relationship of activated carbon 207E4 and methanol is presented in Eq. (2.41) and Eq. (2.12) and (2.13). The threshold temperatures of desorption and adsorption are determined by Eq. (2.37), (2.38) and (2.16).

The heat transfer analysis on the collector in the heating processes was described in chapter 4. The volumetric heat capacity and the effective thermal conductivity of the adsorption/desorption bed are evaluated by Eq. (4.2) to (4.9). The governing equations and conditions are described in Eq. (4.13) to (4.17). The finite-difference equations are presented in Eq. (4.18) to (4.29). The relationship of the temperature and time in the collector tube in the heating processes was obtained by obtained here is used in the following analysis (for the constant heat flux employed, the relationship is Eq. 4.30; for solar radiation simulated, Eq. 8.26).

The energy analysis on the solar adsorption refrigeration cycle was developed in chapter 5. The gross COP of the cycle is expressed by Eq. (5.73). In which, the maximum and minimum concentration is determined by Eq. (5.12) and (5.47), respectively. The mean specific heat of methanol is determined by Eq. (5.18). The mass of the pressure-adjusting gas in the collector is determined by Eq. (5.21b). The change of the enthalpy of the pressure-adjusting gas in the heating process 2-3 is determined by Eq. (5.28f) (for the constant heat flux) and Eq. (8.27) (for solar radiation simulated). The product of the pressure and the specific volume of the saturated methanol liquid is determined by Eq. (5.43). The average heat of desorption (adsorption) is evaluated by Eq. (5.54). The latent heat of liquid-vapour transition is determined by Eq. (5.70).

Chapter 6 conducted the mass adsorption transfer analysis and derived some useful formulae. The amount of adsorption and the rate of the adsorption are expressed by Eq. (6.49) and (6.50), respectively. The rate of refrigeration is calculated by Eq. (6.51). In these equations, the overall mass transfer coefficient k_{of} and k_{op} is evaluated by Eq. (6.29b) and (6.30b), respectively.

In chapter 7, a detailed exergy analysis on the processes and the whole cycle is carried out. The exergy change, the exergy used, and the exergy loss for the heating process 1-2 are expressed by Eq. (7.57b) (or 7.59b), (7.60) and (7.61), respectively. The exergy change, the exergy used, and the exergy loss for the heating process 2-3 are expressed by Eq. (7.73), (7.74), and (7.75), respectively. The exergy loss in the flashing step is expressed by Eq. (7.78a). The gross exergy gain and the exergy loss are expressed by Eq. (7.80b) (or 7.83b) and (7.85b) (or 7.85c). The exergy used and the exergy loss in the whole cycle is expressed by Eq. (7.86) and (7.87), respectively. The exergetic efficiency of the processes (steps) and the whole cycle is expressed by Eq. (7.89). In the above equations, the mean specific heat for entropy calculation is determined by Eq. (7.52). The heat of adsorption is determined by Eq. (5.53). The mole fraction of the adsorbent/refrigerant mixture can be calculated from Eq. (5.12) and (5.47). The mole fraction of the refrigerant vapour and the pressure-adjusting gas can be determined by the same approach as that in section 4.2.2. The mass rate of the pressure-adjusting gas is determined by Eq. (5.27). The specific heat of the methanol vapour is determined by Eq. (7.66). The quality of solar irradiance is evaluated by Eq. (7.30). The mass of the liquid refrigerant at the beginning of the cooling step is determined by Eq. (7.77).

A simulation of the performance of the adsorption refrigeration powered by solar radiation was described in chapter 8. Solar radiation is determined by Eq. (8.1) to (8.15). The performance of the collector is evaluated by Eq. (8.16) to (8.25). By replacing the constant heat flux with the variable heat flux into the equations in chapter 4, the temperature of the collector pipe, the useful heat, and thus the COP and the exergetic efficiency of the system can be simulated.

With these models and equations presented here, the performance of the solar adsorption refrigeration system working at near atmospheric pressure can be evaluated comprehensively.

9

Some Suggestions and Guidelines for the Design of the Prototype

The previous chapters presented a comprehensive analysis of a solar adsorption refrigeration system working around atmospheric pressure. The analysis was compared to results obtained on the indoor experimental rig developed. A simulation of the performance of the adsorption refrigeration cycle powered by solar radiation is also conducted. To investigate this technique further, a prototype must be designed, built and tested. The detailed design, building, and testing of the prototype are beyond the scope of this thesis. This chapter presents some suggestions and guidelines for the prototype design.

9.1 THE COLLECTOR/ADSORPTION BED

- Flat-plate collector is suitable for the system.

- Stainless steel is recommended as the material of the collector pipe. Copper and Aluminium are not suggested since copper may cause the decomposition of methanol and corrosion may occur at the junction between aluminium and other metal materials.

- The heat capacity of the collector (the collector pipe and the contained materials) needs to be selected for particular climate and application (eg. the ambient temperature, the condenser temperature, the evaporator temperature).

- To harvest the solar radiation simply and effectively, the collector pipes can be in contact each other, and the upper half of the pipe shall be painted black or covered by some adsorption film.

- It is useful to have two 'dampers' in the collector. One is at the upper side edge, and the other, the lower side edge, of the collector. In the heating process (during the day), the dampers are closed. In the cooling process (the late day and night) the dampers are open to cool down the adsorption bed quickly and to help keeping the temperature of the adsorption bed as low as possible.

- The cover of the collector could be a single ordinal glass.

- The casing of the collector and the dampers need to be heavily insulated.

- The distance from the collector pipe to the glass cover and from the collector pipe to the back casing may be taken as 50 mm (Hu, 1992).

The collector is schematically shown in Fig. 9.1 and 9.2.
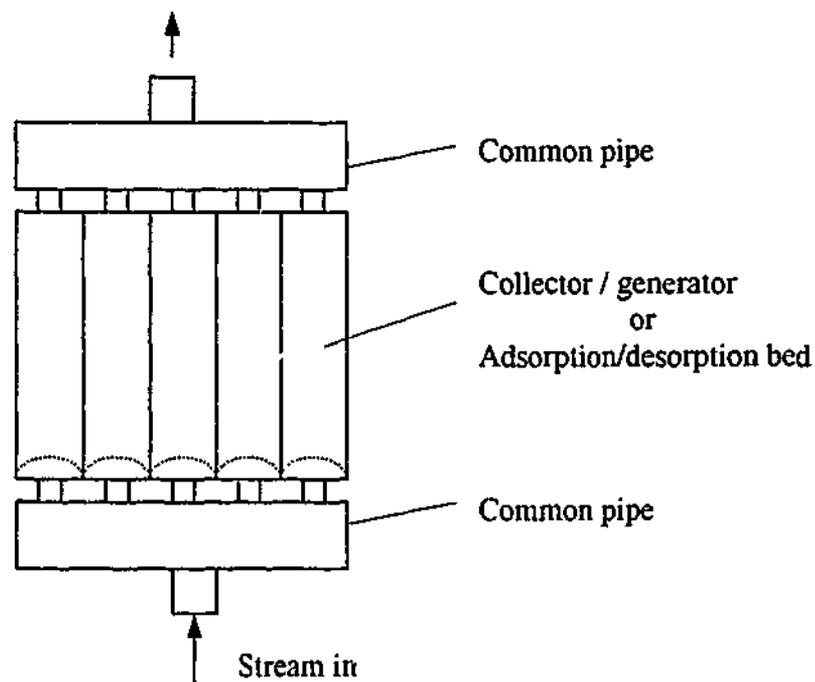
Figure 9.1 The schematic arrangement of the collector pipes
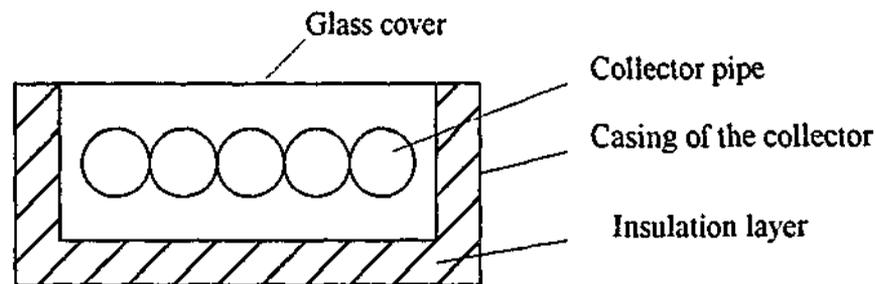
Figure 9.2 The schematic of the relative position of the collector pipe and the casing

9.2 THE CONDENSER

- To simplify the system, the condenser can be a static air cooled one (natural convection).

- To improve heat exchange, fins are employed in the outside of the pipe of the condenser (in the air side).

- To reduce the flow resistance, a grid configuration for the condenser is recommended (Fig. 9.3). The pipes of the condenser are made straight.

- To prevent the condensed refrigerant from being trapped in the condenser, the lower common pipe should be inclined to the outlet of the condenser to allow for drainage. The inclination should be equal to, or greater than, 0.01.

- The condenser pipe can be made of copper or brass.

The condenser is schematically shown in Fig. 9.3.
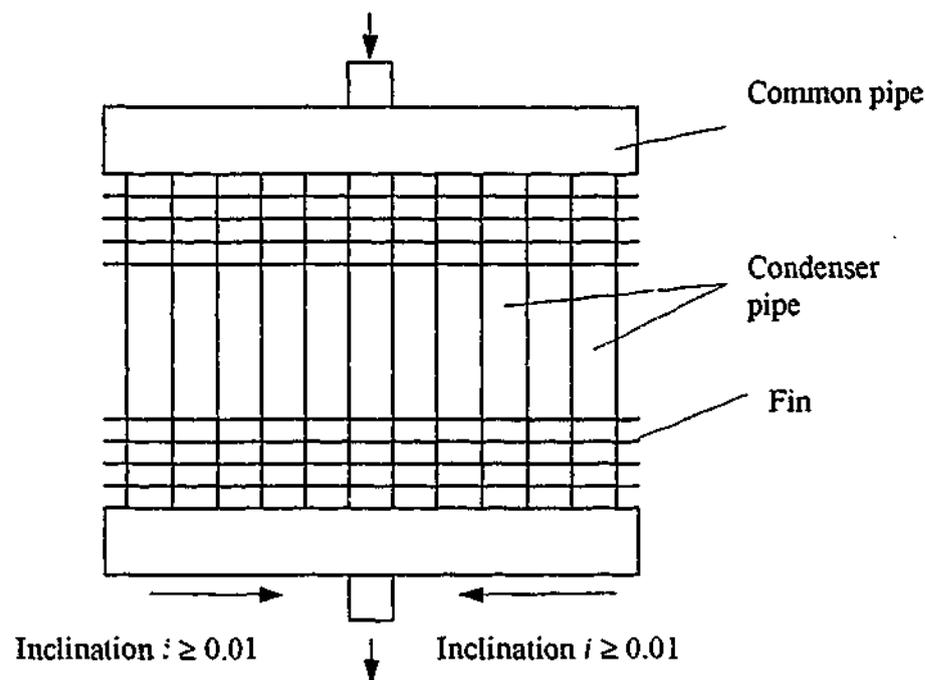
Figure 9.3 The schematic of the condenser

9.3 THE EVAPORATOR/COOLING CHAMBER

- The solar adsorption refrigeration system can be adapted for different purposes with different shapes of evaporators. The evaporator supposed here is for a domestic refrigerator.

- To simplify the system, the evaporator can be a static air cooled one (natural convection).

- To reduce the flow resistance, a grid configuration for the evaporator is also recommended (Fig. 9.4).

- To get a good cooling, the evaporator pipe may be installed in the cooling chamber (Fig 9.5).

- To protect the evaporator pipe, a plate with good thermal conductivity may be employed (plate-type evaporator). This plate also plays the role of a fin increasing the heat exchange.

- The evaporator pipe can be made of copper or brass.

- To protect the bottom pipe/plate of the evaporator, a tray may be employed in which the objects or materials to be cooled is put on.

- A sight glass can be included in the evaporator if the condensing and evaporating processes need to be observed.

The structure of the evaporator is schematically shown in Fig. 9.4, and the assembly of the evaporator/cooling chamber is schematically shown in Fig. 9.5 for the case the pipe being installed in the cooling chamber.
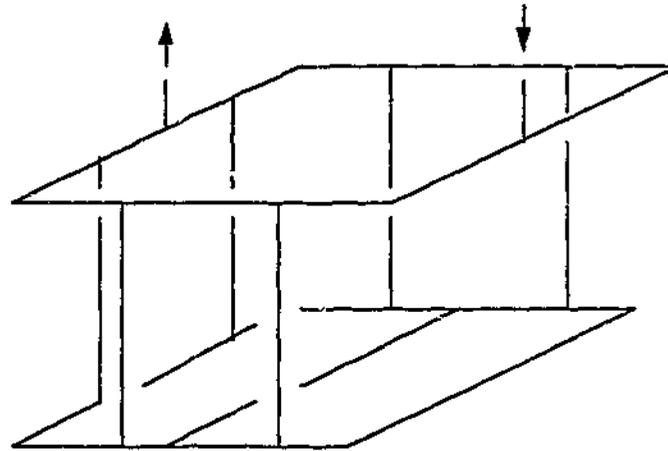

Figure 9.4 The schematic arrangement of the evaporator pipes
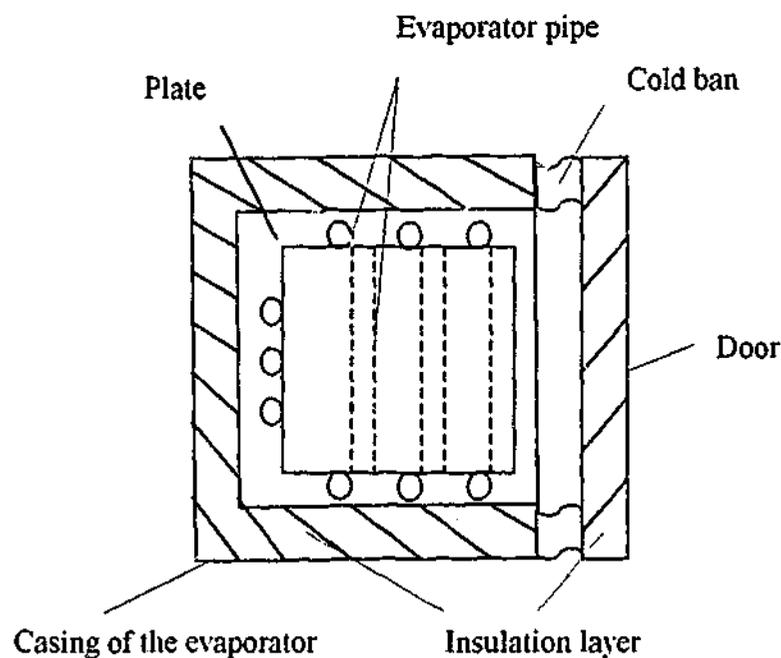
Figure 9.5 The schematic of the relative position of the evaporator and the casing

9.4 THE SYSTEM

- The collector is tilted with a suitable angle to face the solar radiation.

- The condenser is arranged below the collector to shield the direct solar radiation but with enough distance for air convection.

- A pipe connecting the evaporator outlet and the collector inlet and a fan is needed for circulation in the stream. The fan may be powered by a small solar PV plate or battery.

- Measuring meters and instruments. Solar radiation pyranometer, w. \.)eed meter, pressure gauge, thermometers in the collector bed, in the condenser, in the eva_orator, in the cooling space, and in the cooled subjects or materials, in the inlet and out let of each component, etc.

The system is schematically shown in Fig. 9.6.
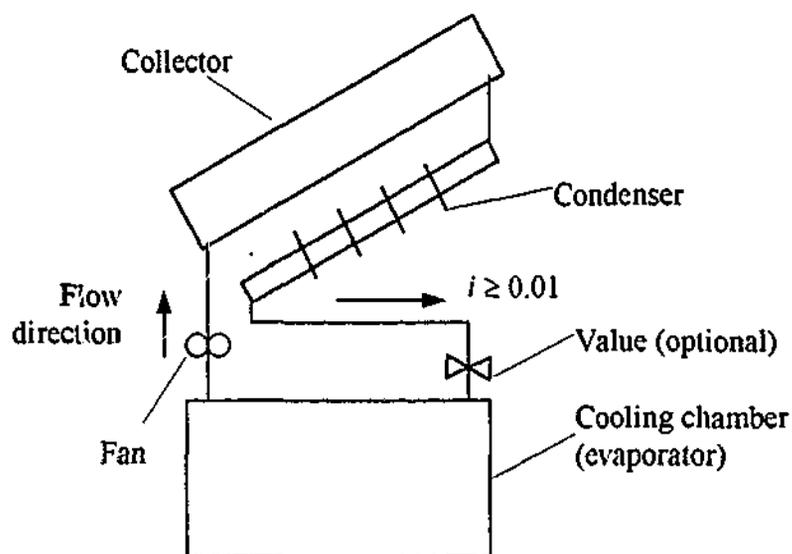
Figure 9.6 The schematic of the solar adsorption refrigeration system

Conclusions

From the research conducted in this thesis, it can be concluded:

- The research hypothesis that the working pressure of the adsorption refrigeration system using methanol as refrigerant could be adjusted to about atmospheric pressure by using a selected adsorbent and introducing a pressure balance gas has been proved experimentally and theoretically.

- Activated Carbon has been found suitable for use as the adsorbent, while Helium used as the pressure-balance gas.

- Some Molecular Sieve samples tested (MS 5A and MS 13X) are not good for this purpose when solar energy is the heating source. Other Molecular Sieves and other refrigerants remain to be explored as the adsorbent/refrigerant pairs.

- The heat transfer analysis yielded descriptions of the temperature distribution in the collector tube and the temperature variation with time in the heating and the heating/desorption processes for the constant heat flux. The results from the theoretical model agreed with the experimental results. So the model was extended to the variable heat flux in the simulation.

- The energy analysis on the solar adsorption refrigeration cycle evaluated the thermodynamic performance of the system. The introduction of the pressure-adjusting gas into the system increases the heat consumed, thus decreases the COP. The optimal COP of the new system is about half of that of the conventional system at the same conditions except the peak temperature. *The most important task in this research is to eliminate the leaking problem for the vacuum system; therefore, the difference of the COPs of the systems with and without the pressure-adjusting gas is not the main concern here.* The COP of the system working around atmospheric pressure can be improved by reducing the velocity of the stream.

- The energy and exergetic analyses showed that for a certain climate (eg, a certain morning temperature and a certain condenser temperature) and a certain application (eg, a specific evaporator temperature), there is an optimal peak temperature at which the COP and the exergetic efficiency of the system are maximized. The optimal peak temperature is in the range

of 70-95°C for our case. Over this optimal peak temperature, the COP and the exergetic efficiency will decrease and will be only about two thirds of the maximum COP when the peak temperature is designed to be 120°C. Thus the solar refrigeration system should be designed and charged specifically for specific situations to achieve the best thermodynamic performance.

- The exergy analysis on the processes and the whole cycle revealed the 'weakest link' of the system. In our case, there is large exergy loss in heating process from state 1 to state 2 and from state 2 to state 3, so if the thermodynamic performance of the system is to be improved, the thermal performance of these processes should be improved firstly. This improvement can be achieved by designing the collector/desorption bed properly for the particular application and reducing the velocity of the stream. Since the detailed exergy analysis for adsorption refrigeration system has not been found reported, the methodology of the analysis developed in this study was a new attempt in this aspect.

- This system is suitable to locations with the low morning temperature, and medium ambient air temperature in the day. From the viewpoint of refrigeration, the larger the difference of the concentrations (the ratio of the amount of refrigerant hold by the adsorbent to the amount of the adsorbent) in a cycle, the larger the cooling capacity, while the lower the morning temperature, the larger the maximum concentration can be hold and the lower the condenser temperature, the lower the minimum concentration can be reached (with the same evaporator temperature and the same peak temperature). However, the lower the minimum concentration, the harder it is to get the refrigerant desorbed. Thus the cycle needs a compromise between the cooling capacity and the heat consumed.

- The adsorption mass transfer model developed in this study described the adsorption process. The adsorption transfer analysis resulted in some useful derivates (eg, the rate of adsorption and the rate of cooling). The rate of cooling, which is strongly subjected to the velocity of the stream, is determined by the insulation of the evaporator.

- The simulation gave a more realistic indication of the cycle performance (eg, COP and exergetic efficiencies) of the performance of the adsorption refrigeration cycle powered by solar radiation in an actual installation. The simulation also shown that there is an optimal peak temperature at which the COP and the exergetic efficiency of the system are maximized. The optimal peak temperature is also in the range of 70-95°C for our case. Over this optimal peak temperature, the COP and the exergetic efficiency will decrease and then level off. The COP corresponding to the peak temperature of 120°C is also only about two thirds of the maximum COP. The simulation can be refereed in the prototype design. In order to make it convenient to find the pertinent equations, an index of the useful formulae was also presented.

- The flat-plate solar collector is suitable for the system. For our activated carbon-methanol-helium system, the optimal peak temperature is in the range (75-95°C) that the flat-plate collector can reach (under 120°C). So there is no need to pursue a higher temperature and no need to employ advanced and expensive collectors.

- Some suggestions and guidelines were also presented for the full scale solar powered prototype design.

Recommendations for Further Work

To implant the solar adsorption refrigeration concept developed in this thesis, more work needs to be done. Some suggestions and recommendations for further work are:

- Modify the indoor experimental rig further. The condenser and the evaporator is the same component which compromises its performance. The advantage of this arrangement is that it is simple and compact, but the drawback is it is hard to measure the cooling effect directly. Although the cooling effect can be calculated (indirectly), it is preferable to measure it directly. That is why the measured cooling effect has not been given in the thesis. The evaporator in the new rig should be an independent one and should be heavily insulated.

- Design and build a prototype and conduct the field measurement. The indoor rig can simulate some of the climate conditions, but not all. A prototype such as the one suggested in chapter 9 should be designed, built, and tested in the realistic conditions.

- Modify the prototype until it works satisfactorily. Then if possible, design and build a sample machine and conduct further tests. Modify the design and the amount of refrigerant charged of the sample machine to make it as effective as possible. If the machine works satisfactorily for a reasonably long time, it can be mass produced.

References

Alam, K.C.A, Saha, B.B., Kang, Y.T., Akisawa, A., and Kashiwagi, T. (2000). Heat Exchanger Design Effect on the System Performance of Silica Gel Adsorption Refrigeration Systems. *Int. J. of Heat & Mass Transfer*, Vol 43, No 24, pp4419-31.

Arnold, J.N., Bonaparte, P.N., Catton, I., and Edwards, D.K. (1974). Experimental investigation of natural convection in a finite rectangular inclined at various angles from 0° to 180°, *Proc. of Heat Transfer Fluid Mech. Inst.*, Stanford University Press, CA, pp.321-9.

ASHRAE. (1995). *Applications Handbook*.

ASHRAE. (1997). *Fundamentals*.

ASHRAE. (1994). *Refrigeration Handbook*.

ASHRAE. (1996). *System and Equipment Handbook*.

Atkins, P.W. (1994). *The Second Law*, Scientific American Books.

Bansal, N.K., Blumenberg, J., Kavasch, H.J. and Rottinger, T. (1997). Performance Testing and Evaluation of Solid Absorption Solar Cooling Unit, *Solar Energy*, Vol. 61, No. 2, pp 127-40.

Bejan, A. (1997). *Advanced Engineering Thermodynamics*, John Wiley & Sons, New York.

Bejan, A. (1984). *Convection Heat Transfer*, John Wiley & Sons, New York.

Bentayeb, F., Lemmini, F., and Guilleminot, J.J. (1995). Adsorption of an adsorptive solar refrigerator to Moroccan climates, *Renewable Energy*,

Bird, R.B., Stewart, W.E., and Lightfoot, E.N. (1960). *Transport Phenomena*, John Wiley & Sons, New York.

Boelman, E.C., Saha, B.B., and Kashiwagi, T. (1997). Parametric Study of a Silica Gel-water Adsorption Refrigeration Cycle-the Influence of Thermal Capacitance and Heat Exchanger UA-values on Cooling Capacity, Power Density, and COP. *ASHRAE Transactions*, Vol 103, No 1, pp137-48.

Boubakri, A., Arsalane, M., Yous, B., Ali-Moussa, L., Pons, M., Meunier, F., Guilleminot, J. (1992). Experimental Study of Adsorptive Solar Powered Ice Makers in Agadia (Morocco)-1 and -2. *Renewable Energy*. Vol.2, No.1, pp.7-13, 15-22.

Boublik, T., Fried, V., and Hala, E. (1973). *The Vapour Pressure of Pure Substances*, Elsevier, Amsterdam.

Carslaw, H.S. and Jaeger, J.C. (1959). *Conduction of Heat in Solids*, Second Edition, Oxford University Press, New York.

Chang, S.C. and Roux, J.A. (1995). Thermodynamic Analysis of a Solar Zeolite refrigeration System. *J. of Solar Energy Engineering*, Vol 107, pp189-95.

Chen, J., Que, X., Chen, Z., and Wang, B. (1996). Experimental Study on Adsorption Refrigeration System Using Activated Carbon-ethanol pair, *Taiyangneng Xuebao*, Vol 17, No 3, pp216-9.

Cheng, W.-H. and Kung, H. (1994). *Methanol Production and Use*, Marcel Deckker, New York.

Cho, Soon-H., and Kim, Jong-N., (1992). Modeling of a Silica Gel/Water Adsorption-Cooling System, *Energy*, Vol. 17, pp.829-39.

Critoph, R.E. (1988). Performance Limitation of Adsorption Cycles for Solar Cooling, *Solar Energy*, Vol.41, No 1, pp.21-31.

Critoph, R.E. (1994). Ammonia Carbon Solar Refrigerator for Vaccine Cooling. *Renewable Energy*, Vol.5, No 1-4, Part I, pp.502-8.

Critoph, R.E. (1996). Towards a one tonne per day solar ice maker, *Renewable Energy*, Vol 9, No 1-4, pp.626-31.

Croft, D.R. and Lilley, D.G. (1977). *Heat transfer Calculations using Finite Difference Equations*, Applied Science Publishers Ltd, London.

Daubert, T.E. and Danner, R.P. (1984). *Data Compilation Tables of Properties of Pure Compounds*, American Institute of Chemical Engineers, New York.

Douss N. and Meunier F. (1989). Experimental Study of ccascading Adsorption Cycles, *Chemical Engineering Science*, Vol. 44, No 2, pp.225-35.

Douss N., Meunier F. and Sun L.M., (1988). Predictive model and experimental results for a two-adsorber solid adsorption heat pump. *Industrial Engineering and Chemical Research*, Vol.27, pp.310-316.

Dubinin, M.M and Astakhov, V.A. (1970). *Adv. Chem. Ser.*, Vol 102, pp69.

Dubinin, M.M. (1960). *Chem. Revs.*, Vol 60, pp235.

Duffie, J.A. and Beckman, W.A. (1991). *Solar Engineering of Thermal Processes*, John Wiley & Sons, Inc., New York.

Eggers-Lura, A. (1978). Solar Refrigeration in Developing Countries, Technology for Solar Energy Utilisation, *UNIDO, Development and Transfer of Technology Series*, No 5, UN, New York, pp107-12.

Eltom, O.M.M., and Sayigh, A.A.M. (1994). Adsorption capability of charcoal: A comparison study

of some activated and non-activated charcoal samples, *Renewable Energy*.

Erhard, A. and Hahne, E. (1997). Test and Simulation of a Solar-powered Absorption Cooling Machine, *Solar Energy*, Vol. 59(4-6), pp155-162.

Exell, R.H.B., Bhattacharya S.C. and Upadhyaya Y.R. (1987). *Final report of research and development of solar powered desiccant refrigeration for cold storage applications* (USAID Grant No. DPE-5542-G-SS-4057-00). AIT.

Follin, S. Goetz, V., and Guillot, A. (1996). Influence of Microporous Characteristics of Activated Carbons on the Performance of an adsorption Cycle for refrigeration, *Industrial & Engineering Chemistry Research*, Vol 35, pp.2632-9.

Gebhart, B. (1993). *Heat Conduction and Mass Diffusion*, McGraw-Hill, New York.

Glueckauf, E. (1955). *Trans. Faraday Soc.*, Vol 51, pp1540.

Grenier Ph. And Pons M., (1983). Experimental and Theoretical results on the use of an activated carbon-methanol intermittent cycle for the application to a solar powered ice maker. *Solar World Congress*, Pergamon Press, pp.500-506.

Grenier, Ph., Guilleminot, J.J., Meunier, F. and Pons, M. (1988). Solar powered solid adsorption cold store, *Journal of Solar Energy Engineering*.

Guilleminot, J.J. and Meunier, F. (1981). Etude experimentale diune glaciere solaire utilisant le cycle zeolithe 13X-eau. *Revue Gen. Therm.* Vol 239, pp825-33.

Guilleminot, J.J. and Meunier, F. (1987). Heat and Mass Transfer in a Non-isothermal Fixed Bed Solid Adsobent Reactor: a Uniform Pressure, Non-uniform Temperature Case, *Int. J. of Heat and Mass Transfer*, Vol 30, No 8, pp1595-1606.

Guilleminot, J.J., Meunier, F., and Mischler B. (1980). Etude de cycle intermittents a adsorption solid pour la refrigeration solaire. *Revue Phys. Appl.* Vol 15, pp441-52.

Hahre, E. (1988). Thermal Energy Storage: Some Views on Some Problems, *Proc. Conf. Heat transfer*, pp279-292.

Hajji, A., Worek, W.M., and Lavan, Z. (1991). Dynamic analysis of a closed-cycle solar adsorption refrigerator using two adsorbent-adsorbate pairs, *International Journal of Ambient Energy*.

Hinotani K. and Kanatani K. (1983). Development of a solar absorption refrigeration system. *Solar World Congress*, Pergamon Press, pp.507-511.

Holman, J.P. (1997). *Heat Transfer*, 8th Edition, McGraw-Hill, New York.

Hottel, H.C. (1976). A simple model for estimating the transmissivity of direct solar radiation through clear atmospheres, *Solar Energy*, Vol. 18, pp.129.

Howell, J.R. and Buckius, R.O. (1992). *Fundamentals of Engineering Thermodynamics*, 2nd Edition, McGraw-Hill, New York.

Hsieh, J.S. (1975). *Principles of Thermodynamics*, McGraw-Hill, New York.

Hu, E. J. (1992). *Study of Solar Powered Charcoal/Methanol Adsorption Refrigerator*. Ph.D. Thesis, Asia Institute of Technology, Bangkok, Thailand.

Hu, E. J. (1996). Simulated results of a non-valve daily cycled solar powered carbon/methanol refrigerator with a tubular solar collector. *Applied Thermal Engineering*. Vol. 16 No.5, pp439-445.

Hu, E. J. (1998). A study of thermal decomposition of methanol in solar powered adsorption refrigeration systems. *Solar Energy*. Vol. 62, No.5, pp325-329.

Hu, J. and Exell., R.H.B. (1993). Adsorptive Properties of Activated Charcoal/Methanol Combinations. *Renewable Energy*. Vol.3, No.6-7, pp567-75.

Huang Zhi-Cheng and Li Zhong-Fu (1992). Design and test of a solar adsorption ice maker, *Second World Renewable Energy Congress*, U.K.

Hunn, B.D., and Calafell, D.O. (1977). Determination of average ground reflectivity for solar collectors, *Solar Energy*, Vol.19, pp. 87.

Iloeje, O.C. (1985). Parametric Effects on the Performance of a Solar Powered Solid Absorption Refrigerator. *Intersol '85*, Pergamon Press, pp.736-741.

Iloeje, O.C., Ndili, A.N., and Enibe, S.O. (1995). Computer simulation of A $CaCl_2$ solid-adsorption solar refrigerator, *Energy*.

Incropera, F.P. and DeWitt, D.P. (1990). *Introduction to Heat Transfer*, John Wiley & Sons, New York.

Jakob, M. (1958). *Heat transfer, Volume I*, John Wiley & Sons, New York.

Kaviany, M. (1995). *Principles of Heat Transfer in Porous Media*, Second Edition, Springer, New York.

Klein, S.A. (1975). Calculation of Flat-Plate Collector Loss coefficients, *Sol. Energy*, vol. 17, pp79-80.

Kluppel, R.P., and Gurgel, J.M.A.M. (1988). Solar Cooled Drinking Fountain. *Sunworld*, Vol 12, No 4, pp113-4.

Kotas, T.J. (1995). *The Exergy Method of Thermal Plant analysis*, Krieger Publishing Company, Florida.

Kreider, J.F. and Rabl, A. (1994). *Heating and Cooling of Buildings*, McGraw-Hill, New York.

Kreith, F and West, R.E. (1997). CRC *Handbook of Energy Efficiency*, CRC Press.

Li, Z. and Sumathy, K. (1999). Solar-powered Ice-maker with the Solid Adsorption Pair of Activated Carbon and Methanol, *Int. J. of Energy Research*, Vol 23, No 6, pp517-27.

Li, M., Wang, R.Z., and Xu Y. (2000). Design of a New Adsorbent Bed about Solid Adsorption Refrigeration Driven by Solar Energy, *J. of Shanghai Jiaotong University*, Vol 34, No 4, pp469-72.

Liley, P.E. (1982). Thermodynamic Properties of Methanol. *Chemical Engineering Data*, No 29, pp50-1.

Liu, B.Y.H., and Jordan, R.C. (1960). The interrelationship and characteristic distribution of direct, diffuse and total solar radiation, *Solar Energy*, Vol. 4, pp.34.

McAdams, W.H. (1954). *Heat transmission*, Third Edition, McGraw-Hill, New York.

Medini N., Marmottant B., El Golli S. and Grenier Ph., (1991). Study of a packed solar ice maker. *Int. J. Refrig.*, Vol.14, pp.363-367.

Meunier F., Grenier Ph., Guilleminot and Pons M., (1986). Solar powered refrigeration using intermittent solid adsorption cycles. *Internal Paper*, Campus Universitaire, Orsay, France.

Meunier, F. and Mischler, B. (1979). Solar Cooling Through Cycles using Microporous Solid Adsorbent, *Sun II*, Pergamon Press, pp676-680.

Mohamad, A.A., Ramadhyani, S., and Viskanta, R. (1994). Modeling of Combustion and Heat Transfer in a Packed Bed with Embeded Coolant Tubes, *Int. J. Heat Mass Transfer* (37/8), pp1181.

Monnier, J.B. and Dupont, M. (1982). Zeolite-water Close Cycle Solar refrigeration; Numerical Optimisation and Field Testing, *Proc. of the American Solar Energy Society Conference*, Houston.

Moran, M.J. (1989). *Availability Analysis*, ASME Press, New York.

Moran, M.J. and Shapiro, H.N. (1995). *Fundamentals of Engineering Thermodynamics*, Third Edition, John Wiley & Sons, New York.

Nielsen P.B. and Worsøe-Schmidt, P. (1977). *Experimental Investigation of the Generation and Absorption Process*, The Technical University of Denmark Report F30-77.

Nielsen P.B. (1981). A Critical Surrey of Intermittent Absorption System for Solar Refrigeration, *Int. Congr. of Refrigeration*, Moscow, Session 1B2.1, pp659-667.

Passos, E.F. and Escobedo, J.F. (1989). Simulation of an intermittent adsorptive solar cooling system, *Solar Energy*, Vol. 42, No. 2, pp.103-11.

Passos E.F., Meunier F., and Gianola, J.C. (1986). Thermodynamic performance improvement of an intermittent solar-powered refrigeration cycle using adsorption of methanol on activated carbon. *Heat Recover Systems*, Vol.6, No.3, pp.259-64.

Plank, R. and Kuprianoff, J. (1960). *In die klainkaltemaschine*, Spring-Verlag, Berlin.

Pons, M., and Grenier, Ph. (1986). A Phenomenological adsorption Equilibrium Law Extracted from Experimental and Theoretical Consideration Applied to the Activated Carbon and Methanol Pair, *Carbon*, Vol 24, No 5, pp615-25.

Pons, M., and Grenier, Ph. (1987). Experimental Data on a Solar-powered Ice Maker Using Activated Carbon and methanol Adsorption Pair. *J. Solar Energy Engineering*, Vol 109, No 4, pp303-10.

Pons, M. and Guilleminot J.J. (1986). Design of an Experimental Solar-powered, Solid-adsorption Ice Maker, *Journal of Solar Energy Engineering*, Vol 108, No 4. pp332-7.

Rohsenow, W. M., Hartnett, J.P., and Cho, Y.I. (1998). *Handbook of Heat Transfer*, 3rd ed., McGraw-Hill.

Ruthven, D.M. (1984). *Principle of Adsorption and Adsorption Processes*, Wiley-Interscience, New York.

Ruthven, D.M. and Lee, L.K. (1981). Kinetics of Non-isothermal Sorption: System with Bed Diffusion Control, *A.I.Ch.E.J.*, Vol 27.

Saha, B.B., Boelman, E.C., and Kashiwagi, T. (1995). Computational analysis of an advanced adsorption-refrigeration cycle, *Energy*, Vol. 20, No 10, pp.983-94.

Saha, B.B., et al. (1997). Silica Gel Water Advanced Adsorption Refrigeration Cycle, *Energy*, Vol. 22, pp.437-47.

Saha, B.B., and Kashiwagi, T. (1997). Experimental Investigation of an Advanced Adsorption Refrigeration Cycle, *ASHRAE Transactions*, Vol. 103 Pt. 2, pp.50-8.

Sakoda A. and Suzuki M., (1984). Fundamental study on solar powered adsorption cooling system. *Journal of Chemical Engineering Japan*, Vol.17, No.1, pp.52-57.

Sakoda A. and Suzuki M., (1986). Simultaneous Transport of heat and adsorbate in closed type adsorption cooling system utilizing solar heat. *J. of Solar Energy Engineering*. Vol.108, pp.239-245.

Satterfield, C.N. and Sherwood, T.K. (1963) *The Role of Diffusion in Catalysis*, Addison-Wesley Publiching Company, Inc., Massachusetts.

Shelton, S V. Wepfer, W J. Miles, D J. (1989). Ramp wave analysis of the solid-vapor heat pump, *AES.*, Advanced Energy Systems Division (Publication) Publ. by ASME, New York, Vol 5. pp 1-11.

Siegel, R. and Howell, J.R. (1981). *Thermal Radiation Heat Transfer*, McGraw-Hill, New York.

Smith, J.M. and ven Ness, H.C. (1987). *Introduction to Chemical Engineering Thermodynamics*, Fourth Edition, McGraw-Hill, New York.

Smith, J.M., ven Ness, H.C., and Abbott, M.M. (1996). *Introduction to Chemical Engineering Thermodynamics*, Fifth Edition, McGraw-Hill, New York.

Sridhar K., (1987). *Study on activated carbon methanol pairs with relevance to ice making*. AIT Thesis, No. ET-87-2.

Suzuki, M. (1990). *Adsorption Engineering*, Kodansha, Tokyo.

Tan, Y.K., Feng, Y., Cui, N., Xu, Zh. (1992). Study of Solar Powered Adsorption Ice Maker, *Taiyangneng Xuebao*, Vol 13 No 3, pp 255-8.

Tan, Z, and Wang, R.Z. (1998). Research on Double Effect Adsorption Refrigeration Cycle. *Taiyangneng Xuebao*, Vol 19 No 2, pp 150-60.

Tanaka S., Hasegawa T. And Waki T., (1983). On the integrated solar collector-chiller using the intermittent adsorption cycle. *I.S.E.S. Solar World Congress*, Perth.

Tchernev, D.I. (1974). Solar Energy Cooling with Zeolites, *Proc. of the NSF/RANN Solar Collector Workshop*, New York, pp262.

Tchernev, D.I. (1978). Solar Energy Application of natural Zeolites, *Natural Zeolite and Its Use*, Pergamon Press, pp479-484. *Proc. of the NSF/RANN Solar Collector Workshop*, New York, pp262.

Tchernev, D.I. (1979). Solar Refrigeration Utilizing Zeolites, *Proc. of 14th Intersociety Energy Conversion.*

Tchernev, D.I. (1982). Solar Air Conditioning and Refrigeration Systems Utilizing Zeolites, *Utilisation of Solar Energy for Refrigeration and Air Conditioning, Refrigeration Science and Technology*, Paris, pp205-211.

Tchernev D.I., (1984). Use of natural zeolite in solar refrigeration. *ASSET*, Vol.6, No.5, pp.21-24.

Threlkeld, J.L. (1970). *Thermal Environmental Engineering*, 2nd ed., Prentice Hall, Englewood Cliffs, N.J.

Tien, C. (1994). *Adsorption Calculations and Modeling*, Butterworth-Heinemann, Boston.

van Wylen, G.J. et al. (1993). *Fundamentals of Classical Thermodynamics*, Fourth Edition, John Wiley & Sons, New York.

Wang, S.K. (1993). *Handbook of Air Conditioning and Refrigeration*, McGraw-Hill, New York.

Wang, R.Z., Jia, J., Teng, Y., Zhu, Y., and Wu, J. (1997). Potential Solid Adsorption Refrigeration Pair – Activated Carbon Fiber – Methanol. Taiyangneng Xuebao, Vol 18, No 2, pp222-7.

Wang, R.Z., Wu, J., Xu, Y., Wang, W., and Gui, Y. (1999). Experiments and Improvement on Heat Regenerative Adsorption Refrigerator and Heat Pump, *Taiyangneng Xuebao*, Vol 20, No 4, pp364-9.

Wark, K. (1995). *Advanced Thermodynamics for Engineers*, McGraw-Hill, New York.

Wark, K. and Richards D. (1999). *Thermodynamics*, 6th ed., McGraw-Hill, Boston.

Watabe Y. and Yanadori M., (1994). Cooling characteristic of adsorpti refrigeration apparatus using silica gel-ethanol system. *Kagaku Kogaku Ronbunshu*, Vol.20, No.4, pp.589-593.

Winter, C.-J., Sizmann, R.L., and Vant-Hull, L.L. (1991). *Solar Power Plants*, Springer-Verlag, Berlin.

Winterbone, D.E. (1997). *Advanced Thermodynamics for Engineers*, Arnold, London.

Worsφe-Schmidt, P. (1979) A Solar powered Solid-absorption Refrigeration System, *Int. J. Refrign.* Vol. 2, pp.75-84.

Yang, R.T. (1997). *Gas Separation by Adsorption Processes*, Imperial College Press, London.

Yoshida, F., Ramaswami, D and Hougen, O.A., (1962) *A.I.Ch.E. Journal*, Vol 8, pp5-11.

You, Y., Ma, Y.T., and Lu C.R. (1993a). The exergetic analysis of heat pump drying system, In: *Proc. of IECEC '93*, Atlanta, USA, Vol. 1, pp. 1913-1917

You, Y., Ma, Y.T., and Lu C.R. (1993b). The thermodynamic analysis of heat pump drying system. Part I: The exergy change of mixing, the exergy of moist air, *Journal of Yangzhou Institute of Technology*, Vol.5, No.1.

You, Y., Ma, Y.T., and Lu C.R. (1993c). The thermodynamic analysis of heat pump drying system. Part II: Experiment results and analysis, *Journal of Yangzhou Institute of Technology*, Vol.5, No.2.

You, Y. and Lu C.R. (1996). The derivation of entropy change for irreversible process, *Journal of Yangzhou Institute of Technology*, Vol.8, No.1, pp69-70.

Zhu, M.S. (1988). *Exergy Analysis on Energy Systems*. Qinghua University Press, Beijing.

Zhu, R., Han, B., Lin, M., and Yu, Y. (1992). Experimental Investigation on an Adsorption System for Producing Chilled Water. *Int. J. of Refrigeration*, Vol 15, No 1, pp31-4.

Publications (Peer Refereed)

1   You, Y., E. Hu and J. Jarvis, "The Derivation of Non-flow Exergy from Several Approaches", *1st International Conference on Heat Transfer, Fluid Mechanics and Thermodynamics*, Kruger National Park, South Africa, 2002 (accepted)

2   You, Y., E. Hu and J. Jarvis, "Deriving Flow Exergy from Several Approaches", *1st International Conference on Heat Transfer, Fluid Mechanics and Thermodynamics*, Kruger National Park, South Africa, 2002 (full paper submitted)

3   You, Y. and S. Harmon, "The Quantum 340 Litre Solar Boosted Heat Pump Water Heater and Its Performance in Real Climate Conditions", *7th International Energy Agency Heat Pump Conference*, Beijing, China, 2002 (abstract submitted)

4   You, Y. and S. Harmon, "A New Heat Pump System for Year-round Water Heating and Seasonal Air Cooling or Heating", *7th International Energy Agency Heat Pump Conference*, Beijing, China, 2002 (abstract submitted)

5   You, Y., E. Hu and J. Jarvis, "Simulation of the solar adsorption refrigeration operating at near atmospheric pressure", *ISES 2001 World Solar Congress*, Adelaide, Australia, 2001 (full paper submitted)

6   You, Y., E. Hu and J. Jarvis, "Solar thermal power systems: a thermodynamic comparison", *ISES 2001 World Solar Congress*, Adelaide, Australia, 2001 (full paper submitted)

7   Hu, E. and Y. You "Solar adsorption refrigeration—an alternative/auxiliary way for thermal storage for air conditioning", *ISES 2001 World Solar Congress*, Adelaide, Australia (full paper submitted)

8   You, Y., E. Hu and J. Jarvis, "Thermodynamic analyses on the influence of heat interchanger on the performance of vapour-compression refrigeration cycle", *CLIMA 2000*, Napoli, Italy, 2001 (full paper submitted)

9   You, Y., E. Hu and J. Jarvis, "A high energy efficiency air conditioning system", *CLIMA 2000*, Napoli, Italy, 2001 (full paper submitted)

10 You, Y. and E. Hu, "A Medium-Temperature Solar Thermal Power System and Its Efficiency Optimisation", *International Journal of Renewable Energy Engineering* (submitted).

11 You, Y. and E. Hu, "A solar thermal power system and its efficiency optimisation", *Applied Thermal Energy* (submitted).

12 Hu, E. and Y. You, "Solar thermal power or solar aided thermal power? A choice between efficiencies", In Proc. of *The 3rd Asia-Pacific Conf. On Sustainable Energy and Environmental Technologies*, Hong Kong, 2000, pp387-91

13 Hu, E. and Y. You, "Solar adsorption ice making — an ideal supplement to the ice storage air conditioning systems", *International Symposium of Air Conditioning in High Rise Buildings' 2000*, Shanghai, China, 2000

14 You, Y., E. Hu, J. Jarvis, and Y. Ibrahim, "Heat transfer analysis on the collector of the new solar adsorption refrigeration system working at around atmospheric pressure", In Proc. of *7th Australasian Heat and Mass Transfer Conference*, Townsville, Australia, 2000

15 You, Y., E. Hu, J. Jarvis, and Y. Ibrahim, "Adsorption analysis of the new solar adsorption refrigeration system working at about atmospheric pressure", In Proc. of *7th Australasian Heat and Mass Transfer Conference*, Townsville, Australia, 2000

16 You, Y., E. Hu and J. Jarvis, "The energy analysis on the solar adsorption refrigeration system working around atmospheric pressure", In Proc. of *Solar 2000. The Annual Conference of the Australia and New Zealand Solar Energy Society*, Brisbane, Australia, 2000

17 You, Y., E. Hu and J. Jarvis, "The exergy (availability) analysis on the solar adsorption refrigeration system working around atmospheric pressure", In Proc. of *Solar 2000. The Annual Conference of the Australia and New Zealand Solar Energy Society*, Brisbane, Australia, 2000

18 You, Y. and E. Hu, "Thermodynamic advantages of using solar energy in the regenerative Rankine power plant", *Applied Thermal Energy*, 19 (1999), pp.1173-80.

19 Hu, E., Y. You and M.A. Hessami, "A Study on Adsorption Refrigeration Systems Operating at Near Atmospheric Pressure", In Proc. of *The 20th International Congress of Refrigeration*, Sydney, 1999.

20 You, Y. and E. Hu, "The considerations of heat and exergy balance for heat exchangers", In Proc. of *The 20th International Congress of Refrigeration*, Sydney, Australia, 1999.

21 Hu, E. and Y. You, "A cleaner way for power generation--Integrate solar energy into conventional Rankine cycle", In Proc. of *The International conference on Industrial Waste Minimisation and Sustainable Development*, 13-17, Dec. 1999, Taipei, Taiwan.

22 You, Y. and E. Hu, "A power cycle proposed for using low-temperature thermal energy", In Proc. of *International Power and Energy Conference*, Victoria, Australia, 1999. pp357-361.

23 Hu, E. and Y. You, "A new solar adsorption refrigeration systems working around the atmosphere pressure and its thermodynamic analysis", In Proc. of *International Power and Energy Conference*, Victoria, Australia, 1999. pp442-447.

24 You, Y. and E. Hu, "Optimum efficiency for a solar thermal regenerative Rankine power cycle", In Proc. of *Solar '99, The Annual Conference of the Australia and New Zealand Solar Energy Society*, Geelong, Australia, 1999.

25 Hu. E. and Y. You, "Mass transfer analysis on the new solar adsorption refrigeration systems working around the atmospheric pressure", In Proc. of *Solar '99, The Annual Conference of the Australia and New Zealand Solar Energy Society*, Geelong, Australia. 1999.

26 You, Y., and E. Hu, "The exergy advantage of using low-grade heat (eg. solar energy) in conventional thermal power cycle", In: Proc. of *Adelaide International Workshop on Thermal Energy Engineering and the Environment*, South Australia, 1998, pp.593-604.

27 You, Y., E. Hu, and Y. Li, "An investigation on the favourable temperature difference for heat exchanger", In: Proc. of *Adelaide International Workshop on Thermal Energy Engineering and the Environment*, South Australia, 1998, pp. 567-578.

28 Hu, E. and Y. You, "Development of a (solar power) adsorption ice maker working at about atmospheric pressure", In Proc. of *Solar '98, The Annual Conference of the Australia and New Zealand Solar Energy Society*, Chrischurch, New Zealand, 1998.

29 You, Y. and E. Hu, "A modified Rankine power cycle for solar thermal energy", In Proc. of *Solar '98. The Annual Conference of the Australia and New Zealand Solar Energy Society*, Chrischurch, New Zealand, 1998.

30 You, Y., E. Hu, and R. Beebe, "Solar aided regenerative Rankine plant", In: Proc. of *1997 International Joint Power Generation Conference, ASME*, USA, 1997, Vol. 2, pp 555-5560.

31 You, Y. and C.R. Lu, "The derivation of entropy change for irreversible process", *Journal of Yangzhou Institute of Technology*, Vol.8, No.1, 1996, pp69-70. (in Chinese)

32 You, Y. and C. Lu "A direct calculation method of friction drag for rectangle duct", *Journal of Ventilation and Dust-Removing*, Vol.15, No.2, 1996, pp. 47-49 (in Chinese) (selected in <<*Science & Technology Treasury Of China Constructions*>>)

33 You, Y. et al, "An exact algorithm for the thermodynamic calculation of and some improvements on the double-effect $LiBr/H_2O$ absorption refrigerating machine of parallel-flow type", ' *96 National Conference on HVAC&R*, Nanjing, China, 1996. (in Chinese)

34 You, Y., "Refrigerant CO_2 and the new exploration for its applications", ' *96 National Conference on HVAC&R*, Nanjing, China, 1996. (in Chinese)

35 You, Y. and G. Wang, "Probe into the mean temperature (difference) of heaters in the hairpin type one-pipe heating system", *Journal of Yangzhou Institute of Technology*, Vol.7, No.1, 1995.

36 You, Y., Y.T. Ma, and C.R. Lu, "A new refrigeration / heat pump system of continuous capacity control with NARMs", In: Proc. of *International Conference on Energy and Environment*, Shanghai, China May 1995.

37 You, Y., Y.T. Ma, and C.R. Lu, "A new refrigeration system of continuous capacity control with NARMs", ' *94 National Conference on HVAC&R*, Zhang Jiajie, China, 1994. (in Chinese)

38 You, Y., Y.T. Ma, and C.R. Lu, "The thermodynamic analysis of heat pump drying system. Part I: The exergy change of mixing, the exergy of moist air", *Journal of Yangzhou Institute of Technology*, Vol.5, No.1, 1993. (in Chinese)

39 You, Y., Y.T. Ma, and C.R. Lu, "The thermodynamic analysis of heat pump drying system. Part II: Experiment results and analysis", *Journal of Yangzhou Institute of Technology*, Vol.5, No.2, 1993. (in Chinese)

40 You, Y., Y.T. Ma, and C.R. Lu, "The exergetic analysis of heat pump drying system", In: *Proc. of IECEC '93*, Atlanta, USA, Vol. 1, pp. 1913-7.

41 You, Y., Y.T. Ma, and C.R. Lu, "Experimental study on the capacity control of heat pump using NARM R22/R142b", In: *Proc. of IECEC '93*, Atlanta, USA, Vol. 1, pp 1909-12.

42 You, Y. and D. Zhou, "CFCs and environment", *Journal of Yangzhou Institute of Technology*, Vol.3, No.2, 1991, pp 63-9. (in Chinese, excellent paper award by Jiangsu HVAC society)

43 You, Y., Y.T. Ma, and C.R. Lu, "Experimental study on the capacity control of heat pump using NARM R22/R142", *Journal of Yangzhou Institute of Technology*, Vol.2, No.1, 1990, pp 17-21. (in Chinese, excellent paper award by Yangzhou Science and Technology Association, 1991)

44 You, Y., "*Study on the heat pump drying system and the new continuous capacity control heat pump system with non-azeotropic refrigerant mixtures*", Master's Thesis, Tianjin University, Tianjin, China, 1989.

45 You, Y., Y.T. Ma, and C.R. Lu, "A new heat pump system of continuous capacity control with non-azeotropic refrigerant mixtures", In: *Proc. of IECEC '89*, Washington D. C., USA, Vol. 4, pp 2117-2119.

46 You, Y., Y.T. Ma, and C.R. Lu, "A new continuous capacity control water-to-water heat pump system with NARMs" *'89 National Conference on Refrigeration and Heat Pump*, Wuxi, China, 1989. (in Chinese)

47 You, Y., "The calculation of cold air infiltration capacity of high rise buildings", *'85 Jiangsu HVAC&R Annual Conference*, Suzhou, China, 1985. (in Chinese)